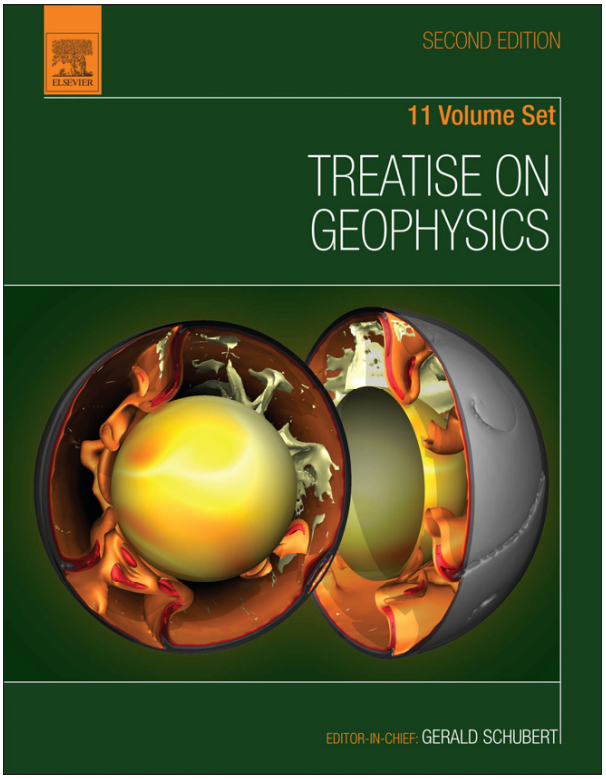

Cloetingh S., Ziegler P.A., Beekman F., Burov E.B., Garcia-Castellanos D. and Matenco L Tectonic Models for the Evolution of Sedimentary Basins. In: Gerald Schubert (editor-in-chief) Treatise on Geophysics, 2nd edition, Vol 6. Oxford: Elsevier; 2015. p. 513-592.

6.12 Tectonic Models for the Evolution of Sedimentary Basins

S Cloetingh, Utrecht University, Utrecht, The Netherlands
PA Ziegler†, University of Basel, Basel, Switzerland
F Beekman, Utrecht University, Utrecht, The Netherlands
EB Burov, Université Pierre et Marie Curie, Paris, France; Centre National de la Recherche Scientifique, Paris, France
D Garcia-Castellanos, Instituto de Ciencias de la Tierra Jaume Almera, Barcelona, Spain
L Matenco, Utrecht University, Utrecht, The Netherlands

This chapter is a revision of the previous edition chapter by S.Cloetingh and P.A. Ziegler, volume 6, pp. 485–611, © 2007, Elsevier B.V.

6.12.1 Introduction

Understanding the processes that drive sedimentary basin formation (e.g. Cloetingh et al., 1994; Ziegler, 1994) is a key element in elucidating the geologic evolution of the continental lithosphere. During the last decades, substantial progress was made in the understanding of thermomechanical properties and processes controlling the evolution of sedimentary basins and the isostatic response of the lithosphere to surface loads such as sedimentary basins. Much of this progress stems from improved insights into the mechanical properties of the lithosphere, from the development of new modeling techniques, and from the evaluation of new, high-quality datasets from previously inaccessible areas of the globe. The focus of this chapter is on tectonic models for

†Deceased.

Treatise on Geophysics, 2nd edition, (2015), vol. 6, pp. 513-592

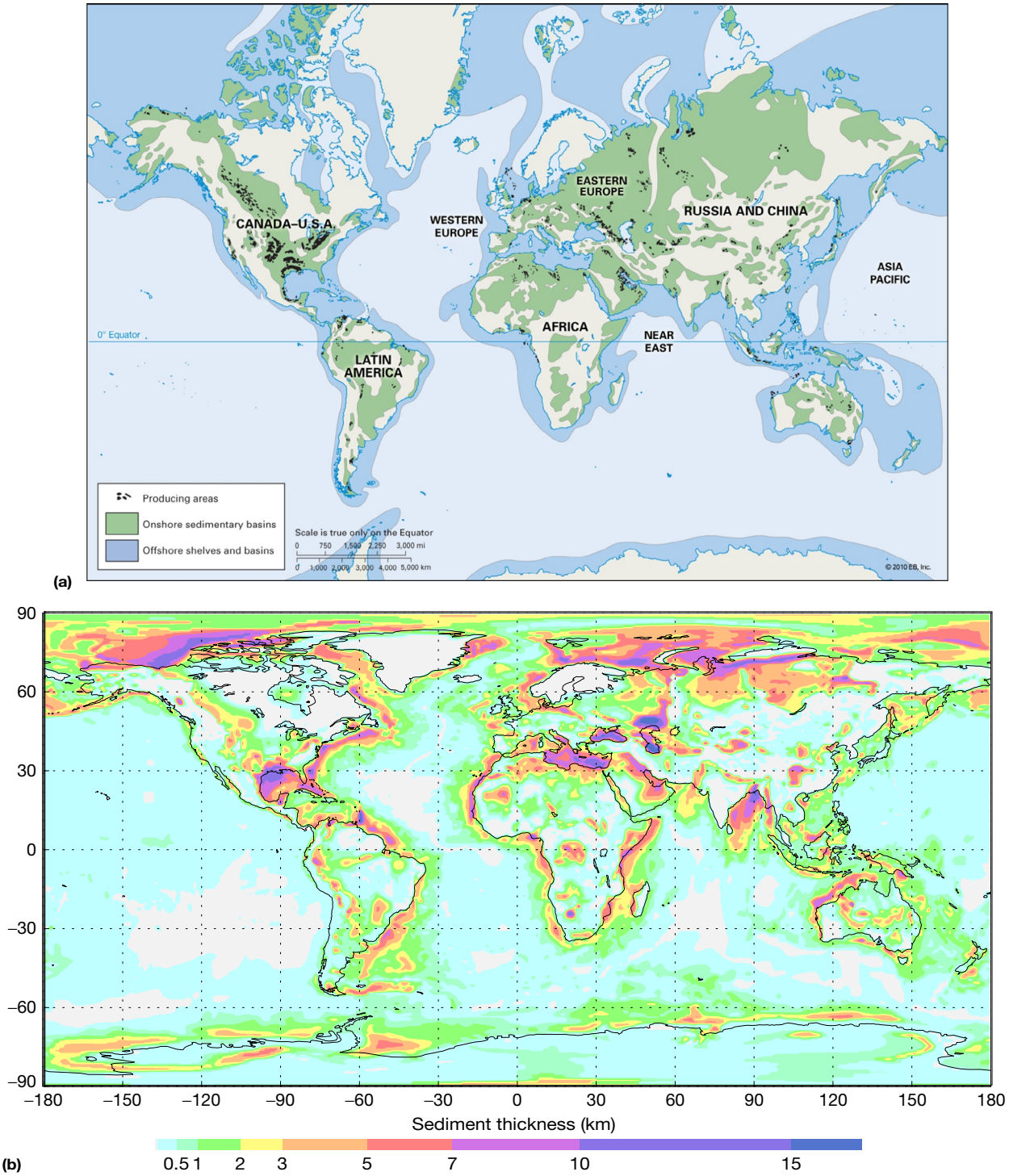

Figure 1 (a) Sedimentary basins and petroleum-producing areas of the world (the sizes of petroleum-producing areas are exaggerated in this map). (Adapted from Petroleum Publishing Co./PenWell (1970) Worldwide offshore activity and sedimentary basins. Oil and Gas Journal.) (b) Global map of sediment thickness, outlining the major onshore and offshore sedimentary basins of the world (reproduced from Laske G and Masters G (1997) A global digital map of sediment thickness. *Eos, Transactions of the American Geophysical Union* 78: F483).

processes controlling the evolution of sedimentary basins around the globe (Figure 1).

After the realization that subsidence patterns of Atlantic-type margins, corrected for effects of sediment loading and paleobathymetry, displayed the typical time-dependent decay characteristic of ocean-floor cooling (Sleep, 1971), a large number of studies were undertaken that aimed at restoring the quantitative subsidence history of basins on the basis of well data and outcropping sedimentary sections. With the introduction of backstripping analysis algorithms (Bond and Kominz, 1984; Steckler and Watts, 1982), the late 1970s and early 1980s marked a phase during which basin analysis

essentially stood for backward modeling, namely, reconstructing the tectonic subsidence from sedimentary sequences. These quantitative subsidence histories provided constraints for the development of conceptually driven forward basin models. For extensional basins, this commenced in the late 1970s with the appreciation of the importance of the lithospheric thinning and stretching concepts in basin subsidence (Salveson, 1976). After initiation of mathematical formulations of stretching concepts in forward extensional basin modeling (McKenzie, 1978), a large number of basin fill simulations focused on the interplay between thermal subsidence, sediment loading, and eustatic sea-level changes. To arrive at commonly observed more episodic and irregular subsidence curves, the smooth postrift subsidence behavior was modulated by changes in sediment supply and eustatic sea-level fluctuations. Another approach frequently followed was to input a subsidence curve, thus rendering the basin modeling package essentially a tool to fill in an adopted accommodation space (Burton et al., 1987; Lawrence et al., 1990). For the evolution of extensional basins, this approach made a clear distinction between their synrift stage and postrift stage, relating exponentially decreasing postrift tectonic subsidence rates to a combination of thermal equilibration of the lithosphere–asthenosphere system and lithospheric flexure (Watts et al., 1982).

A similar set of assumptions were made to describe the synrift phase. In the most simple version of the stretching model (McKenzie, 1978), lithospheric thinning was described as resulting from more or less instantaneous extension. In these models, a component of lithospheric mechanics was obviously lacking. On a smaller scale, tilted fault block models were introduced for modeling of the basin fill at the scale of half-graben models. Such models essentially decouple the response of the brittle upper crust from deeper lithospheric levels during rifting phases (e.g., see Kusznir et al., 1991).

A noteworthy feature of most modeling approaches in the 1990s was their emphasis on the basin subsidence record and their very limited capability to handle differential subsidence and uplift patterns in a process-oriented, internally consistent manner (e.g., see Doré et al., 1993; Kusznir and Ziegler, 1992; Larsen et al. 1992). More recently, increasing evidence is accumulating for compressional reactivation of extensional basins (e.g., Cloetingh et al., 2008; Johnson et al., 2008).

Compressional basin modeling also underwent a change in focus. The importance of the lithospheric flexure concept, relating topographic loading of the crust by an overriding mountain chain to the development of accommodation space, was recognized as early as 1973 by studying the foreland of the Canadian Rocky Mountain thrust belt (Price, 1973). Also here it took several years before quantitative approaches started to develop, investigating the effects of lithospheric flexure on foreland basin stratigraphy (Beaumont, 1981). The success of flexural basin stratigraphy modeling, capable of incorporating subsurface loads related to plate tectonic forces operating on the lithosphere (e.g., Peper et al., 1995; Van der Beek and Cloetingh, 1992), led in the 1990s to the need to incorporate more structural complexity in these models, also in view of implications for the simulation of thermal maturation and fluid migration (e.g., Parnell, 1994). The necessary understanding of lithospheric mechanics and basin deformation was subsequently developed after a bridge was established between researchers studying deeper lithospheric processes and those who analyzed the record of vertical motions, sedimentation, and erosion in basins (e.g., Cloetingh et al., 2007; Cloetingh and Negendank, 2010; Garcia-Castellanos and Cloetingh, 2012). This permitted the development of basin analysis models that integrate structural geology and lithosphere tectonics (see Roure et al, 2010c for an overview).

In the following sections of this chapter, we review recent advances in modeling the initiation and evolution of sedimentary basins in their lithospheric context on a global and more regional scale. To the latter purpose, we follow a natural laboratory approach selecting some well-documented basins of Europe. In this way, a review of recent advances and data interactive modeling integrating process modeling with geologic and geophysical data is given, covering key aspects of extensional basins, foreland basins, and basins formed by lithospheric folding. As will become clear from these sections, polyphase evolution of basin systems is the rule rather than an exception. Another important aspect has been the quantification of mechanical coupling of lithospheric processes to the near-surface expression of tectonic controls on basin fill. This invoked a process-oriented approach, linking different spatial and temporal scales in the basin record. Crucial in this was the testing and validation of modeling predictions in natural laboratories for which high-quality databases were available at deeper crustal levels (deep reflection and refraction seismic) and the basin fill (reflection seismic, wells, and outcrops), demanding a close cooperation between academic and industrial research groups (e.g., Roure et al., 2010c).

In **Section 6.12.2**, we first analyze the finite strength of the lithosphere, which plays an important role in the development of both extensional and compressional basins. This applies both to the geometry of the basin shape and to the record of vertical motions during and after rifting. We highlight the connection between the bulk rheological properties of the lithosphere and the evolution of some of Europe's main sedimentary basins. These include some of the best-documented sedimentary basin systems of the world.

In **Section 6.12.3**, we start with a review of the dynamics of extensional basin systems. First, we discuss the genetic types of extensional basins followed by an overview of the characteristics of thermal thinning of the lithosphere, doming and flood basalt extrusion, and aspects of particular importance to volcanic-rifted margins. We examine the record of vertical motions during and after rifting in the context of stretching models developed to quantify rifted basin development. We also address the tectonic control on postrift evolution of extensional basins. In **Section 6.12.3.7**, we develop the treatment of polyphase deformation of extensional basins by reviewing two European back-arc basin systems as natural laboratories: the Black Sea basin system and the Pannonian–Carpathian Basin system, both located in eastern Europe. We concentrate on rheological controls on basin formation and its consequences for large-scale basin stratigraphy and rift-shoulder dynamics. We also discuss the role of intraplate stresses and lithospheric strength evolution during the postrift phase and implications for neotectonic reactivation of the Black Sea basin system. The Pannonian–Carpathian Basin system is the site of pronounced contrasts of lithospheric strength between the Pannonian area, which is probably underlain by the hottest and weakest lithosphere of Europe,

and the particularly strong East European Platform lithosphere bounding the Carpathian arc to the east. Noteworthy features of the Pannonian system are the short duration of rifting phases in a back-arc setting affected by extensional collapse and subsequent compressional reactivation.

In Section 6.12.4, we review the development and evolution of compressional basins in a lithospheric context. We focus on foreland basins and basins that evolved as a result of large-scale compressional folding of intraplate continental lithosphere and present and discuss examples of both types of basins in the first part of the section. In the first part of Section 6.12.4, we address the role of flexure in compressional basin evolution and the interplay between lithosphere dynamics and topography in compressional basin systems. Basins developed on folded continental lithosphere have characteristic features. We illustrate this in the second part of Section 6.12.4 by the basins of central Asia, the folded lithosphere of Iberia, the NW European Platform, the Pannonian Basin and the South Caspian Basin.

The closing Section 6.12.5 draws some general conclusions and addresses future perspectives.

6.12.2 Rheological Controls on Basin Evolution

6.12.2.1 Rheological Stratification of the Lithosphere

The strength of *continental* lithosphere is controlled by its depth-dependent rheological structure in which the thickness and composition of the crust, the thickness of the lithospheric mantle, the potential temperature of the asthenosphere, and the presence or absence of fluids, as well as strain rates, play a dominant role (Burov, 2007; Cloetingh and Burov, 1996; Kusznir and Park, 1987; Watts, 2001, 2007; see also Watts, Chapter 6.01 and Burov, Chapter 6.03). Rheological models indicate that thermally stabilized continental lithosphere typically consists of the mechanically strong upper crust, which is separated by a weak lower crustal layer from the strong upper part of the mantle–lithosphere that in turn overlies the weak lower mantle–lithosphere (Figure 2).

By contrast, *oceanic* lithosphere has a more homogeneous composition and is characterized by a much simpler rheological structure. The strength of *oceanic* lithosphere depends mainly on its thermal regime, which controls its essentially

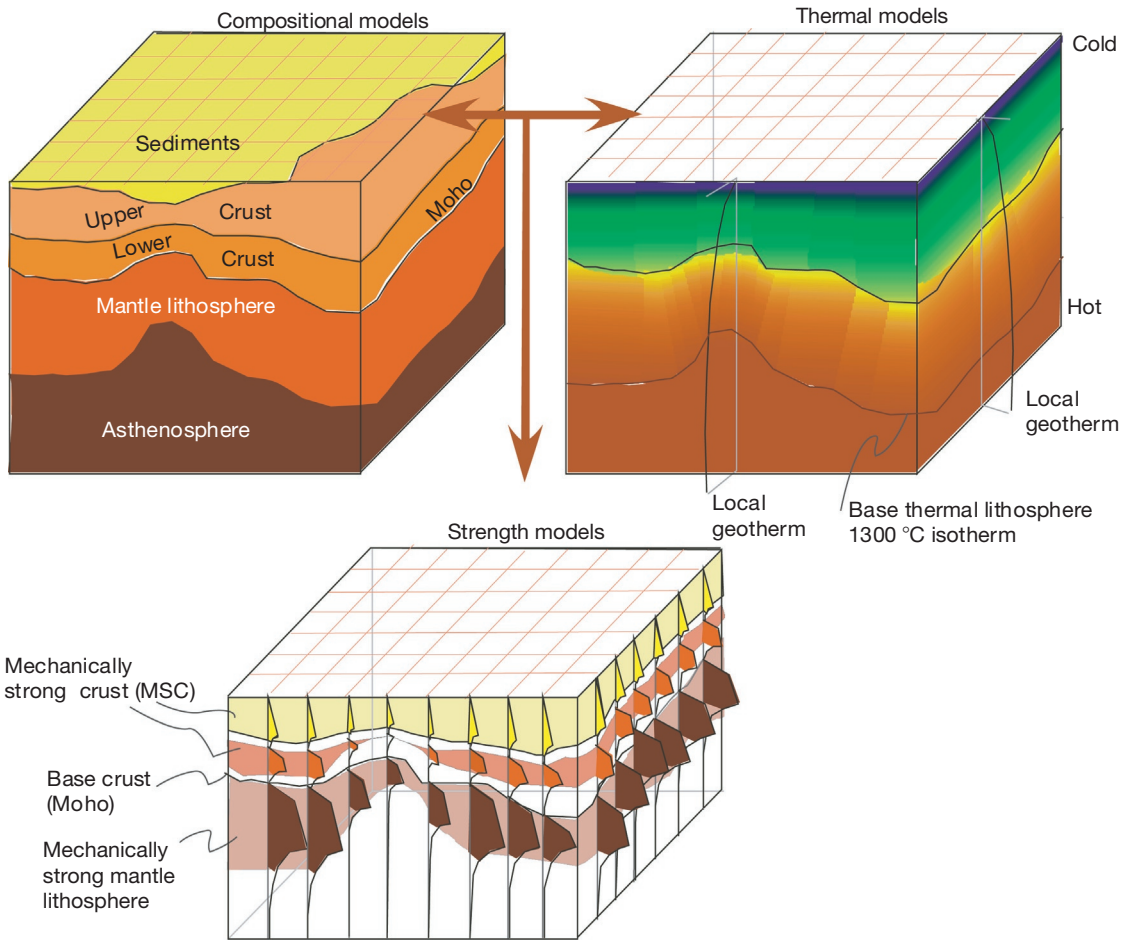

Figure 2 From crustal thickness (top left) and thermal structure (top right) to lithospheric strength (bottom): conceptual configuration of the thermal structure and composition of the lithosphere, adopted for the calculation of 3-D strength models. Reproduced from Cloetingh S, Ziegler PA, Beekman F, Andriessen PAM, Hardebol N, and Dèzes P (2005) Intraplate deformation and 3D rheological structure of the Rhine Rift System and adjacent areas of the northern Alpine foreland. *International Journal of Earth Sciences* 94: 758–778.

age-dependent thickness. Rheologically speaking, thermally stabilized oceanic lithosphere is considerably stronger than all types of continental lithosphere.

The strength of continental crust depends also on the availability of preexisting crustal discontinuities (Burov, 2007; see also Burov, this volume). Deep-reaching crustal discontinuities, such as thrust and wrench faults, cause significant weakening of the otherwise mechanically strong upper parts of the crust. As such discontinuities are apparently characterized by a reduced frictional angle, particularly in the presence of fluids (Van Wees, 1994), they are prone to reactivation at stress levels that are well below those required for the development of new faults. Deep reflection-seismic profiles show that the crust of late Proterozoic and Paleozoic orogenic belts is generally characterized by a monoclinal fabric that extends from upper crustal levels down to the Moho either at which it soles out or by which it is truncated (see Ziegler and Cloetingh, 2004). This fabric reflects the presence of deep-reaching lithologic heterogeneities and shear zones.

The strength of the continental upper lithospheric mantle depends to a large extent not only on the thickness of the crust but also on its age and thermal regime (Jaupart and Mareschal, 2007; see Jaupart and Mareschal, this volume). Thermally stabilized stretched continental lithosphere with a 20 km thick crust and a 50 km thick lithospheric mantle is mechanically stronger than unstretched lithosphere with a 30 km thick crust and a 70 km thick lithospheric mantle. Extension of stabilized continental crustal segments precludes ductile flow of the lower crust, and faults will be steep to listric and propagate toward the hanging wall, that is, toward the basin center (Bertotti et al., 2000). Under these conditions, the lower crust will deform by distributing ductile shear in the brittle–ductile transition domain. This is compatible with the occurrence of earthquakes within the lower crust and even close to the Moho (e.g., southern Rhine Graben: Bonjer, 1997; East African Rift: Shudofsky et al., 1987).

On the other hand, in young orogenic belts, which are characterized by crustal thicknesses of up to 60 km and an elevated heat flow, the mechanically strong part of the crust is thin and the lithospheric mantle is also weak. Extension of this type of lithosphere, involving ductile flow of the lower and middle crust along pressure gradients away from areas lacking upper crustal extension into zones of major upper crustal extensional unroofing, can cause crustal thinning and thickening, respectively. This deformation mode gives rise to the development of core complexes with faults propagating toward the hanging wall (e.g., Basin and Range Province: Bertotti et al., 2000; Buck, 1991; Wernicke, 1990). However, crustal flow will cease after major crustal thinning has been achieved, mainly due to extensional decompression of the lower crust (Bertotti et al., 2000).

Generally, the upper mantle of thermally stabilized, old cratonic lithosphere is considerably stronger than the strong part of its upper crust (Moisio et al., 2000). However, the occurrence of upper mantle reflectors, which generally dip in the same direction as the crustal fabric and probably are related to subducted oceanic and/or continental crustal material, suggests that the continental lithospheric mantle is not necessarily homogenous but can contain lithologic discontinuities that enhance its mechanical anisotropy (Vauchez et al., 1998; Ziegler et al., 1998). Such discontinuities, consisting of eclogitized crustal material, can potentially weaken the strong upper part of the lithospheric mantle. Moreover, even in the face of similar crustal thicknesses, the heat flow of deeply degraded late Proterozoic and Phanerozoic orogenic belts is still elevated as compared to adjacent old cratons (e.g., Pan-African belts of Africa and Arabia; Janssen, 1996). This is probably due to the younger age of their lithospheric mantle and possibly also to a higher radiogenic heat generation potential of their crust. These factors contribute to weakening of former mobile zones to the end that they present rheologically weak zones within a craton, as evidenced by their preferential reactivation during the breakup of Pangaea (Janssen et al., 1995; Ziegler, 1989b; Ziegler et al., 2001).

From a rheological point of view, the thermally destabilized lithosphere of tectonically active rifts, as well as of rifts and passive margins that have undergone only a relatively short postrift evolution (e.g., 25 Ma), is considerably weaker than that of thermally stabilized rifts and of unstretched lithosphere (Ziegler et al., 1998). In this respect, it must be realized that during rifting, progressive mechanical and thermal thinning of the lithospheric mantle and its substitution by the upwelling asthenosphere is accompanied by a rise in geotherms causing progressive weakening of the extended lithosphere. In addition, its permeation by fluids causes its further weakening. Upon decay of the rift-induced thermal anomaly, rift zones are rheologically speaking considerably stronger than unstretched lithosphere. However, the accumulation of thick syn- and postrift sedimentary sequences can cause by thermal blanketing a weakening of the strong parts of the upper crust and lithospheric mantle of rifted basins (Stephenson, 1989). Moreover, as faults permanently weaken the crust of rifted basins, they are prone to tensional and compressional reactivation (Ziegler et al., 1995, 1998, 2001, 2002).

In view of its rheological structure, the continental lithosphere can be regarded under certain conditions as a two-layered viscoelastic beam (Reston, 1990; Ter Voorde et al., 1998). The response of such a system to the buildup of extensional and compressional stresses depends on the thickness, strength, and spacing of the two competent layers and on stress magnitudes and strain rates and the thermal regime (Watts and Burov, 2003; Zeyen et al., 1997). As the structure of continental lithosphere is also laterally heterogeneous, its weakest parts start to yield first once tensional and compressional intraplate stress levels equate their strength.

6.12.2.2 Rheological Controls on Basin Evolution: Europe's Continental Lithosphere

Studies on the rheological properties of the European lithosphere revealed a direct link between its thermotectonic age and bulk strength (Cloetingh and Burov, 1996; Cloetingh et al., 2005a,b; Pérez-Gussinyé and Watts, 2005). On the other hand, inferences from *P*- and *S*-wave tomography (Goes et al., 2000a,b; Ritter et al., 2000, 2001) and thermomechanical modeling (Garcia-Castellanos et al., 2000) point to a pronounced weakening of the lithosphere in the Lower Rhine area owing to high upper mantle temperatures. However, the late Neogene and Quaternary tectonics of the Ardennes–Lower Rhine area appears to form part of a much wider neotectonic deformation system that overprints the late Paleozoic and Mesozoic basins of NW Europe. This is supported by

geomorphological evidence and the results of seismicity studies in Brittany (Bonnet et al., 2000) and Normandy (Lagarde et al., 2000; Van Vliet-Lanoë et al., 2000) and by data from the Ardennes–Eifel region (Van Balen et al., 2000), the southern parts of the Upper Rhine Graben (Nivière and Winter, 2000), the Bohemian Massif (Ziegler and Dèzes, 2005, 2007), and the North German Basin (Bayer et al., 1999).

Lithospheric-scale folding and buckling, in response to the buildup of compressional intraplate stresses, can cause uplift or subsidence of relatively large areas at timescales of a few My and thus can be an important driving mechanism of neotectonic processes. For instance, the Pliocene–Pleistocene accelerated subsidence of the North Sea basin is attributed to downbuckling of the lithosphere in response to the buildup of the present-day stress field (Van Wees and Cloetingh, 1996). Similarly, uplift of the Vosges–Black Forest Arch, which at the level of the crust–mantle boundary extends from the Massif Central into the Bohemian Massif, commenced during the Burdigalian (±18 Ma) and persisted until at least Early Pliocene times. Uplift of this arch is attributed to lithospheric folding controlled by compressional stresses originating at the Alpine collision zone (Dèzes et al., 2004; Ziegler and Dèzes, 2005, 2007; Ziegler et al., 2002).

An understanding of the temporal and spatial strength distribution of continental lithosphere (e.g., Cloetingh and Van Wees, 2005; Cloetingh et al., 2005a,b, 2006, 2007, 2011, 2013; Tesauro et al., 2007, 2009b, 2012b, 2013) may offer quantitative insights into the patterns of its intraplate deformation (basin inversion and upthrusting of basement blocks) and particularly into the pattern of lithospheric-scale folding and buckling. So far, strength envelopes and the effective elastic thickness (EET) of the lithosphere have been calculated for a number of locations in Europe (e.g., Cloetingh and Burov, 1996). However, as such calculations were made for scattered points only, or along transects, they provide limited information on lateral strength variations of the lithosphere. Although lithospheric thickness and strength maps have already been constructed for the Pannonian Basin (Lankreijer et al., 1999) and the Baltic Shield (Kaikkonen et al., 2000), such maps were until recently not yet available for all of Europe.

As evaluation and modeling of the response of the lithosphere to vertical and horizontal loads require an understanding of its strength distribution, dedicated efforts were made to map the strength of the European foreland lithosphere by implementing 3-D strength calculations (Cloetingh et al., 2005a,b; Tesauro et al., 2009b). Owing to the large amount of high-quality geophysical data acquired during the last 20 years in Europe, its lithospheric configuration is rather well known though significant uncertainties remain in many areas about the seismic and thermal thickness of the lithosphere (Artemieva, 2006, 2011; Artemieva and Mooney, 2001; Artemieva et al., 2006; Babuska and Plomerova, 1992). Nevertheless, available data help to constrain the rheology of the European lithosphere, thus enhancing our understanding of its strength.

Strength calculations of the lithosphere depend primarily on its thermal and compositional structure and are particularly sensitive to thermal uncertainties (Burov and Diament, 1995; Ranalli, 1995; Ranalli and Murphy, 1987). For this reason, the workflow aimed at the development of a 3-D strength model for Europe was twofold: (1) constructing a 3-D compositional model and (2) calculating a 3-D thermal cube. The final 3-D strength cube (**Figure 2**) was obtained by calculating 1-D strength envelopes for each lattice point (x,y) of a regularized raster covering NW Europe. For each lattice point, the appropriate input values were obtained from a 3-D compositional and thermal cube. A geologic and geophysical geographic database was used as reference for the construction of the input models.

For continental realms, a 3-D multilayer compositional model was constructed, consisting of one mantle–lithosphere layer, 2–3 crustal layers, and an overlying sedimentary cover layer, whereas for oceanic areas, a one-layer model was adopted. For the depth to the different interfaces, several regional- or European-scale compilations were available that are based on deep seismic reflection and refraction or surface wave dispersion studies (e.g., Artemieva et al., 2006; Blundell et al., 1992; Calcagnile and Panza, 1987; Du et al., 1998; Panza, 1983; Suhadolc and Panza, 1989; Tesauro et al., 2008). For the Moho depth, we relied on the EuCRUST-07 model of Tesauro et al. (2008) (**Figure 3**). Regional compilation maps of the seismogenic lithospheric thickness were used as reference to the base of the thermal lithosphere in subsequent thermal modeling (Babuska and Plomerova, 1993, 2001; Plomerova et al., 2002; Tesauro et al., 2010a,b).

Figure 4(a) shows the integrated strength under compression of the entire lithosphere of western and central Europe (Tesauro et al., 2009b), whereas **Figure 4(b)** displays the integrated strength of the crustal part of the lithosphere. As evident from **Figure 4**, European lithosphere is characterized by major spatial mechanical strength variations, with a pronounced contrast between the strong Proterozoic lithosphere of the East European Platform to the east of the Teisseyre–Tornquist Line and the relatively weak Phanerozoic lithosphere of western Europe. A similar strength contrast occurs at the transition from strong Atlantic oceanic lithosphere to the relatively weak continental lithosphere of western Europe. Within the Alpine foreland, pronounced northwest–southeast trending weak zones are recognized that coincide with such major geologic structures as the Rhine Graben system and the North Danish–Polish Trough that are separated by the high-strength North German Basin and the Bohemian Massif. Moreover, a broad zone of weak lithosphere characterizes the Massif Central and surrounding areas.

The presence of thickened crust in the area of the Teisseyre–Tornquist suture zone (**Figure 3**) gives rise to a pronounced mechanical weakening of the lithosphere, particularly of its mantle part. Whereas the lithosphere of Fennoscandia is characterized by a relatively high strength, the North Sea rift system corresponds to a zone of weakened lithosphere. Other areas of high lithospheric strength are the Bohemian Massif and the London–Brabant Massif, both of which exhibit low seismicity (**Figure 5**). A pronounced contrast in strength can also be noticed between the strong Adriatic indenter and the weak Pannonian Basin area.

Comparing **Figure 4(a)** with **4(b)** reveals that the lateral strength variations of Europe's intraplate lithosphere are primarily caused by variations in the mechanical strength of the lithospheric mantle, whereas variations in crustal strength appear to be more modest. The variations in lithospheric mantle strength are primarily related to variations in the thermal structure of the lithosphere that can be related to thermal perturbations of the sublithospheric upper mantle imaged by seismic tomography (Goes et al., 2000a), with lateral variations in crustal thickness

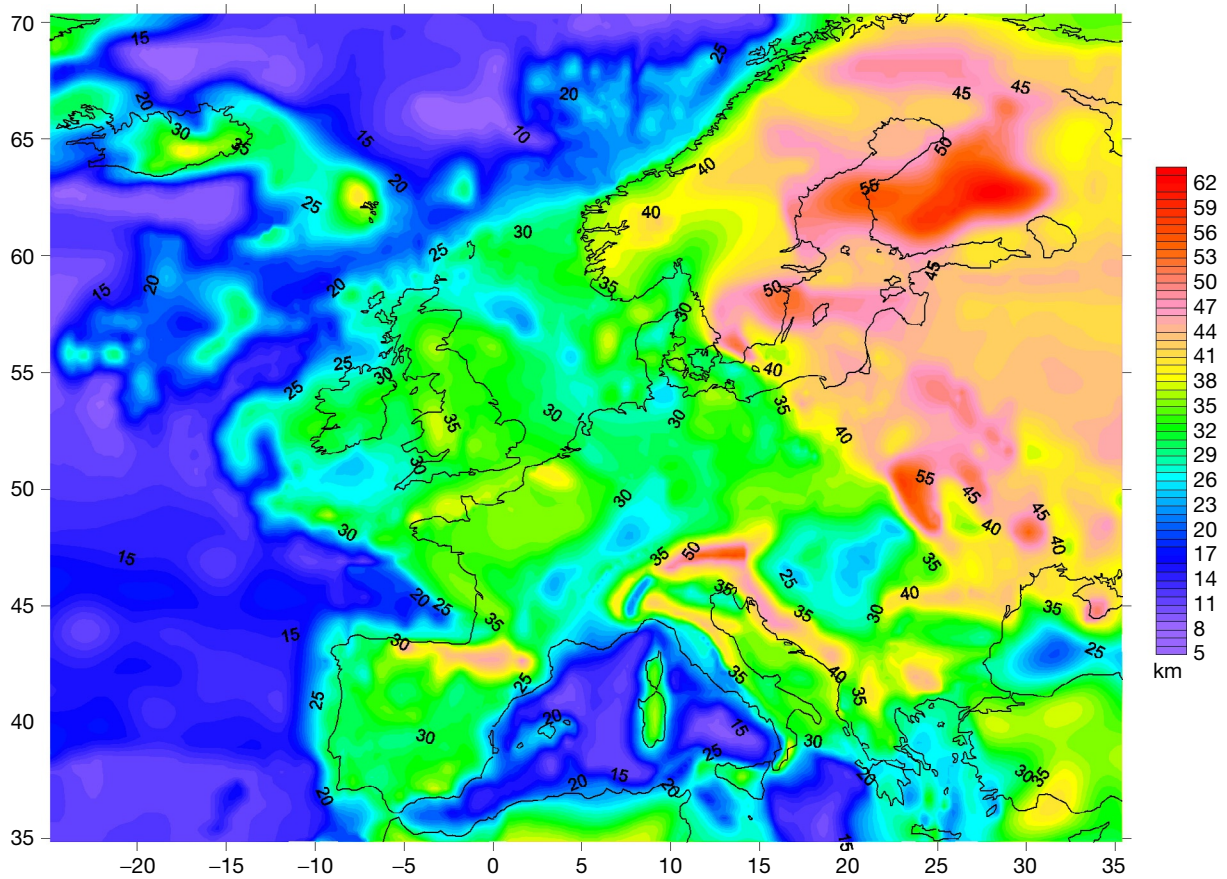

Figure 3 Map of Moho depth discontinuity for western Europe, constructed by integration of published regional maps. Reproduced from Tesauro M, Kaban MK, and Cloetingh SAPL (2008) EuCRUST-07: A new reference model for the European crust. *Geophysical Research Letters* 35: L05313.

playing a secondary role, apart from Alpine domains that are characterized by deep crustal roots. High strength in the East European Platform, the Bohemian Massif, the London–Brabant Massif, and the Fennoscandian Shield reflects the presence of old, cold, and thick lithosphere, whereas the European Cenozoic Rift System coincides with a major axis of thermally weakened lithosphere within the Northwest European Platform. Similarly, weakening of the lithosphere of southern France can be attributed to the presence of tomographically imaged plumes rising up under the Massif Central (Granet et al., 1995; Wilson and Patterson, 2001).

The major lateral strength variations that characterize the lithosphere of extra-Alpine Phanerozoic Europe are largely related to its late Cenozoic thermal perturbation and to Mesozoic and Cenozoic rift systems and intervening stable blocks and not so much to the Caledonian and Variscan orogens and their accreted terranes (Dèzes et al., 2004; Ziegler and Dèzes, 2006). These lithospheric strength variations are primarily related to variations in the thermal structure of the lithosphere and, therefore, are compatible with inferred variations in the EET of the lithosphere (see Cloetingh and Burov, 1996; Pérez-Gussinyé and Watts, 2005). The most important strong inliers in the lithosphere of the Alpine foreland lithosphere correspond to the early Paleozoic London–Brabant Massif and the Variscan Armorican, Bohemian, and west Iberian Massifs. The strong Proterozoic Fennoscandian–East European Craton flanks the weak Phanerozoic European lithosphere to the northeast, whereas the strong Adriatic indenter contrasts with the weak lithosphere of the Mediterranean collision zone.

Spatial variations in lithospheric strength and relatively hot upper mantle under the lithosphere of central and western Europe can lead to ductile crustal flow not only on continental scale in European lithosphere (Tesauro et al., 2011) but also on the scale of rifted margin systems such as the southern Norwegian rifted margin (Pascal and Cloetingh, 2009).

6.12.2.3 Loading, Flexure, and Rheology of the Lithosphere

The major, directly measurable proxy for the integrated strength of the lithosphere is its EET (or T_e, see Watts, 2001 and references therein). By comparing observations of flexure in the region of long-term loads such as ice, sediment, and volcanoes to the predictions of elastic plate flexure models, T_e of the lithosphere in a wide range of geologic settings could be estimated (**Table 1**). Flexure studies on oceanic lithosphere suggest that its T_e ranges between 2 and 40 km and depends on plate age and sedimentary load. The T_e of continental lithosphere ranges

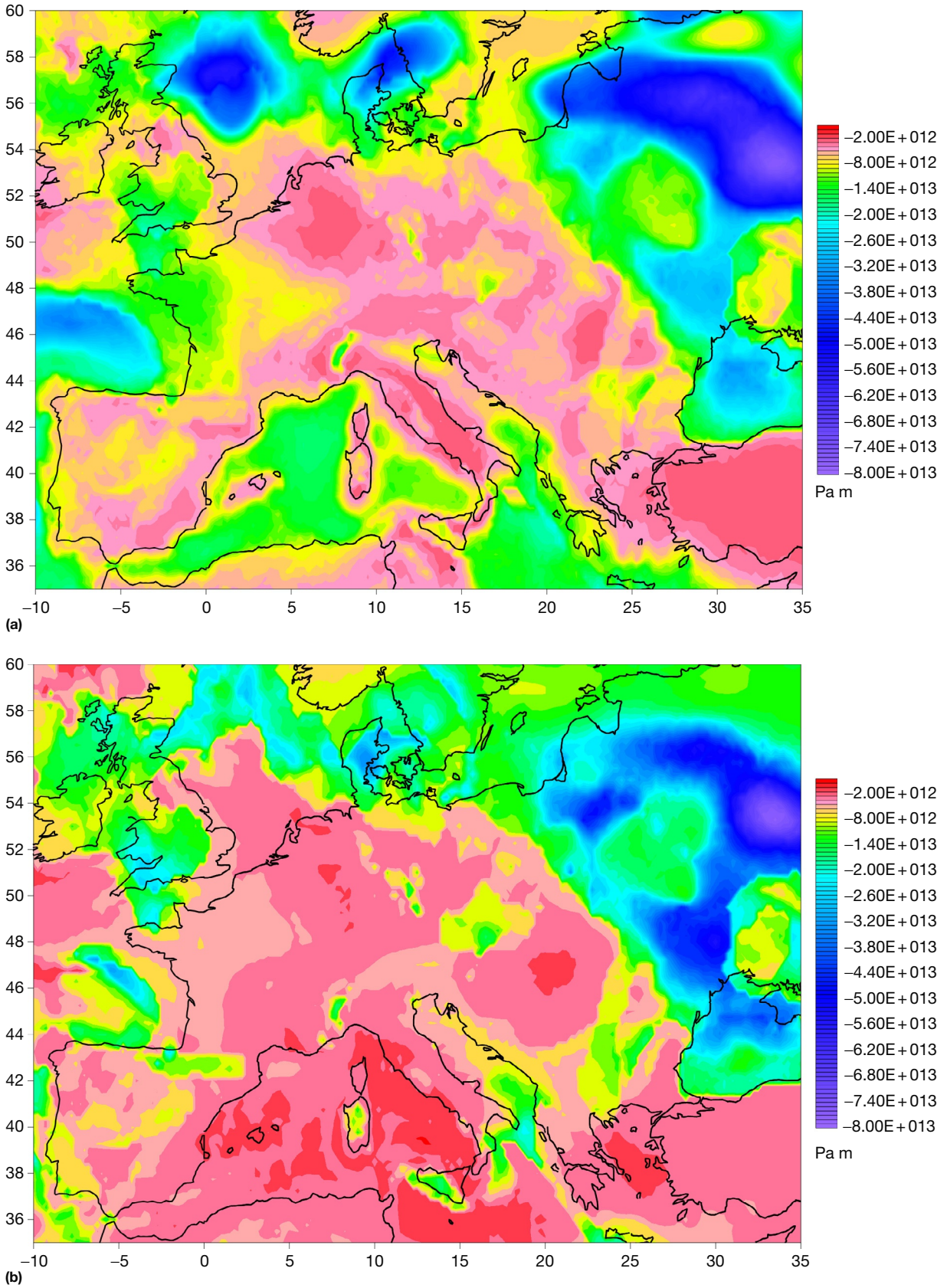

Figure 4 Integrated strength maps for intraplate Europe. Contours represent integrated strength in compression for (a) total lithosphere and (b) crust. Reproduced from Tesauro M, Kaban MK, and Cloetingh SAPL (2009a) A new thermal and rheological model of the European lithosphere. *Tectonophysics* 476: 478–495.

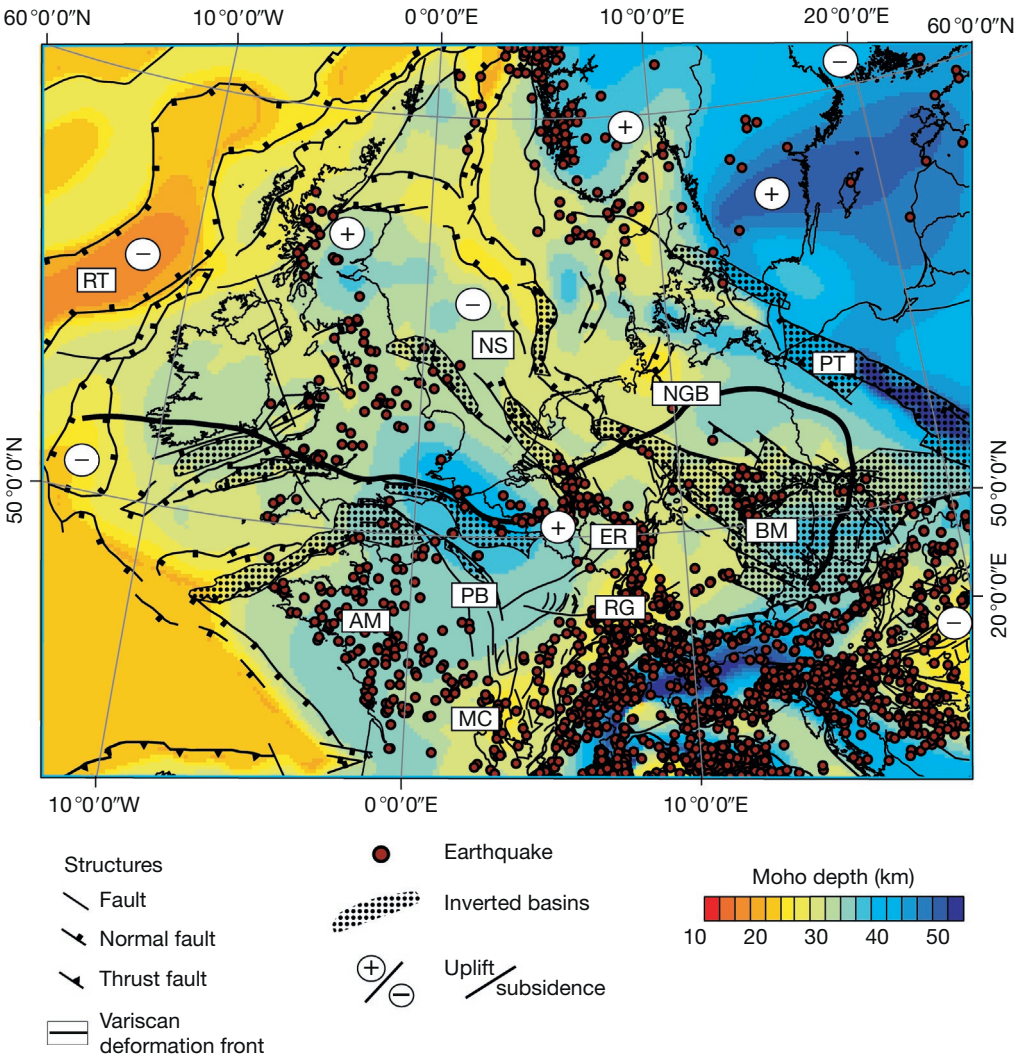

Figure 5 Seismicity (after Grünthal et al., 1999) superimposed on map of depth to Moho (reproduced from Ziegler PA and Dèzes P (2006) Crustal evolution of Western and Central Europe. *Geological Society, London, Memoirs* 32: 43–56) of northwest Europe. Neogene uplift and subsidence anomalies are indicated by circled plus and minus symbols, respectively (cf. Japsen and Chalmers, 2000). Also shown are locations of inverted basin structures (modified from Brun JP and Nalpas T (1996) Graben inversion in nature and experiments. *Tectonics* 15: 677–687). Note concentrations of intraplate seismicity in areas of crustal thickness contrast between basinal and Paleozoic massif areas, as well as in areas of crustal contrast along northeastern Atlantic rifted margins. Notable exception is seismicity along neotectonically active Rhine Graben (RG). BM, Bohemian Massif; ER, Eifel region; MC, Massif Central; NS, North Sea basin; NGB, North German Basin, PB, Paris Basin; PT, Polish Trough; RT, Rockall Trough; AM, Armorican Massif. Reproduced from Cloetingh S and Van Wees JD (2005) Strength reversal in Europe's intraplate lithosphere: Transition from basin inversion to lithospheric folding. *Geology* 33: 285–288.

from 0 to 100 km and shows no clear relationship with the consolidation age of the crust (Watts, 2001).

The thermomechanical age concept provides the framework for EET estimates of the lithosphere. Figure 6 (Cloetingh et al., 2013) illustrates the general trend of increasing elastic plate thickness with increasing thermomechanical age. Also plotted are predictions for the bulk rheology of the lithosphere based on extrapolations from rock-mechanical data, constrained by crustal geophysical data and thermal models. A characteristic feature of these models is the incorporation of a quartz-dominated upper crustal rheology and an olivine-controlled mantle rheology. These models are cast in terms of the depth to the base of the mechanically strong upper part of the crust (MSC) and the mechanically strong part of the upper mantle–lithosphere (MSL). The analysis of Figure 6 demonstrates that the mechanical properties of the crust are little affected by its age-dependent cooling, whereas the thickness and strength of the lithospheric mantle are very strongly age-dependent.

Oceanic flexural studies have shown that EET increases as the tectonic plate becomes older and gradually decreases after load emplacement ceases, because viscous stress relaxation makes the plate appearing weaker (Nádai, 1963). However, these relationships remain often unclear for continents (Watts, 2001). Adopting a quartz–diabase–olivine composition, the intrinsic strength of upper crust, lower crust, and lithospheric mantle increases with depth, in competition with

Table 1 Compilation of elastic thicknesses (EET) obtained from forward flexural modeling of foreland basins (see also **Figure 6**)

Plate	*Load/orogen*	*Basin*	*EET (km)*	*Error ± (km)*	*Source*
South Iberia	Betics W	Guadalquivir	10.0	5.0	Van der Beek and Cloetingh (1992) and Garcia-Castellanos et al. (2002)
South Iberia	Betics E	Guadalquivir	2.5	2.5	Van der Beek and Cloetingh (1992) and Garcia-Castellanos et al. (2002)
Central Iberia	Iberian Central System	Duero/Tajo/Madrid	7.0	5.0	Andeweg (2002)
North Iberia	Pyrenees, Iberian Chain, CCR	Ebro	22.5	10.0	Gaspar-Escribano et al. (2001) and Zoetemeijer et al. (1990)
W European Platform	Pyrenees	Aquitaine	25.5	5.0	Brunet (1986)
W European Platform	W Alps	North Alpine	25.0	15.0	Gutscher (1995), Macario et al. (1995), Stewart and Watts (1997), Ford et al. (1999), and Karner and Watts (1983)
W European Platform	E Alps	North Alpine	35.0	12.0	Gutscher (1995), Steward and Watts (1997), and Karner and Watts (1983)
Adriatic N	Alps/Apennines	Po west	20.0	5.0	Carrapa and Garcia-Castellanos (2005) and Kroon (2002)
Adriatic N	Alps/Apennines	Po east	10.0	8.0	Tang et al. (1992), Kroon (2002), and Barbieri et al. (2004)
Adriatic N	Apennines	Adriatic	28.0	3.0	Kroon (2002)
Adriatic center	Apennines	Adriatic	6.5	3.5	Kroon (2002)
Adriatic	Apennines/Dinarides	Apennine–Dinaridic	14.0	10.0	Royden (1988a,b) and Kruse and Royden (1994)
Adriatic S	Apennines		28.0	3.0	Kroon (2002)
Adriatic S	Calabria–Hellenides/Sicily		11.0	8.0	Cogan et al. (1989) and Moretti and Royden (1988)
Moesian Platform	S Carpathian	Getic Depression	11.0	2.0	Matenco et al. (1997a,b)
E European Platform	SE Carpathian	E Carpathian	12.0	5.0	Matenco et al. (1997a,b) and Steward and Watts (1997)
E European Platform	Carpathian		35.0	10.0	Royden and Karner (1984), Roure et al. (1993), and Raileanu et al. (1993)
E European Platform	NE Carpathian	E Carpathian	18.0	7.0	Matenco et al. (1997a,b), and Oszczypko et al. (2005)
E European Platform	NW Carpathian	W Carpathian	12.0	4.0	Oszczypko et al. (2005)
E European Platform	E Caucasus	N Caucasian	55.0	15.0	Ruppel and McNutt (1987) and Ershov et al. (1999)
E European Platform	W Caucasus	N Caucasian	70.0	15.0	Ruppel and McNutt (1987) and Ershov et al. (1999)
E European Platform	Urals		75.0	25.0	Kruse and McNutt (1988)
E European Platform	Urals		120.0	20.0	Piwowar and LeDrew (1996)
Scandinavia	Caledonian	Caledonian	87.0	20.0	Samuelsson and Middleton (1999)
Scandinavia	Caledonian	Caledonian	39.0	31.0	Poudjom-Djomani et al. (1999)
Mongolia, central			7.0	3.0	Bayasgalan et al. (2005)
Mongolia, south	Gobi-Altai		15.0	5.0	Bayasgalan et al. (2005)
Mongolia, west			40.0	10.0	Bayasgalan et al. (2005)
Siberian Platform	Verkhoyansk	Verkhoyansk	50.0	10.0	McNutt and Kogan (1987) and McNutt et al. (1988)
Arabian Shield	Zagros		50.0	25.0	Snyder and Barazangi (1986)
Arabian Shield	Oman mountain	N Oman	13.0	3.0	Ravaut et al. (1993)
Turkmenistan–Iran	Kopet Dag	Trans-Caspian	25.0	5.0	Artemjev et al. (1994)
Asia	Karakoram		121.0	10.0	Caporali (1995)
Tarim S	Kunlun	Tarim	44.0	25.0	Lyon-Caen and Molnar (1984), Fan and Ma (1990), and Teng (1991)
Tarim N	Tian Shan	Tarim	53.0	20.0	McNutt and Kogan (1987), McNutt et al. (1988), and Liu et al. (2006)
Dzungarian		Junggar	12.5	12.5	Burov et al. (1990), Burov and Kogan (1990)
Tadjik depression	Pamirs		15.0	5.0	McNutt et al. (1988)
China	Indosinian orogeny	Longmenshan	48.0	5.0	Yong et al. (2003)

(*Continued*)

Table 1 (Continued)

Plate	*Load/orogen*	*Basin*	*EET (km)*	*Error ± (km)*	*Source*
Indian shield	Karakoram		99.0	10.0	Caporali (1995)
Indian shield	Himalayas E	Ganges	90.0	15.0	Karner and Watts (1983), Lyon-Caen and Molnar (1985), and Royden (1993)
Indian shield	Himalayas W	Ganges	34.0	6.0	Karner and Watts (1983), Lyon-Caen and Molnar (1985), and Royden (1993)
Indian shield	Himalayas	Ganges	25.0	5.0	Hetényi et al. (2006)
Taiwan W	Taiwan	W Taiwan	15.0	6.5	Grotzinger and Royden (1990) and Lin and Watts (2002)
Papua New Guinea E			20.0	10.0	Haddad and Watts (1999)
Papua New Guinea W			75.0	10.0	Haddad and Watts (1999)
New Zealand		Wanganui	17.0	8.0	Holt and Stern (1991) and Stern et al. (1993)
E Australia	New Zealand (S Island)		22.5	12.5	Stern (1995)
N Australia	Banda Arc (Timor)		79.1	10.0	Londoño and Lorenzo (2004) and Tandon et al. (2000)
NW Australia	Banda Arc (Timor)		55.0	25.0	Lorenzo et al. (1998)
East Antarctic			62.0	37.0	Bott and Stern (1992)
S Am. Platform	Burdwood Bank	South Falkland	13.0	7.0	Bry et al. (2004)
S Am. Platform (Arg.)	E Andes? Volcanic?		14.0		Bahlburg and Furlong (1996)
S Am. Platform (Arg.)	Andes	Ordovician Puna	14.0		Bahlburg and Furlong (1996)
S Am. Platform (Arg.)	Andes	Puna 22,24 N	20.0		Prezzi (1999)
S Am. Platform (Bolivia)	Andes	Chaco	30.5	0.5	Coudert et al. (1995)
S Am. Platform (Peru)	Andes		40.0	15.0	Fan et al. (1996)
S Am. Platform (Ecuador)	Andes		25.0	20.0	Stewart and Watts (1997)
S Am. Platform (Colombia)	Andes	Llanos	70.0		Cardozo (1997)
S California	Transverse Ranges N		50.0	5.0	Sheffels and McNutt (1986)
S California	Transverse Ranges S		10.0	5.0	Sheffels and McNutt (1986)
N Am. Platform	Appalachians		105.0	25.0	Karner and Watts (1983), Hinze and Braile (1988), and Rankin et al. (1991)
N Am. Platform	Appalachians		70.0	15.0	Steward and Watts (1997)
N Am. Platform	Rocky Mountains (Paleozoic and Ancestral)	Pennsylvanian–Permian Paradox	25.0		Barbeau (2003)
N Am. Platform W		Idaho Wyoming	22.0		Jordan (1981)
N Am. Platform NW	Arctic Alaska	Colville	65.0	5.0	Nunn et al. (1987)

Reproduced from Garcia-Castellanos D and Cloetingh S (2012) Modeling the interaction between lithospheric and surface processes in foreland basins. In: Busby C and Azor A (eds.) *Tectonics of Sedimentary Basins: Recent Advances*, pp. 152–181.

the weakening induced by the geothermal gradient. This can lead to two weak zones, capable of mechanically decoupling the upper crust, the lower crust, and the lithospheric mantle. Burov and Diament (1992, 1995) provided a formulation to capture the dependence of EET on the degree of coupling between these layers and on inelastic (plastic) failure during plate bending. For a lithosphere behaving as three completely welded elastic plates, the EET (T_e) would be the addition of the individual thicknesses:

$$T_e = h_{UC} + h_{LC} + h_{ML}$$

where h_{UC}, h_{LC}, and h_{ML} are the mechanical thicknesses of the upper crust, lower crust, and mantle–lithosphere, respectively. If these three layers are completely decoupled, then

$$T_e = \sqrt[3]{h_{UC}^3 + h_{LC}^3 + h_{ML}^3}$$

The EET bands for the mechanically strong upper crust and upper lithospheric mantle (**Figure 6**) describe the integrated EET of the lithosphere that has a bearing on its response to loads imposed on it. The degree of coupling and/or decoupling between these two mechanically strong layers and the scatter of data points reflects to a large extent the importance of mechanical weakening of the lower crust by tectonic stresses (Cloetingh and Burov, 1996). Burov and Diament (1995) showed that a rheological model in which a weak lower crust is sandwiched between a strong brittle–elastic upper crust and an elastic–ductile mantle ('jelly sandwich' model; Jackson, 2002) accounts for the wide range of lithospheric T_e values

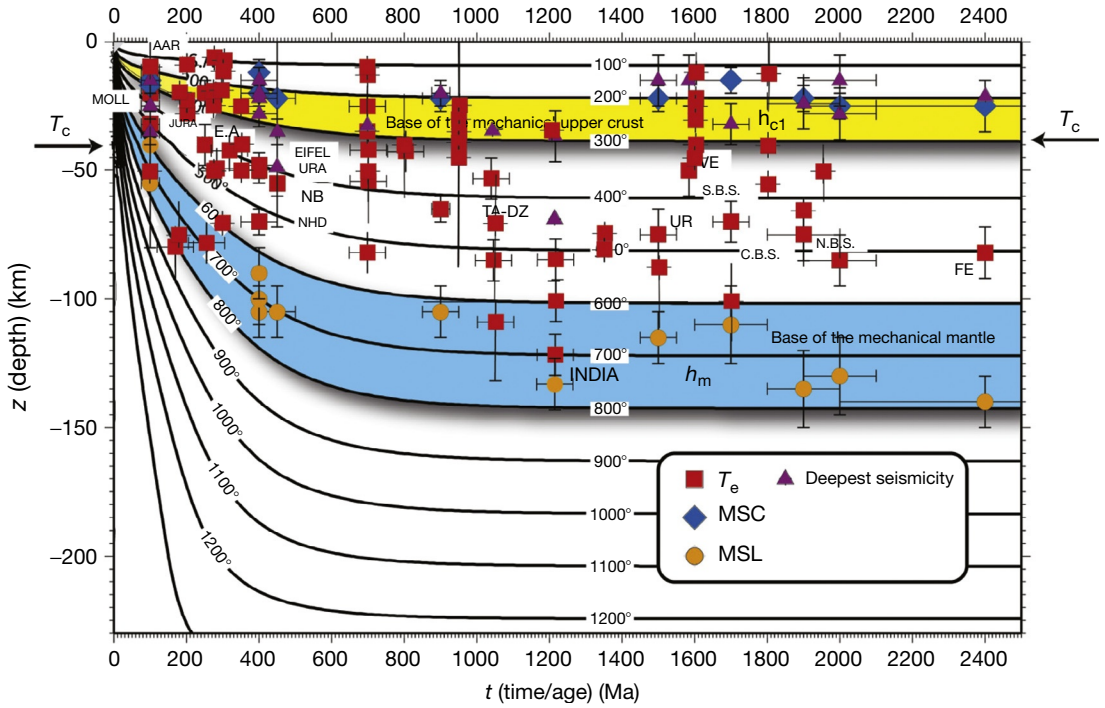

Figure 6 Compilation of observed and predicted values of effective elastic thickness (T_e, EET), depth to bottom of mechanically strong crust (MSC), and depth to bottom of mechanically strong lithospheric mantle (MSL) plotted against the age of the continental lithosphere at the time of loading and comparison with predictions from thermal models of the lithosphere. Labeled contours are isotherms. Isotherms marked by 'solid lines' are for models that account for additional radiogenic heat production in the upper crust. 'Dashed lines' correspond to pure cooling models for continental lithosphere. The equilibrium thermal thickness of the continental lithosphere is 250 km. 'Shaded bands' correspond to depth intervals marking the base of the mechanical crust (MSC) and the mantle portion of the lithosphere (MSL). 'Squares' correspond to EET estimates, 'circles' indicate MSL estimates, and 'diamonds' correspond to estimates of MSC. 'Bold letters' correspond to directly estimated EET values derived from flexural studies on, for example, foreland basins. 'Thinner letters' indicate indirect rheological estimates derived from extrapolation of rock-mechanics studies. The dataset includes (I): old thermomechanical ages (1000–2500 Ma): northernmost (N.B.S.), central (C.B.S.), and southernmost Baltic Shield (S.B.S.); Fennoscandia (FE); Verkhoyansk plate (VE); Urals (UR); Carpathians; Caucasus, (II): intermediate thermomechanical ages (500–1000 Ma): North Baikal (NB); Tarim and Dzungaria (TA-DZ); Variscan of Europe: URA, NHD, EIFEL; and (III): younger thermomechanical ages (0–500 Ma): Alpine belt: JURA, MOLL (Molasse), AAR; southern Alps (SA) and Eastern Alps (EA); Ebro basin; Betic rifted margin; Betic Cordilleras. Reproduced from Cloetingh S, Burov E, Matenco L, Beekman F, Roure F, and Ziegler PA (2013) The Moho in extensional tectonic settings: Insights from thermo-mechanical models. *Tectonophysics* 609: 558–604.

observed due to wide variations in crustal thickness and composition and geothermal gradients. At the same time, it was realized that rheological decoupling of the upper crust and lithospheric mantle also plays an important role in the structural style of intraplate compressional deformations (e.g., Rocky Mountains and Bohemian Massif; Ziegler et al., 1995, 2002).

Rheological decoupling of the crust and mantle parts of the lithosphere can contribute to the spread in EET values (Figure 6). However, a precise interpretation of continental EET is not trivial in the absence of a simple method to estimate an a priori EET based on regional parameters such as plate age and/or load age (Watts, 2001). At the same time, forward modeling of integrated lithospheric strength based on an integration of available constraints on lithospheric structure, thermal regime, and composition has provided a quantitative framework for present-day lithospheric strength on a continental scale (e.g., Cloetingh et al., 2005a,b; Tesauro et al., 2009a). Such an approach has demonstrated strong lateral heterogeneity in EETs in Europe (Figure 7), with low values in the Cenozoic rifts and relatively high values eastward of the Trans-European Suture Zone (see also Perez-Gussinyé and Watts, 2005).

Recently, the first global EET distributions have been published based on both admittance study approaches (Audet and Burgmann, 2011) and forward modeling of rheology (Tesauro et al., 2012a, 2013). A subsequent comparison of rheological and inverse approaches has demonstrated the existence of fairly robust spatial patterns in strength, with high values of EET associated with cratons and relatively low values of EET associated with rifts and convergence zones (Tesauro et al., 2009b, 2012a,b).

Sedimentary basins and continental topography are intrinsically coupled. This is the case not only in terms of the transfer of sediments from their source areas to the basins but also in terms of the support of surface loads by the underlying lithosphere. In discussions on the nature of controls on dynamic topography (e.g., Moucha and Forte, 2011), the role of spatial variations in structure and mechanical properties of the lithosphere (e.g., Tesauro et al., 2012a,b) is not always recognized. Constraints on upper mantle and crustal structure are of paramount importance in deciphering dynamic topography

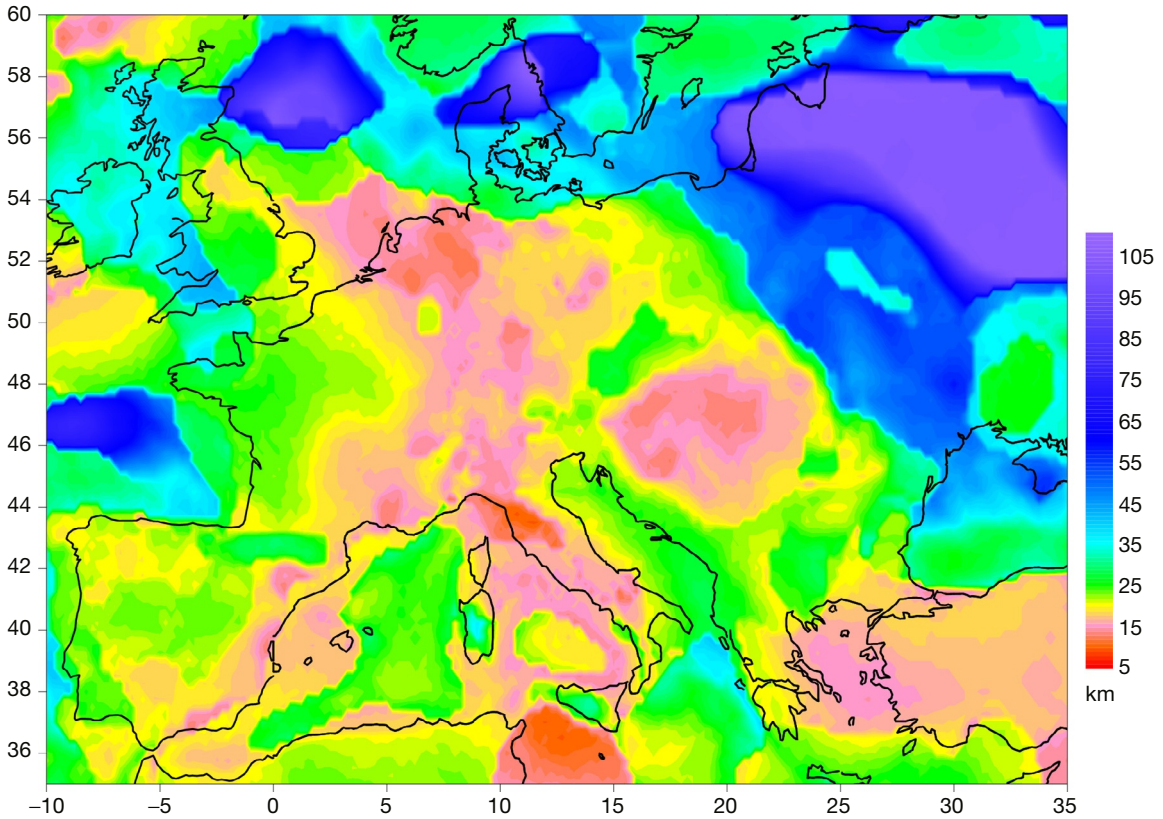

Figure 7 Effective elastic thickness (T_e) distribution of the European lithosphere derived from integrated strength of the lithosphere (km). Reproduced from Tesauro M, Kaban MK, and Cloetingh SAPL (2009) How rigid is Europe's lithosphere? *Geophysical Research Letters* 36: L16303.

attributed to mantle convective processes (Boschi et al., 2010). These authors predict for the Mediterranean area patterns in residual topography inferred from mantle flow (Faccenna and Becker, 2010) characterized by overall uplift of Iberia and overall subsidence in the eastern Mediterranean area. In contrast, predictions for basins in western Mediterranean area and Anatolia show striking differences dependent on the assumed crustal models (**Figure 8**). Availability of reliable crustal models is also crucial in separating the static isostatic and dynamic components of the topographic signal (Flament et al., 2013). This shows the need for more detailed models for crustal and upper mantle structures in the assessment of the relative contribution of mantle convection to regional-scale topography and the evolution of long-wavelength vertical motions in sedimentary basin systems.

6.12.3 Extensional Basin Systems

Tectonically active rifts, paleorifts, and passive margins form a group of genetically related extensional basins that play an important role in the spectrum of sedimentary basin types (Bally and Snelson, 1980; Buck, 2007; Ziegler and Cloetingh, 2004; see also **Chapter 6.08**). Extensional basins cover large areas of the globe and contain important mineral deposits and energy resources, including geothermal energy (e.g., Cloetingh et al., 2010; Lenkey et al., 2002). A large number of major hydrocarbon provinces are associated with rifts (e.g., North Sea, Sirte, and West Siberian basins and Dnieper–Donets and Gulf of Suez grabens) and passive margins (e.g., Campos Basin; Gabon, Angola, mid-Norway, and NW Australian shelves; and Niger and Mississippi Deltas; Ziegler, 1996). On these basins, the petroleum industry has acquired large databases that document their structural styles and allow detailed reconstruction of their evolution. Academic research programs have provided information on the crustal and lithospheric configuration of tectonically active rifts, paleorifts, and passive margins (e.g., Abadi et al., 2008; Beglinger et al., 2012a,b,c,d; Corver et al., 2009, 2011; Dupré et al., 2007, 2011). Petrologic and geochemical studies have advanced the understanding of rift-related magmatic processes. Numerical models, based on geophysical and geologic data, have contributed at lithospheric and crustal scales toward the understanding of dynamic processes that govern the evolution of rifted basins. In the succeeding text, we summarize basic concepts on dynamic processes that control the evolution of extensional basins.

A natural distinction can be made between tectonically active and inactive rifts and rifts that evolved in continental and oceanic lithosphere. Tectonically active intracontinental (intraplate) rifts, such as the Rhine Graben, the East African Rift, the Baikal rift, and the Shanxi Rift of China, correspond to important earthquake and volcanic hazard zones.

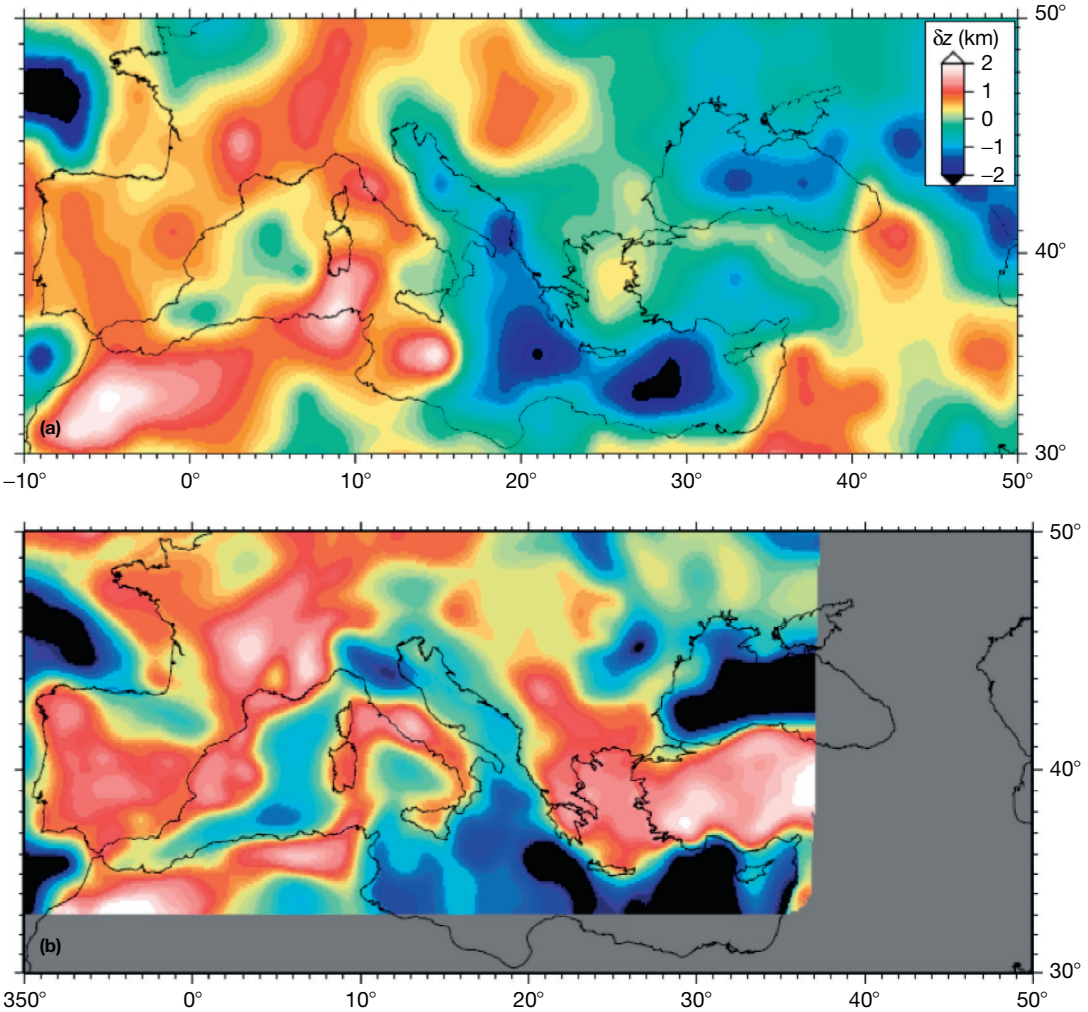

Figure 8 (a) Residual topography after correcting for isostatic adjustment based on the crustal model CRUST 2.0 (Bassin, 2000). (b) Same as (a), isostatic adjustment computed from EuCRUST-07 (Tesauro et al., 2008), with density values taken, again from CRUST 2.0. Reproduced from Boschi L, Faccenna C and Becker TW (2010) Mantle structure and dynamic topography in the Mediterranean Basin. *Geophysical Research Letters* 37: L20303.

The globe-encircling mid-ocean ridge system forms an immense intraoceanic active rift system that encroaches onto continents in the Red Sea and the Gulf of California. Rifts that are tectonically no longer active are referred to as paleorifts, aulacogens, inactive or aborted rifts, and failed arms, in the sense that they did not progress to crustal separation. Conversely, the evolution of successful rifts culminated in the breakup of continents, the opening of new oceanic basins, and the development of conjugate pairs of passive margins.

In the past, a genetic distinction was made between 'active' rifting and 'passive' rifting (Olsen and Morgan, 1995; Sengör and Burke, 1978). 'Active' rifts are thought to evolve in response to thermal upwelling of the asthenosphere (Bott and Kusznir, 1979; Dewey and Burke, 1974), whereas 'passive' rifts develop in response to lithospheric extension driven by far-field stresses (McKenzie, 1978). It is, however, questionable whether such a distinction is justified as the study of Phanerozoic rifts revealed that rift-related volcanic activity and doming of rift zones are basically a consequence of lithospheric extension and are not the main driving force of rifting. The fact that rifts can become tectonically inactive at all stages of their evolution, even if they have progressed to the Red Sea stage of limited seafloor spreading (e.g., Bay of Biscay–Pyrenean rift), supports this concept. However, as extrusion of large volumes of rift-related subalkaline tholeiites must be related to a thermal anomaly within the upper mantle, a distinction between 'active' rifting and 'passive' rifting is to a certain degree still valid, though not as 'black and white' as originally envisaged.

Rifting activity preceding the breakup of continents is probably governed by forces controlling the movement and interaction of lithospheric plates. These forces include plate boundary stresses, such as slab pull, slab rollback, ridge push, and collisional resistance, and frictional forces exerted by the convecting mantle on the base of the lithosphere (Bott, 1993; Forsyth and Uyeda, 1975; Wessel and Müller, 2007; Ziegler, 1993a,b; see also **Chapter 6.02**). On the other hand, deviatoric tensional stresses, inherent to the thickened lithosphere of young orogenic belts, as well as those developing in the lithosphere above upwelling mantle convection cells and mantle plumes (Bott, 1993), do not appear to cause, on their own, the

breakup of continents. However, if such stresses interfere constructively with plate boundary and/or mantle drag stresses, the yield strength of the lithosphere may be exceeded, thus inducing rifting (Figure 9).

It must be understood that mantle drag forces are exerted on the base of a lithospheric plate if its velocity and direction of movement differ from the velocity and direction of the mantle flow. Mantle drag can constructively or destructively interfere with plate boundary forces and thus can either contribute toward plate motion or resist it. Correspondingly, mantle drag can give rise to the buildup of extensional as well as compressional intraplate stresses (Artemieva and Mooney, 2002; Bott, 1993; Forsyth and Uyeda, 1975; Warners-Ruckstuhl et al., 2012). Although the present lithospheric stress field can be readily explained in terms of plate boundary forces (Cloetingh and Wortel, 1986; Richardson, 1992; Zoback, 1992), mantle drag probably contributed significantly to the Triassic–Early Cretaceous breakup of Pangaea, during which Africa remained nearly stationary and straddled an evolving upwelling and radial outflowing mantle convection cell (Pavoni, 1993; Ziegler, 1993a,b; Ziegler et al., 2001).

Mechanical stretching of the lithosphere and thermal attenuation of the lithospheric mantle are associated with the development of local deviatoric tensional stresses, which play an increasingly important role during advanced rifting stages (Bott, 1992; Ziegler, 1993a,b). This has led to the development

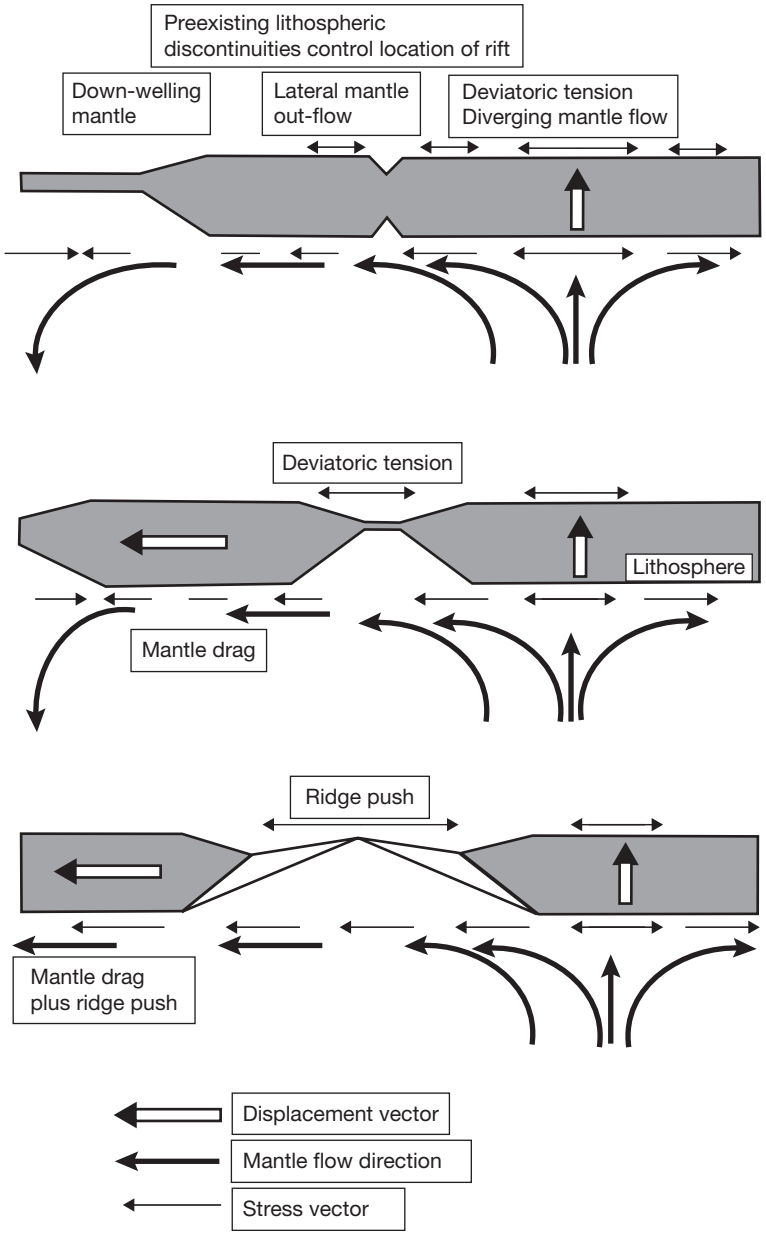

Figure 9 Diagram illustrating the interaction of shear traction exerted on the base of the lithosphere by asthenospheric flow, deviatoric tension above upwelling mantle convection cells, and ridge push forces. Reproduced from Ziegler PA, Cloetingh S, Guiraud R, and Stampfli GM (2001) Peri-Tethyan platforms: Constraints on dynamics of rifting and basin inversion. *Mémoires du Muséum national d'histoire naturelle* 186: 9–49.

of the concept that many rifts go through an evolutionary cycle starting with an initial 'passive' phase that is followed by a more 'active' stage during which magmatic processes play an increasingly important role (Burov and Cloetingh, 1997; Huismans et al., 2001a; Wilson, 1993a).

6.12.3.1 Modes of Rifting and Extension

6.12.3.1.1 Atlantic-type rifts

Atlantic-type rift systems evolve during the breakup of major continental masses, presumably in conjunction with a reorganization of the mantle convection system (Ziegler, 1993a,b). During early phases of rifting, large areas around future zones of crustal separation can be affected by tensional stresses, giving rise to the development of complex graben systems. In time, rifting activity concentrates on the zone of future crustal separation, with tectonic activity decreasing and ultimately ceasing in lateral graben systems. In time and as a consequence of progressive lithospheric attenuation and ensuing crustal doming, local deviatoric tensional stresses play an important secondary role in the evolution of such rift systems. Upon crustal separation, the diverging continental margins (pericontinental rifts) and the 'unsuccessful' intracontinental branches of the respective rift system become tectonically inactive. However, during subsequent tectonic cycles, such aborted rifts can be tensional and compressional-reactivated (Cloetingh et al., 2008; Johnson et al., 2008; Ziegler et al., 1995, 1998, 2001, 2002). The development of Atlantic-type rifts is subject to great variations mainly in terms of duration of their rifting stage and the level of volcanic activity (Ziegler, 1988, 1990a, 1996a).

6.12.3.1.2 Back-arc rifts

Back-arc rifts are thought to evolve in response to a decrease in convergence rates and/or even a temporary divergence of colliding plates, ensuing steepening of the subduction slab and development of a secondary upwelling system in the upper plate mantle wedge above the subducted lower plate lithospheric slab (Uyeda and McCabe, 1983). Changes in convergence rates between colliding plates are probably an expression of changes in plate interaction. Back-arc rifting can progress to crustal separation and the opening of limited oceanic basins (e.g., Sea of Japan, South China Sea, and Black Sea). However, as convergence rates of colliding plates are variable in time, back-arc extensional basins are generally short-lived. Upon a renewed increase in convergence rates, back-arc extensional systems are prone to destruction by back-arc compressional stresses (e.g., Variscan Rhenohercynian Basin, Sunda Arc and East China rift systems, and Black Sea domain; Cloetingh et al., 1989; Jolivet et al., 1989; Letouzey et al., 1990; Nikishin et al., 2001; Uyeda and McCabe, 1983; Ziegler, 1990a).

6.12.3.1.3 Synorogenic rifting and wrenching

Synorogenic rift/wrench deformations can be related to indenter effects and ensuing escape tectonics, often involving rotation of intramontane stable blocks (e.g., Pannonian Basin: Royden and Horváth, 1988; Late Carboniferous Variscan fold belt: Ziegler, 1990b), and to lithospheric overthickening in orogenic belts, resulting in uplift and extension of their axial parts (Peruvian and Bolivian Altiplano: Dalmayrac and Molnar, 1981; Mercier et al., 1992). Furthermore, collisional stresses exerted on a craton may cause far-field tensional or transtensional reactivation of preexisting fracture systems and thus the development of rifts and pull-apart basins. This model may apply to the Late Carboniferous development of the Norwegian–Greenland Sea rift in the foreland of the Variscan orogen, the Permo-Carboniferous Karoo rifts in the hinterland of the Gondwanaland orogen, the European Cenozoic Rift System in the Alpine foreland, and the Neogene Baikal rift in the hinterland of the Himalayas (Dèzes et al., 2004; Ziegler et al., 2001). Under special conditions, extensional structures can also develop in fore-arc basins (e.g., Talara Basin, Peru; see Ziegler and Cloetingh, 2004).

6.12.3.1.4 Postorogenic extension

Extensional disruption of young orogenic belts, involving the development of grabens and pull-apart structures, can be related to their postorogenic uplift and the development of deviatoric tensional stresses inherent to orogenically overthickened crust (Dewey, 1988; Sanders et al., 1999; Stockmal et al., 1986). The following mechanisms contribute to postorogenic uplift: (1) locking of the subduction zone due to decay of the regional compressional stress field (Whittaker et al., 1992), (2) rollback and ultimately detachment of the subducted slab from the lithosphere (Andeweg and Cloetingh, 1998; Bott, 1993; Fleitout and Froidevaux, 1982), and (3) retrograde metamorphism of the crustal roots, involving in the presence of fluids the transformation of eclogite to less dense granulite (Le Pichon et al., 1997; Straume and Austrheim, 1999). Although tensional collapse of an orogen can commence shortly after its consolidation, for example, the Variscan orogen (Ziegler, 1990a; Ziegler et al., 2004), it may be delayed by as much as 30 My, as in the case of the Appalachian–Mauritanides (Ziegler, 1990a). The Permo-Triassic West Siberian basin that is superimposed on the juncture of the Uralides and Altaides is in an example of a postorogenic tensional basin that began to subside shortly after the consolidation of these orogens (Nikishin et al., 2002; Vyssotski et al., 2006). In addition, modifications in the convergence direction of colliding continents and the underlying stress reorientation can give rise to the development of wrench fault systems and related pull-apart basins, controlling early collapse of an orogen, such as the Devonian collapse of the Arctic–North Atlantic Caledonides (Ziegler, 1989b; Ziegler and Dèzes, 2006) or the Stephanian–early Permian disruption of the Variscan fold belt (Ziegler et al., 2004).

The Basin and Range Province of North America is a special type of postorogenic rifting. Oligocene and younger collapse of the US Cordillera is thought to be an effect of the North American craton having overridden at about 28 Ma the East Pacific Rise in conjunction with rapid opening of the Atlantic Ocean (Verrall, 1989). In the area of the southwestern US Cordillera, regional compression waned during the late Eocene and the orogen began to collapse during late Oligocene with main extension occurring during the Miocene and Pliocene (Parsons, 1995). By contrast, the Canadian Cordillera remained intact. During the collapse of the US Cordillera, the heavily intruded, at middle and lower levels, ductile crust of the Basin and Range Province was subjected to major extension at high strain rates, resulting in uplift of ductilely deformed core complexes by 10–20 km. The area affected by extension, crustal thinning, volcanism, and uplift measures 1500×1500 km

(Wernicke, 1990). The Eocene–Oligocene magmatism of the Basin and Range Province bears a subduction-related signature, suggestive of an initial phase of back-arc extension, whereas lithospheric mantle- and asthenosphere-derived magmas play an increasingly important role from Miocene times onward, presumably due to the opening of asthenospheric windows in the Farallon slab during its detachment from the lithosphere and gradual sinking into the mantle (Parsons, 2006).

6.12.3.2 Thermal Thinning and Stretching of the Lithosphere

Mechanical stretching of the lithosphere, triggering partial melting of its basal parts and the upper asthenosphere, is followed by the segregation of melts and their diapiric rise into the lithosphere, an increase in conductive and advective heat flux, and consequently an upward displacement of the thermal asthenosphere–lithosphere boundary. Small-scale convection in the evolving asthenospheric diapir may contribute to mechanical thinning of the lithosphere by facilitating lateral ductile mass transfer (**Figure 10**; Mareschal and Gliko, 1991; Richter and McKenzie, 1978). Progressive thermal and mechanical thinning of the higher-density lithospheric mantle and its replacement by lower-density asthenosphere induces progressive doming of rift zones. At the same time, deviatoric tensional stresses developing in the lithosphere contribute to its further extension (Bott, 1992).

Although major hot-spot activity is thought to be related to a thermal perturbation within the asthenosphere caused by a deep mantle plume, smaller-scale 'plume' activity may also be the consequence of lithospheric stretching triggering partial melting by adiabatic decompression in areas characterized by an anomalously volatile-rich asthenosphere/lithosphere (Wilson, 1993a; White and McKenzie, 1989). In this context, it is noteworthy that extension-induced development of a partially molten asthenospheric diapir that gradually rises into the lithosphere causes by itself further decompression of the underlying asthenosphere and consequently more extensive partial melting and melt segregation at progressively deeper levels. Thus, the evolving diapir may grow not only upward but also downward. Similarly, acceleration of plate divergence and the ensuing increase in seafloor spreading rates probably cause at spreading axes partial melting and melt segregation at progressively deeper asthenospheric levels reaching down to 80–100 km, as imaged by seismic tomography (Anderson et al., 1992).

Melts, which intrude the lithosphere and pond at the crust/mantle boundary, provide a further mechanism for thermal doming of rift zones (**Figure 10**). Emplacement of such asthenoliths, consisting of a mixture of indigenous subcrustal

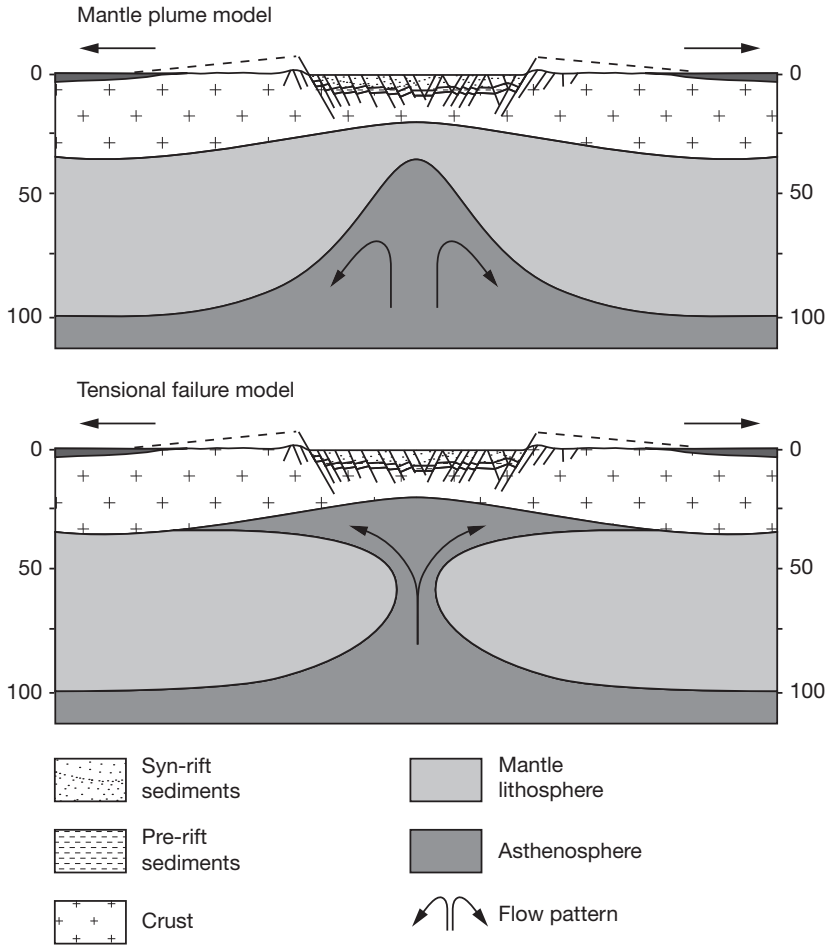

Figure 10 Rift models.

mantle material and melts extracted from deeper lithospheric and upper asthenospheric levels, may cause temporary doming of a rift zone and a reversal in its subsidence pattern, such as the Mid-Jurassic central North Sea arch (Ziegler, 1990a) or the Neogene Baikal arch (Suvorov et al., 2002).

Volcanic-rifted margins cannot always be linked directly to hot-spot areas. Different rifts show a wide range in lag time between rifting and the impingement of plumes on zones of crustal extension (Franke, 2013): nearly synchronous in the South Atlantic and Labrador Sea, while with a lag of 15 My in the Central Atlantic, 70 My in the Indian Ocean, and as long 280 My of intermittent crustal extension in the Norwegian–Greenland Sea (Nikishin et al., 2002; Ziegler and Cloetingh, 2004). Ziegler and Cloetingh (2004) concluded that initial magma generation in intracontinental rifts generally occurs in the 100–200 km depth range, corresponding to the lower parts of the lithosphere and the upper asthenosphere (Wilson, 1997). Moreover, several observations are difficult to reconcile with a deep mantle origin of the melts (Franke, 2013). Gradual changes of mantle properties and dynamics should generate a smooth transition from magma-starved to volcanic rifting over at least a hundred or a few hundreds of kilometers. However, observations of abrupt change in emplaced magmatic volume argue against the hypothesis that gradual along-margin variations in the thermal regime of the lithosphere and sublithospheric mantle (the traditional plume-driven model) are solely responsible for the formation of volcanic-rifted margins (Franke, 2013).

Depending on the applicability of the 'pure shear' (McKenzie, 1978) or the 'simple shear' model (Wernicke, 1985), or a combination thereof (Kusznir et al., 1991), the zone of upper crustal extension, corresponding to the subsiding rift, may coincide with the zone of lithospheric mantle attenuation (pure shear and combined shear) or may be laterally offset from it (simple shear; see **Figure 11**). Under conditions of pure

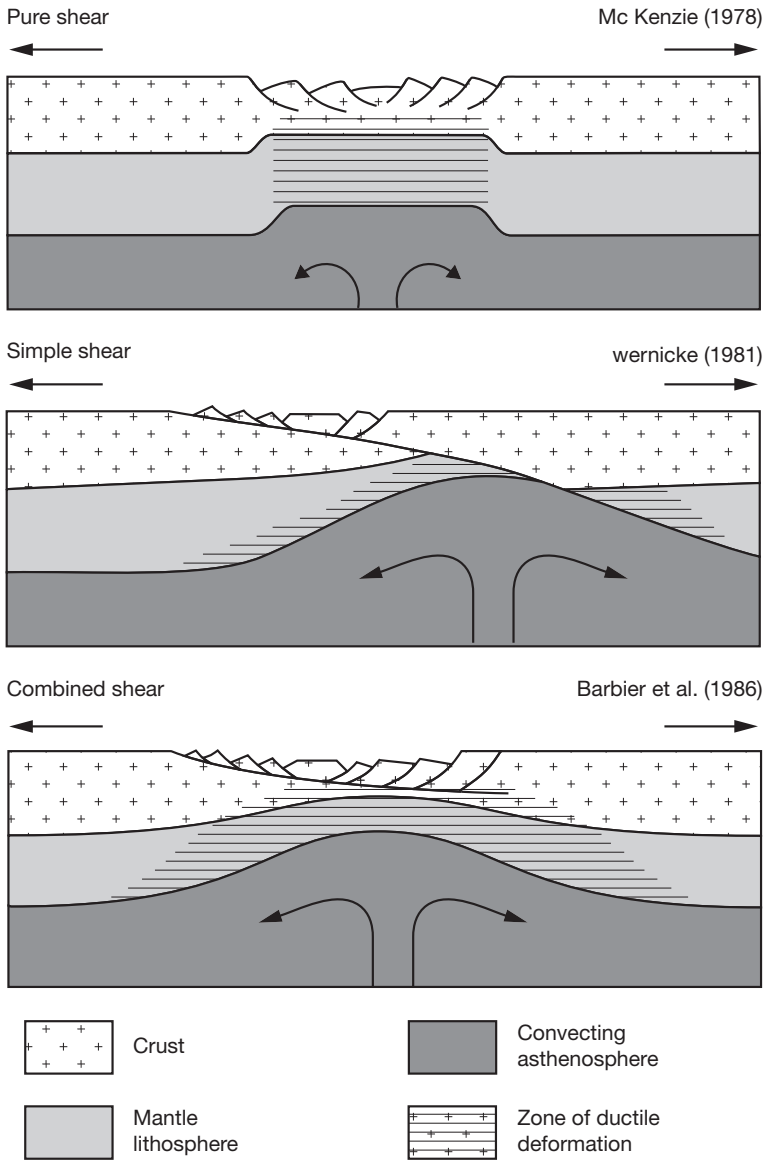

Figure 11 Lithospheric shear models.

shear lithospheric extension, magmatic activity should be centered on the rift axis where in time also mid-oceanic ridge basalt (MORB)-type magmas can be extruded after a high degree of extension has been achieved. By contrast, under simple shear conditions, magmatic activity is asymmetrically distributed with respect to the rift axis, and MORB-type extrusives may occur on one of the rift flanks (e.g., the Basin and Range Province (Jones et al., 1992), the Red Sea (Favre and Stampfli, 1992), and the Ethiopian Rift (Kazmin, 1991)).

A modification to the pure shear model is the 'continuous depth-dependent' stretching model that assumes that stretching of the lithospheric mantle affects a broader area than the zone of crustal extension (**Figure 12**; Rowley and Sahagian, 1986). In both models, it is assumed that the asthenosphere wells up passively into the space created by mechanical attenuation of the lithospheric mantle. In depth-dependent stretching models, this commonly gives rise to flexural uplift of the rift shoulders, whereas in the flexural cantilever model, which assumes ductile deformation of the lower crust, this produces footwall uplift of the rift flanks and intrabasin fault blocks (Kusznir and Ziegler, 1992). By the same mechanism, the simple shear model predicts asymmetrical doming of a rift zone or even flexural uplift of an arch located to one side of the zone of upper crustal extension (Wernicke, 1985). A modification to the simple shear model envisages that massive upper crustal extensional unloading of the lithosphere causes its isostatic uplift and passive inflow of the asthenosphere (Wernicke, 1990).

The structural style of rifts, as defined at upper crustal and synrift sedimentary levels, is influenced by the thickness and thermal state of the crust and lithospheric mantle at the onset of rifting, by the amount of crustal extension and the width over which it is distributed, the mode of crustal extension (orthogonal or oblique and simple shear or pure shear), and the lithologic composition of the pre- and synrift sediments (Cloetingh et al., 1995b; Ziegler, 1996a).

A major factor controlling the structural style of a rift zone is the magnitude of the crustal extensional strain that was achieved across it and the distance over which it is distributed (δ factor). Although quantification of the extensional strain and of the stretching factor δ is of basic importance for the understanding of rifting processes, there is often a considerable discrepancy between estimates derived from upper crustal extension by faulting, the crustal configuration, and quantitative subsidence analysis (Ziegler and Cloetingh, 2004).

6.12.3.3 Synrift Subsidence and Duration of Rifting Stage

The balance of two mechanisms controls the synrift subsidence of a sedimentary basin. Firstly, elastic/isostatic adjustment of the crust to stretching of the lithosphere and its adjustment to sediment loading causes subsidence of the mechanically thinned crust (**Figures 11** and **12**; Jarvis and McKenzie, 1980; Keen and Boutilier, 1990; McKenzie, 1978). Depending on the depth of the lithospheric necking level, this is accompanied by either flexural uplift or downwarping of the rift zone (**Figure 13**; Braun and Beaumont, 1989; Kooi, 1991; Kooi et al., 1992). Secondly, uplift of a rift zone is caused by upwelling of the asthenosphere into the space created by mechanical stretching of the lithosphere, thermal upward displacement of the asthenosphere–lithosphere boundary, thermal expansion of the lithosphere, and intrusion of melts at the base of the crust (**Figure 10**; Turcotte and Emerman, 1983). Thus, the geometry of a rifted basin is a function of the elastic/isostatic

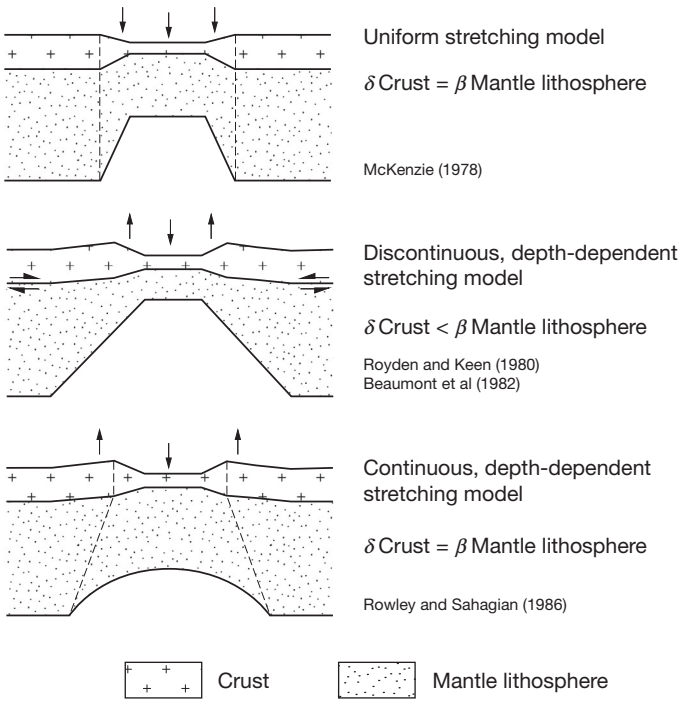

Figure 12 Lithospheric stretching models.

response of the lithosphere to its mechanical stretching and related thermal perturbation (Van der Beek et al., 1994).

The duration of the rifting stage of intracontinental rifts (aborted) and passive margins (successful rifts) is highly variable (Figures 14 and 15; Ziegler, 1990a; Ziegler and Cloetingh, 2004; Ziegler et al., 2001). Overall, it is observed that in time, rifting activity concentrates on the zone of future crustal separation with lateral rift systems becoming inactive. However, as not all rift systems progress to crustal separation, the duration of their rifting stage is obviously a function of the persistence of the controlling stress field. On the other hand, the time required to achieve crustal separation is a function of the strength (bulk rheology) of the lithosphere, the buildup rate, magnitude and persistence of the extensional stress field, constraints on lateral movements of the diverging blocks (on-trend coherence, counteracting far-field compressional stresses), and apparently not so much of the availability of preexisting crustal discontinuities that can be tensionally reactivated.

Crustal separation was achieved in the Liguro–Provençal Basin after 9 My of crustal extension and in the Gulf of

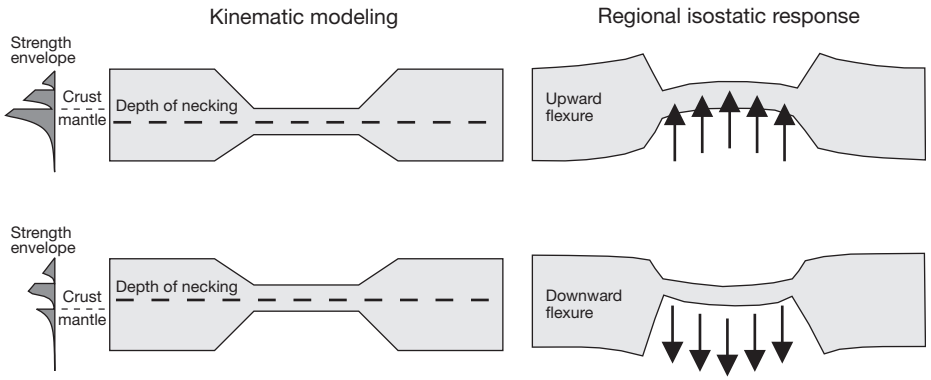

Figure 13 Concept of lithospheric necking. The level of necking is defined as the level of no vertical motions in the absence of isostatic forces. (left) Kinematically induced configuration after rifting for different necking depths. (right) Subsequent flexural isostatic rebound.

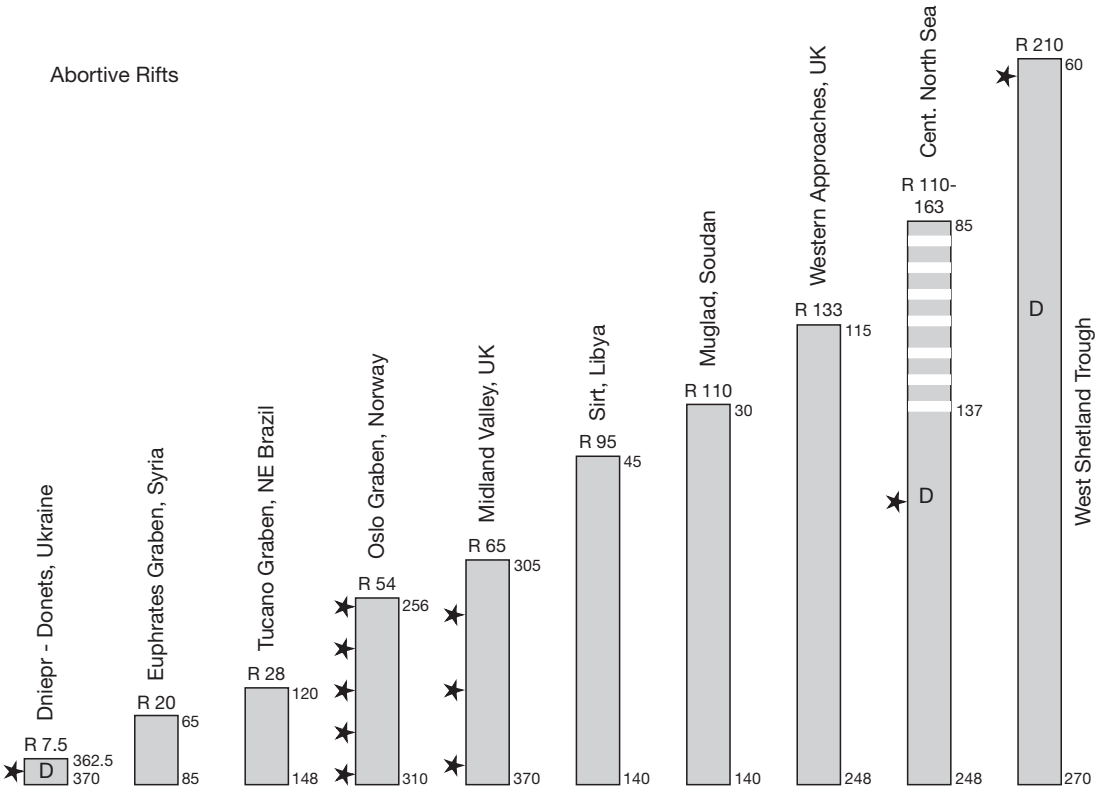

Figure 14 Duration of rifting stage of 'abortive' rifts (paleorifts and failed arms). Vertical columns in My; numbers on side of vertical columns indicate onset and termination of rifting stage in My; numbers under R on top of each column give the duration of rifting stage in My; stars indicate periods of main volcanic activity; D indicates periods of doming. Reproduced from Ziegler PA and Cloetingh S (2004) Dynamic processes controlling evolution of rifted basins. *Earth-Science Reviews* 64: 1–50.

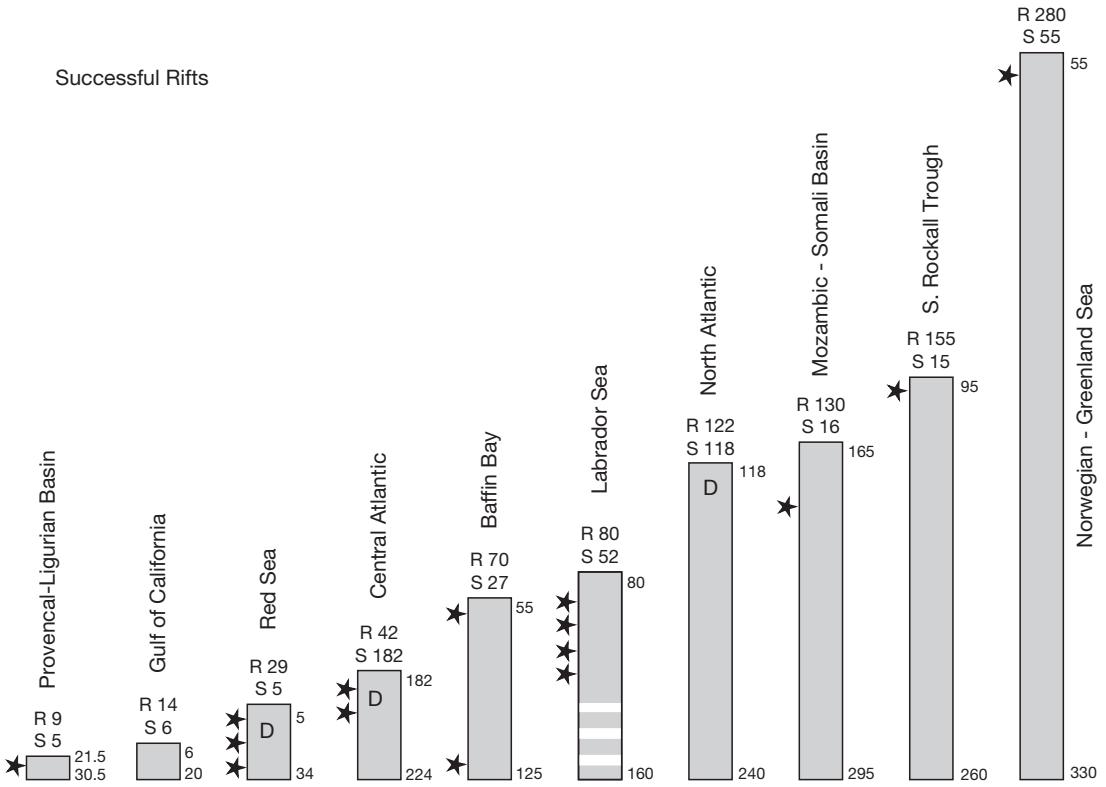

Figure 15 Duration of rifting stage of 'successful' rifts. Legend same as **Figure 14**. Numbers beside letter 'S' indicate duration of seafloor spreading stage in My. Reproduced from Ziegler PA and Cloetingh S (2004) Dynamic processes controlling evolution of rifted basins. *Earth-Science Reviews* 64: 1–50.

California after about 14 My of rifting, whereas opening of the Norwegian–Greenland Sea was preceded by an intermittent rifting history spanning some 280 My (Ziegler, 1988; Ziegler and Cloetingh, 2004). There appears to be no obvious correlation between the duration of the rifting stage (R) of successful rifts (**Figure 15**), which are superimposed on orogenic belts (Liguro–Provençal Basin, Pyrenees $R = 9$ My; Gulf of California, Cordillera $R = 14$ My; Canada Basin, Innuitian fold belt $R = 35$ My; Central Atlantic, Appalachians $R = 42$ My; and Norwegian–Greenland Sea, Caledonides $R = 280$ My), and the duration of those that developed within stabilized cratonic lithosphere (southern South Atlantic $R = 13$; northern South Atlantic $R = 29$ My; Red Sea $R = 29$ My; Baffin Bay $R = 70$ My; and Labrador Sea $R = 80$ My). This suggests that the availability of crustal discontinuities, which regardless of their age (young orogenic belts and old Precambrian shields) can be tensionally reactivated, does not play a major role in the time required to achieve crustal separation. However, by weakening the crust, such discontinuities play a role in the localization and distribution of crustal strain. Moreover, by weakening the lithosphere, they contribute to the preferential tensional reactivation of young and old orogenic belts (Janssen et al., 1995; Ziegler et al., 2001).

6.12.3.4 Postrift Subsidence

Similar to the subsidence of oceanic lithosphere, the postrift subsidence of extensional basins is mainly governed by thermal relaxation and contraction of the lithosphere, resulting in a gradual increase of its flexural strength, and by its isostatic response to sedimentary loading. Theoretical considerations indicate that subsidence of postrift basins follows an asymptotic curve, reflecting the progressive decay of the rift-induced thermal anomaly, the magnitude of which is thought to be directly related to the lithospheric stretching value (Beaumont et al., 1982; McKenzie, 1978; Royden et al., 1980; Sleep, 1973; Steckler and Watts, 1982; Watts et al., 1982). During the postrift evolution of a basin, the thermally destabilized continental lithosphere reequilibrates with the asthenosphere (McKenzie, 1978; Steckler and Watts, 1982; Wilson, 1993b). In this process, in which the temperature regime of the asthenosphere plays an important role, new lithospheric mantle consisting of solidified asthenospheric material is accreted to the attenuated old continental lithospheric mantle (Ziegler et al., 1998). In addition, densification of the continental lithosphere involves crystallization of melts that accumulated at its base or were injected, subsequent thermal contraction of the solidified rocks, and under certain conditions their phase transformation to eclogite facies. The resulting negative buoyancy effect is the primary cause of postrift subsidence.

However, in a number of basins, significant departures from the theoretical thermal subsidence curve are observed. These can in some cases be explained as effects of compressional intraplate stresses and related phase transformations (Cloetingh and Kooi, 1992a,b; Lobkovsky et al., 1996; Van Wees and Cloetingh, 1996). It appears that in many areas,

the postrift evolution is characterized by initial rift-related subsidence, sometimes followed by accelerated subsidence of the central parts of an extensional sedimentary basin, simultaneously occurring with broad uplift in adjacent areas flanking the depocenter. Examples can be found in the Atlantic margin of Morocco (Ghorbal et al., 2008; Gouiza et al., 2010), the southern Atlantic rifted margins (Beglinger et al., 2012a,b,c,d; Dupré et al., 2007, 2011), and the Sirte Basin in Libya (Abadi et al., 2008).

6.12.3.4.1 Shape and magnitude of rift-induced thermal anomalies

The shape and dimension of rift-induced asthenosphere–lithosphere boundary anomalies essentially control the geometry of the evolving postrift thermal sag basin (**Figure 11**). Thermal-sag basins associated with aborted rifts are broadly saucer-shaped and generally overstep the rift zone, with their axes coinciding with the zone of maximum lithospheric attenuation.

Pure shear-dominated rifting gives rise to the classical 'steer's head' configuration of the syn- and postrift basins (White and McKenzie, 1989) in which both basin axes roughly coincide, with the postrift basin broadly overstepping the rift flanks. This geometric relationship between syn- and postrift basins is frequently observed (e.g., North Sea rift: Ziegler, 1990b; West Siberian basin: Artyushkov and Baer, 1990; Dnieper–Donets graben: Kusznir et al., 1996; Stephenson et al., 2001; Gulf of Thailand: Hellinger and Sclater, 1983; Watcharanantakul and Morley, 2000; and Sudan rifts: McHargue et al., 1992). Such a geometric relationship is compatible with discontinuous, depth-dependent stretching models that assume that the zone of crustal extension is narrower than the zone of lithospheric mantle attenuation (**Figure 12**). The degree to which a postrift basin oversteps the margins of the synrift basin is a function of the width difference between the zone of crustal extension and the zone of lithospheric mantle attenuation (White and McKenzie, 1988) and the EET of the lithosphere (Watts et al., 1982).

Conversely, simple shear-dominated rifting gives rise to a lateral offset between the syn- and the postrift basin axes. An example is the Tucano graben of northeastern Brazil, which ceased to subside at the end of the rifting stage, whereas the coastal Jacuipe–Sergipe–Alagoas Basin, to which the former was structurally linked, was the site of crustal and lithospheric mantle thinning culminating in crustal separation and subsequent major postrift subsidence (Chang et al., 1992; Karner et al., 1992). Moreover, the simple shear model can explain the frequently observed asymmetry of conjugate passive margins and differences in their postrift subsidence pattern (e.g., Central Atlantic and Red Sea: Favre and Stampfli, 1992). Discrepancies in the postrift subsidence of conjugate margins are attributed to differences in their lithospheric configuration at the crustal separation stage. At the end of the rifting stage, a relatively thick lithospheric mantle supports lower plate margins, whereas upper plate margins are underlain by a strongly attenuated lithospheric mantle and partly directly by the asthenosphere. Correspondingly, lower plate margins are associated at the crustal separation stage with smaller thermal anomalies than upper plate margins (Stampfli et al., 2001; Ziegler et al., 1998). These differences in lithospheric configuration of conjugate simple shear margins have repercussions on their rheological structure, even after full thermal relaxation of the lithosphere, and their compressional reactivation potential (see succeeding text; Ziegler et al., 1998).

The magnitude of postrift tectonic subsidence of aborted rifts and passive margins is a function of the thermal anomaly that was introduced during their rifting stage and the degree to which the lithospheric mantle was thinned. Most intense anomalies develop during crustal separation, particularly when plume-assisted and asthenospheric melts well up close to the surface. The magnitude of thermal anomalies induced by rifting that did not progress to crustal separation depends on the magnitude of crustal stretching (δ-factor) and lithospheric mantle attenuation (β-factor), the thermal regime of the asthenosphere, the volume of melts generated, and whether these intruded the lithosphere and destabilized the Moho (**Figure 10**).

About 65% (after 60 My) and about 95% (after 180 My) of deep-seated thermal anomalies associated with a major pull-up of the asthenosphere–lithosphere boundary have decayed (mantle plume model; **Figure 10**). Thermal anomalies related to intralithospheric intrusions (tensional-failure model; **Figure 10**) have apparently a faster decay rate. For instance, the Mid-Jurassic North Sea rift dome had subsided below the sea level, 20–30 My after its maximum uplift, that is, well before crustal extension had terminated (Underhill and Partington, 1993; Ziegler, 1990a).

6.12.3.4.2 Stretching factors derived from quantitative subsidence analysis

The thickness of the postrift sedimentary column that can accumulate in passive margin basins and in thermal-sag basins above aborted rifts is a function not only of the magnitude of the lithospheric mantle and crustal attenuation factors β and δ but also of the crustal density and the water depth at the end of their rifting stage, as well as of the density of the infilling postrift sediments (carbonates, evaporites, and clastics). Moreover, it must be kept in mind that during the postrift cooling process, the flexural rigidity of the lithosphere increases gradually, resulting in the distribution of the sedimentary load over progressively wider areas.

Quantitative postrift subsidence analyses of extensional basins, neglecting intraplate stresses, are thought to give a measure of the thermal contraction of the lithosphere and, conversely, of lithospheric stretching factors, as suggested by the McKenzie (1978) model and its early users (e.g., Barton and Wood, 1984; Sclater and Christie, 1980). Such analyses, assuming Airy isostasy, yield often considerably larger δ-factors than indicated by the populations of upper crustal faults (Watcharanantakul and Morley, 2000; Ziegler, 1983, 1990a). This discrepancy is somewhat reduced when flexural isostasy is assumed (Roberts et al., 1993). However, as during rifting attenuation of the lithosphere is achieved not only by its mechanical stretching but also by convective and thermal upward displacement of the asthenosphere–lithosphere boundary, the magnitude of a thermal anomaly derived from the postrift subsidence of a basin cannot be directly related to a mechanical stretching factor. Moreover, intraplate compressional stresses and phase transformations in the lower crust and lithospheric mantle have an overprinting effect on postrift subsidence and can cause significant departures from a purely thermal subsidence curve

(Cloetingh and Kooi, 1992a,b; Lobkovsky et al., 1996; Van Wees and Cloetingh, 1996).

Furthermore, during rifting, the ascent of mantle-derived melts to the base of the crust can cause destabilization of the Moho, magmatic inflation of the crust, and its metasomatic reactivation and secondary differentiation (Morgan and Ramberg, 1987; Mohr, 1992; Stel et al., 1993; Watts and Fairhead, 1997). For instance, lower crustal velocities of 6.30–7.2 km s^{-1} and densities of 3.02×10^3 kg m^{-3} characterize the highly attenuated crust of the Devonian Dnieper–Donets rift almost up to the base of its synrift sediments, probably owing to its synrift permeation by mantle-derived melts (Stephenson et al., 2001; Yegorova et al., 1999).

Moreover, the accumulation of very thick postrift sedimentary sequences can cause phase transformation of crustal rocks to granulite facies, with the resulting densification of the crust accounting for accelerated basin subsidence. This process can be amplified in the cases of eclogite transformation of basaltic melts that were injected into the lithospheric mantle or that had accumulated at its base (Lobkovsky et al., 1996). However, it is uncertain whether large-scale eclogite formation can indeed occur at crustal thicknesses of 30–40 km (Carswell, 1990; Griffin et al., 1990). Although phase transformations, entailing an upward displacement of the geophysical Moho, are thought to occur under certain conditions at the base of very thick Proterozoic cratons (increased confining pressure due to horizontal intraplate stresses and/or ice load and possible cooling of asthenosphere; Cloetingh and Kooi, 1992a,b), it is uncertain whether physical conditions conducive to such transformations can develop in response to postrift sedimentary loading of paleorifts and passive margins as, for example, suspected for the East Newfoundland Basin (Cloetingh and Kooi, 1992a,b) and the West Siberian basin (Lobkovsky et al., 1996).

As rifting processes can take place intermittently over very long periods of time (e.g., Norwegian–Greenland Sea rift: Ziegler, 1988, 1989a), thermal anomalies introduced during early stretching phases start to decay during subsequent periods of decreased extension rates. Thus, the thermal anomaly associated with a rift may not be at its maximum when crustal stretching terminates and the rift becomes inactive. Similarly, late rifting pulses and/or regional magmatic events may interrupt and even reverse lithospheric cooling processes (e.g., Paleocene thermal uplift of northern parts of Viking Graben due to Iceland plume impingement: Nadin and Kusznir, 1995; Ziegler, 1990a). Therefore, analyses of the postrift subsidence of rifts that have evolved in response to multiple rifting phases spread over a long period need to take their entire rifting history into account.

Intraplate compressional stresses may cause amplification of the deflection of the lithosphere under basins and thus can overprint the thermal subsidence of postrift basins (Cloetingh et al., 1985; Zoback et al., 1993). The example of the Pliocene–Pleistocene evolution of the North Sea shows that the buildup of regional compressional stresses can cause a sharp acceleration of postrift subsidence (**Figure 16**; Cloetingh, 1988; Cloetingh et al., 1990; Kooi and Cloetingh, 1989; Kooi et al., 1991; Van Wees and Cloetingh, 1996). Similar contemporaneous effects are recognized in North Atlantic passive margin basins (Cloetingh et al., 1987, 1990) as well as in the Pannonian Basin (Horváth and Cloetingh, 1996). Also the late Eocene accelerated subsidence of the Black Sea basin can be

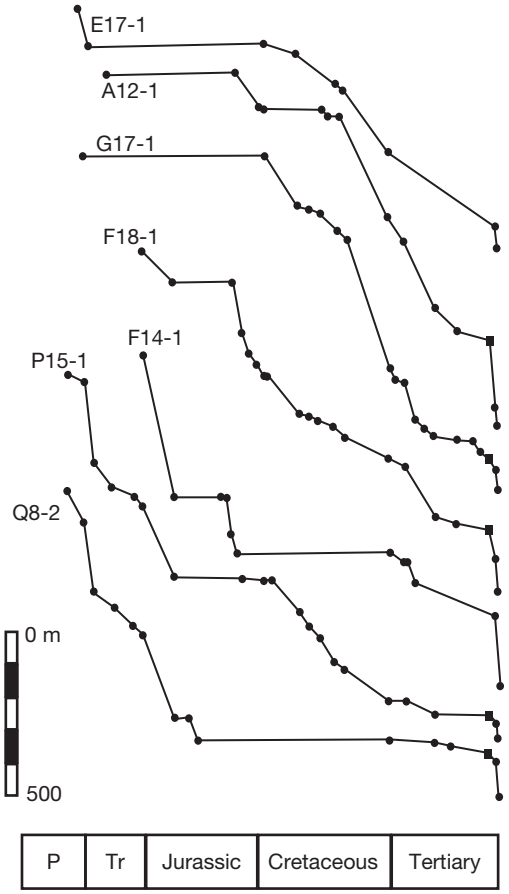

Figure 16 Tectonic subsidence curves of southern North Sea, showing accelerated subsidence during Pliocene–Pleistocene. Postrift stage starts during the Cretaceous. Reproduced from Kooi H (1991) *Tectonic Modelling of Extensional Basins: The Role of Lithospheric Flexure, Intraplate Stress and Relative Sea-level Change*, 183 pp. PhD Thesis, VU University, Amsterdam.

attributed to the buildup of a regional compressional stress field (Cloetingh et al., 2003; Robinson et al., 1995).

At present, many extensional basins are in a state of horizontal compression as documented by stress indicators summarized in the World Stress Map (Zoback, 1992) and the European Stress Map (e.g., Gölke et al., 1996). The magnitude of stress-induced vertical motions of the lithosphere during the postrift phase, causing accelerated basin subsidence and tilting of basin margins, depends on the ratio of the stress level and the strength of the lithosphere inherited from the synrift phase. Moreover, horizontal stresses in the lithosphere strongly affect the development of diapirism, accounting for local subsidence anomalies (Cloetingh and Kooi, 1992a,b), and have a strong impact on the hydrodynamic regime of rifted basins (Van Balen and Cloetingh, 1993, 1994) by contributing to the development of overpressure, as seen in parts of the Pannonian Basin (Van Balen et al., 1999). Glacial loading and unloading can further complicate postrift lithospheric motions, a better insight into the nature of which is required (Solheim et al., 1996).

These considerations indicate that stretching factors derived from the subsidence of postrift basins must be treated with reservations. Nevertheless, quantitative subsidence studies,

combined with other data, are essential for the understanding of postrift subsidence processes by giving a measure of the lithospheric anomaly that was introduced during the rifting stage of a basin and by identifying deviations from purely thermal cooling trends.

6.12.3.4.3 Postrift compressional reactivation potential

Paleostress analyses give evidence for changes in the magnitude and orientation of intraplate stress fields on timescales of a few My (Bergerat, 1987; Dèzes et al., 2004; Letouzey, 1986; Philip, 1987). Thus, in an attempt to understand the evolution of a postrift basin, the effects of tectonic stresses on subsidence must be separated from those related to thermal relaxation of the lithosphere (Cloetingh and Kooi, 1992a,b). In response to the buildup of far-field compressional stresses, rifted basins, characterized by a strongly faulted and thus permanently weakened crust, are prone to reactivation at all stages of their postrift evolution, resulting in their inversion (Ziegler, 1987, 1990a; Ziegler et al., 1995, 1998, 2001). Only under special condition can gravitational forces associated with topography around a basin cause its inversion (Bada et al., 2001).

Rheological considerations indicate that the lithosphere of thermally stabilized rifts, lacking a thick postrift sedimentary prism, is considerably stronger than the lithosphere of adjacent unstretched areas (Ziegler and Cloetingh, 2004). This contradicts the observation that rift zones and passive margins are preferentially deformed during periods of intraplate compression (Ziegler et al., 2001). However, burial of rifted basins under a thick postrift sequence contributes by thermal blanketing to weakening of their lithosphere (Stephenson, 1989; Van Wees, 1994), thus rendering them prone to tectonic reactivation.

In order to quantify this effect and to assess the reactivation potential of conjugate simple shear margins during subduction initiation, their strength evolution was modeled and compared to that of oceanic crust (Ziegler et al., 1998). By applying a 1-D two-layered lithospheric stretching model, incorporating the effects of heat production by the crust and its sedimentary thermal blanketing (Table 2), the thermomechanical evolution of the lithosphere was analyzed in an effort to predict its paleorheology (Bertotti et al., 1997; Van Wees et al., 1996).

For modeling purposes, a time frame of 100 My was chosen. Of this, the first 10 My (between 100 and 90 My in Figure 17) corresponds to the rifting stage, culminating in the separation of the conjugate upper and lower plate margins, and the following 90 My to the seafloor spreading stage during which oceanic lithosphere is accreted to the diverging plates. For modeling purposes, it was assumed that the prerift crustal and lithospheric mantle thicknesses are 30 and 70 km, respectively, and that at the end of the rifting stage, the upper plate margin has a crustal thickness of 15 km ($\delta = 2$) and a remaining lithospheric mantle thickness of 7 km ($\beta = 10$) (δ and β are, respectively, the crustal and subcrustal stretching factors (Royden and Keen, 1980)), while the lower plate margin has a crustal thickness of 10 km ($\delta = 3$) and a lithospheric mantle thickness of 63.6 km ($\beta = 1.1$; Figure 17(a) and 17(b)). Results show that through time, the evolution of strength envelopes for lower and upper plate passive margins differs strongly. In principle, during rifting, increased heating of the lithosphere causes its weakening; this effect is most pronounced at the moment of crustal separation. However, upper and lower plate margins show a very different evolution, both during the rifting and postrift stage.

At the moment of crustal separation, upper plate margins are very weak due to strong attenuation of the mantle–lithosphere and the ascent of the asthenospheric material close to the base of the crust. During the postrift evolution of such a margin, having a crustal thickness of 15 km, the strength of the lithosphere increases gradually as new mantle is accreted to its base and cools during the reequilibration of the lithosphere with the asthenosphere (Figures 17(a) and 18(a)). In contrast, the evolution of a sediment-starved lower plate margin with a crustal thickness of 10 km is characterized by a synrift strength increase due to extensional unroofing of the little attenuated mantle–lithosphere; the strength of such a margin increases dramatically during the postrift stage due to its progressive cooling (Figures 17(b) and 18(b)). At the time frame of 0 My, a sediment-starved lower plate margin is considerably stronger than the conjugate upper plate margin for which a sedimentary cover of about 7 km was assumed. The strength evolution of an upper plate margin is initially controlled by the youthfulness of its lithospheric mantle and its thicker crust and subsequently by the thermal blanketing effect of sediments infilling the available accommodation space. On the other hand, the strength of oceanic lithosphere that is covered by thin sediments only increases dramatically during its 90 My evolution and ultimately exceeds the strength of both margins, even if these are sediment-starved (Figures 17(c) and 18). However, the strength of 90 My old oceanic lithosphere that has been progressively covered by very thick sediments is significantly reduced (Figure 17(d)) to the point that it approaches the strength of a sediment-filled lower plate margin (Figure 18).

To test the effects of sediment infill and thermal blanketing on the strength evolution of upper and lower plate passive margins, a wide range of models was run assuming that sediments completely fill the tectonically created accommodation space (sediment overfilled; Figure 18), adopting different sediment densities and corresponding sediment thickness variations (Table 2). Results show that a thick syn- and postrift sedimentary prism markedly reduces the integrated strength of a margin. However, despite the strong sediment fill effect on the integrated strength, earlier identified first-order differences between upper and lower plate margins remain. Compared to oceanic lithosphere, with both a 1 km sedimentary cover (Figures 17(c) and 18) and a 15 km thick cover (Figure 17(d)), a sediment

Table 2 Rheological and thermal parameters of crust and lithospheric materials, adopted for the rheological models shown in Figure 17

Layer	*Rheology*	*Conductivity* ($W\,m^{-1}K^{-1}$)	*Heat production* ($10^{-6}\,W\,m^{-3}$)
Sediments (models A, B, and C)	Quartzite	2	0.2
Sediments (model D)	Quartzite	1.4	1.8
Upper crust	Quartzite	2.6	1.88
Lower crust	Diorite	2.6	0.5
Lithospheric mantle	Olivine	3.1	0

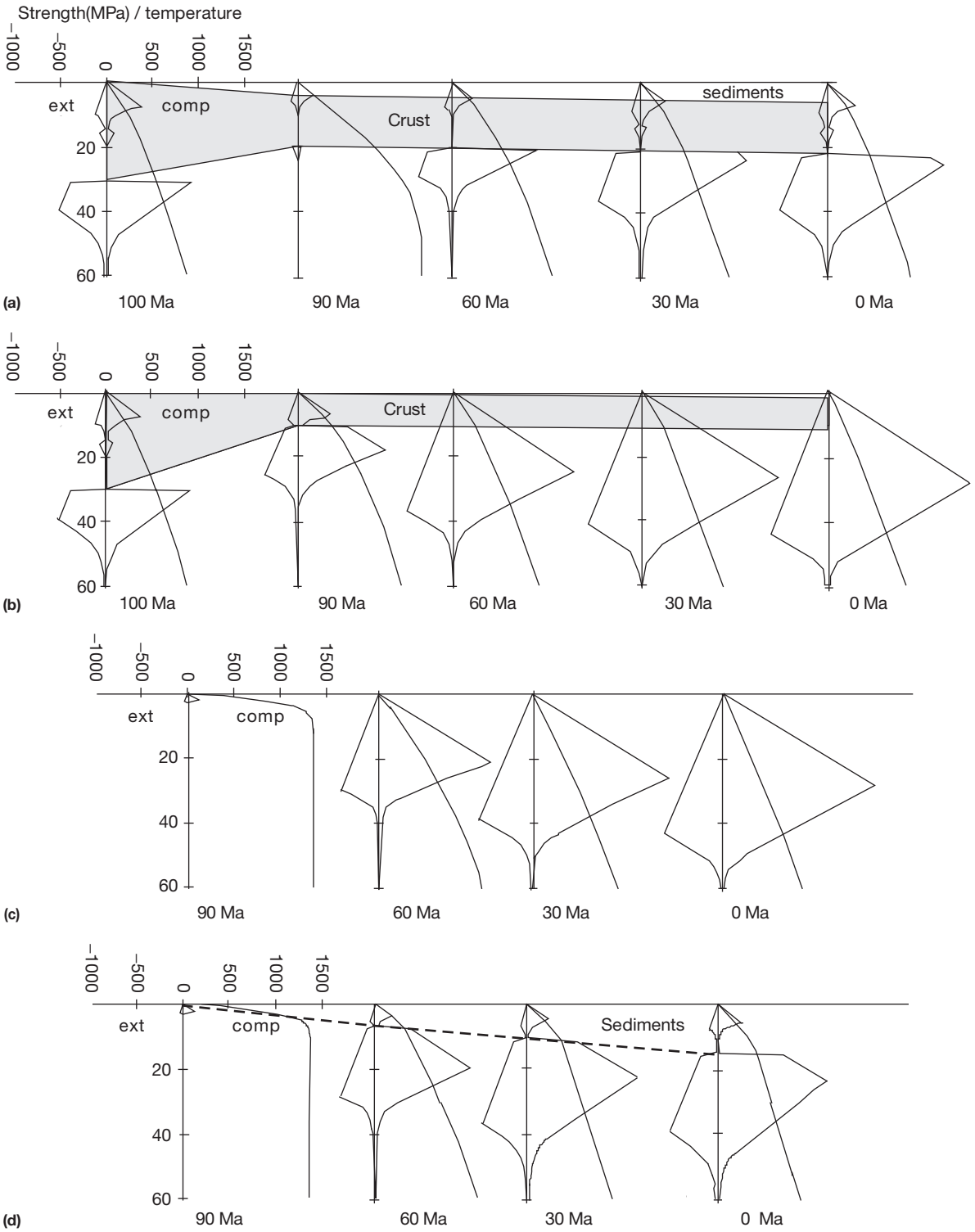

Figure 17 Depth-dependent rheological models for the evolution of lower plate and upper plate passive margins and oceanic lithosphere. For modeling parameters, see **Tables 2** and **3**. (a) Upper plate passive margin ($\delta = 2$, $\beta = 10$), characterized at the end of postrift phase by complete sediment fill of accommodation space ($\rho_s = 2100$ kg m^{-3}, 7.084 km sediments). (b) Lower plate passive margin ($\delta = 3$, $\beta = 1.1$), marked by sediment starvation at the end of postrift phase (1 km sediments). (c) Oceanic lithosphere with a thin sedimentary cover of 1 km. (d) Oceanic lithosphere with a gradually increasing sedimentary cover reaching a maximum of 15 km. Reproduced from Ziegler PA, Van Wees JD, and Cloetingh S (1998) Mechanical controls on collision-related compressional intraplate deformation. *Tectonophysics* 300: 103–129.

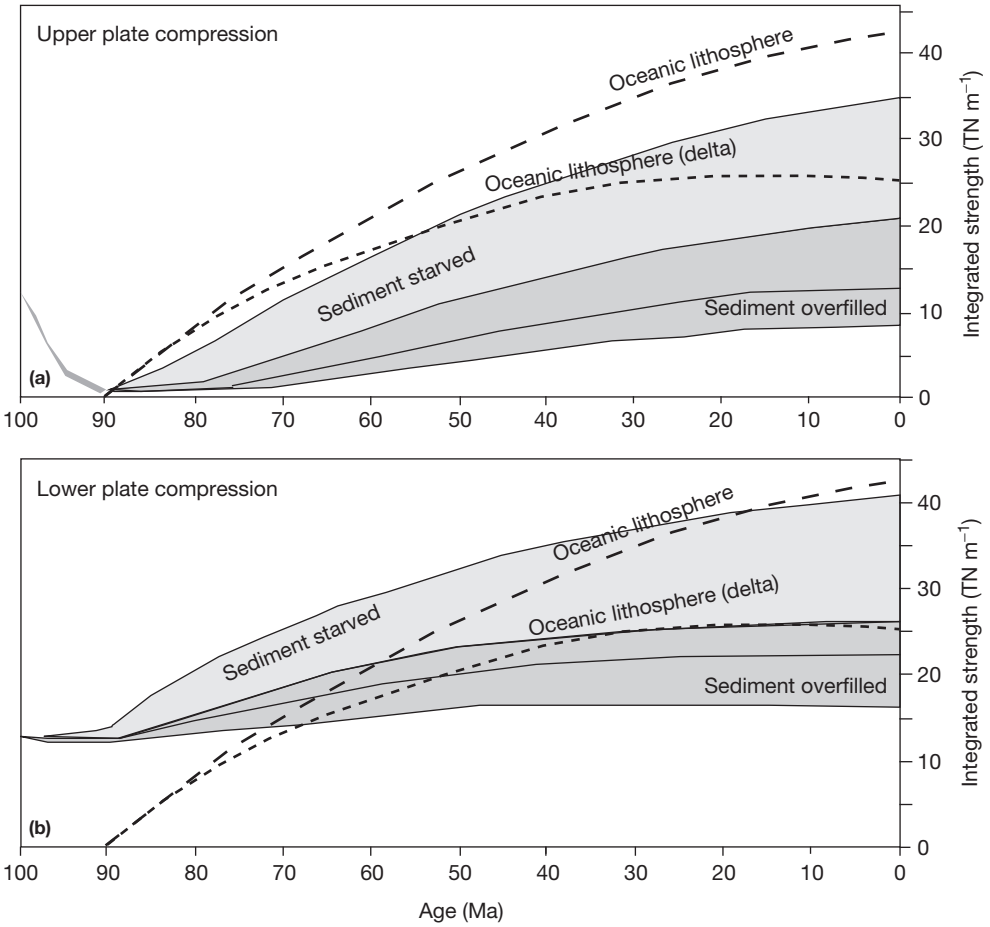

Figure 18 Integrated compressional strength evolution of sediment-starved and sediment-filled (a) upper plate and (b) lower plate passive margins, compared to the integrated strength evolution of oceanic lithosphere with thin and thick sediment cover as in **Figure 17**. Shaded areas demonstrate strong sensitivity of integrated strength to sediment infilling, ranging from sediment starvation (highest strength values) to complete fill of accommodation space (dark shading, lowest strength values). Curves in dark-shaded area correspond to different sediment densities and related range in sediment thickness (see **Table 3**). Reproduced from Ziegler PA, Van Wees JD, and Cloetingh S (1998) Mechanical controls on collision-related compressional intraplate deformation. *Tectonophysics* 300: 103–129.

overfilled upper plate margin (applying $\rho_s = 2100\ \mathrm{kg\ m^{-3}}$) is characterized by lower integrated strength values throughout its evolution. However, for a lower plate margin, conditions are dramatically different. Up to 20–70 My after rifting, the lower plate integrated strength values are significantly higher than those for oceanic lithosphere, with both a thin sedimentary cover and a thick sedimentary cover.

From these strength calculations, it is evident that at any stage, the upper plate margin is weaker than oceanic lithosphere and the conjugate lower plate margin. This suggests that the upper plate margin is the most likely candidate for compressional reactivation and the initiation of a subduction zone. For realistic sediment density and infill values ($\rho_s <= 2500\ \mathrm{kg\ m^{-3}}$), also, the upper plate margin tends to grow stronger in time, indicating that after a prolonged postrift stage (>70 My), localization of deformation and subduction along such a margin, instead of on the adjacent continent, should be facilitated by weakening mechanisms that are not incorporated in our standard rheological assumptions for the lithosphere, such as preexisting crustal and mantle discontinuities and the boundaries between old and newly accreted lithospheric mantle.

The modeling shows that the compressional yield strength of passive margins can vary considerably, depending on their lithospheric configuration, sedimentary cover, and thermal age. Lower plate margins, at which much of the old continental mantle–lithosphere is preserved, are considerably stronger than upper plate margins at which asthenospheric material has been accreted to the strongly attenuated old mantle–lithosphere. Although mature oceanic lithosphere is characterized by a high compressional yield strength, it can be significantly weakened in areas where thick passive margin sedimentary prisms or deep-sea fans prograde onto it (e.g., Gulf of Mexico: Worrall and Snelson, 1989; Niger Delta: Doust and Omatsola, 1989; Bengal fan: Curray and Moore, 1971).

6.12.3.5 Finite Strength of the Lithosphere in Extensional Basin Formation

In recent approaches to extensional basin modeling, the implementation of finite lithospheric strengths is an important step forward (see **Section 6.12.3** for a review). Advances in the understanding of lithospheric mechanics (e.g., Burov and

Table 3 Sediment-overfilled scenario (up to water surface), adopted in Figure 18

			Accumulated sediment fill (m)		
		Tectonic air-loaded subsidence (m)	$\rho_s = 2100$ kg m^{-3}	$\rho_s = 2500$ kg m^{-3}	$\rho_s = 2650$ kg m^{-3}
Upper plate	Synrift	1474	4396	7065	9148
	Postrift	2375	7084	11384	14739
Lower plate	Synrift	2599	7752	7752	16130
	Postrift	3332	9939	15972	20679

Diament, 1995; Ranalli, 1995) demonstrate that early stretching models that assumed zero lithospheric strength during rifting are not valid. Moreover, the notion of a possible decoupling zone between the strong upper crust and the strong upper lithospheric mantle (see Section 6.12.3.1) is also important in the context of extensional basin formation. During the past decades, the relative importance of pure shear (McKenzie, 1978) and simple shear (Wernicke, 1985) mode of extension has been a matter of debate. In the presence of a weak lower crustal layer decoupling of the mechanically strong upper crust from the even stronger upper lithospheric mantle, the zone and symmetry of upper crustal extension do not necessarily have to coincide with the zone and symmetry of lithospheric mantle extension. This is particularly the case if the upper crust is weakened by preexisting discontinuities favoring its simple shear extensional deformation (Ziegler, 1996). A better appreciation of the role played by rheology during basin formation and the advent of corresponding modeling capabilities during the past few years has increasingly shifted the focus of attention away from these end-members of lithospheric extension. Finite element models have explored the large-scale implications of a finite lithospheric strength and particularly its sensitivity to the presence of fluids in the crust and lithospheric mantle (Bassi, 1995; Braun and Beaumont, 1989; Dunbar and Sawyer, 1989; Govers and Wortel, 1993). These dynamic models, which require intensive computing, are expensive to run and thus are not suitable for an industry user-oriented environment. However, they have provided the background for a more user-friendly class of kinematic models targeted at modeling rift-shoulder uplift and basin fill (Cloetingh et al., 1995c). These kinematic models invoke the concept of lithospheric necking around one of its strong layers during extensional basin formation (see Braun and Beaumont, 1989; Kooi et al., 1992; Spadini et al., 1995b). Figure 13 illustrates the basic features of these models and their relation to the strength distribution within the lithosphere. In the presence of a strong layer in the subcrustal mantle, the level of lithospheric necking is deep, inducing pronounced rift-shoulder topography. This type of response is to be expected if extension affects cold and correspondingly strong intracontinental lithosphere; it is commonly observed in intracratonic rifts and rifted margin such as the Red Sea and the Transantarctic Mountains (Cloetingh et al., 1995a).

For Alpine/Mediterranean basins, which developed on a weak lithosphere with a thickened crust, the necking level is generally located at shallower depths). An example of such a situation is found in the Pannonian Basin (Horváth and Cloetingh, 1996; Van Balen et al., 1995, 1999) where the necking level is located at depths between 5 and 10 km within the upper crust. In this case, the strength of the lithospheric upper mantle has decreased to almost zero (see also Figure 13). Important exceptions to this general pattern do occur, however, such as in the southern Tyrrhenian Sea for which our modeling indicates a deep necking level to fit observational data (Spadini and Podladchikov, 1996; Spadini et al., 1995a,b). This is primarily attributed to the fact that the southern Tyrrhenian Basin developed essentially on Hercynian lithosphere with significant bulk strength of its mantle component. In other areas, this concept has led to a better understanding of lateral variations in basin structure and sedimentary fill within one and the same basin. This is exemplified by the Black Sea (see Section 6.12.5), where modeling deciphered important variations in necking level and thermal conditions between its eastern and western subbasins that can be attributed to differences in the timing and mode of their development (Cloetingh et al., 2003; Robinson et al., 1995; Spadini et al., 1996, 1997).

The interdependence of the necking depth and such parameters as prerift crustal and lithospheric thicknesses, the EET of the lithosphere, and strain rates was investigated in a comparative study on several basins, using the same modeling technology (Cloetingh et al., 1995a,b). Results of this study are summarized in Figure 19, illustrating that for Alpine/Mediterranean basins, the position of the necking level depends primarily on the prerift crustal thickness and strain rate, whereas the key controlling factors in intracratonic rifts appear to be the prerift lithospheric thickness and strain rate. This figure also illustrates where other basin formation processes have played a role. For instance, the Saudi Arabia–Red Sea margin is characterized by the presence of plume-related activity in the upper mantle that explains the systematic misfit of this case. The importance of the prerift lithospheric rheology for the subsequent basin geometry and the patterns of vertical motions are evident from these models. Moreover, they demonstrate that the better we are able to constrain the prerift evolution of an area, the greater the chance we have to define the parameter range that has to be to adopted for large-scale synrift mechanics.

6.12.3.6 Rift Shoulder Development and Architecture of Basin Fill

As discussed earlier, the finite strength of the lithosphere has important implications for the crustal structure of extensional basins and the development of accommodation space in them. The development of significant rift-shoulder topography in response to lithospheric extension has drawn attention to the need to constrain the coupled vertical motion of the shoulders and the subsiding basin (Kusznir and Ziegler, 1992). Whereas

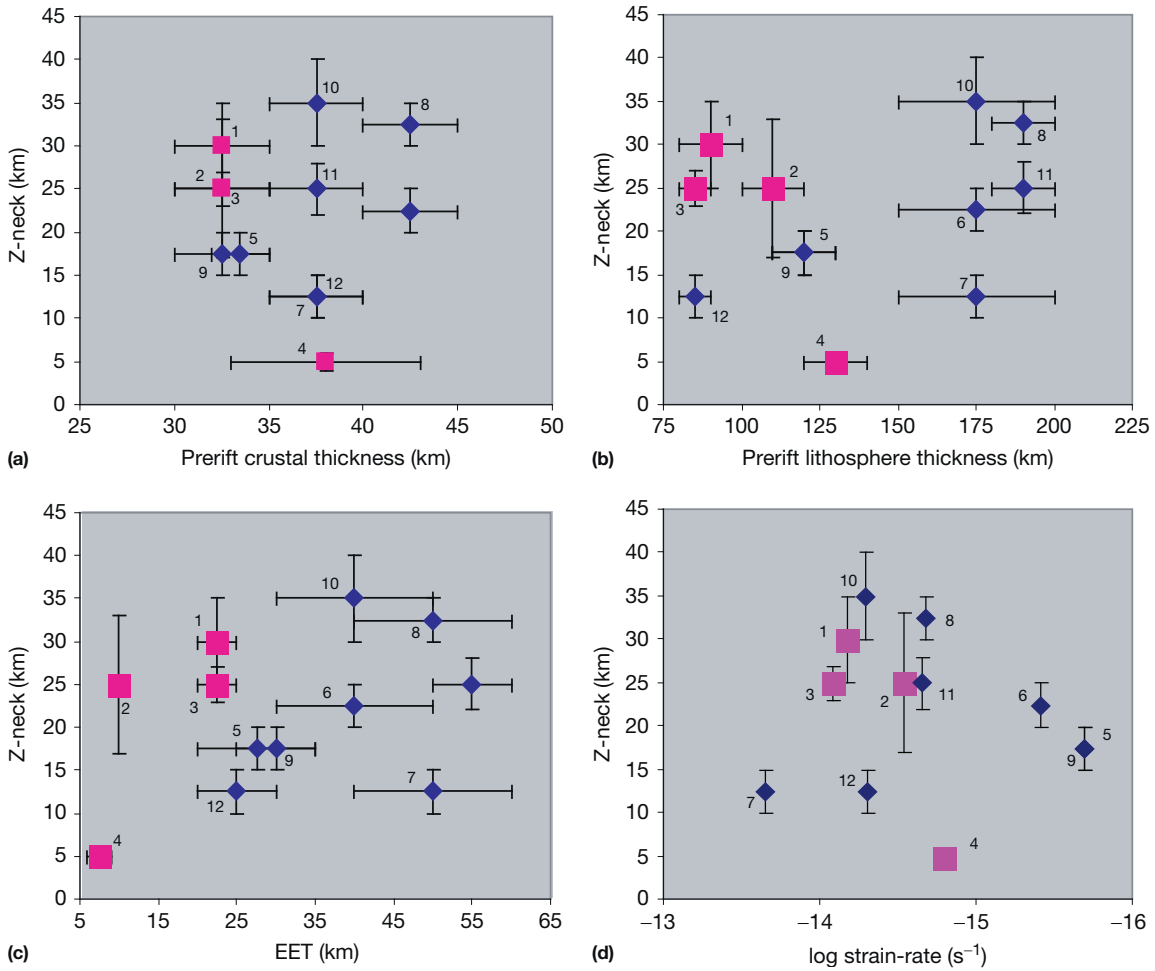

Figure 19 Correlation diagrams for the relationship between (a) necking depth and prerift crustal thickness, (b) necking depth and prerift lithospheric thickness, (c) EET and necking depth, and (d) necking depth and strain rate. *Circles* and *diamonds* indicate data from Alpine/Mediterranean basins and intracratonic rifts, respectively. Numbers refer to the following basins: *1* Gulf of Lion; *2* Valencia trough; *3* southern Tyrrhenian Sea; *4* Pannonian Basin; *5* North Sea; *6* Baikal rift; *7* Saudi Arabia Red Sea; *8* Transantarctic Mountains; *9* Barents Sea; *10* East African Rift; *11* western Black Sea; *12* eastern Black Sea. Reproduced from Cloetingh S, DArgenio B, Catalano R, Horvath F, and Sassi W (1995) Interplay of extension and compression in basin formation: Introduction. *Tectonophysics* 252: 1–5.

the standard approach in basin analysis focused until recently primarily on the subsiding basin, treating sediment supply as an independent parameter, necking models highlight the need for linking sediment supply to the rift-flank uplift and erosion history. To this end, a twofold approach was followed. The first research line aimed at constraining the predicted uplift histories by geothermochronology. Modeling of the distribution of fission-track length permits to back-stack the eroded sediments from their present position in the basin to their source on the rift shoulder in an effort to obtain a better reconstruction of the rift-shoulder geometries (e.g., Rohrman et al., 1995; Van der Beek et al., 1995). This has led to a better understanding of the timing and magnitude of rift-shoulder uplift, for example, on the Norwegian margin, shedding light on the observed relationship between onshore uplift and the presence of thick late Cenozoic sedimentary wedges in the adjacent offshore basin.

A second research line focused on the development of a model for basin fill simulation, integrating the effects of rift-shoulder erosion through hillslope transport and river incision with sediment deposition in the basin. As illustrated in Figure 20 (see Van Balen et al., 1995), these models predict the progradation of sedimentary wedges into extensional basins and the development of hinterland basins having a distinctly different stratigraphic signature than predicted by standard models, which invoke stretching and postrift flexure and which are commonly applied in the existing packages. Testing of this new model against a number of rifted margins around the world demonstrates that erosion of the rift-shoulder topography, created during extension of a lithosphere with a finite strength, eliminates to a large extent the need to invoke eustatic sea-level changes to explain the most commonly encountered large-scale stratigraphic features of rifted basins and associated hinterland basins.

On the scale of individual half-grabens, faulting exerts the main control on the basin architecture. Modeling studies have focused on the coupling of fault block tilting and the flexural behavior of the extending lithosphere. In a first step, modeling technology was developed to quantify the thermal effects of faulting on an extending lithosphere (Ter Voorde and Bertotti, 1994; Ter Voorde et al., 2007). Subsequently, models were

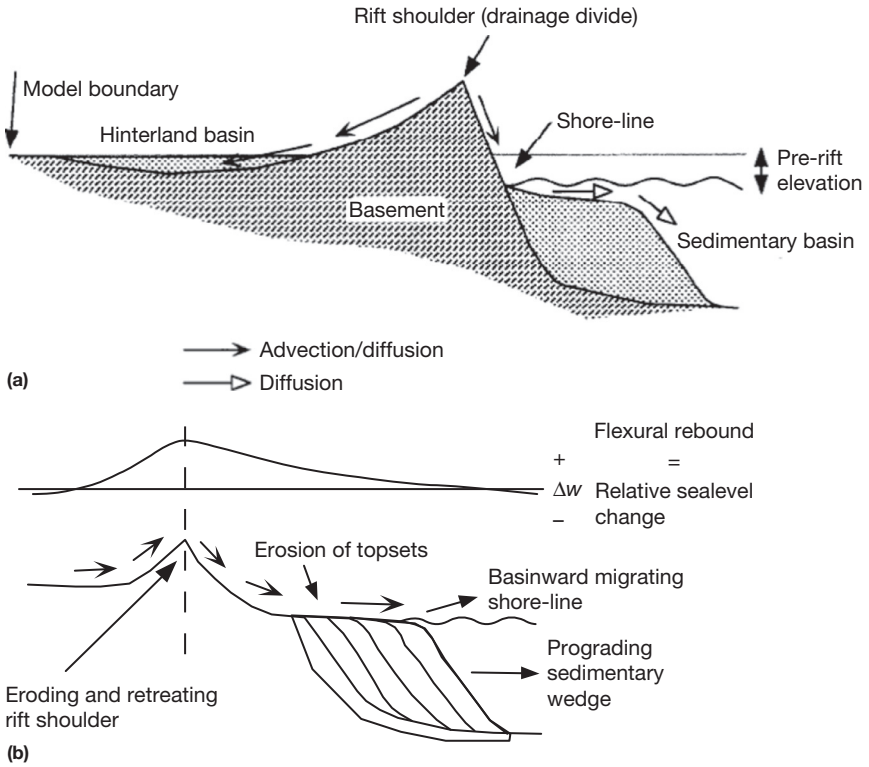

Figure 20 (a) Cartoon of the rift-shoulder erosion model. The isostatic response to necking of the lithosphere during extension causes a flexurally supported rift shoulder. In a landward direction, the rift shoulder is flanked by a flexural downwarp, the hinterland basin. The erosion products of the rift shoulder are transported to the offshore rifted basin and the hinterland basin. When the hinterland basin is completely filled, the sediments are taken out at the location indicated by 'model boundary.' These sediments are reintroduced into the model at the shoreline position in the offshore basin, establishing conservation of mass in the model. (b) Cartoon illustrating the mechanism of initial postrift coastal offlap at passive margins. Flexural rebound in response to erosional unloading at the rift shoulder causes uplift extending far into the offshore basin. The uplift causes erosional truncation of the topsets of the sedimentary wedge. Coastal onlap will occur when the rate of erosion-induced uplift is less than the subsidence caused by sedimentary loading, thermal contraction, and the flexural response to the increase in rigidity. Δw shows the instantaneous flexural uplift (+) and subsidence (−) pattern caused by rift-shoulder erosion. Reproduced from Van Balen RT, Vanderbeek PA, and Cloetingh SAPL (1995) The effect of rift shoulder erosion on stratal patterns at passive margins – Implications for sequence stratigraphy. *Earth and Planetary Science Letters* 134: 527–544.

developed that link the evolution of individual half-grabens to the extensional response of the deeper lithospheric (Ter Voorde and Cloetingh, 1996). The second step aimed at validating and testing these models against closely constrained natural examples, such as the well-exposed Mesozoic southern Alpine rifted margin, where extensive radiometric dating and the application of Ar/Ar laser-probing techniques permitted to constrain with high accuracy the thermal evolution of the extending lithosphere at subbasin and basin-wide scales (Bertotti and Ter Voorde, 1994). Testing and validation of the stratigraphic modeling component were carried out by a case-history study of the Oseberg field in the Norwegian part of the Viking Graben (Ter Voorde et al., 1997). This study demonstrated the need to establish a regional framework, linking the mechanics of the Oseberg block to the crustal evolution of adjacent areas, as a prerequisite for more detailed reservoir modeling.

Considering the notion that in synrift basins, different spatial and temporal scales are by their very nature linked, ignorance of constraints and structural information on surrounding areas will severely limit the quality of reservoir modeling. Modeling provides a quantitative tool to assess tectonic controls on synrift depositional sequences at a subbasin scale (see also Nottvedt et al., 1995). The amount of footwall uplift of an individual fault block appears to depend directly on the lithospheric necking level, controlling the large-scale response of the lithosphere to extension, and, therefore, should not only be attributed to factors restricted to the subbasin scale.

6.12.3.7 Back-Arc Extensional Basins

Back-arc extensional basins evolve in response to a decrease in the convergence rate or even a temporary divergence of colliding plates, causing steepening and rollback of the subducting lower plate lithospheric slab and the development of a secondary upwelling system in the upper plate mantle wedge above the subducting slab (e.g., Doglioni et al., 2007; Uyeda and McCabe, 1983). Back-arc basins can be developed over oceanic and continental lithosphere. Continental back-arc rifting can progress to the opening of limited oceanic basins (e.g., Sea of Japan, Black Sea, and South China Sea). However, as convergence rates between colliding plates vary in time, back-arc extensional basins are generally short-lived. Upon a renewed increase in convergence rates and shallowing of the subducting lower plate lithospheric slab, back-arc extensional basins are subjected to compressional stresses that can lead to their inversion and closure. Typical examples may include the Variscan

geosyncline, Sunda Arc and East China, or the Black Sea (Cloetingh et al., 1989; Hall et al., 2011; Jolivet et al., 1989; Munteanu et al., 2011; Nikishin et al., 2012; Uyeda and McCabe, 1983; Ziegler, 1990b). The sedimentary geometry and architecture of back-arc basins are controlled by such parameters as the age of subducted lithosphere, the subduction direction, the type of underlying lithosphere (oceanic versus continental), or the uplift of the orogenic arc (e.g., Dewey, 1980; Doglioni et al., 2007; Mathisen and Vondra, 1983; Uyeda and Kanamori, 1979). These parameters control the large variety of back-arc basins of various ages presently overlying different types of crust, such as the Caribbean, Banda–Sunda back-arcs, or the Black Sea basin (e.g., Hall et al., 2011; Meschede and Frisch, 1998; Munteanu et al., 2011; Spakman and Hall, 2010).

An observation that is common to many extensional back-arc basins floored by continental crust is the discrepancy between the observed amounts of crustal and lithospheric mantle stretching as derived from the magnitude, the upper crustal faulting and crustal/lithospheric thicknesses, and thus major differences between the corresponding stretching factors. This type of back-arc basin is often characterized by a much thicker postrift basin fill than predicted by synrift stretching as seen in the Pannonian Basin (Lenkey, 1999; Horváth et al., 2006). Such contrasting features occur in the hinterland of subduction-driven orogens (sensu Doglioni et al., 2007; Royden and Burchfiel, 1989), as, for example, the case of subduction driving the highly arcuate Mediterranean orogens (e.g., the Pannonian–Transylvanian system, the Aegean Sea, or the western Mediterranean, Faccenna et al., 2004; Jolivet and Brun, 2010; Krézsek and Bally, 2006; Matenco and Radivojević, 2012) or SE Asia subduction zones (e.g., the Malay and Pattani Basins; Morley and Westaway, 2006).

In the following, two large-scale extensional back-arc basins that underwent significant amounts of inversion postdating extensional episodes are discussed: the Black Sea and the Pannonian–Transylvanian Basin system of central Europe.

6.12.3.7.1 Black Sea basin

The Black Sea is superimposed on the Euxinus orogenic system that developed along the southern margin of the East European Craton during the closure of the Rheic and Paleo-Thethys Oceans. The Euxinus orogen was repeatedly subjected to back-arc extension and compression during the Triassic to Early Cretaceous final closure of the Paleo-Tethys Ocean and the opening of the Neo-Tethys Ocean (**Figure 21**; e.g., Nikishin et al., 2012; Okay et al., 1996; Robinson et al., 1996; Saintot et al., 2006; Şengör, 1987; Stephenson et al., 2004). The western Black Sea opened in Late Cretaceous times (e.g., Finetti et al., 1988; Görür, 1988; Munteanu et al., 2011; Nikishin et al., 2001, 2012), commonly interpreted as an extensional back-arc basin related to the N-ward subduction of the Neo-Tethys (e.g., Letouzey et al., 1977; Nikishin et al., 2012; Okay et al., 1994). Although a coeval opening of all domains of the Black Sea during Late Cretaceous times has been inferred (e.g., Nikishin et al., 2003; Zonenshain and Le Pichon, 1986), most studies agree that the eastern Black Sea has opened later, during Paleocene–Eocene times (e.g., Banks, 1998; Kazmin et al., 2000; Robinson et al., 1996; **Figure 21**; see also Okay et al., 1994), creating thinned continental to oceanic crust (Edwards et al., 2009; Shillington et al., 2008). The Early Cretaceous opening of the western Black Sea took place in a number of deformation phases (Munteanu et al., 2011) creating possibly oceanic crust, followed by overall seafloor spreading and subsidence during Late Cretaceous and Cenozoic times (Finetti et al., 1988; Görür, 1988; Nikishin et al., 2012; Starostenko et al., 2004). The Early Cretaceous back-arc opening was followed by a main Late Cretaceous extensional episode in the Pontides (Görür, 1988; Yilmaz et al., 1997). This can be followed laterally also onshore in the Balkanides (e.g.,

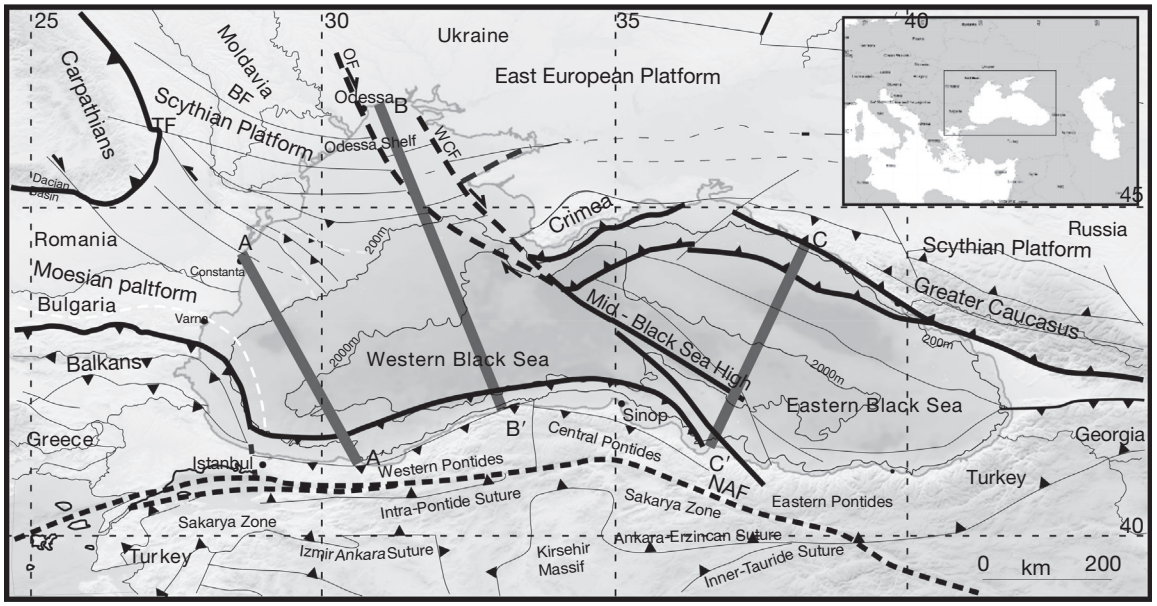

Figure 21 Tectonic map of the Black Sea and adjacent areas (simplified and modified from Munteanu, 2012) with the location of profiles shown in **Figure 22**. Reproduced from Munteanu I (2012) *Evolution of the Western Black Sea: Kinematic and Sedimentological Inferences from Geological Observations and Analogue Modelling*. Dissertation, Utrecht University.

Georgiev et al., 2001). The Eocene opening of the eastern Black Sea (e.g., Görür, 1988) has induced renewed extension in the western basin (e.g., Robinson et al., 1996; Dinu et al., 2005; Munteanu et al., 2011; Tari et al., 2009). The passive margin evolution that is interrupted by the late (middle) Eocene collision recorded the major tectonic units of the Pontides and Taurides (Okay et al., 1994; Şengör and Yilmaz, 1981). The major contraction taking place at the southern margin of the Black Sea led to the onset of inversion recorded in the extensional basins and to the formation of other foreland and thrust-sheet top basins (e.g., Dinu et al., 2005; Finetti et al., 1988; Nikishin et al., 2003; Robinson et al., 1996; Sunal and Tüysüz, 2002). In the western Black Sea basin, the contraction gradually migrated in time N-ward until the Odessa shelf (Munteanu et al., 2011), where the shortening continued during Miocene–Pliocene times (Khriachtchevskaia et al., 2009). The eastern Black Sea was inverted with an opposite polarity, the Crimean and Caucasus orogens being thrusted S-ward over the Black Sea domain starting with Oligocene times (e.g., Munteanu et al., 2013; Stovba et al., 2009). The change in polarity is accommodated by the transcurrent movements recorded by the Odessa–West Crimean fault system and along the Mid-Black Sea High (Munteanu et al., 2011, 2014).

In the context of the endemic Eastern Paratethys, the Neogene evolution of the western Black Sea basin is of special interest (Popov et al., 2006; Vasiliev et al., 2013). While fine clastic to pelagic Lower–Middle Miocene sediments are generally thin throughout the western Black Sea, higher subsidence rates are recorded during latest Miocene–Quaternary times (Cloetingh et al., 2003; Munteanu et al., 2012; Nikishin et al., 2003). The sea-level drop of the Messinian Salinity Crisis in the Mediterranean (e.g., Krijgsman et al., 1999) is recorded in the Black Sea by large-scale shelf erosion and massive progradation of clastics during the lower Pliocene transgressive and highstand, the estimated sea-level drop probably exceeding 1 km (e.g., Bartol and Govers, 2009; Bartol et al., 2012; Gillet et al., 2007; Hsü and Giovanoli, 1979; Munteanu et al., 2012). Rapid sea-level changes are also inferred for the Pliocene–Quaternary evolution of the western Black Sea (Lericolais et al., 2013; Winguth et al., 2000). Consequently, thick successions of mass-transport and turbiditic deposits are observed along a number of deep-sea fans in front of modern rivers discharging into the Black Sea (e.g., Popescu et al., 2001).

In the succeeding text, we address the relationship between the prerift finite strength of the lithosphere and the geometry of extensional basins in the Black Sea area and discuss the effects of differences in prerift rheology on the Mesozoic–Cenozoic stratigraphy of the western and eastern Black Sea basin. These findings raise important questions on postrift tectonics and on intraplate stress transmission into the Black Sea basin from its margins.

6.12.3.7.1.1 Rheology and back-arc rift basin formation

Inferred differences in the mode of basin formation between the western and eastern Black Sea basins can be largely explained in terms of paleorheologies. The prerift lithospheric strength of the western Black Sea (**Figure 22**) appears to be primarily controlled by the combined mechanical response of a strong upper crust and strong upper mantle (Spadini et al., 1996). The shallow necking level in the eastern Black Sea is compatible with a prerift strength controlled by a strong upper crust decoupled from the weak hot underlying mantle (**Figure 22**). These differences point to important differences in the thermotectonic age of the lithosphere of the two subbasins (Cloetingh and Burov, 1996). The inferred lateral variations between the western and eastern Black Sea suggest thermal stabilization of the western Black Sea prior to rifting, while the lithosphere of the eastern Black Sea was apparently already thinned and thermally destabilized by the time of Eocene rifting. The inferred differences in the necking level and in the timing of rifting between the western and eastern Black Sea suggest an earlier and more pronounced development of rift shoulders in the western Black Sea basin as compared with the eastern Black Sea (Robinson et al., 1995).

6.12.3.7.1.2 Strength evolution and neotectonic reactivation during the postrift phase

Automated backstripping studies and results of forward models of lithospheric stretching (Van Wees et al., 1998) provide estimates of the integrated lithospheric strength at various syn- and postrift stages. Top panel in **Figure 23** shows a comparison of observed and forward modeled tectonic subsidence curves for the center of the western Black Sea basin. Automated backstripping yields a stretching factor of 6. Modeling fails, however, to predict the pronounced late Neogene subsidence acceleration, documented by the stratigraphic record that may be attributed to late-stage compression. As postrift cooling of the lithosphere leads in time to a significant increase in its integrated strength, its early postrift deformation is favored. Present-day lithospheric strength profiles calculated for the center and margin of western Black Sea (Figure 23 bottom panels) show a pronounced difference. On the contrary, the onset of the basin inversion during late Middle Eocene times at short times after the extension ceased earlier during Middle Eocene means that the lithosphere was weak when compression was activated. The presence of relatively strong lithosphere in the basin center in the very late stages of Pliocene inversion and weaker lithosphere at the basin margins favors the deformation of the latter during late-stage compression.

In **Figure 24**, (top panel) the observed and forward modeled tectonic subsidence curves for the center of eastern Black Sea basin are compared, adopting for modeling a stretching factor of 2.3 that is compatible with the subsidence data and consistent with geophysical constraints. During the first 10 My of postrift evolution, integrated strengths are low but subsequently increase rapidly owing to cooling of the lithosphere. This would correspond to the initial moments of post-Middle Eocene inversion.

At short time after the ultimate cessation of rifting (~10 My) in Middle Eocene times, the basing was still underlain by very weak and extended lithosphere. This is the moment when the entire Black Sea basin was inverted due to the collision recorded in the Pontides domain (e.g., Nikishin et al., 2012). It should be noted, however, that with a cooling-related progressive increase of the integrated lithospheric strength, with time increasingly higher stress levels are required to cause large-scale deformation (**Figures 23** and **24**, middle panels). This is probably why the amplitude of contractional deformation decreases in time in the western Black Sea basin (Munteanu et al., 2012). Important in this context is also that, due to substantial crustal thinning, a strong upper mantle layer is present in the central part of the basin at relatively shallow depths that may contrast substantially with an inherited weaker

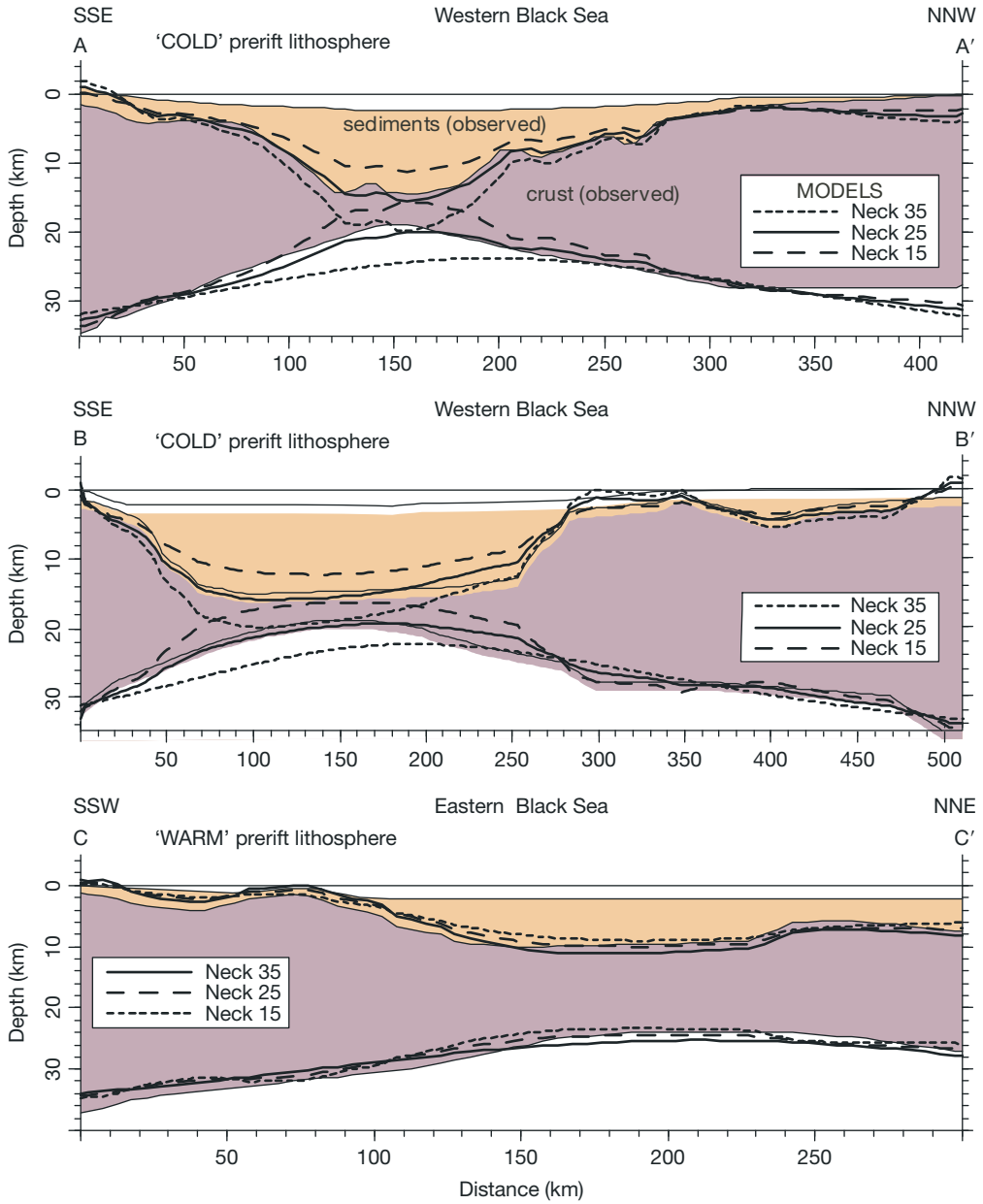

Figure 22 Crustal-scale models for basin evolution for the western and eastern Black Sea. For location of cross sections, see **Figure 21**. A comparison of predicted and observed Moho depths provides constraints on levels of necking and thermal regime of the prerift lithosphere. The models support the presence of cold prerift lithosphere compatible with a deep necking level of 25 km in the western Black Sea. For the eastern Black Sea, the models suggest the presence of a warm prerift lithosphere with a necking level of 15 km. Reproduced from Cloetingh S, Spadini G, Van Wees JD, and Beekman F (2003) Thermo-mechanical modelling of Black Sea Basin (de)formation. *Sedimentary Geology* 156: 169–184.

lower crust and, therefore, favor the transmission of contractional stresses over large distances (Munteanu, 2012).

Based on the present thermomechanical configuration (Figures 23 and 24) with relatively strong lithosphere in the basin center and relatively weak lithosphere at the basin margins, we predict that the bulk of shortening will be taken up in the margins of the basin during the initial phase of shortening, while the late-stage shortening induced by orogenic activity in the surrounding areas will be taken up along the basin center. The relative difference in rheological strength of the marginal and central parts of the basin is more pronounced in the eastern than in the western Black Sea. These predictions are in agreement with data mapping deformation in the Black Sea (e.g., Dondurur et al., 2013; Munteanu et al., 2012).

Basement and surface heat flow in the eastern and western Black Sea show markedly different patterns in timing of the rift-related heat flow maximum. The predicted present-day heat flow is considerably lower in the western than in the eastern subbasin. This is attributed to the presence of more heat-producing crustal material in the eastern than in the western Black Sea that is partly floored by oceanic crust. In heat flow modeling studies, the effects of sedimentary blanketing were

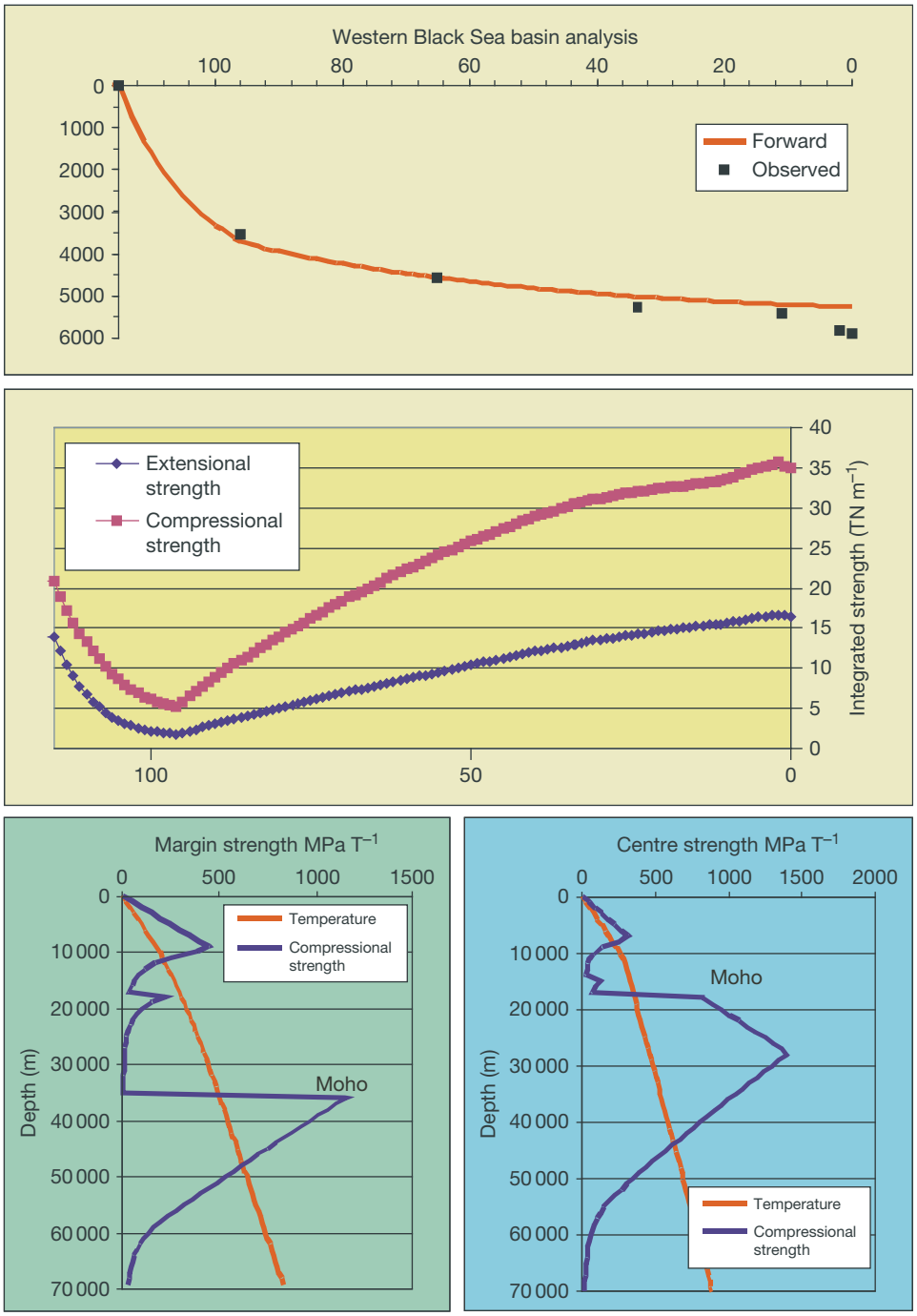

Figure 23 (Upper panel) Comparison of observed and forward modeled tectonic subsidence for the western Black Sea basin center. Automated backstripping yields an estimated stretching factor of 6. Postrift cooling leads in time to a significant increase in the predicted integrated strength for both compressional and extensional regimes (middle panel; 1 TN m^{-1} = 10^{12} N m^{-1}). (Middle panel) Present-day lithospheric compressional strength profiles calculated for the center and margin of western Black Sea show with depth a pronounced difference (bottom panels). Temperature profiles (in ^{o}C) and Moho depth are given for reference. Note the important role of the actual Moho position in terms of mechanical decoupling of the upper crust and mantle parts of the Black Sea lithosphere. Reproduced from Cloetingh S, Spadini G, Van Wees JD, and Beekman F (2003) Thermo-mechanical modelling of Black Sea Basin (de)formation. *Sedimentary Geology* 156: 169–184.

taken into account (Van Wees and Beekman, 2000). Heat flow values vary between 30 mW m^{-2} in the center of the basins and up to 70 mW m^{-2} at the Crimean and Caucasus margins (Nikishin et al., 2003). With its sedimentary thickness of up to 15 km, thermal blanketing has a pronounced effect on the heat flow in the western Black Sea. As a result, its present-day integrated strength is not that much higher than its initial strength. By contrast, the integrated strength of the eastern

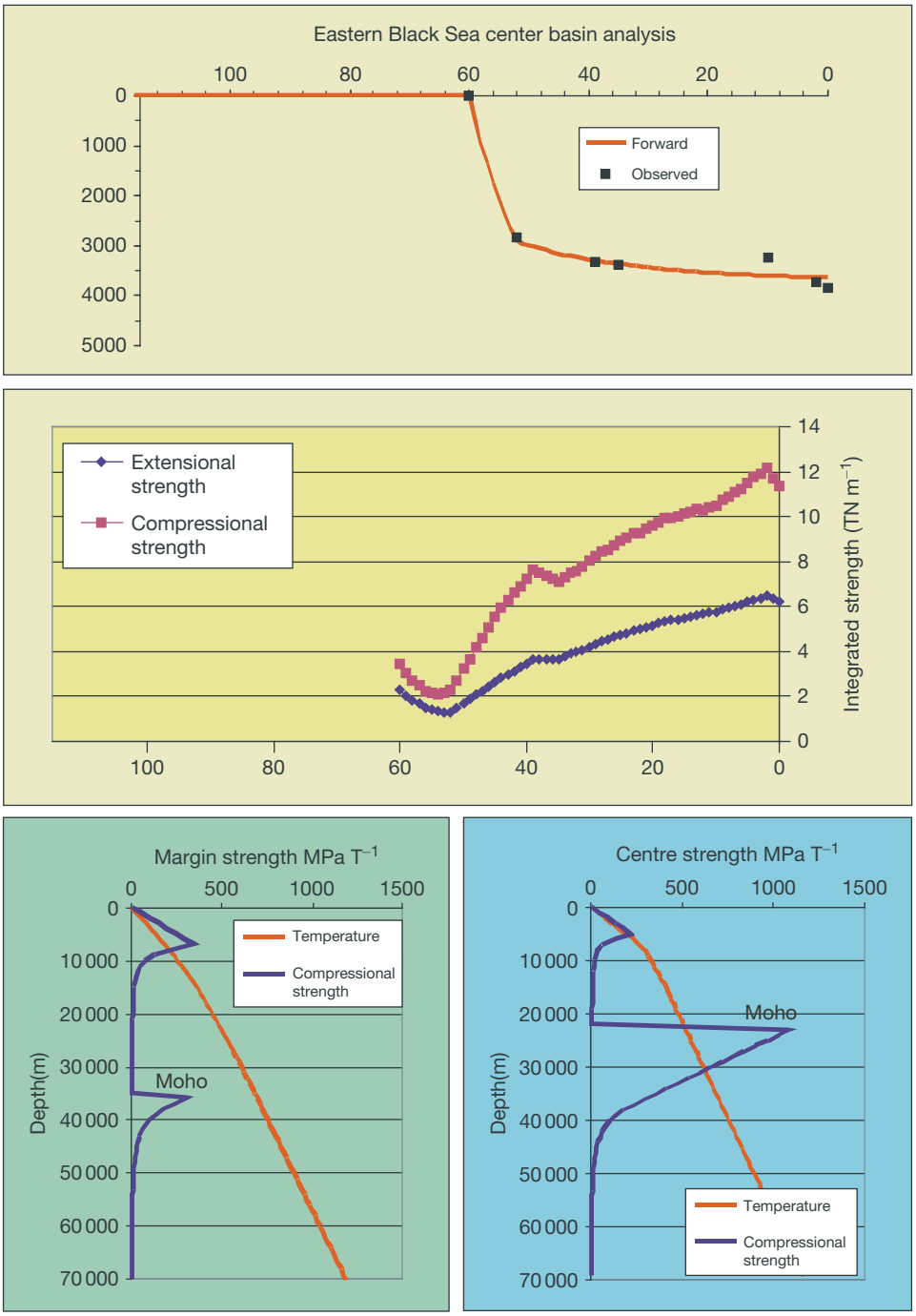

Figure 24 Comparison of observed and forward modeled tectonic subsidence for the eastern Black Sea basin center. Automated backstripping yields an estimated stretching factor of 2.3 (upper panel). Postrift cooling leads in time to a significant increase in the predicted integrated strength for both compressional and extensional regimes (middle panel 1 TN m^{-1} = 10^{12} N m^{-1}). Present-day lithospheric strength profiles calculated for the center and margin of the eastern Black Sea show with depth a pronounced difference (bottom panels). Reproduced from Cloetingh S, Spadini G, Van Wees JD, and Beekman F (2003) Thermo-mechanical modelling of Black Sea Basin (de)formation. *Sedimentary Geology* 156: 169–184.

Black Sea is much higher than its initial strength as the blanketing effect of its up to 12 km thick sedimentary fill is less pronounced and as water depths are greater.

The western Black Sea center is marked by a thermomechanical age of around 100 My with rheological modeling indicating mechanical decoupling of the crust and lithospheric mantle (see Figures 23 and 24). These models imply an EET of at least 40 km (Burov and Diament, 1995) and folding wavelengths of 100–200 km for the mantle and 50–100 km for the upper crust (Cloetingh et al., 1999). For the eastern Black Sea, a probably significantly younger thermomechanical lithospheric age of 55 My implies an EET of no more than 25 km and indicates mantle folding at wavelengths of 100–150 km and a crustal folding wavelength similar to the western Black Sea.

The large dimension of the preexisting rift basin causes during the late stages of inversion a pronounced increase in the wavelength of the stress-induced downwarp (Cloetingh et al., 1999; Munteanu et al., 2011). This effect has been observed in the North Sea basin (Van Wees and Cloetingh, 1996) and the Pannonian Basin (Horváth and Cloetingh, 1996), both of which are characterized by large sediment loads and a wide rift basin. This provides an alternative to previous explanations for recent differential motions in the northern Black Sea basin (Smolyaninova et al., 1996) that were attributed to convective mantle flow.

6.12.3.7.2 Pannonian–Transylvanian Basin system

The Pannonian–Transylvanian Basin system is surrounded by the Carpathian and Dinaridic orogens (**Figure 25**) and has been the focus of major research efforts integrating a wide range of geophysical and geologic data, thus representing a key area for quantitative basin studies and the study of the dynamics of basin–orogen interaction (see Cloetingh et al., 2006; Horváth et al., 2006; Neubauer et al., 1997; Schmid et al., 2008, for recent reviews). A vast geophysical and geologic database has been established during the last decades as a result of major international research collaborations in this area, largely carried out in the framework of European programs such as the EU Integrated Basin Studies project (Cloetingh et al., 1995b; Durand et al., 1999), the EUROPROBE–PANCARDI (Decker et al., 1998) programs, the Peri-Tethys Programme (Brunet and Cloetingh, 2003; Ziegler and Horváth, 1996b; Ziegler and Roure, 1996), and more recently the ESF EUROCORES TOPO-EUROPE initiative and its dedicated subprojects, such as the Source–Sink and TOPO-Alps projects (Cloetingh et al., 2007; Matenco et al. (2013)).

An important asset of this natural laboratory is the high-quality constraints both on the evolution of Neogene basins such as the Pannonian or Transylvanian Basins and on the mechanics of surrounding orogens (see Cloetingh et al., 2006; Horváth et al., 2006; Leever et al., 2011; Matenco et al., 2010). A focal area has been the Vrancea seismogenic area of the SE Carpathians that displays a high-velocity teleseismic intermediate mantle anomaly commonly related to the rapid rollback evolution of a slab inherited from the evolution of the Alpine Tethys (e.g., Cloetingh et al., 2004; Ismail-Zadeh et al., 2012; Martin and Wenzel, 2006, and references therein). This anomalous seismicity can be related with significant recent tectonic activity and associated natural hazards (e.g., Cloetingh et al., 2005a,b; Matenco et al., 2007; Merten et al., 2010; Necea et al., 2005).

In the Pannonian–Transylvanian Basin system, extensive industrial reflection-seismic coverage and well data acquired in the context of petroleum exploration and surface studies permitted to construct a high-resolution kinematic, structural, sedimentologic, and stratigraphic framework (e.g., Bada et al., 2007; Horváth et al., 2006; Krezsek and Bally, 2006; Krezsek et al., 2010; Matenco and Radivojević, 2012; Sacchi et al., 1999; Sztanó et al., 2013; Tari et al., 1999; Tilita et al., 2013; Vasiliev et al., 2010) that set the stage for numerical and analog modeling (e.g., Bada et al., 1998; Dombradi et al., 2010; Jarosinski et al., 2011).

The Pannonian–Carpathian system, therefore, permits to test models for the development of sedimentary basins and their subsequent deformation and for ongoing continental collision. The lithosphere of the Pannonian Basin is a particularly sensitive recorder of changes in lithospheric stress induced by near-field intraplate and far-field plate boundary processes (Bada et al., 2001).

6.12.3.7.2.1 Neogene development and evolution of the Pannonian Basin

The Pannonian Basin of central Europe (**Figure 25**) is a classical extensional back-arc basin formed during Miocene times in

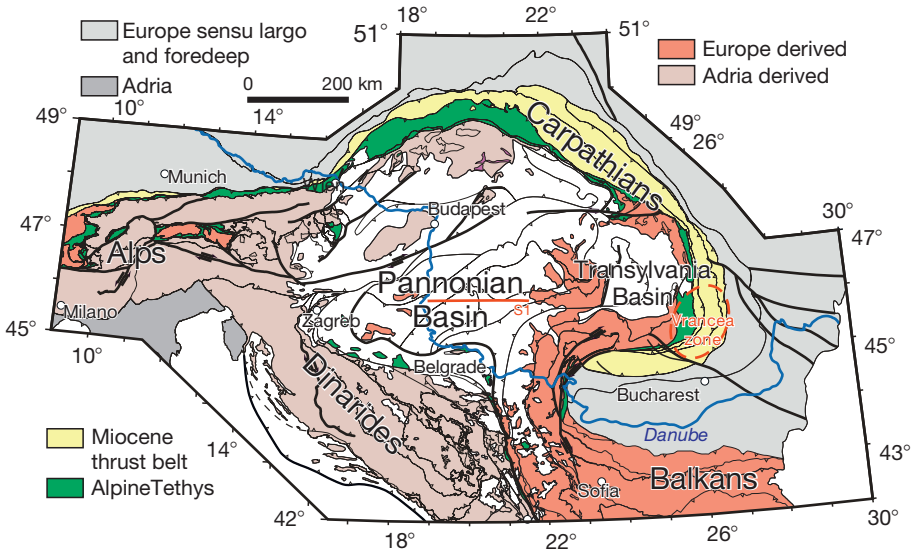

Figure 25 Tectonic map of the Alpine–Carpathian–Dinaridic system with the extent of the large Pannonian and Transylvanian back-arc basins and the location of other Miocene basins superposed over the Dinarides and Carpathians structures. Red line S1 indicates location of transect shown in Figure 28. Reproduced from Matenco L and Radivojević D (2012) On the formation and evolution of the Pannonian Basin: Constraints derived from the structure of the junction area between the Carpathians and Dinarides. *Tectonics* 31: TC6007 and Schmid SM, Bernoulli D, Fugenschuh B, et al. (2008) The Alpine-Carpathian-Dinaridic orogenic system: Correlation and evolution of tectonic units. *Swiss Journal of Geosciences* 101: 139–183.

response to the rapid rollback of a slab attached to the European continent, which is still underlain by highly thinned continental lithosphere (e.g., Balla, 1986; Cloetingh et al., 2006; Horváth, 1993; Horváth et al., 2006; Royden, 1988a,b). The rollback is partly responsible for the creation of the highly arcuate geometry of the Carpathian Mountains (e.g., Matenco et al., 2010), a process that is common with many other Mediterranean orogens (e.g., Faccenna et al., 2004; Jolivet and Faccenna, 2000). The Pannonian Basin is spatially juxtaposed over an orogenic area that formed in Cretaceous–Paleogene times in response to the subduction and closure of a number of oceanic domains that were kinematically linked with the evolution of the larger Alpine Tethys and Neo-Tethys oceans (e.g., Csontos and Voros, 2004; Schmid et al., 2008). Evolutionary models of the Pannonian Basin assume the onset of extension at ~20 Ma, subsequently followed by a peak tectonic activity along normal faults during Middle Miocene times, followed by a postrift, thermal-sag phase starting in Late Miocene times (e.g., Tari et al., 1999 and references therein). A latest Miocene–Quaternary contractional event has subsequently overprinted the basin during the translation and counterclockwise rotation of the Adriatic indenter (Bada et al., 2007; Fodor et al., 2005; Horváth, 1995; Horváth and Cloetingh, 1996; Pinter et al., 2005).

6.12.3.7.2.2 Dynamic models of basin formation

Several models have been proposed to explain the dynamics of Neogene rifting in the Pannonian Basin (Bada and Horváth, 2001), which take into account such prominent features of the Pannonian–Carpathian system as thinned and hot versus thickened and colder lithosphere in its central and peripheral sectors, respectively. Some of these models have proposed the presence of a mantle diapir beneath the intra-Carpathian area. Other models proposed rifting as the driving mechanism for the Pannonian Basin (Horváth et al., 1975), attributed to thermal thinning of the Pannonian lithosphere in response to upwelling of the mantle above the subducted European and Adriatic lithospheric slabs that dip beneath the Pannonian domain.

At a different scale and with a different mechanical behavior, the plume model has been also recently inferred by Burov and Cloetingh (2010) to be responsible for the formation of the asthenospheric upwelling beneath the Pannonian Basin and the initiation of subduction in neighboring Carpathian and Dinaridic orogens.

Other models stress the back-arc position of the Pannonian domain with respect to the Carpathian arc and postulate that gravity-driven passive rollback of the subducting European lithospheric slab is the driving force for the tensional subsidence of the Pannonian Basin (e.g., Csontos, 1995; Csontos et al., 1992; Horváth, 1993; Linzer, 1996; Royden and Horváth, 1988; Royden and Karner, 1984). In a modification of this model, eastward mantle flow is thought to control rollback of the subducted slab and related retreat of its hinge line.

Based on thermomechanical finite element modeling, Huismans et al. (2001b) were able to simulate temporal changes in rifting style in the Pannonian Basin, suggesting a two-phase evolutionary scheme for the system. According to their model, the initial early Middle Miocene basin subsidence was driven mainly by passive rifting in response to rollback of the subducted Carpathian slab, involving gravitational collapse of the thickened prerift Pannonian lithosphere. This triggered small-scale convective upwelling of the asthenosphere that has favored the late-stage thermal subsidence (Horváth, 1993) and the compressional inversion of the Pannonian domain during Late Miocene–Pliocene times (e.g., Bada et al., 1999; Fodor et al., 2005).

Another category of models involves lithospheric mantle instabilities for the formation of the asthenospheric up rise beneath the Pannonian Basin and the high-velocity anomalies observed by teleseismic tomography in neighboring orogens (e.g., Dando et al., 2011; Gemmer and Houseman, 2007; Houseman and Gemmer, 2007; Ren et al., 2012). These models assume a convective mantle removal beneath the Pannonian Basin, correlated with high heat flow and interpreted as upwelling asthenosphere correlated with a fast anomaly extending outward as far as the Carpathians, the Dinarides, and the Eastern Alps. This higher velocity mantle material is interpreted as being produced by a mantle downwelling, whose detachment from the lithosphere above may have triggered the extension of the Pannonian Basin.

6.12.3.7.2.3 Stretching models and subsidence analysis

Sclater et al. (1980) were the first to apply the stretching model of McKenzie (1978) to the intra-Carpathian basins. They found that the development of peripheral basins could be fairly well simulated by the uniform pure shear extension concept with a stretching factor of about 2. For the more centrally located basins, however, their considerable thermal subsidence and high heat flow suggested unrealistically high stretching factors up to 5. Thus, they postulated differential extension of the Pannonian lithosphere with moderate crustal stretching (δ factor) and larger stretching of the lithospheric mantle (β factor). Building on this and using a wealth of well data, Royden et al. (1983) introduced the nonuniform stretching concept according to which the magnitude of lithospheric thinning is depth-dependent. This concept accounts for a combination of uniform mechanical extension of the lithosphere and thermal attenuation of the lithospheric mantle (Ziegler, 1992, 1996b; Ziegler and Cloetingh, 2004). This is compatible with the subsidence pattern and thermal history of major parts of the Pannonian Basin that suggest a greater attenuation of the lithospheric mantle as compared to the finite extension of the crust. Horváth et al. (1988) further improved this concept by considering radioactive heat generation in the crust and the thermal blanketing effect of basin-scale sedimentation. By reconstructing the subsidence and thermal history, and by calculating the thermal maturation of organic matter in the central region of the Pannonian Basin (Great Hungarian Plain), a major step forward was made in the field of hydrocarbon prospecting by means of basin analysis techniques.

These studies highlighted difficulties met in explaining basin subsidence and crustal thinning in terms of uniform extension and point toward the applicability of anomalous subcrustal mantle thinning. This issue was central to subsequent investigations involving quantitative subsidence analyses (backstripping) of an extended set of Pannonian Basin wells and cross sections and their forward modeling (Juhász et al., 1999; Lankreijer et al., 1995; Lenkey, 1999; Sachsenhofer et al., 1997). Kinematic modeling, incorporating the concept of necking depth and finite strength of the lithosphere during and after rifting (Van Balen et al., 1999), as well as dynamic modeling studies (Huismans et al., 2001b), suggested that the

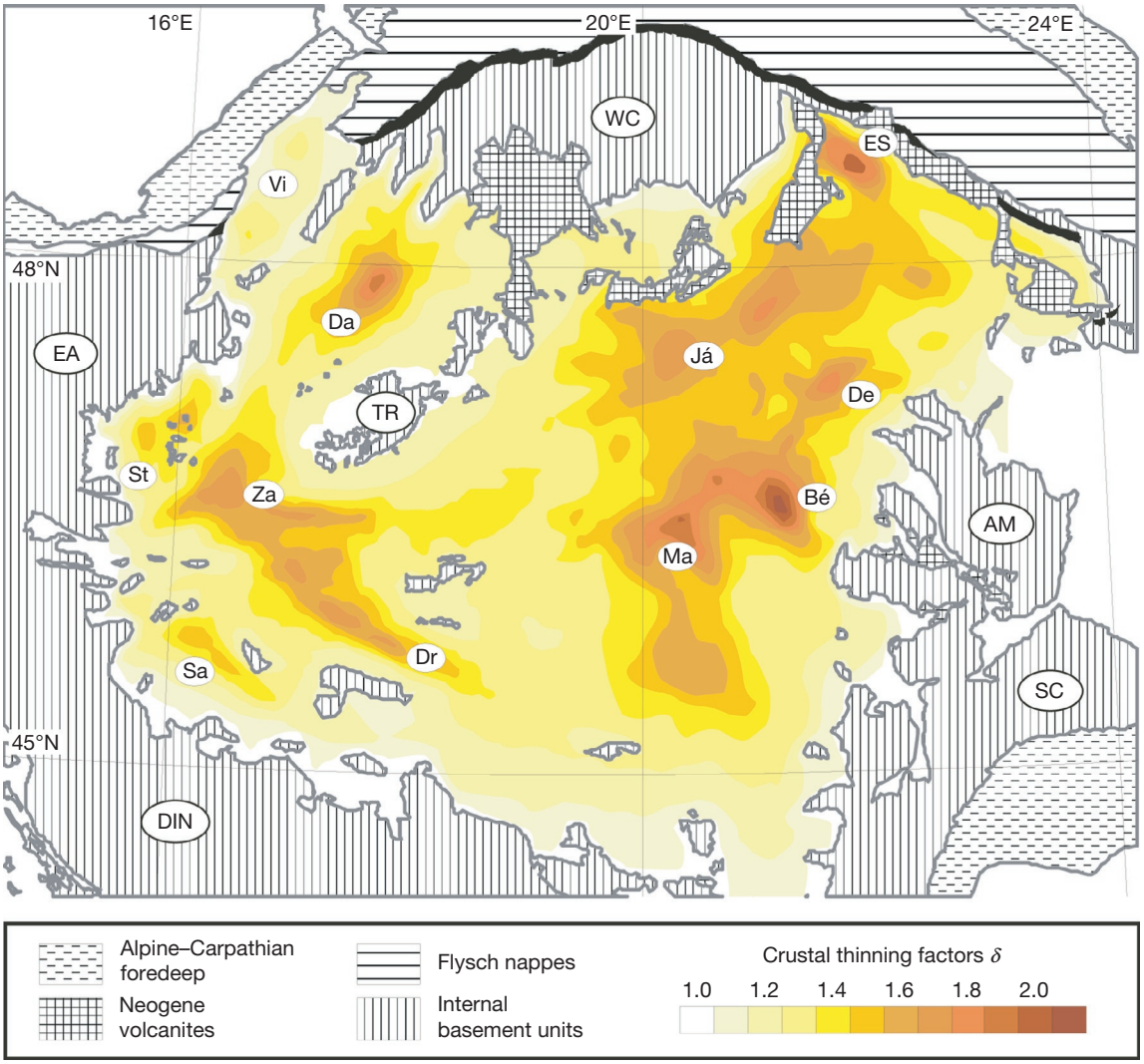

Figure 26 Crustal thinning factors calculated by forward modeling for the Pannonian Basin applying the nonuniform stretching concept and taking the effects of lateral heat flow and flexure of the lithosphere into account. Note the pronounced lateral variations in crustal extension controlling the development of deep subbasins separated by areas of limited deformation. AM, Apuseni Mts.; DIN, Dinarides; EA, Eastern Alps; TR, Transdanubian Range; SC, WC, Southern and Western Carpathians, respectively. Local depressions of the Pannonian Basin system: Be, Békés; Da, Danube; De, Derecske; Dr, Drava; ES, East Slovakian; Ja, Jászság; Ma, Makó; Sa, Sava; St, Styrian; Vi, Vienna; Za, Zala. Reproduced from Lenkey L (1999) Geothermics of the Pannonian Basin and Its Bearing on the Tectonics of Basin Evolution, 215 pp. PhD Thesis, VU University, Amsterdam.

transition from passive to active rifting was controlled by the onset of subcrustal flow and small-scale convection in the asthenosphere. In order to quantify basin-scale lithospheric deformation, Lenkey (1999) carried out forward modeling applying the concept of nonuniform lithospheric stretching and taking into account the effects of lateral heat flow, flexure, and necking of the lithosphere. Calculated crustal thinning factors (δ) indicate large lateral variation of crustal extension in the Pannonian Basin (**Figure 26**). This is consistent with the areal pattern of the depth to the pre-Neogene basement (Horváth et al., 2006). The indicated range of crustal thinning factors of 10–100% crustal extension is in good agreement with the prerift palinspastic reconstruction of the Pannonian Basin and the amount of cumulative shortening in the Carpathian orogen (e.g., Fodor et al., 1999; Roure et al., 1993).

As a major outcome of basin analysis studies, Royden et al. (1983) provided a two-stage subdivision for the evolution of the Pannonian Basin with a synrift (tectonic) phase during Early to Middle Miocene times and a postrift thermal subsidence phase during the Late Miocene–Pliocene. Further development of the stratigraphic database, however, demonstrated the need to refine this scenario. According to Tari et al. (1999), the regional Middle Badenian unconformity, marking the termination of the synrift stage, is followed by a postrift phase that is characterized by only minor tectonic activity. Nevertheless, the subsidence history of the Pannonian Basin can be subdivided into three main phases that are reflected in the subsidence curves of selected subbasins (**Figure 27**). The initial synrift phase is characterized by rapid tectonic subsidence, starting synchronously at about 20 Ma in the entire Pannonian Basin. This phase of pronounced crustal extension is recorded everywhere in the basin system and was mostly limited to relatively narrow, fault-bounded grabens or subbasins. During the subsequent postrift phase, much broader areas began to subside, reflecting

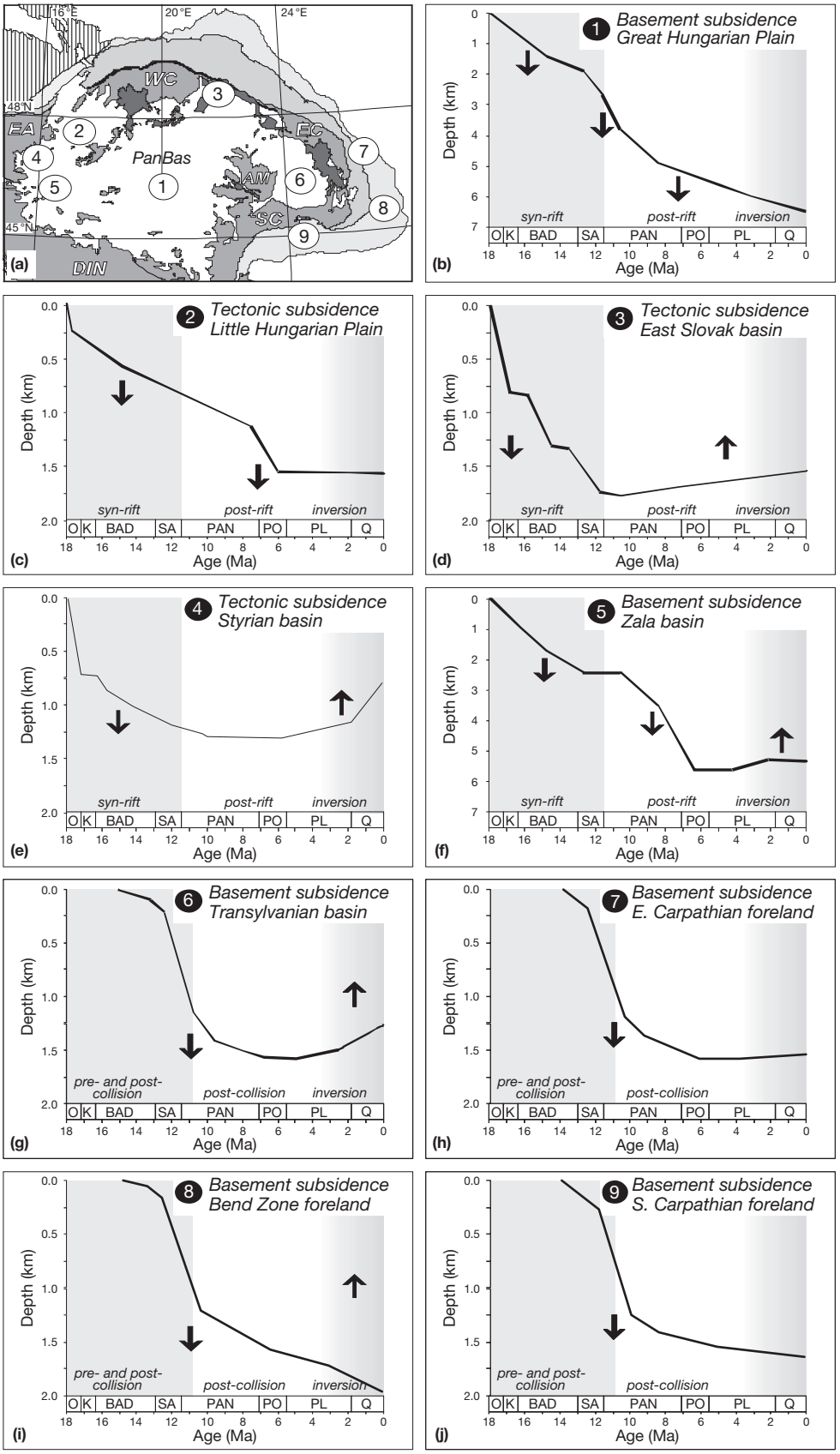

Figure 27 Subsidence curves for selected subbasins of the Pannonian Basin and the Carpathian foreland. Note that after a rapid phase of general subsidence throughout the entire Pannonian Basin, the subbasins show distinct subsidence histories from Middle Miocene times onward. Arrows indicate generalized vertical movements. O, K, Ottnangian and Karpatian, respectively (Early Miocene); BAD, SA, Badenian and Sarmatian, respectively (Middle Miocene); PAN, PO, Pannonian and Pontian, respectively (Late Miocene); PL, Pliocene; Q, Quaternary. AM, Apuseni Mts.; DIN, Dinarides; EA, Eastern Alps; PanBas, Pannonian Basin; SC, WC, Southern and Western Carpathian foreland basins, respectively. Reproduced from Cloetingh S, Bada G, Matenco L, Lankreijer A, Horváth F, and Dinu C (2006). Thermo-mechanical modelling of the Pannonian-Carpathian system: Modes of tectonic deformation, lithospheric strength and vertical motions. In: Gee D and Stephenson R (eds.) *European Lithosphere Dynamics*, Geological Society, London, Memoirs 32: 207–221.

general downwarping of the lithosphere in response to its thermal subsidence. This is particularly evident in the central parts of the Pannonian Basin, suggesting that in this area, synrift thermal attenuation of the lithospheric mantle played a greater role than in the marginal areas (e.g., Royden and Dövényi, 1988; Sclater et al. (1980)). The third and final phase of basin evolution is characterized by the gradual structural inversion of the Pannonian Basin system during the Late Pliocene–Quaternary. During these times, intraplate compressional stresses gradually built up and caused basin-scale buckling of the Pannonian lithosphere that was associated with late-stage subsidence anomalies and differential vertical motions (Horváth and Cloetingh, 1996). As evident from subsidence curves (**Figure 27**), accelerated late-stage subsidence characterized the central depressions of the Little and Great Hungarian Plains (**Figure 27(b)** and **27(c)**), whereas the peripheral Styrian and East Slovakian subbasins were uplifted by a few hundred meters after mid-Miocene times (**Figure 27(d)** and **27(e)**) and the Zala basin during the Pliocene–Quaternary (**Figure 27(f)**). The importance of tectonic stresses, during both the rifting phase (extension) and subsequent inversion phase (compression), is highlighted by this late-stage tectonic reactivation, as well as by other episodic inversion events in the Pannonian Basin (Fodor et al., 1999; Horváth, 1995).

A more recent analysis of the subsidence evolution of the Pannonian Basin in the sector connecting the Carpathians with the Dinarides has observed significant discrepancies with the aforementioned models by analyzing the development of syn- and postrift sedimentation (Matenco and Radivojević, 2012). This study has documented large-scale erosional unconformities between the classically defined syn- and postrift phases that migrate in time from the Dinarides to the Carpathians, while the postrift deposition for the Early and Middle Miocene rifting is largely missing (**Figure 28**). Therefore, these authors propose that the low-angle Early–Middle Miocene normal faults responsible for the basin formation are connected to a lower crustal detachment that was prolonged eastward beneath the Apuseni Mountains and affected the mantle–lithosphere below the Transylvanian Basin. The coupling between the mechanical extension of the Pannonian Basin and its thermal effects recorded in the Transylvanian Basin should have taken place in such a way that the intervening Apuseni Mountains did not underwent any significant Miocene vertical movements. The related exhumation and large-scale domal structure is mainly the effect of Cretaceous–Paleogene deformations (Merten et al., 2011). In contrast to earlier periods of extension, massive thermal-sag sedimentation is observed in direct relationship with and postdating the Pannonian–Lower Pontian detachments and/or normal faults (such as the Makó depression, **Figure 28**). The main depocenters of the thermal-sag sedimentation overlie these asymmetrical extensional structures. Furthermore, this thermal-sag sedimentation has a far larger areal extent than one of the half-grabens, covering an area that corresponds to the asthenospheric up rise presently observed beneath the Pannonian Basin (Horváth et al., 2006; Matenco and Radivojević, 2012).

These studies demonstrated the close relationship that existed between the timing and the nature of stress changes in extensional basins and structural episodes in the surrounding thrust belts, pointing to mechanical coupling between the orogen and its back-arc basin. In parallel, significant efforts have been devoted to reconstruct the spatial and temporal variations in thrusting along the Carpathian orogen (Matenco and Bertotti, 2000; Matenco et al., 2007; 2010; Roure et al., 1993; Schmid et al., 1998) and its relationship to foredeep depocenters (Cloetingh et al., 2005a,b; Matenco et al., 2003; Meulenkamp et al., 1996; Necea et al., 2005; Tarapoanca et al., 2004), changes in foreland basin geometry, and lateral variations in the flexural rigidity of the foreland lithosphere.

6.12.3.7.2.4 Lithospheric strength in the Pannonian–Carpathian system

The Pannonian–Carpathian system shows remarkable variations in crustal thickness (**Figure 29**) and thermomechanical properties of the lithosphere. Lithospheric rigidity varies in space and time, giving rise to important differences in the tectonic behavior of different parts of the system. As rheology controls the response of the lithosphere to stresses, and thus the formation and deformation of basins and orogens, the characterization of rheological properties and their temporal changes has been a major challenge to constrain and quantify tectonic models and scenarios. This is particularly valid for the Pannonian–Carpathian region where tectonic units with a different history and rheological properties are in close contact.

By conversion of strength predictions to EET values at a regional scale, Lankreijer (1998) mapped the EET distribution for the entire Pannonian– Carpathian system (**Figure 30**). Calculated EET values are largely consistent with the spatial variation of lithospheric strength of the system. Lower values are characteristic for the weak central part of the Pannonian Basin

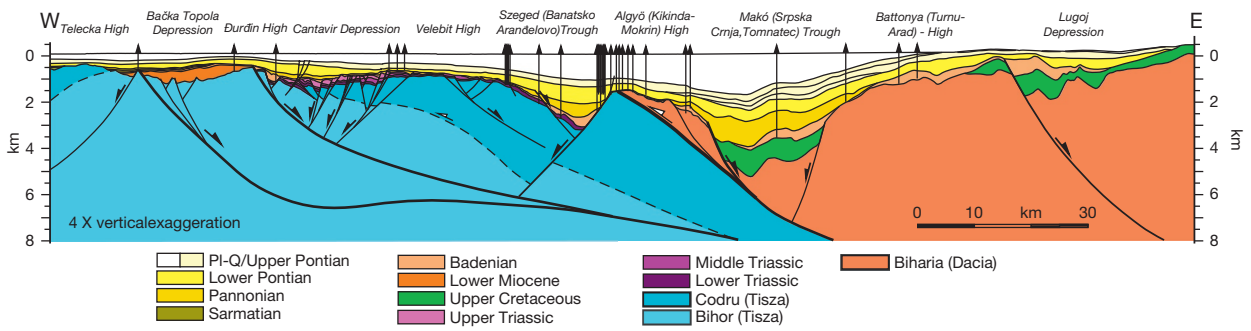

Figure 28 Depth converted regional transects over the Pannonian Basin of Serbia and Romania. Location of the transect is indicated in Figure 25. Reproduced from Matenco L and Radivojević D (2012) On the formation and evolution of the Pannonian Basin: Constraints derived from the structure of the junction area between the Carpathians and Dinarides. *Tectonics* 31: TC6007.

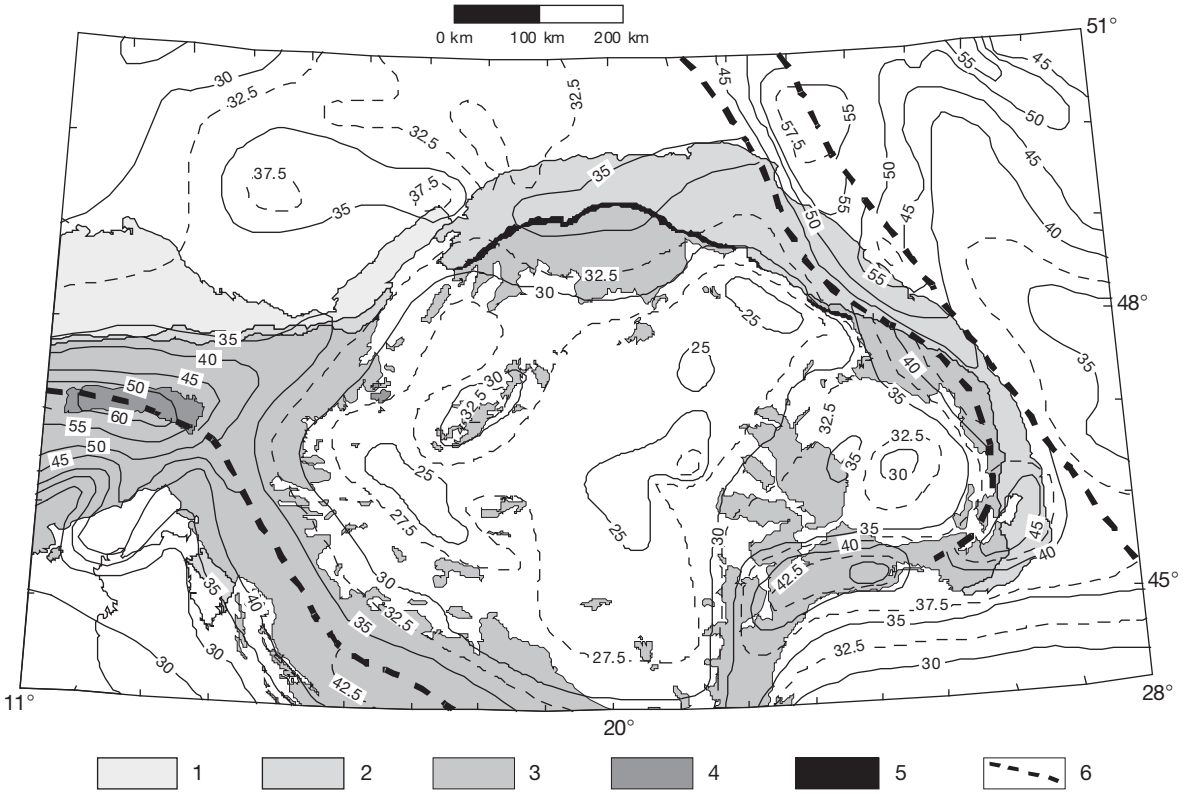

Figure 29 Crustal thickness in the Pannonian Basin and the surrounding mountains. Values are given in km. 1, foreland (molasse) foredeep; 2, flysch nappes; 3, pre-Tertiary units on the surface; 4, Penninic windows; 5, Pieniny Klippen Belt; 6, trend of abrupt change in crustal thickness. Reproduced from Horváth F, Bada G, Szafián P, Tari G, Ádám A, and Cloetingh S (2006) Formation and deformation of the Pannonian Basin: Constraints from observational data. *Geological Society, London, Memoir* 32: 191–206.

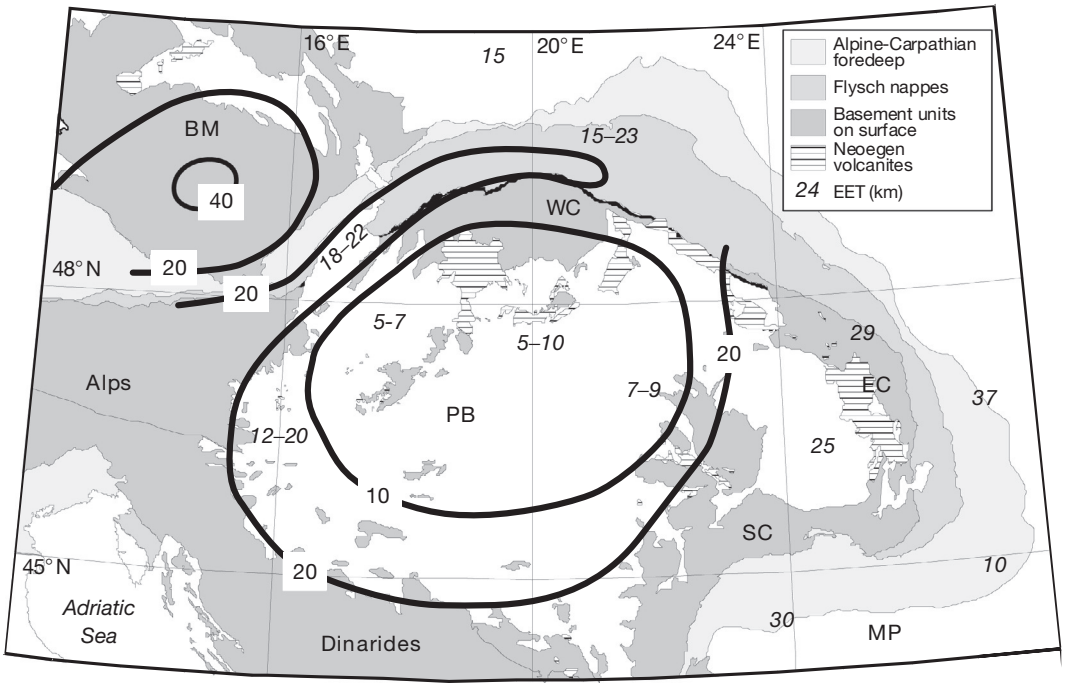

Figure 30 Effective elastic thickness (EET – in km) of the lithosphere in and around the Pannonian Basin predicted from rheological calculations. BM, Bohemian Massif; MP, Moesian Platform; PB, Pannonian Basin; EC, SC, WC, Eastern, Southern, and Western Carpathians, respectively. Reproduced from Lankreijer AC (1998) Rheology and Basement Control on Extensional Basin Evolution in Central and Eastern Europe: Variscan and Alpine-Carpathian-Pannonian Tectonics, 158 pp. PhD Thesis. VU University, Amsterdam.

(5–10 km), whereas EET increases toward the Dinarides and Alps (15–30 km) and particularly toward the Bohemian Massif and Moesian Platform (25–40 km). This trend is in good agreement with EET estimates obtained from flexural studies and forward modeling of extensional basin formation. Systematic differences, however, can occur and may be the consequence of significant horizontal intraplate stresses (e.g., Cloetingh and Burov, 1996) or of mechanical decoupling of the upper crust and uppermost mantle that can lead to a considerable reduction of EET values.

The range of calculated EET values reflects the distinct mechanical characteristics and response of the different domains forming part of the Pannonian–Carpathian system to the present-day stress field. These characteristics can be mainly attributed to the memory of the lithosphere. In this respect, it must be kept in mind that the tectonic and thermal evolution of these domains differed considerably during the Cretaceous–Neogene Alpine development of both the outer and the intra-Carpathian units and the Neogene extension of the Pannonian Basin, resulting in a wide spectrum of lithospheric strengths. These, in turn, exert a strong control on the complex present-day pattern of ongoing tectonic activity.

6.12.3.7.2.5 Deformation of the Pannonian–Carpathian system

The present-day deformation pattern and related topography development in the Pannonian–Carpathian system is characterized by pronounced spatial and temporal variations in the stress and strain fields (Figure 31; e.g., Cloetingh et al., 2006). Horváth and Cloetingh (1996) established the importance of Late Pliocene and Quaternary compressional deformation of the Pannonian Basin that explains its anomalous uplift and subsidence, as well as intraplate seismicity. Based on the case study of the Pannonian–Carpathian system, these authors established a novel conceptual model for the structural reactivation of back-arc basins within orogens. At present, the Pannonian Basin has reached an advanced evolutionary stage as compared to other Mediterranean back-arc basins (e.g., Bache et al., 2010) in so far as it has been partially inverted during the last few million years. Inversion of the Pannonian Basin can be related to temporal changes in the regional stress field, from one of tension that controlled its Miocene extensional subsidence to one of Pliocene–Quaternary compression resulting in deformation, contraction, and flexure of the lithosphere associated with differential vertical motions.

Model calculations are in good agreement with the overall topography of the system (Figure 31). Several flat-lying, low-elevation areas (e.g., Great Hungarian Plain and Sava and Drava troughs) subsided continuously since the Early Miocene beginning of basin development and contain 300–1000 m thick Quaternary alluvial sequences. By contrast, the periphery of this basin system, as well as the Transdanubian Range, the Transylvanian Basin and the adjacent Carpathians underwent late-stage uplift. Therefore, the spatial distribution of uplifting and subsiding areas within the Pannonian Basin can be interpreted as resulting from the buildup of intraplate compressional stresses, causing large-scale positive and negative

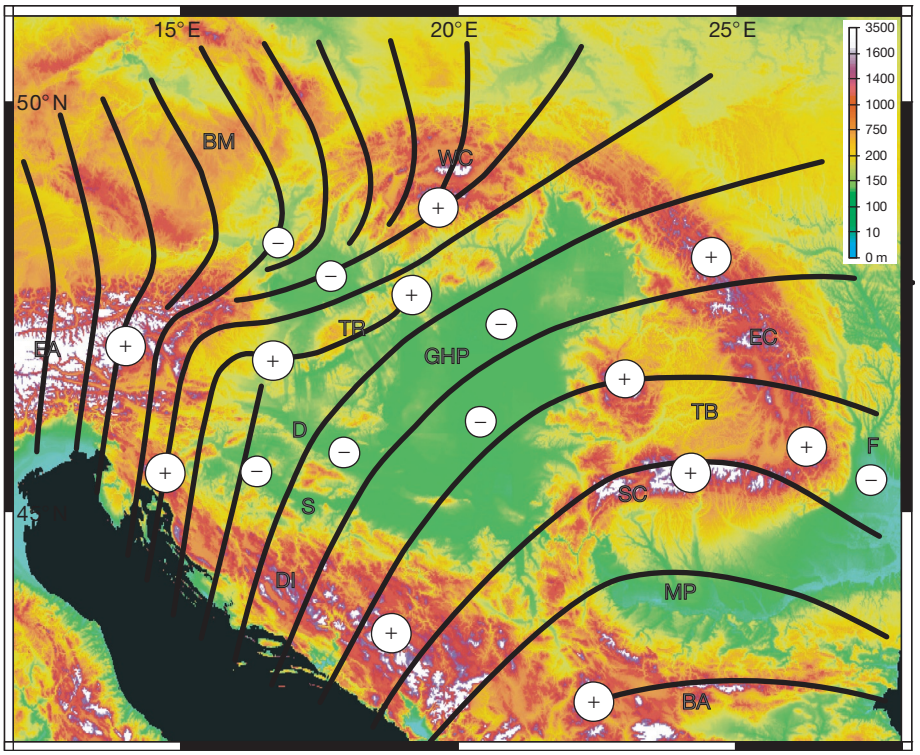

Figure 31 Topography of the Pannonian–Carpathian system showing present-day maximum horizontal stress (SHmax) trajectories (Reproduced from Bada G, Horváth F, Cloetingh S, Coblentz DD, and Toth T (2001) Role of topography-induced gravitational stresses in basin inversion: The case study of the Pannonian basin. *Tectonics* 20: 343–363). '+' and '–' symbols denote areas of Quaternary uplift and subsidence, respectively. BA, Balkanides; BM, Bohemian Massif; D, Drava trough; DI, Dinarides; EA, Eastern Alps; EC, Eastern Carpathians; F, Focşani Depression; MP, Moesian Platform; PB, Pannonian Basin; S, Sava trough; SC, Southern Carpathians; TB, Transylvanian Basin; TR, Transdanubian Range; WC, Western Carpathians. Reproduced from Cloetingh et al. (2006).

deflection of the lithosphere at various scales. This includes basin-scale positive reactivation of Miocene normal faults, and large-scale folding of the system leading to differential uplift and subsidence of anticlinal and synclinal segments of the orogen which were uplifted and considerably eroded from Late Miocene–Pliocene time onward (see **Figure 31**). Quantitative subsidence analyses confirm that late-stage compressional stresses caused accelerated subsidence of the central parts of the Pannonian Basin (Van Balen et al., 1999), while the Styrian Basin (Sachsenhofer et al., 1997), the Vienna and East Slovakian Basins (Lankreijer et al., 1995), and the Transylvanian Basin (Ciulavu et al., 2002) were uplifted by several hundred meters starting in Late Miocene–Pliocene times (**Figure 31**). The mode and degree of coupling of the Carpathians and Dinarides with their foreland control the Pliocene to Quaternary deformation patterns in their hinterland in the Pannonian–Transylvanian Basins (Ciulavu et al., 2002; Dombradi et al., 2007; Jarosinski et al., 2011). These findings can be related to the results of seismic tomography that highlight upwelling of hot mantle material under the Pannonian Basin and progressive detachment of the subducted lithospheric slab that is still ongoing in the Vrancea area (Wenzel et al., 2002; Wortel and Spakman, 2000).

In summary, results of forward basin modeling show that an increase in the level of compressional tectonic stress during Pliocene–Quaternary times can explain the first-order features of the observed pattern of accelerated subsidence in the center of the Pannonian Basin and uplift of basins in peripheral areas. Therefore, both observations and modeling results lead to the conclusion that compressional stresses can cause considerable differential vertical motions in the Pannonian–Carpathian back-arc basin–orogen system (Dombradi et al., 2007; Horváth et al., 2006; Jarosinski et al., 2011).

6.12.4 Compressional Basin Systems

In this section, we discuss basic concepts and observations for large-scale compressional basin systems. In doing so, we focus on flexural foreland basins (**Section 6.12.4.1**) and basins initiated by lithospheric folding (**Section 6.12.4.2**).

Flexural foreland basins are dynamic systems that provide key information on the interplay between lithospheric and surface processes (see also Garcia-Castellanos and Cloetingh, 2012, for a recent review). Their evolution can be constrained by various types of observations, including structural, paleogeographic, sedimentologic, paleoclimatic, potential field (gravity and geoid), and seismic data. These data allow extraction of the thermomechanical properties of the underlying continental lithosphere and are crucial in reconstruction of continental paleotopography. Flexural isostasy is a simple model and will certainly remain valid and useful as a first approach to isostasy, for example, to study first-order interactions with other processes based on synthetic experiments (e.g., Garcia-Castellanos, 2002; Pelletier, 2007). By their nature, foreland basins are in general undergoing a polyphase evolution, to a large extent conditioned by their overall regional tectonic setting. Of particular importance are the associated temporal and lateral variations in plate rigidity and stress fields. These features explain deviations in their record of vertical motions and basin geometries from predictions from simple foreland flexural models. Lateral variations in lithospheric rigidity are also of significant influence for the drainage history of foreland basins and their connectivity with adjacent back-arcs. Temporal variations in rigidity associated with preorogenic extension have a profound effect on the subsequent foreland basin subsidence. This feature is highly relevant in the context of subsidence histories of retroforedeep basins with a subsidence history strongly deviating from predictions of flexural foredeep models (Naylor and Sinclair, 2008). Flexural forebulges are highly sensitive to changes in tectonic regime and inherited lateral lithospheric heterogeneities and might be enhanced by the progressive viscous relaxation of stresses during and after tectonic loading. Forebulges can in some cases determine the drainage history of the basin. Strong feedbacks exist between lithospheric and surface processes in foreland basins. The integration of numerical and analog modeling (Athmer et al., 2010; Persson et al., 2004) appears to be particularly promising to explore the coupling of tectonics and climate in orogenic foreland basin systems. A different example of inherited properties strongly affecting the basin development is provided by topography. Preflexural topography can not only modify estimates of tectonic load in flexural calculations but also overprint the effects of tectonic vertical motions on drainage development.

Sedimentary basins controlled by lithospheric folding are characterized by a number of features in their basin architecture, subsidence history, thermal evolution, and faulting patterns, making them distinctly different from other basin systems (see also Cloetingh and Burov, 2011, for a recent review). Of particular importance are the relatively short temporal scales involved in their evolution, whereas their spatial scales vary from tens to several hundreds of km, depending on the rheological stratification of the lithosphere and its thermomechanical age. Subsidence patterns are characterized by an acceleration of subsidence in the depocenters during compressional basin formation, occurring simultaneously with accelerated uplift of and erosion from flanking basin highs. In contrast with asymmetrical foreland basins, basins on folded lithosphere are symmetrical with equal dimensions for linearly trending topographic highs and lows. The thermal history of these basins is not characterized by an initial thermal perturbation, unless folding occurs in interaction with plume activity. In the absence of interplay with lithospheric-scale thermal perturbations, their thermal evolution will be primarily controlled by the burial history of the sediments deposited in the accommodation space created by the folding process. Intrabasinal faulting and the formation of pop-up structures and inverted basins at upper crustal levels are important in the structural evolution of these basin systems. The intensity of the brittle deformation peaks with ongoing shortening of the lithosphere during folding, but faulting activity is dramatically reduced after the cessation of folding. At this stage, with equilibrium between sedimentation and erosion, minor faulting occurs as a result of stress relaxation due to erosion of folded highs. During overall uplift of basins on folded lithosphere, their accommodation space is further reduced by unflexing and associated stress release through faulting.

6.12.4.1 Flexural Foreland Basins

Foreland basins owe their existence to the capacity of the lithosphere to support loads, such as the topography of

orogenic wedges or subducted lithospheric slabs (Garcia-Castellanos and Cloetingh, 2012). The lithosphere deforms by flexurally bending downward over areas often exceeding the spatial scale of these loads (Figure 32). The width of the resulting depression, the foreland basin, provides information on the mechanical strength of the underlying lithosphere. Under an imposed load, a zero-strength lithosphere would simply sink vertically into the mantle (Airy isostasy), thus not accounting for the development of a foreland basin. By contrast, a mechanically strong lithosphere, characteristic of cratonic forelands, allows for the subsidence of wide and relatively shallow foreland basins (flexural isostasy). Such wide foreland basins are associated with the Canadian Rocky Mountains of Alberta and British Columbia and the Appalachian fold-and-thrust belts (Figure 33) that are superimposed on the North American Proterozoic cratonic crust (e.g., Beaumont, 1981; Quinlan and Beaumont, 1984). By contrast, the much narrower Alpine foreland basins of Europe (Figure 33; Mascle, 1998) developed on considerably younger lithosphere that equilibrated with the asthenosphere after the Variscan orogeny and was modified by Mesozoic rifting activity. The time elapsed between rifting and the synorogenic flexural deformation of this foreland lithosphere was very variable (Pyrenees: *c*.30 Ma; Apennines: *c*.130 Ma). The relatively modest widths of the foreland basins of the Carpathians (Matenco et al., 1997a,b; Zoetemeijer et al., 1999), Pyrenees (Millan et al., 1995), the Betic Cordillera (Van der Beek and Cloetingh, 1992), the Apennines (Zoetemeijer et al., 1993), and the Eastern Alps (Andeweg and Cloetingh, 1998) reflect a relatively weak lithosphere.

In addition to topographic loading by orogenic wedges and loading by the sedimentary fill of the foreland basins, additional forces operate on the lithosphere, such as slab pull, slab detachment, and slab rollback, and play an important role in shaping the geometry of prowedge and retrowedge foreland basins (Figure 34; e.g., Millan et al., 1995; Ziegler et al., 2002). Moreover, depending on mechanical coupling/decoupling of the orogenic wedge and the foreland lithosphere, horizontal compressional stresses can be exerted onto the latter, influencing the geometry of an evolving flexural foreland basin (Ziegler et al., 2002).

In a first generation of flexural foreland basin models, the different loading components and forces were represented by a system of vertical loads, shear forces, and bending moments (Royden, 1988a,b, 1993). This approach is illustrated in Figure 32. A characteristic feature of these models is that horizontal stresses were neglected. Nevertheless, these have been shown to play a potentially important role in the geometry of foreland basins and the architecture of their sedimentary fill (Peper et al., 1995). These models were utilized to extract information on the mechanical properties of the lithosphere that was treated as an elastic plate rather than as a depth-dependent rheologically stratified beam. Consequently, the models yielded rough estimates for the EET of the lithosphere and a first approximation for the bulk rheology of the continents. This approach permitted to examine the effect of the time elapsed since the last

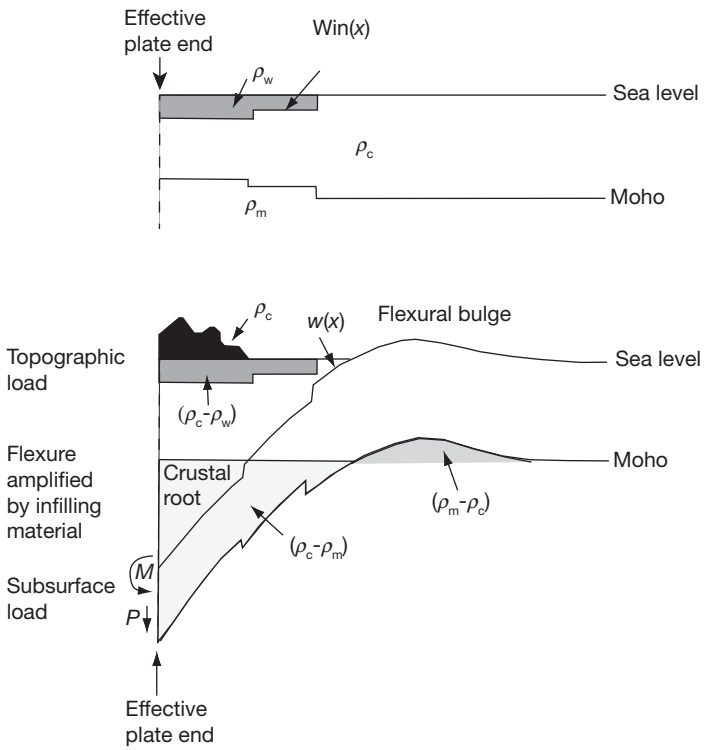

Figure 32 Concept of lithospheric flexure during foreland basin evolution. Deflection of the subducting lower plate lithosphere is the combined result of topographic loading by the mountain chain of the upper plate, the weight of the sediments in the foreland basin, and the weight of the subducted slab. The shape of the flexural foreland depression is controlled by the interplay between the lithospheric strength of the lower plate, the magnitude of the differential loads imposed on it, and the level of collision-related compressional stresses transmitted into it (see also Ziegler et al., 2002). Reproduced from Royden LH (1993) The tectonic expression slab pull at continental convergent boundaries. *Tectonics* 12: 303–325.

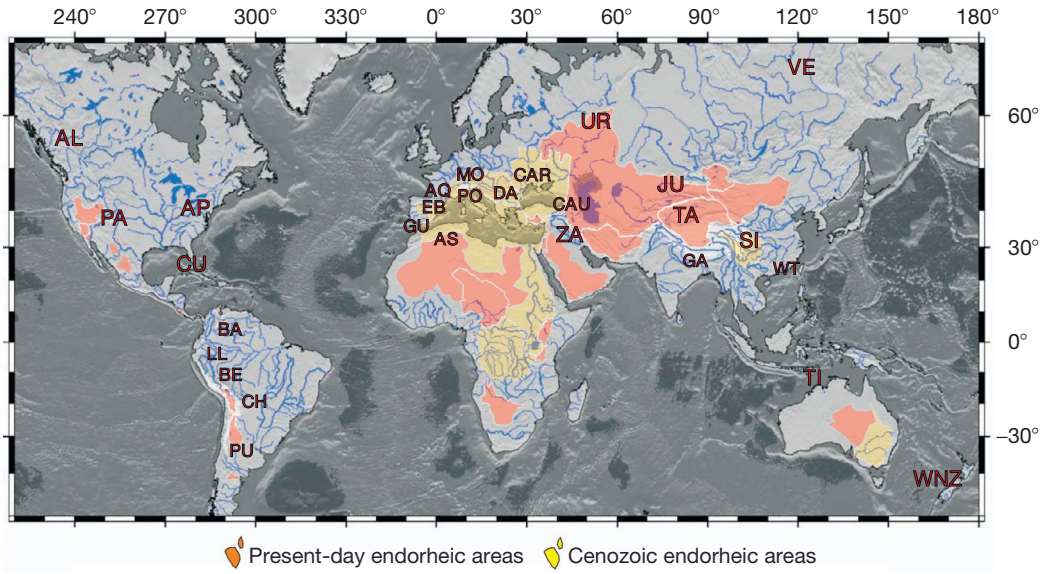

Figure 33 Location of the main foreland basins discussed in this study. Present-day endorheic areas and examples of areas that underwent endorheism during the Cenozoic are indicated by the color shading. Their singularity in terms of sediment transport affects a significant part of these basins. Foreland basins from west to east: AL, Alberta Basin; PA, Paradox Basin; AP, Appalachian; CU, Cuba; LL, Llanos (Andes); BA, Barinas; BE, Beni; CH, Chaco (Andes); PU, Puna (Andes); GU, Guadalquivir (Betics); EB, Ebro (Pyrenees); AQ, Aquitaine; AS, Algerian–Saharan Atlas; MO, Molasse (North Alpine); PO, Po and Piedmont (South Alpine); DA, Dacic Basin (South Carpathian); CAR, Subcarpathian; CAU, Caucasian; ZA, Zagros; UR, Uralian; JU, Junggar; TA, Tarim; GA, Ganges; SI, Sichuan; VE, Verkhoyansk; WT, west Taiwan; TI, Timor; WNZ, West New Zealand. Reproduced from Garcia-Castellanos D and Cloetingh S (2012) Modeling the interaction between lithospheric and surface processes in foreland basins. In: Busby C and Azor A (eds.) *Tectonics of Sedimentary Basins: Recent Advances*, pp 152–181.

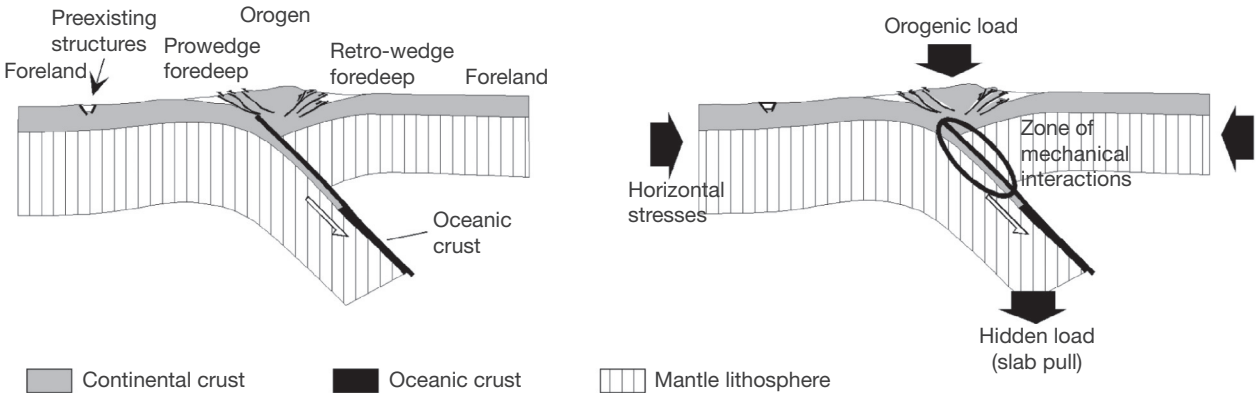

Figure 34 Conceptual model illustrating forces controlling the subsidence of retro- and prowedge foreland basins and showing zone of potential mechanical coupling between the upper and the lower plate. Reproduced from Ziegler PA, Bertotti G, and Cloetingh S (2002) Dynamic processes controlling foreland development Â the role of mechanical (de) coupling of orogenic wedges and forelands. In: *Stephan Mueller Special Publication Series*, vol. 1, 17–56.

thermal perturbation of the lithosphere (generally a rift phase) on its deflection during the subsequent foreland basin development phase. In this respect, Desegaulx et al. (1991) explained the rapid Cenozoic subsidence of the Aquitaine foreland basin (SW France) in terms of preorogenic synrift extensional thinning and associated thermal perturbation of the lithosphere and its postrift thermal subsidence and sedimentary loading.

The term foreland basin was introduced by Dickinson (1974) to refer to thick sediment accumulations in the undeformed areas (*forelands*) bounding orogens resulting from compressional tectonics. He proposed two broad categories: *peripheral foreland basins* related to continent–continent collision (e.g., the Indo-Ganges basin and the North Alpine basin; Figure 33) and *retroarc foreland basins* related to the subduction of oceanic lithosphere (e.g., the late Mesozoic–Cenozoic Rocky Mountain basins). Foreland basins are strongly asymmetric in cross section, with maximum depths next to the orogen and a wedge shape along its passive (undeformed) margin (Allen et al., 1986). Inspired by the early findings of marine geologic and geophysical studies (Vening-Meinesz, 1941), it soon

became widely accepted that foreland basins form primarily by flexural isostatic subsidence of the foreland (plate bending), in response to the growing weight of the tectonic units stacked by shortening in the orogen (Price, 1973). Presently, the weight of sediments and water in the foredeep and horizontal compression, slab pull, and, in the case of slab retreat, lateral asthenospheric push during the opening of the back-arc and delamination of the retreating delaminated mantle–lithosphere are all recognized as important ingredients for driving flexural subsidence in foreland basin settings (**Figure 35**).

More recent modeling studies implementing the initiation of subduction during continental collision (starting by Johnson and Beaumont, 1995) suggested that peripheral foreland basins can be further classified into retroforeland (forming on the overriding plate, e.g., the Aquitaine Basin, not to be confused with retroarc basins defined earlier) and proforeland basins (forming on the underthrusting plate, e.g., the Ebro basin and northern Pyrenees).

Various types of foreland basins have also been differentiated in relationship to the position of the Moho underlying the orogenic belt and the position of the backstop (the overriding plate). True subduction applies only for oceanic lithosphere, where also the crust is recycled in the mantle. Retroforeland basins, like the Canadian Rocky Mountain foreland basin (e.g., Hardebol et al., 2009, 2013), develop at the rear of an oceanic subduction zone. In the Canadian example, there is a complete preservation of the continental crustal thickness, the Moho being continuous from the foreland to the hinterland, perhaps indicating absence of continental subduction and only a limited amount of lateral flow in the lower crust. In collisional orogens, such as the Alps or the Pyrenees, the Moho is offset by a mantle indenter, the Moho of the lower plate deepening toward the plate boundary and accounting for a crustal root where most of the lower crust of the downgoing plate is progressively stacked (Roure et al., 1989, 2010b). In the case of slab retreat and back-arc development (i.e., Carpathians (Tomek, 1993), Apennines (Patacca et al., 2008), and Brooks Range in Alaska (Fuis et al., 1997)), there is no vertical offset of the Moho under the orogen, as in the Canadian Rocky Mountains. A possible interpretation for this is the delamination of the mantle–lithosphere (see also Bocin, 2010; Matenco et al., 2010).

Consistent with their flexural origin, foreland basins are generally characterized, in comparison with other sedimentary basins, by an overall acceleration of tectonic subsidence (i.e., *convex-up* subsidence curve), though eventually reflecting the periodicity of thrust loading (e.g., Xie and Heller, 2009) and with a less clear pattern in the case of retroforeland and retroarc basins (Naylor and Sinclair, 2008; see **Figure 36**). Many foreland basins have experienced a polyphase evolution characterized by preorogenic extension that might introduce a thermal, convex-down component in their subsidence record, which affects their vertical motions during the foreland basin stage. Examples are found in the Aquitaine Basin (southern France; Desegaulx et al., 1991) and the Romanian Carpathian foredeep (Tarapoanca et al., 2004). Alternatively, numerous foreland basins have recorded late-stage episodes of vertical uplift and unroofing, for instance, in the North American Cordillera, from the Canadian Rocky Mountains in the north (Hardebol et al., 2013) to the Mexican Cordoba Platform in the south (Roure, 2008; Roure et al., 2009), where uplift might be related to mantle convection at the rear of the Pacific subduction. Other examples can be found in United Arab Emirates, north

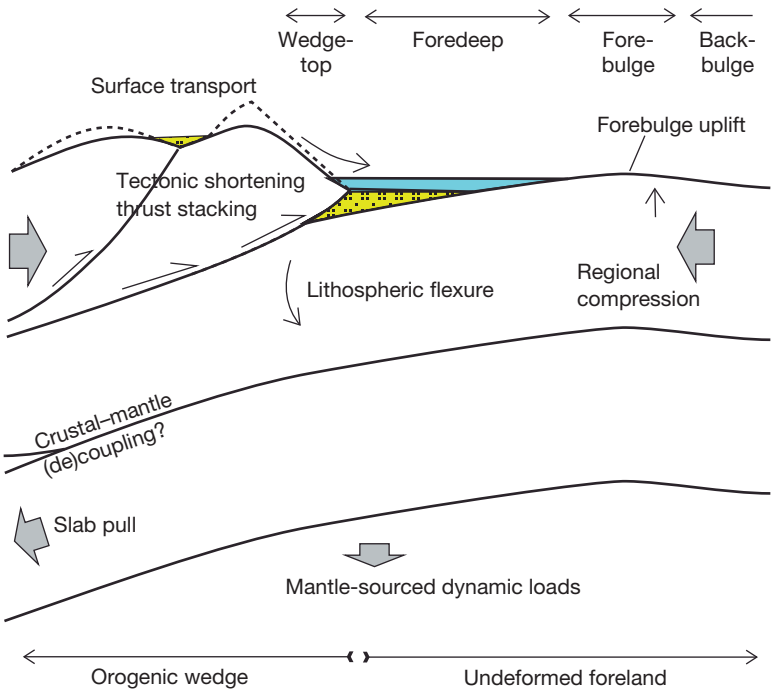

Figure 35 Simplified cartoon (not to scale) showing the standard partition of foreland basins and the main processes involved in their evolution. The crustal/mantle segment of the sketch applies mainly to retroarc basins and not to configurations with a true backstop. Reproduced from Garcia-Castellanos D and Cloetingh S (2012) Modeling the interaction between lithospheric and surface processes in foreland basins. In: Busby C and Azor A (eds.) *Tectonics of Sedimentary Basins: Recent Advances*, pp. 152–181.

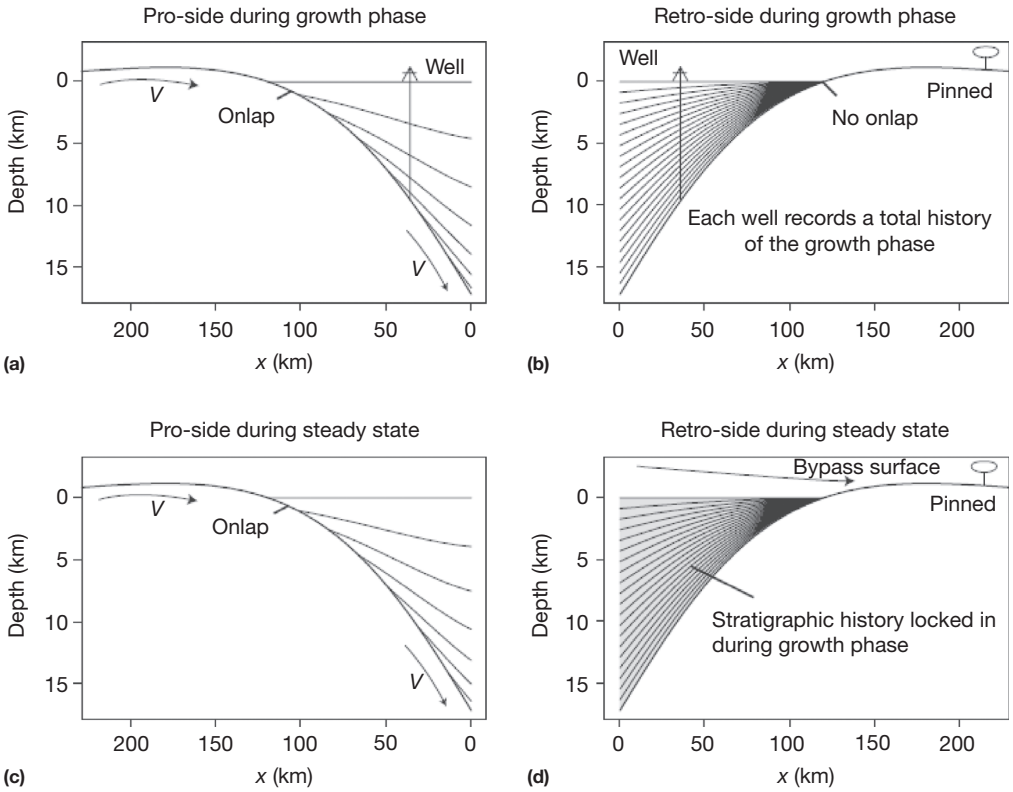

Figure 36 Typical basin fill geometries obtained from flexural modeling for pro- and retroforeland basins. A vertical end load is applied at x = 0 during the growth phase (a and b) and during the steady-state phase (c and d). The stratigraphic horizons are spaced at 3.55 My intervals, with a total duration for each simulation of 71 My. A synthetic well drilled in the retrobasin records the entire growth phase, whereas in the proside, it records only the recent advection of the basin. Reproduced from Naylor M and Sinclair HD (2008) Pro- vs. retro-foreland basins. *Basin Research* 20: 285–303.

Algeria, and the Apennines, where recent uplift relates to slab detachment and back-arc asthenospheric upwelling (Ali and Watts, 2009; Roure et al., 2010a; Tarapoanca et al., 2010; Van der Meulen et al., 1999).

The equation governing the bending of a thin elastic plate resting on an inviscid fluid (Turcotte and Schubert, 2014) is often used as a proxy for lithospheric flexure on the asthenosphere. This model shows that the flexural subsidence next to the orogenic wedge is wider and shallower for larger plate thicknesses and predicts a small uplift (forebulge) of the undeformed plate (foreland) of a few hundreds of meters or less (Turcotte and Schubert, 2014). Marine geophysical studies of plate flexure seaward off trenches and under volcanic island chains provide an interesting analog for the height of the foreland bulge not affected by surface erosion (e.g., Watts, 2001). These studies have drawn attention to the order in magnitude difference between the height of the bulge and the depth of adjacent flexural depocenter. Although the same is true for the relationship between the magnitude of the foreland bulge and the depth of foreland depocenter, subaerial erosion of the bulge usually hampers accurate estimates of bulge height. Integrating this model with field observations brings to the distinction of four depozones in foreland basins (DeCelles and Giles, 1996) sketched in **Figure 35**: wedge-top (sediments deposited on top of the deformation wedge, including piggyback basins), foredeep (sediments at the maximum flexural subsidence), forebulge (sedimentary cover of the foreland basin, if any), and backbulge (sedimentary cover beyond the forebulge, if any).

The first foreland basin modeling studies (Beaumont, 1981; Jordan, 1981, 1982; Flemings and Jordan, 1989; Sinclair et al., 1991) provided the numerical methods to calculate the EET of the continental lithosphere and established general relationships between sedimentary infill and tectonic shortening implied by simple flexural isostatic models. The simple approaches adopted for surface transport and tectonic deformation could only capture first-order interactions between these processes. For example, Beaumont (1981) showed that a purely elastic lithosphere bending under a prograding wedge would normally produce a prograding onlapping stratigraphy, while viscous relaxation of stress within the lithosphere might induce large-scale offlapping geometries and shift of depocenters toward the orogen. This latter geometric relationship was observed at that time in the Alberta Basin and later documented in many foreland basin settings (e.g., Carrapa and Garcia-Castellanos, 2005). The basin infill geometries predicted by those models were, however, subject to their 2-D nature (they modeled a vertical cross section) and the lack of mass conservation between erosion and sedimentation at the scale of the orogen–basin system.

The polyphase nature of foreland basins explains deviations in the geometry and record of vertical motions from predictions from simple flexural models of foreland basin evolution

(e.g., Cloetingh and Ziegler, 2007; Roure, 2008; Roure et al., 2010b). This is particularly important for the interpretation of EET values extracted from the geometry of the foredeeps or their gravity field. Temporal and spatial variations of EET (e.g., Prezzi et al., 2009) as well as temporal variations in horizontal stress are leading to a natural spread of EET when compared to the depth of isotherms in the lithosphere.

6.12.4.1.1 Role of preorogenic extension and late-stage compression

Many present-day foreland basins have been formed at the sites of preexisting rifts or rifted continental margins (Stockmal et al., 1986; Desegaulx et al., 1991). This fact has a number of important implications not only for the mode of shortening of the lithosphere but also for its subsidence history and thermal evolution. **Figure 37** illustrates the temporal evolution from rift to foredeep as reconstructed for the Aquitaine Basin (Desegaulx et al., 1991), which is the *retro*foreland basin of the Pyrenees. At the onset of foreland basin formation, the heat impulse in the lithosphere generated by preorogenic extension of the Gulf of Biscay region (**Figure 37**) was not yet relaxed. As a result, this basin has experienced considerable postrift thermal subsidence (**Figure 38**). In this case, a further complication comes from the obliquity of the rifting with respect to the main axis of subsequent compression, with a lateral movement during the Albian, prior to Late Cretaceous to Eocene frontal collision. The Romanian Carpathian foredeep also was affected by preorogenic extension (Tarapoanca et al., 2004). The superposition of preorogenic extension and foreland flexure results in subsidence patterns that deviate from predictions of standard flexural foreland basin models (Cloetingh and Ziegler, 2007). Furthermore, lateral variations in rheological properties in the downflexed lithosphere also occur in this situation, strongly affecting the subsidence patterns.

In addition to preorogenic extension, foreland subsidence can also be enhanced by late-stage compression associated with changes in the convergence rate. Examples can be found in the Aquitaine Basin and the Carpathian foredeep (Tarapoanca et al., 2004), as well as in the Alpine Piedmont Basin (Carrapa and Garcia-Castellanos, 2005). As pointed out by Cloetingh et al. (2004), slab detachment during final stages of continental collision can lead toward drastic changes in stress regime in the overriding plate with high levels of compression. In the case of the Romanian Carpathian foredeep, this has led to a more symmetrical shape of the foredeeps than predicted by foreland flexure alone. The superposition of preorogenic extension, foreland flexure, and late-stage compression also provides an explanation for cases of ultradeep foredeeps. An example of this is the Romanian Carpathians, with more than 12 km of Neogene sediments accumulating in the Focşani Depression flanked by the Carpathian orogen, where geothermochronology studies have provided evidence

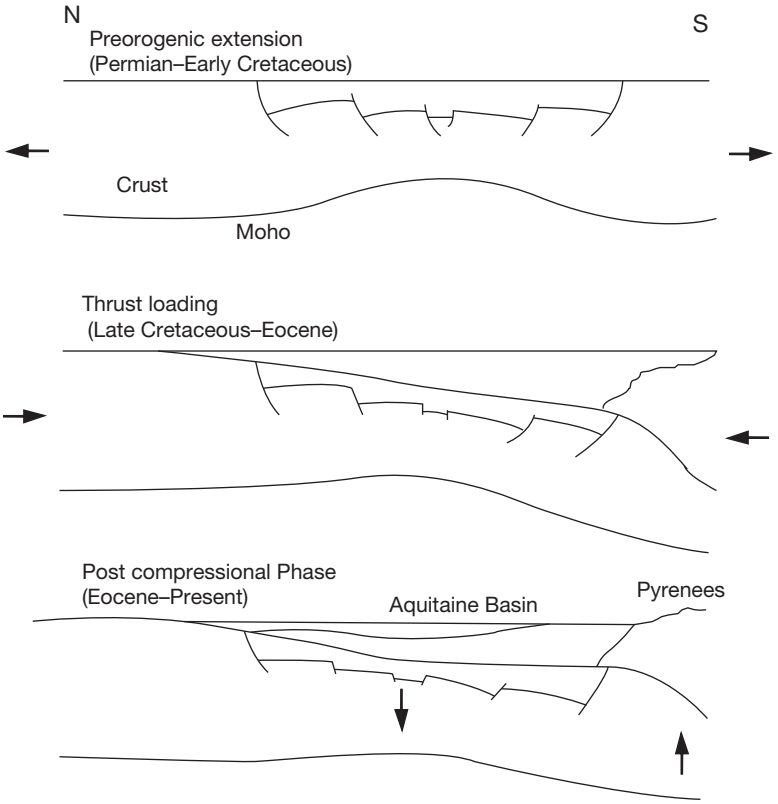

Figure 37 Schematic evolution of the Aquitaine foreland basin. (top) (Permian–Early Cretaceous) preorogenic extension phase; rifting of the European domain. (middle) (Late Cretaceous–Eocene) compression; formation of the Aquitaine foredeep. (bottom) (Eocene–present) postcompressive phase associated with unflexing. Reproduced from Desegaulx P, Kooi H, and Cloetingh S (1991) Consequences of foreland basin development on thinned continental lithosphere – Application to the aquitaine basin (Sw France). *Earth and Planetary Science Letters* 106: 116–132.

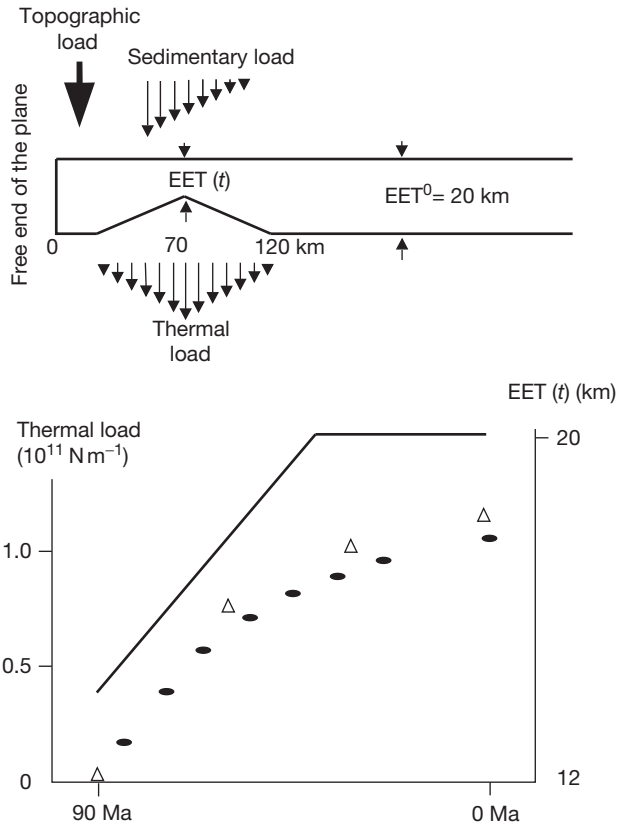

Figure 38 Cartoon illustrating the effect of extensionally induced weakening and ongoing thermal subsidence on foreland basin subsidence. (top) Thinning of the elastic plate coincides in space with the thermal load. A prograding topographic (thrust) load is applied. (bottom) Triangles denote the change of plate thickness through time EET (*t*) for the center of the preorogenic basin. Dotted line shows the evolution of thermal loading. Reproduced from Desegaulx P, Kooi H, and Cloetingh S (1991) Consequences of foreland basin development on thinned continental lithosphere – Application to the aquitaine basin (Sw France). *Earth and Planetary Science Letters* 106: 116–132.

for erosion of more than 4 km during the last 12 My (Merten et al., 2010; Necea, 2010; Sanders et al., 1999).

The Tertiary Piedmont Basin is the retroforeland basin of the Western Alps characterized by a noncylindrical geometry due to the superposition with the Ligurian Alps, oriented in an oblique direction (Bertotti and Mosca, 2009; Bertotti et al., 2006). Within the limitations imposed by this, cross-sectional modeling suggests that the presence of a compressional horizontal force during the formation of that basin enhanced the remarkable *toplap* sedimentary geometry shown in **Figure 39** (Carrapa and Garcia-Castellanos, 2005), with younger sediment filling only the basin areas closer to the Alps and gradually older sequences outcropping further toward the foreland.

6.12.4.1.2 Feedback between lithospheric and surface processes

Much effort in foreland basin modeling has been directed to understanding landscape evolution and surface processes (e.g., Bonnet, 2009 and references therein). A by-product of these studies is the development of a series of models integrating 3-D surface sediment transport with the dynamics of basin evolution (Johnson and Beaumont, 1995). Computer simulations coupling planform flexural isostasy and 3-D fluvial sediment erosion/transport have shown that river transport, on its own, is not capable of producing significant sediment accumulation on the foreland in the absence of flexural subsidence at intermediate EET values (Garcia-Castellanos, 2002). These findings are similar to the classical notion that, to generate significant accommodation space, kilometer-scale tectonic subsidence by lithospheric downflexing over a sizable area in front of the orogen is a prerequisite. More specifically, if the strength of the lithosphere is too low or too high, the creation of accommodation space next to the orogen becomes negligible, and rivers will transport their sediment load out of the orogen–basin system.

Whereas early diffusive models for erosion (Flemings and Jordan, 1989; Sinclair et al., 1991) produced significant amounts of sediment accumulation even for large rigidities, the more sophisticated models show that river transport does not allow such sediment accumulation in the absence of differential vertical motions, as in the case of very high rigidity. The dependence between the basin volumes predicted by these models and EET shows a remarkable similarity with the observed EET histogram (Garcia-Castellanos, 2002). This suggests that the EET *measurements* might be biased by a focus of studies on large sedimentary basins. An open question is to what extent the presence of middle EET values (20–40 km), responsible for 'large' sedimentary basins, is overestimated relative to larger and smaller values, which generate small basins. An example of this could be the Atlas orogen in Morocco, for which no forward flexural modeling has been performed in the tiny foreland basins formed in the vicinity. The absence of modeling is probably due to the fact that the associated foreland basin is relatively insignificant in both sedimentary thickness (<700 m) and width (<35 km in Ouarzazate). Preliminary flexural models of the Ouarzazate basin yield EET values below 4 km (Teson et al., 2006), a low value that may be linked to a mantle upwelling under the Moroccan Atlas Mountains, which would also explain the high topography relative to the small amounts of shortening, and the spatial coincidence of a gravity low and a geoid high in this orogen (Teixell et al., 2005). Other examples are the small Klagenfurt and Styrian Basins (Austrian Eastern Alps), where EET values between 1 and 5 km have been linked to strong decoupling of the upper crust (Nemes et al., 1997; Sachsenhofer et al., 1997).

6.12.4.1.2.1 Modeling the sedimentary infill geometry

Several researchers have focused numerical models to non-instantaneous orogenic loading, incorporating some simplified approach to fault propagation within the basement and the sediment (Garcia-Castellanos et al., 1997; Sassi et al., 1993; Sassi and Rudkiewicz, 2000; Toth et al., 1996). These studies aim to better constrain the tectonic evolution based on the sedimentary record or vice versa. To that purpose, a pure elastic plate responding instantaneously to loading is insufficient, and the transient viscous response of the lithosphere must be considered (Beaumont, 1981). Viscous relaxation during basin development induces basin narrowing and deepening, similar to the result of an EET reduction through time. The application of a viscoelastic model to the Guadalquivir Basin (Garcia-Castellanos et al., 2002) and the Tertiary Piedmont Basin (Carrapa and Garcia-Castellanos, 2005) shows that viscous

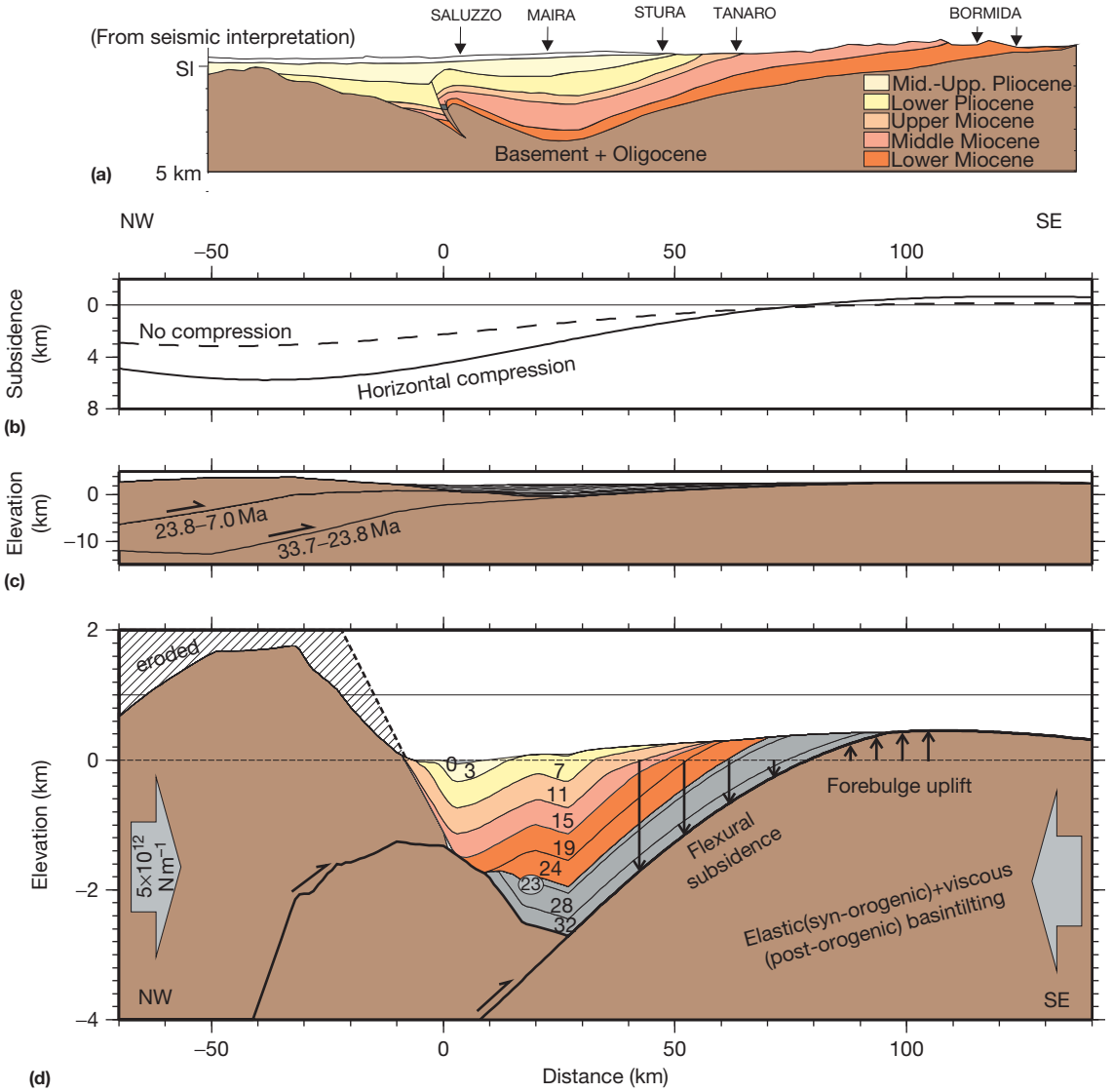

Figure 39 (a) Sedimentary infill geometry of the Piedmont Basin constrained by seismic surveys (see for location **Figure 33**). (b) Calculated vertical motions. Dashed line corresponds to an identical model without horizontal compression. (c) Final model geometry (no vertical exaggeration) obtained from a viscoelastic flexural model. (d) Basin geometry (vertically exaggerated). Reproduced from Carrapa B and Garcia-Castellanos D (2005) Western Alpine back-thrusting as subsidence mechanism in the Tertiary Piedmont Basin (Western Po Plain, NW Italy). *Tectonophysics* 406: 197–212.

basin narrowing may exceed the velocity of wedge motion, inducing a retreat of the subsiding area toward the orogen. Under such circumstances, older sedimentary units may outcrop in the distal parts of the foreland basin (**Figure 39**). A shift toward the orogen of the pinch out of sedimentary units is observed in the previously mentioned foreland basins and also in the Alberta Basin (Beaumont, 1981) and the Swiss Molasse basin (Schlunegger et al., 1997). In the Alberta Basin, the entire lithosphere, in both the foreland and the hinterland, has been uplifted (Hardebol et al., 2013). In the Swiss Molasse basin, the pinch out relates partially to post-Messinian inversion of Paleozoic grabens beneath the Jura Mountains, which accounts for a refolding of the intra-Triassic decollement, and differential topography between the Jura and the Molasse basin (Philippe, 1994; Roure et al., 1994). Models incorporating viscous relaxation, therefore, still require these mechanisms or the additional vertical or horizontal forces mentioned in the previous section to be able to fit the basin architecture.

6.12.4.1.2.2 Forebulge uplift

The magnitude of the forebulge might fluctuate with time as a result of temporal variations in regional stress fields (Cloetingh et al., 1989), stress accumulation and relaxation prior and upon thrusting (Peper et al., 1992), and spatial variations in rheology of the lithosphere underlying the foreland basin (Waschbusch and Royden, 1992). Numerical modeling has shown that the position of the forebulge should not be expected to migrate steadily toward the foreland even when the tectonic wedge does. Instead, this shift might slow down or accelerate if lateral EET variations are present (*Waschbusch and Royden, 1992*) or even

reverse direction and move toward the orogen due to viscous relaxation of stresses (Beaumont, 1981; Garcia-Castellanos et al., 2002). Forebulge uplift is therefore not necessarily stationary in time and space. In fact, the presently active forebulge might mark the current limit of the flexural basin geometry, whereas the basin fill might also have recorded an older forebulge, which is now buried under the foredeep depocenter.

In parallel, results from 3-D computer experiments (Garcia-Castellanos, 2002) show that forebulges may not easily be represented as drainage divides, since limited amounts of inherited (preflexural) topographic relief may be more decisive in determining the future drainage network than the vertical uplift associated with the forebulge (usually smaller than 200 m). This can be further complicated by the discrete localization of the forebulge as the front of deformation jumps toward the foreland. Still, these models do not exclude that forelands with small inherited topographic gradients and an initially poorly incised river network can develop drainage patterns that reflect forebulge uplift of a few hundred meters or even backbulge subsidence in the order of tens of meters (Horton and DeCelles, 1997; Roddaz et al., 2005). Such topographic anomalies can also occur in relation to foreland basement inversion such as documented for the US Rocky Mountains, Mérida Andes, and Saharan Atlas, which generate high topography inside a formerly continuous foreland (Colletta et al., 1997; Gries, 1983; Roure et al., 1997; Roure et al., 2010b).

In some foreland basins, such as along the eastern flank of the Andes, the sedimentary infill has overflowed the forebulge crest and the subsequent sedimentary cover extends beyond that. Computer simulations (**Figures 39** and **40**) show that changes in the balance between tectonic equilibrium and erosional equilibrium (in absence of eustatic base level changes or independent subsidence of the foreland) cannot result in overflowing an active forebulge (a forebulge being still uplifted by tectonic loading). As long as the basin is continental and exorheic, the drainage network generally adapts to these changes and copes with any increase in sediment delivery from the orogen or with any reduction in the rate of generation of accommodation space, transporting along-strike the excess mass to the open ocean (Garcia-Castellanos, 2002). Thus, forebulges buried under basin sediments are either a relic of former stages when the tectonic load was more distant from the foreland or active forebulges subdued below sea level by other subsidence mechanisms. This later interpretation is consistent with the notion by Dávila et al. (2007) that dynamic loading sourced in the mantle produced additional subsidence of the sub-Andean peripheral bulge allowing it to be overlain by later sediments. In addition to static loads, dynamic loading underneath the basin (e.g., viscous mantle corner flow above a subducting plate; Catuneanu et al., 1997) may cause long-wavelength subsidence and forebulge sediment overflow. Our understanding of these dynamic forces as the result of mantle convection has improved in the last years (e.g., Pysklywec and Mitrovica, 1997). The interaction of static (isostatic) and dynamic (e.g., coupling with mantle flow) forces might also be responsible for the formation and preservation of stacking patterns that do not conform to the predictions of simple elastic flexural models (Catuneanu et al., 1997). A more detailed possibly quantitative implementation of regional upper mantle flow studies in the analysis of foreland basins could provide additional understanding of these systems in the future.

6.12.4.1.2.3 Basin exhumation

Modeling studies during the last two decades have shown that erosion and deposition strongly influence tectonic processes, tuning the style of deformation in compressional belts (Avouac and Burov, 1996; Beaumont et al., 1992; Willett, 1999) and demonstrating the importance of feedback between uplift and erosion as well as deposition in the foredeep and the return flow in the lower crust (Garcia-Castellanos, 2002). The feedback between surface processes, isostatic reaction, and subsurface crustal flow can result in accelerated growth of topography in the area of strongest subsurface uplift. Examples are central Asia, the Cordilleran–Sub-Andean basins, and areas with lithospheric delamination, as all the crust remains attached to the upper plate. This mechanism is probably also important in the Eastern Alps where only the mantle–lithosphere is downthrusted, as proposed by Laubscher (2010). The lower crust in this case can then be viewed as rather ductile and flowing between the brittle upper crust and the underlying brittle mantle.

Similar feedback relationships between thrusting dynamics, foreland basin formation, and accretionary wedges have received considerable attention from numerical (e.g., Braun, 2006; Garcia-Castellanos, 2002; Garcia-Castellanos and Cloetingh, 2012; Simpson, 2006) and analog (e.g., Persson and Sokoutis, 2002; Smit et al., 2003, 2013) modelers. Combination of analog and numerical modeling benefits from the 3-D capabilities of analog tectonic experiments to implement preexisting structures, as well as the capability of numerical models to handle 3-D surface mass redistribution. The validation of modeling results requires the availability of high-quality datasets, including deep seismic profiles (Roure et al., 1989, 1996; Tomek, 1993), seismostratigraphic interpretations, and paleothermometers (Roure et al., 2010a).

The reciprocal interactions between surface and tectonic processes have been studied through hybrid numerical–analog models, fully coupling the dynamics of an analog deformation model (sandbox) and the fluvial transport numerical model (**Figure 40**; Athmer et al., 2010; Persson et al., 2004). In this technique, a backstop acts as an indenter at the upper boundary, compressing the initially flat sand layers. During shortening, a scanner is used to digitize the sandbox topography, which is then scaled and passed to the numerical surface process model. The calculated erosion and deposition are then downscaled and mechanically applied to the sandbox by respectively subtracting and adding sand to its surface. The drainage pattern evolving on top of the topography induces lateral differences in surface sediment redistribution, which disrupts the lateral (along-strike) symmetry of the initial setting. The modeling approach used in **Figure 40** is similar to that in Persson et al. (2004), except that here, a computer-calculated flexural isostasy is applied, which permits the formation of large flexural sedimentary basins. The initial topography is slightly tilted (0.5 degrees) toward the west (left). During the experiment, episodic sediment delivery toward the basin results from drainage reorganizations in the orogen and not from changes in tectonic shortening rates, which are not incorporated to this model. Hence, drainage reorganization is a mechanism of episodic sediment delivery, alternative to tectonic or climatic periodicity (Sobel et al., 2003). The forebulge is not migrating continuously toward the foreland, but in fact records two stages of discrete localization at a distance of ~300 and 150 km from the lower boundary of the model, linked with

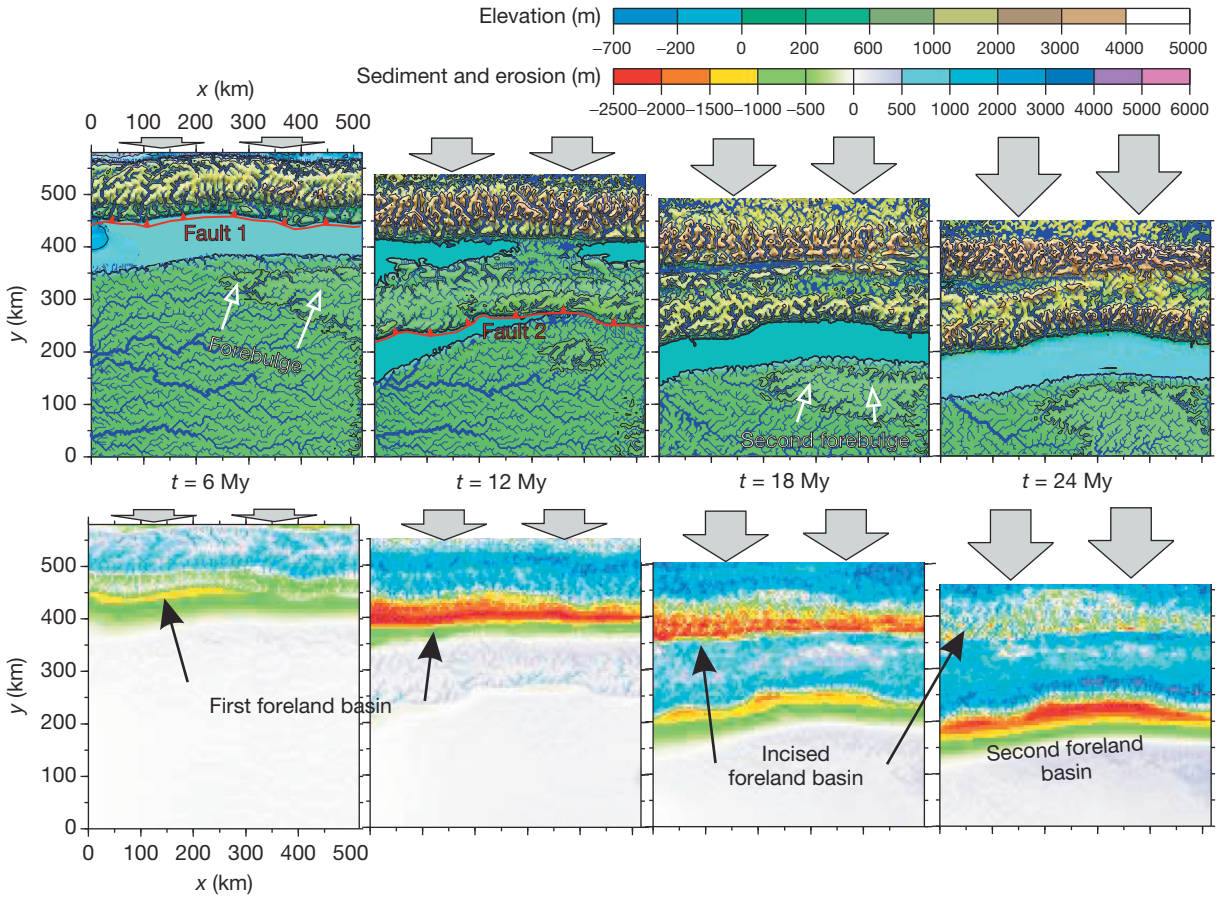

Figure 40 Results from a combined analog–numerical model following a technique similar to Persson et al. (2004) but here incorporating flexural isostasy for the calculation of topography. The formation of topography and tectonic load is simulated with a sandbox compressed from the northern (upper) boundary. Gray arrows indicate cumulative backstop motion. The sand surface is scanned and passed to a computer program (*TISC*), which calculates river incision and sediment transport (Garcia-Castellanos et al., 2002). The calculated erosion/deposition is then downscaled and manually applied to the analog experiment. Four stages are shown at 6, 12, 18, and 24 My. The initial stage (0 My) consists of a flat surface with a slight tilt toward the left boundary, 100 m lower than the right one. Within the orogen, the drainage network develops in N–S direction, perpendicular to the tectonic structures, until a second major thrust develops in the sand ($t = 12$ My) further toward the south. The topography generated by this new fault induces a large drainage reorganization in the direction along the strike of the orogen ($t = 18$ and 24 My). The sediment accumulation produced in the foreland basin is *cannibalized* as the tectonic shortening is accommodated further to the south, as observed in a variety of geologic settings (e.g., DeCelles and Giles, 1996). Two major forebulge areas are uplifted in response to the two major deformation fronts. Both forebulges become drainage divides between the basin and the foreland, although the initial E–W drainage trend is essentially not modified. Cannibalization of piggyback basins and episodic motion of the forebulge is consistent with observations by, for example, Hippolyte et al. (1994) in the southern Apennines. Reproduced from Garcia-Castellanos D and Cloetingh S (2012) Modeling the interaction between lithospheric and surface processes in foreland basins. In: Busby C and Azor A (eds.) *Tectonics of Sedimentary Basins: Recent Advances*, pp. 152–181.

successive offsets of the active thrust front and flexed domain. Hippolyte et al. (1994) and Casero (2004) proposed such successive lateral jumps for the Messinian to Middle Pliocene depocenters in the Apennines. These experiments also show that lateral heterogeneities in erosion and sediment transport induce lateral tectonic diachronism and perturb the initial E–W symmetry of the sandbox setting, affecting the distribution of deformation in a way similar to that described through earlier 2-D numerical models of orogenesis (Willett, 1999). The experiments performed by Persson et al. (2004) and the one shown in **Figure 40** account for 3-D river sediment transport and suggest that axial transport in the orogen and along the foreland basin may induce lateral changes in the tectonic evolution of the orogen–basin system. An obvious challenge is to separate in the field these effects from those induced by inherited heterogeneities and lateral changes in the tectonic forcing.

To improve our understanding of the dynamics of foreland basins, future basin models must incorporate the full dynamics of lithospheric deformation (lithospheric flexure and folding, crustal thrusting, sediment deformation, subduction of the lithospheric mantle, and lower crustal and asthenospheric flow) and surface processes (incorporating to some degree climatic processes). Dynamic tectonic models have improved significantly our understanding of orogenesis (Burov and Toussaint, 2007; Garcia-Castellanos, 2007; Jiménez-Munt et al., 2005; Whipple, 2009; Willett, 1999; Willett et al, 2006) and currently start to contribute similarly at the basin scale (Simpson, 2010). These models are currently moving into 3-D (Braun, 2006),

incorporating more realistic surface processes. Surface process models have shown that there is substantial information waiting in the landscape record, which can contribute to a better quantitative understanding of orogen–basin systems.

6.12.4.2 Compressional Basin Formation by Lithospheric Folding

Folding of the lithosphere, involving positive and negative deflections (Figure 41), appears to be of more importance in the large-scale deformation of intraplate domains than hitherto realized (Cloetingh and Burov, 2011; Cloetingh et al., 1999). As discussed by Cloetingh and Burov (2011), folding can be observed at different spatial scales. At the scale of a microcontinent that was affected by a succession of collisional events, Iberia illustrates lithospheric folding and interplay between neotectonic and surface processes (Cloetingh et al., 2002). An important factor favoring a lithosphere-folding scenario for Iberia is the compatibility of the thermotectonic age of its lithosphere and the wavelength of observed deformations. Other well-documented examples of continental lithospheric folding occur in other regions across the globe (Figure 42). Prominent examples occur in central Asia and surrounding regions (e.g., Delvaux et al., 2013; Smit et al., 2013) involving a lithosphere with thermotectonic ages from 150 Ma (Kazakh shield, Fergana and Tadjik basins, and likely Dzungarian Basin) to 400 Ma (Tarim Basin). In this area, mantle and crustal wavelengths are 360 and 50 km, respectively, with a shortening rate of ~10–20 mm year^{-1} and 200–250 km of shortening during 10–15 My (Burov and Molnar, 1998; Burov et al., 1993). Three-dimensional fold structures in the Tibetan Plateau have been inferred from GRACE satellite gravity data, demonstrating prevailing fold wavelengths of 300–420 km (Shin et al, 2009).

Although the India–Eurasia collision is by far the most dominating factor in the eastern segment of the Alpine–Himalayan collision belt (e.g., Hatzfeld and Molnar, 2010), the contribution of the Arabian indenter to the deformation of western central Asia cannot be neglected. The stress system generated by both indenters is affecting the intraplate topography of (western) central Asia up to distances of the order of a few thousands of kilometers, leading to significant differential

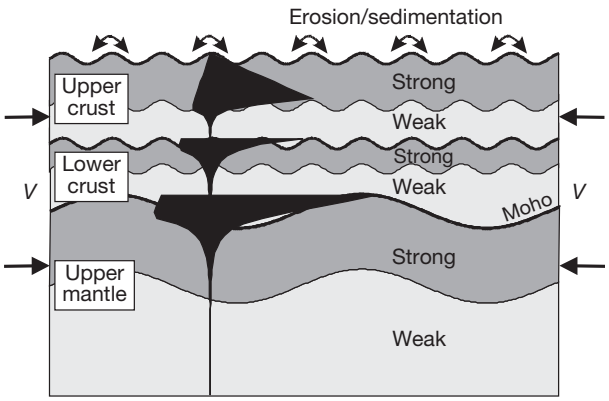

Figure 41 Concepts of folding in rheologically stratified lithosphere and feedback with sedimentation in downfolded areas and erosion of adjacent highs. Different simultaneously occurring wavelengths of crustal and mantle folding are a consequence of the rheological stratification of the lithosphere. Surface wavelengths can be affected also by feedback with surface processes.

Figure 42 Map with examples of well-documented areas affected by lithospheric folding. Areas: Central Indian Ocean Basin (CIOB) (Geller et al., 1983; Stein et al., 1989); NW European Platform (Bourgeois et al., 2007; Lefort and Agarwal, 1996; Marotta et al., 2000); Pannonian Basin (Dombradi et al., 2010); Iberia (Cloetingh et al., 2002; De Vicente et al., 2007; Fernández-Lozano et al., 2011, 2012); central Asia (Burov et al., 1993; Nikishin et al., 1993; Burov and Molnar, 1998); Tibetan/Himalayan syntaxis belt (Burg and Podlachikov, 1999; Shin et al., 2009); Central Australia (Stephenson and Lambeck, 1985; Lambeck, 1983); Arctic Canada (Stephenson et al., 1990); Transcontinental Arch of North America (Ziegler et al., 1995); South Caspian Basin (Guest et al., 2007); Laramide foreland (the United States) (Tikoff and Maxson, 2001); Barents Sea (Ritzmann and Faleide, 2009).

vertical motions. Smit et al. (2013) pointed out that collision of the Eurasian plate with the Arabian and Indian Plates generates folding of the Eurasian lithosphere in two different directions with their interference manifested in the regional geology, gravity, and topography. The wavelengths of the observed lithospheric deformation are consistent with the inferences from thermomechanical models constructed for the lithosphere in western central Asia. Differences in the convergence velocities of the Indian and Arabian indenters with respect to Eurasia and spatial variations in thermomechanical structure of the lithosphere west and east of the Kugitang–Tunka Line appear to be of key importance.

The inferred wavelength of these neotectonic lithospheric folds is consistent with the general relationship between the wavelength of lithospheric folds and the thermotectonic age of the lithosphere shown by a global inventory of lithospheric folds (**Figure 43**; Cloetingh and Burov, 1996; Cloetingh et al., 2005a,b). In some other areas of continental lithospheric folding, smaller wavelength crustal folds have also been detected (Burov et al., 1993; Nikishin et al., 1993). Thermal thinning of the mantle–lithosphere, often associated with volcanism and doming, enhances lithospheric folding and appears to affect the wavelengths of folds (Burov and Cloetingh, 2009).

As has been shown (Burov et al., 1993; Cloetingh et al., 1999; Gerbault et al., 1999; Nikishin et al., 1993; Schmalholz and Podladchikov, 2000), viscoelastic folding starts to develop from the onset of compression and, in contrast to elastic folding, does not require specifically large intraplate stresses. Folding may continue until the background strain-rate drops, for example, due to the localization of deformation in a specific area or to reduction of far-field forces. Such intraplate deformation results from transmission of intraplate stress fields away from plate boundaries into continental forelands (Tesauro et al., 2005; Van der Pluijm et al., 1997; Ziegler et al., 1998).

In continental lithosphere, several wavelengths of folding are expected to develop as a result of the presence of several rheologically competent layers decoupled from each other by weak layers (**Figures 41** and **43**). Crustal folding can be traced from the surface topography, neotectonic movements, and free air gravity. The crust–mantle boundary (Moho) topography reflects mantle folding, because the mantle strength is highest at this interface, and thus, the geometry of Moho deflection is most likely to correspond to that of mantle folding. This wavelength can be traced from Bouguer gravity anomalies because the crust–mantle boundary represents also the main density contrast in the lithosphere. It is to be expected that the base of the mechanical lithosphere (MLB) has roughly the same geometry as the Moho deflection. Likely, the lithosphere–asthenosphere boundary (LAB) has little to do with mantle–lithospheric folding except some specific cases, as the MLB (roughly corresponding to 700 °C depth) is found well above the LAB (1330 °C). Consequently, the low-viscosity zone between MLB and LAB may damp the deformation in a way that the LAB remains even flat. Due to the low viscosity of gravitating mantle between the LAB and the MLB, the LAB is not necessarily advected or downwarped with deflection of the MLB, or at least the relations between the deformation of the MLB and that of LAB are not straightforward. In particular,

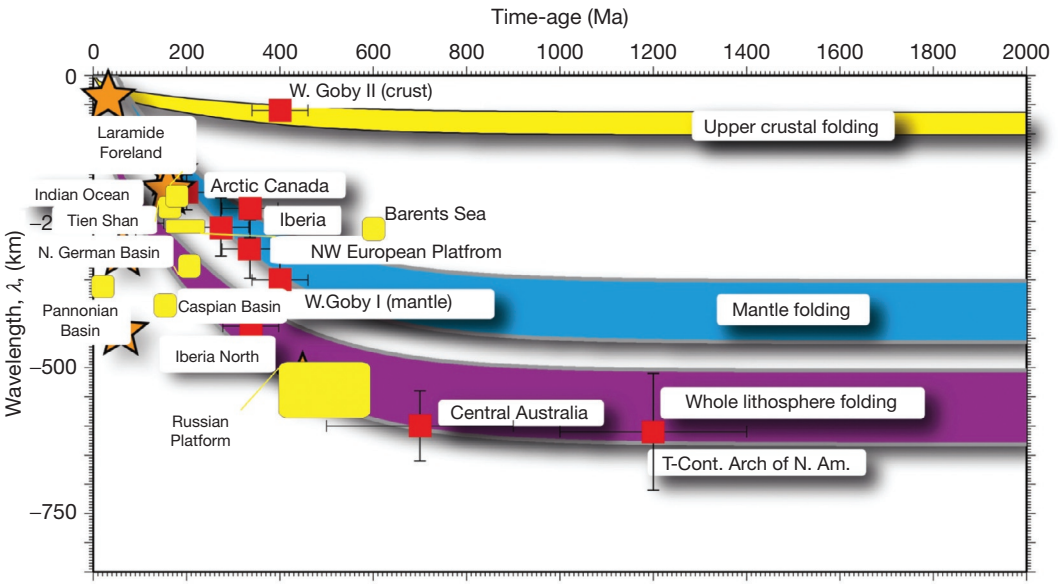

Figure 43 Characteristics of lithospheric folding. Polyharmonic folding concept: due to rheological stratification, the lithosphere can develop different folding wavelengths in response to tectonic compression. Surface topography will reflect superposition of different wavelengths. The colored zones correspond to theoretically folding wavelengths derived for the upper crust, mantle, and coupled whole mantle folding, based on an analytic model that accounts for strength variations as a function of thermomechanical age. Theoretically predicted wavelengths as function of thermotectonic age (for different lithospheric layers as well as whole-lithospheric folding) are compared to observed wavelengths and thermotectonic ages. See also **Table 4**. Reproduced from Cloetingh S, Burov E, and Poliakov A (1999) Lithosphere folding: Primary response to compression? (From central Asia to Paris basin). *Tectonics* 18: 1064–1083; Cloetingh S and Burov E (2011) Lithospheric folding and sedimentary basin evolution: A review and analysis of formation mechanisms. *Basin Research* 23: 257–290.

Table 4 Wavelengths and ages of basins located on folded lithosphere (see Figure 42 for locations)

	Area	*Thermotectonic age (Ma)*	*Folding wavelength λ (km)*	*References*
1	Tian Shan	175	200–250	Burov and Molnar (1998) and Burg et al. (1994)
2	Western Gobi	175–400	300–360	Nikishin et al. (1993) and Burov et al. (1993)
3	Central Asia	370–430	50–70 (crust) 300–400 (lithosphere–mantle)	Nikishin et al. (1993) and Burov et al. (1993)
4	Himalayan syntaxis belt	8–10	150	Burg and Podladchikov (1999)
5	Central Australia	500–900	550–650	Lambeck (1983), Stephenson and Lambeck (1985), and Beekman et al. (1997)
6	Russian Platform	400–600	500–600	Nikishin et al. (1997)
7	South Caspian Basin	125–155	350–450	Guest et al. (2007)
8	Eastern Black Sea	40–80	50–100 (crust) 100–150 (lithosphere–mantle)	Cloetingh et al. (2008)
9	Western Black Sea	75–125	50–100 (crust) 100-200 (lithosphere–mantle)	Cloetingh et al. (2008)
10	Pannonian Basin system	20	200–250	Horváth and Cloetingh (1996), Matenco et al. (2007), and Dombradi et al. (2010)
11	NW European Platform	180–230	270	Bourgeois et al. (2007)
12	Brittany	210–290	225–275	Bonnet et al. (2000)
13	Iberia	330–370	40–80 (crust) 125–275 (lithosphere–mantle)	Cloetingh et al. (2002)
14	Barents Sea	215–245	550–650	Ritzmann and Faleide (2009)
15	Canadian Arctic	150–250	170–230	Stephenson et al. (1990)
16	Transcontinental Arch of North America	1000–1400	500–700	Ziegler et al. (1995)
17	Laramide foreland (the United States)	175–225	190	Tikoff and Maxson (2001)

gravity instabilities or convective movements not related to folding can perturb the LAB without impact on the MLB.

Folding has important implications for vertical motions, sedimentary basin architecture, and the evolution of hydrocarbon systems (Ziegler et al., 1995; 1998). The large wavelength of vertical motions associated with lithospheric folding necessitates the integration of data from large areas (Allen and Davies, 2007; Elfrink, 2001), often beyond the scope of regional structural and geophysical studies that target specific structural provinces. Recent studies on the North German Basin show neotectonic reactivation by lithospheric folding (Marotta et al., 2000). Similarly, acceleration of the Pliocene–Pleistocene subsidence in the North Sea basin is attributed to stress-induced buckling of its lithosphere (Van Wees and Cloetingh, 1996). Folding of the Variscan lithosphere has been documented for Brittany (Bonnet et al., 2000; Lagarde et al., 2000), the adjacent Paris Basin (Lefort and Agarwal, 1996), and the Vosges–Black Forest Arch (Bourgeois et al., 2007; Dèzes et al., 2004; Ziegler and Dèzes, 2007). Lithospheric folding, therefore, appears to be an effective mechanism for the propagation of tectonic deformation from active plate boundaries far into intraplate domains (e.g., Burov et al., 1993; Stephenson and Cloetingh, 1991; Ziegler et al., 1995, 1998).

6.12.4.2.1 The role of lithospheric rheology

Folding is commonly associated with periodic deformation of layered structures with contrasting mechanical properties. As a consequence, the harmonic spatial periodicity is often believed to be its primary, almost synonymous, identifying factor. However, from a mechanical point of view, constant wavelength is not a necessary requirement. Folding is a compressional instability developing in stiff layers embedded in a weaker material. The harmonic solution of the equilibrium and conservation equations is a possible solution (Burov and Molnar, 1998; Cloetingh et al., 1999; Muhlhaus et al., 1998). The physical mechanism of folding is well understood. In a continuously layered medium, the stresses and strains must be continued across the interfaces between the layers. In multilayer systems with contrasting mechanical properties (e.g., strong and weak layers), this requirement may be difficult to satisfy, because the same amount of shortening in a stiffer layer would require much larger stress than in the neighboring weaker layer. The system becomes unstable and, in attempting to reduce the stress and strain unconformities at the interfaces between the layers, starts to fold (or buckle) in response to very small perturbations. In nonelastic media with strain-dependent properties, locally increased flexural strain at the fold limbs can create weakened zones that significantly facilitate further deformation. These weak or softened plastic or viscous zones are often referred to as inelastic hinges, since the system easily folds at such weakened zones. Homogeneous shortening of the lithosphere under horizontal compression requires more work than required by an equivalent amount of shortening by folding. However, shortening by underthrusting/subduction of the lithosphere may be more mechanically efficient than folding but may be blocked or unable to start immediately after the onset of shortening. For this reason, folding is likely to be a primary and common response to tectonic compression. Folding probably may continue, in an attenuated form, even after the beginning of subduction (Cloetingh et al., 1999) or reappear when the subduction channel is locked or during the aftermath of collision (Cloetingh et al., 2004; Matenco et al., 2007).

The rheological structure of the lithosphere (see **Section 6.12.2**) is a key factor in lithospheric folding (Watts and Burov, 2003). Compressional stresses must build up to a level comparable with the integrated strength of the lithosphere in order to induce folding. Prior to the advent of rheological models based on extrapolation of laboratory experiments (Carter and Tsenn, 1987; Goetze and Evans, 1979), lithospheric stresses were thought to be incapable of reaching the failure levels required for folding (Turcotte and Schubert, 2014).

The simplest expression of the folding process is in oceanic lithosphere, characterized by an absence of a rheological stratification, and with thermomechanical ages spanning a limited age window with a maximum of 200 My (Geller et al., 1983). Because weak lithosphere is easier to fold than strong lithosphere, one would expect the first observations of lithospheric folding from the rheologically weak continental plate interiors. However, the observation of folding of the relatively strong lithosphere of the central Indian Ocean with a thermomechanical age of 80 Ma and with wavelengths of 200-250 km (Bull and Scrutton, 1992; Geller et al., 1983; McAdoo and Sandwell, 1985; Stein et al., 1989) triggered the interest in this mode of deformation. There may be two reasons for this. First, the recognition of folding, by mapping of basin reflectors and gravity anomalies, requires spatial scales of several hundreds of kilometers. This is feasible with marine geophysical surveys but generally in excess of the spatial scales covered by land surveys. An exception has been the systematic mapping of basins in Central Australia, located on strong lithosphere with a thermomechanical age of ~700 Ma (Lambeck, 1983; Stephenson and Lambeck, 1985). The Indo-Australian Plate is under an exceptionally high level of compression (Stein et al., 1989), as a result of its collision with the Eurasian Plate. Under these conditions, high stresses might have been more important than the rheology of the plate interior (Beekman et al., 1996; Gerbault, 2000; Gerbault et al., 1999).

Secondly, folding in oceanic lithosphere is not affected by surface erosion, making it relatively easy to recognize. The presence of only one dominant folding wavelength characteristic of nonstratified oceanic lithosphere also facilitated a quantitative interpretation. Following the early studies in the Indian Ocean and in Central Australia in the rear of the Indian–Eurasian collision, attention shifted to the other side of the plate contact in central Asia. Large-scale folding patterns were recognized through the analysis of geophysical data, including gravity and topography (Burov et al., 1993; Burov and Molnar, 1998; Nikishin et al., 1993) as well as detailed geologic studies (Cobbold et al., 1993).

6.12.4.2.2 Observations

On the basis of an inventory of currently available results of studies of folded *continental* lithosphere, it appears that in general, the observed wavelengths of folding follow theoretical predictions for wavelengths as a function of thermomechanical age remarkably well (see **Figure 43**). Basins that developed on folded continental lithosphere have characteristic features. We illustrate this by largely concentrating on the basins of central Asia, the folded lithosphere of Iberia, the NW European Platform, the Pannonian Basin, and the South Caspian Basin.

6.12.4.2.2.1 Compressional basins of central Asia (Tian Shan and Fergana)

The young Fergana and Tadjik basins are compressional basins northwest and north of the Pamirs and south of the Tian Shan ranges (Burov and Molnar, 1998; Delvaux et al., 2013; Smit et al., 2013). In this area, the lithosphere underwent Jurassic reactivation and is characterized by relatively young thermomechanical ages (175 Ma; Burov and Molnar, 1998; Burg et al., 1994). In addition to having undergone thermal weakening, the lithosphere underlying these basins also probably has a weak, quartz-dominated lower crustal rheology. This has resulted in low values for the effective elastic plate thickness (EET) of the order of 15 km.

The central Tian Shan consists of an alternation of ranges and basins separated by reverse faults. The Tian Shan terminates west of the right-lateral Talas–Fergana Fault by splaying into two narrow mountain chains that surround the Fergana Valley. A narrow belt of mountains parallel to the central section of the fault slopes downward to the Fergana Valley, underlain by a deep basin with as much as 8 km of Cretaceous–Cenozoic sediments (Cobbold et al., 1993). Gravity data suggest that the Fergana and Tadjik basins are gravitationally overcompensated. The negative Bouguer gravity anomalies indicate a Moho several km deeper than predicted by models of local Airy isostasy (Burov and Molnar, 1998). This points to Moho downwarping due to nonisostatic processes and most probably, in this compressional context, to lithospheric folding. As demonstrated by numerical thermomechanical experiments (Burov and Molnar, 1998), the approximately north–south shortening of the relatively thin lithosphere could have created central downwarping and anticline mountains north and south of the basin. According to this model, this shortening has produced a folding instability in the mantle–lithosphere that has warped the basement immediately surrounding the basin upward and has forced the basin floor down beneath the Fergana Valley (with an estimate for the folding wavelength of the order of 200–250 km), possibly also producing deep mantle faulting (seen as Moho offsets in seismic reflection data).

Preexisting thermal structure and variations in crustal thickness have played a major control on the styles and distribution of faulting in this region (**Figure 44**; see also Burov and Molnar, 1998; Cobbold et al., 1993; Delvaux et al., 2013). Primary faults appear before the folding develops with a spacing that is proportional to brittle layer thickness. Subsequently, the two processes, faulting and folding, coexist in such a way that faults localize at the inflection points of folds. At this stage, the appearance of faults does not significantly influences the wavelength of folding. Because of the weakness of the lower crust, the upper crust should be completely decoupled from the mantle and interact with it only by flow in the lower crust. Lower crustal flow changes the wavelength and amplitude of the surface folding, which is terminated by the development of a single downwarped megafold (Cloetingh et al., 1999).

Liu et al. (2007) reported evidence for lithospheric folding in the central/north China Tarim Basin region, initiated during Pliocene times, with good time constraints provided by Ar/Ar dating. Two wavelengths are found of 30 and 400 km. The thermomechanical age of the lithosphere is estimated to be 250 Ma, as the main thermal perturbation was associated with

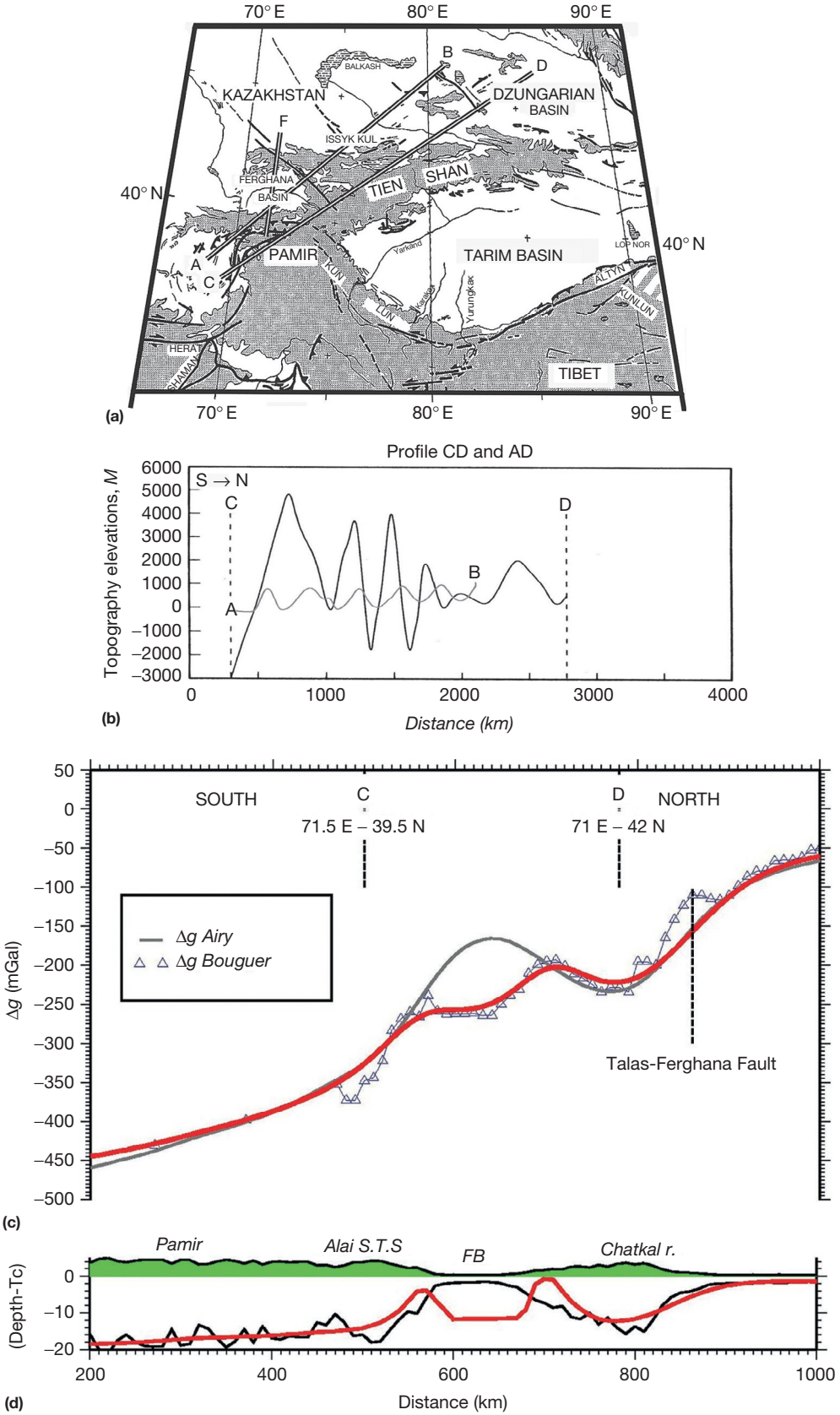

Figure 44 (a) Map showing major tectonic features of Tian Shan area of central Asia, with location of folding profiles discussed in Burov et al. (1993), Burov and Molnar (1998), and Cloetingh et al. (1999). (b) Neotectonic movements along the profiles AD and CD (Burov et al., 1993). (c) Measured and calculated Bouguer gravity anomalies for lithosphere under horizontal compression along profile F across the Fergana basin with corresponding topography profile. (d) Predicted topography and Moho geometry for Airy and best-fitting folding scenario. During compression, the amplitude of plate deflection changed significantly, while the wavelength of folding stayed constant (Burov and Molnar, 1998). Red lines are Bouguer anomaly predicted by folding model and Moho depression, respectively. Solid gray line is Airy isostasy. Solid black line is Airy Moho. Triangles indicate observed Bouguer anomaly. Green is topography above sea level. FB, Fergana basin. Reproduced from Cloetingh S, Burov E, and Poliakov A (1999) Lithosphere folding: Primary response to compression? (from central Asia to Paris basin). *Tectonics* 18: 1064–1083.

a major orogenic phase at 250 Ma ago. These findings are consistent with models in which decoupled lithospheric folds with 30 and 400 km wavelength correspond to, respectively, crustal folding and mantle folding. Deep seismic data for basins north of and within the Tibetan Plateau (Liu et al., 2006; Zhao et al., 2006) show that folding is not limited to the Tibetan Plateau (see also Shin et al, 2009).

6.12.4.2.2.2 Folded lithosphere of Iberia

As reviewed by Cloetingh et al. (2002), Tertiary lithospheric folding of Iberia occurs in Variscan lithosphere with wavelengths of 300 km, leading to the development of a system of parallel trending basins and highs (**Figure 45(a)**). This folding generated the distribution of basins and mountain chains, bounded by folds and faults (Cloetingh et al., 2002; De Vicente et al., 2007). The regularity of the fluvial network pattern of the central-western part of Iberia also indicates large-scale lithospheric folding. Alpine (mainly Cantabrian–Pyrenean-related) compressional tectonics was the principal factor for closing internally drained sedimentary basins, including the Ebro, Duero, and Tagus basins (Casas-Sainz and De Vicente, 2009).

A large body of geophysical and geologic observations is available on the crustal geometries and stress regimes of Iberia (De Vicente et al., 2007, 2008). This is supplemented by geothermochronology data (De Bruijne and Andriessen, 2000, 2002; Ter Voorde et al., 2004, 2007), demonstrating accelerated uplift of the highs during Late Miocene–Pliocene times. In spite of the existence of recent localized volcanism in the inner part of the Iberian plate, an important contribution from thermal uplift is questionable due to the distribution of crustal thickness (Casas-Sainz and De Vicente, 2009). Fernández-Lozano et al. (2011, 2012) have constructed a three-layer analog model consisting of brittle upper crust, ductile lower crust, and ductile upper mantle for Iberia. These models show that folding is associated with the deformation of narrow mountain ranges separated by basins (see **Figure 45(b)**). The narrow mountain ranges representing upper crustal pop-ups form the main topographic reliefs. Shortening is accommodated within the viscous crust beneath the pop-ups leading to lateral thickness variations of the ductile crust. These results are consistent with seismic and gravity data collected in the Cantabrian Mountains, the Spanish Central System, and the Toledo mountains (see also **Figure 45(a)**).

Serpelloni et al. (2013) recently carried out an extensive analysis of continuous Global Positioning System (GPS) data to constrain present-day vertical deformation rates in the Mediterranean region. Their study demonstrates the existence of long-wavelength undulations of vertical velocities in Iberia (**Figure 46**) at spatial scales compatible with predictions from models of lithospheric folding presented earlier.

6.12.4.2.2.3 The European Alpine foreland

Geophysical and geomorphological studies (e.g., Lefort and Agarwal, 1996; 2000; 2002; Marotta et al., 2000) indicate large-scale compressional deformation of the European Alpine foreland lithosphere. Although different in structural grain and rheological structure (Cloetingh et al., 2005a,b; Tesauro et al., 2007) inherited from differences in their Paleozoic–Mesozoic history, different segments of the lithosphere in the northern Alpine European foreland share many similarities in their Cenozoic intraplate deformation. Seismic and geologic evidence shows that the North German Basin cannot be explained by classical models of basin formation (Marotta et al., 2000). The basin underwent a polyphase history (Scheck and Bayer, 1999; Littke et al., 2008) of extension in the Late Triassic followed by lithospheric-scale folding in the Late Cretaceous–early Cenozoic (Mazur et al., 2005; Marotta et al., 2000). 3-D volumetric analysis shows that the compressional event was followed by faster subsidence during the Cenozoic (Scheck and Bayer, 1999). A similar observation was made by Van Wees and Cloetingh (1996) for the North Sea basin. Lithospheric folding modified a basin formed initially by deep-seated thermal perturbations (Scheck and Bayer, 1999) with a thinned crust and shallow Moho. The Moho updoming with a high of 3 km for the height of the bulge in the southern part of the North German Basin appears to be the consequence of flexural buckling of the previously thinned lithosphere by a compressive stress perpendicular to the strike of the basin.

From earliest Triassic to Late Jurassic, the Paris Basin (**Figure 47(a)**) subsided in an extensional framework and was larger than the present basin (Guillocheau et al., 2000). The western margin of the Paris Basin and the rifted Atlantic margin of France were subject to thermal rejuvenation during Mesozoic extension related to North Atlantic rifting (Robin et al., 2003; Ziegler and Dèzes, 2006). Subsequent compressional intraplate deformation (Ziegler et al., 1995) also affected the Paris Basin (Lefort and Agarwal, 1996). Numerical modeling indicates that the amplitude of the compression-induced vertical deflection in the Paris Basin is relatively small, requiring additional mechanisms such as flexure due to the load by the Alpine system (Bourgeois et al., 2007; Ziegler and Dèzes, 2007). However, periodic deformation at the same wavelength occurs northwest of the Paris Basin (**Figure 47(a)**, Bourgeois et al., 2007), which would not be the case if the northeastern part of the basin was flexed down by the load of the Alps. Bourgeois et al. (2007) carefully analyzed basement geometry and timing of vertical motions in the NW European Platform. They separated the contributions from the European Cenozoic Rift System (ECRIS) and the contributions from long-wavelength folding striking NE and located between the Alpine front and the North Sea. According to their analysis, the ECRIS developed mostly between 37 and 17 Ma, whereas lithospheric folds developed between 17 Ma and present, with a wavelength of 270 km and amplitude of 1500 m (see **Figure 47(b)**).

Quaternary folding of the Variscan lithosphere in the area of the Armorican Massif (Bonnet et al., 2000) developed folds with a wavelength of 250 km, pointing to a lithospheric mantle control on deformation. The timing and spatial pattern of uplift inferred from river incision studies in Brittany are incompatible with a glacioeustatic origin. Therefore, Bonnet et al. (2000) related the vertical motions to the deflection of the lithosphere by the present-day NW–SE-directed compressional intraplate stress field. Stress-induced uplift of the area appears to control fluvial incision rates and the position of the main drainage divides. Leveling studies (LeNotre et al., 1999) indicate its ongoing deformation.

6.12.4.2.2.4 The South Caspian Basin

The South Caspian Basin with an estimated sedimentary thickness up to 20 km (Brunet and Cloetingh, 2003; Egan et al.,

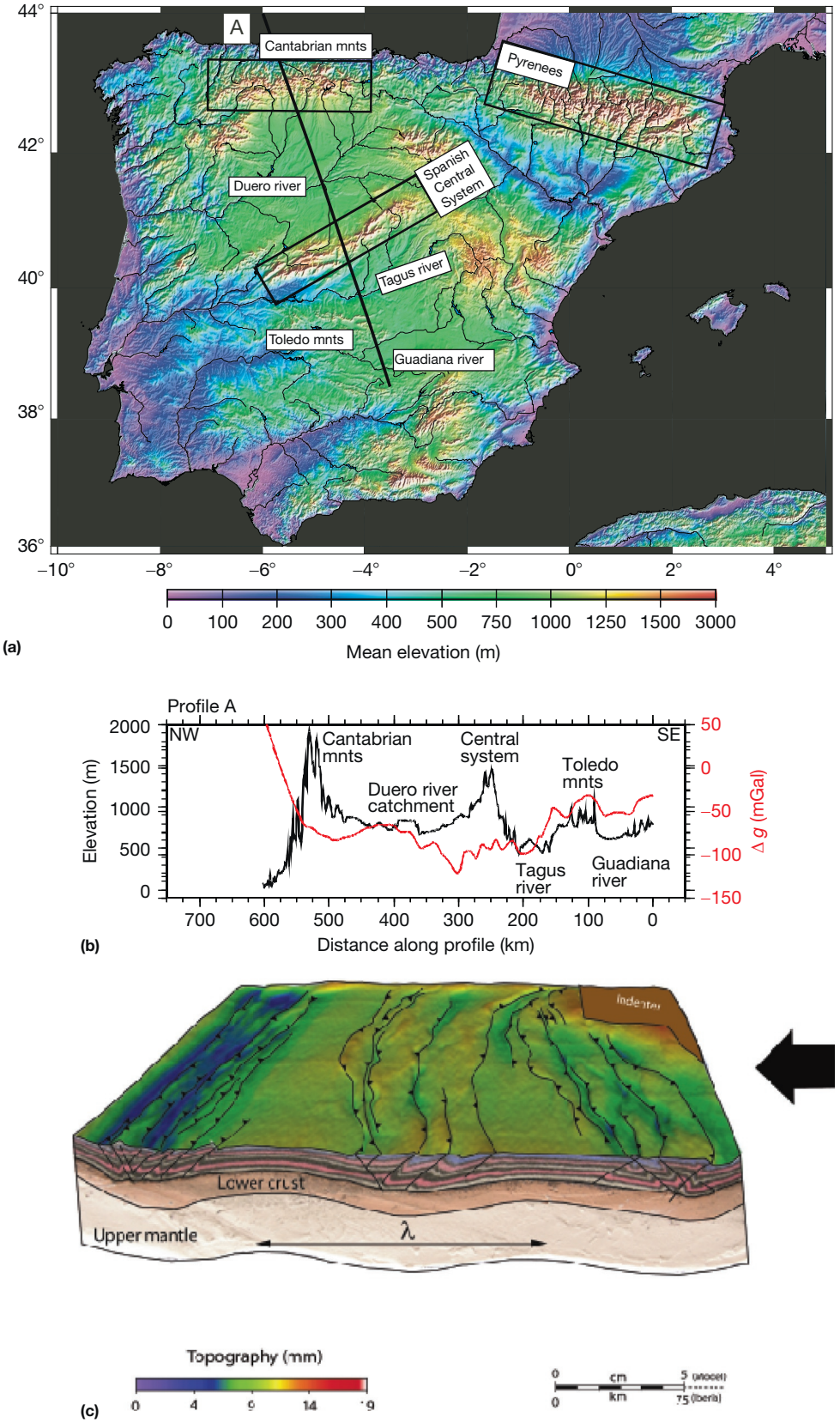

Figure 45 (a) First-order features of basin geometry of folded lithosphere of Iberia. (b) Topography displaying cylindrical patterns of alternating parallel trending highs and lows and corresponding gravity anomalies (red line) (see Cloetingh et al., 2002). (c) Results from analog modeling experiments, displaying pop-up structures underlying topographic highs, accompanied by folding of the Moho (Fernández-Lozano et al., 2011, 2012). Top panel shows final top view of the analog model and location of the cross section shown below. Arrow indicates the direction of the moving wall. λ is the wavelength of folding.

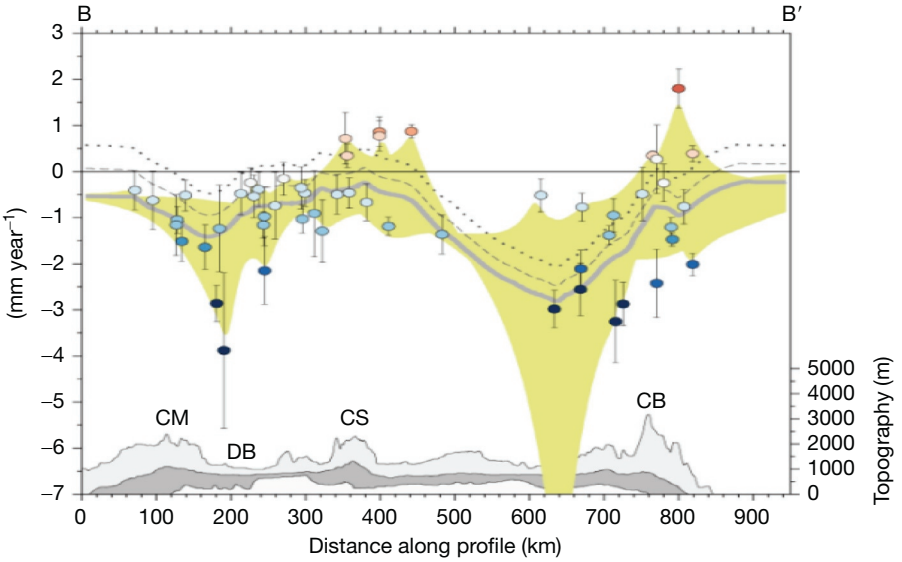

Figure 46 Observed vertical velocity field over the Iberian region (after Serpelloni E, Faccenna C, Spada G, Dong D, and Williams SD (2013) Vertical GPS ground motion rates in the Euro-Mediterranean region: New evidence of vertical velocity gradients at different spatial scales along the Nubia-Eurasia plate boundary. *Journal of Geophysical Research: Solid Earth* 118: 6003–6024). The cross section of the observed vertical velocities (colored circles), with 1σ uncertainty error bars, of GPS stations along cross section B–B′ in **Figure 45(a)**. The gray line shows the median value estimated from the smoothed spline fit of the vertical velocity field, while the yellow envelope shows the minimum and maximum vertical rates values in the swath, filtered using a 10 km Gaussian filter. Dark gray profile shows the average (median) topography, while the light gray and white profiles show the maximum and minimum elevations, respectively. The dotted and dashed lines show the median value estimated from the smoothed spline fit of the vertical velocity field corrected for the GIA component using two different models. DB, Duero basin; CS, Central System; CM, Cantabrian Mountains; and CB, Betic Cordillera.

2009) is probably one the deepest basins in the world. It is flanked by the Alborz Mountains to the south, with an elevation of 2–4 km (see **Figure 48**). The transition between basin and flanking high is abrupt and coincides with a coastline bounded by a major fault system. The formation of the South Caspian Basin is enigmatic. Attempts to explain it as an extensional basin or as a foreland basin have been unsuccessful. There is a lack of evidence for basin extension, and both stretching models and topographic loads and slab pull operating on downflexed lithosphere in foreland basin systems cannot explain differential vertical motions of this order of magnitude. As a result, phase changes in continental crust have been proposed as a mechanism for the formation of this superdeep basin (Artyushkov, 2007). A limitation in conclusively resolving the basin formation mechanism is the lack of multichannel seismic reflection data capable of imaging crustal structure below the thick sedimentary sequences. Over the last few years, however, other constraints on the area have become available (e.g., Guest et al., 2007).

Figure 48 presents a cross section of northern Iran and the South Caspian Basin (Guest et al., 2007). As shown, wavelengths for compressional folding of the lithosphere are typically in the range of 400 km. Although the actual basin formation mechanism for the Caspian Basin is not well resolved (e.g., Artyushkov, 2007), late Neogene folding has been affecting a lithosphere probably thermally reset by middle Late Jurassic marginal basin formation (Guest et al., 2007) with a thermomechanical age at the onset of collision of 130–150 Ma. Satellite data demonstrate an exceptionally large gravity anomaly over the basin (Kaban, 2002). Seismic tomography shows slab detachment under the Iranian plateau (Alinaghi et al., 2007; Hafkenscheid et al., 2006) beginning at about 10–15 Ma.

Basin analysis has shown that basement inversion has occurred 20 Ma ago, simultaneously with the slowing of Arabian/Eurasian Plate convergence and the onset of accumulation of Neogene clastics in foreland basins (e.g., Fakhari et al., 2008). By 10 Ma, contraction occurred by underplating of the Arabian crustal units beneath the Iranian Plate. Estimated shortening rates from current geodetic surveys (Vernant et al., 2004) are 7 mm year^{-1}. Results from geothermochronology demonstrate rapid uplift of the Alborz Mountains, with rates of 0.7 km My^{-1} exhumation between 6 and 4 Ma (Axen et al., 2001), implying $\sim$10 km of uplift. This uplift was nearly synchronous with rapid South Caspian subsidence (Nadirov et al., 1997) and subsequent folding (Devlin et al., 1999). South Caspian sedimentation rates locally increased more than tenfold at ca 6 Ma, with more than 10 km of sediments deposited since then. Axen et al. (2001) argued that if $\sim$10 km of post-6 Ma sediments is present in this basin, then as much as 20 km (equivalent to 80%) of the structural relief of about 25 km between the high Alborz and the southernmost Caspian basement may be younger than 6 Ma.

Folds in the southernmost Caspian Basin (Devlin et al., 1999) and in the Neogene of the northern Alborz foothills imply contraction. The lack of a crustal root under the Alborz Mountains also points to a flexural support by the South Caspian basement (Axen et al., 2001). The simultaneous reversal of Zagros strike slip and extrusion of central Iran, coarse Zagros molasse deposition, Dead Sea transform reorganization, and Red Sea oceanic spreading (Chu and Gordon,

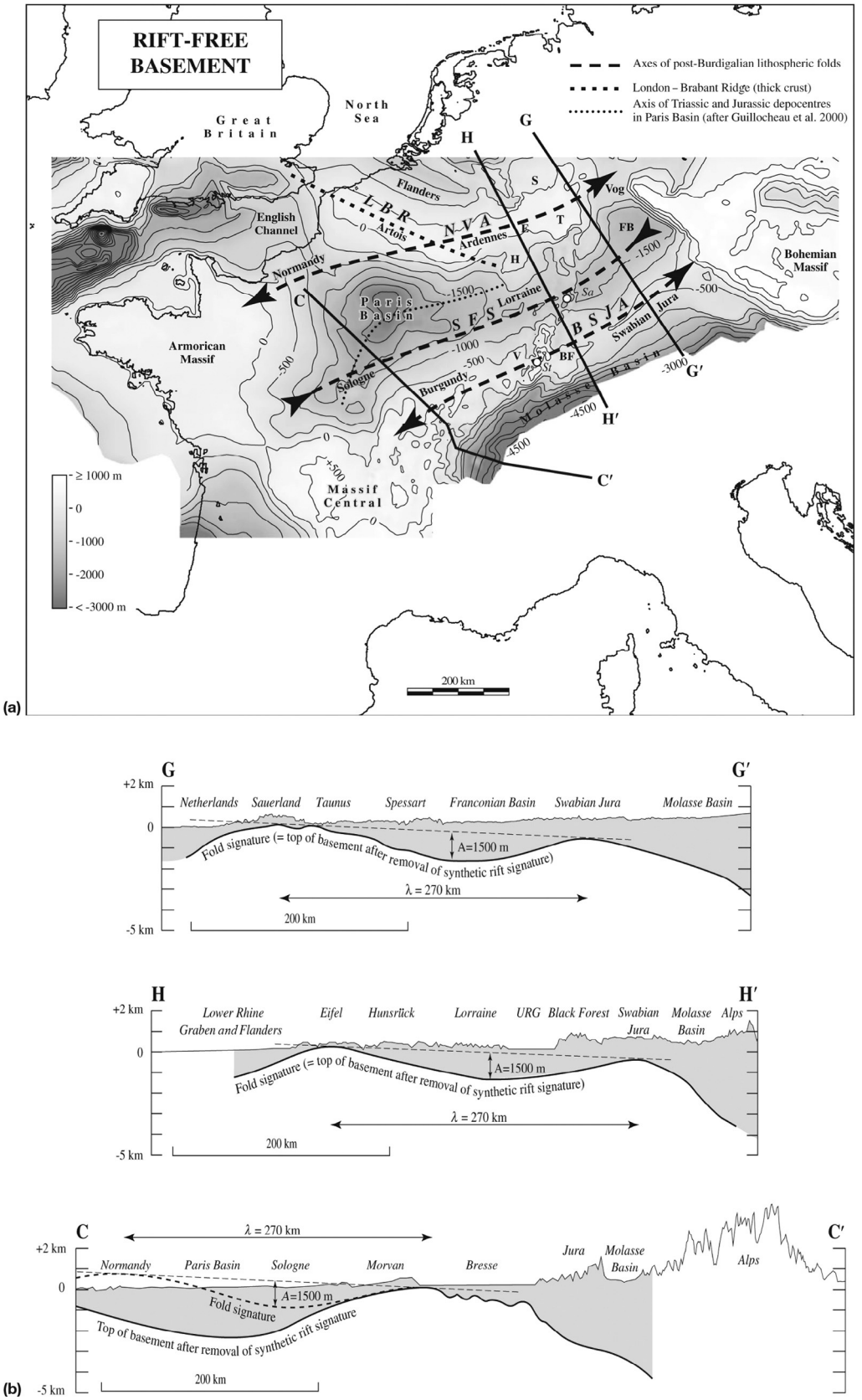

Figure 47 (a) Map of elevation of basement in the NW Alpine foreland with rift signature removed from the map of actual basement (reproduced from Bourgeois O, Ford M, Diraison M, et al. (2007) Separation of rifting and lithospheric folding signatures in the NW-Alpine foreland. *International Journal of Earth Sciences* 96: 1003–1031). Dashed lines show axes of late Neogene lithospheric folds, with a succession of anticlines and synclines: the Normandy–Vogelsberg anticline (NVA), Sologne–Franconian Basin Syncline (SFS), and the Burgundy–Swabian Jura Anticline (BSJA). LBR, London–Brabant Ridge with thick crust; BF, Black Forest; FB, Franconian Basin; E, Eifel; H, Hunsrück; S, Sauerland; T, Taunus; V, Vosges. (b) Cross sections of top basement in the NW Alpine foreland with rift signatures removed (Bourgeois et al., 2007; see for location Figure 47(a)). Thin line: Actual topography surface. Bold line: Elevation of top basement as predicted in the absence of rifting. Fold signatures are similar with a wavelength λ of 270 km and amplitude A of 1500 m in the Franconian Basin (cross section G–G′) and in the upper Rhine Graben area (cross section H–H′). In the Paris Basin, the development of folds with assumed same wavelength and amplitude (stippled bold line in cross section C–C′) implies subsidence of Sologne and uplift of Normandy.

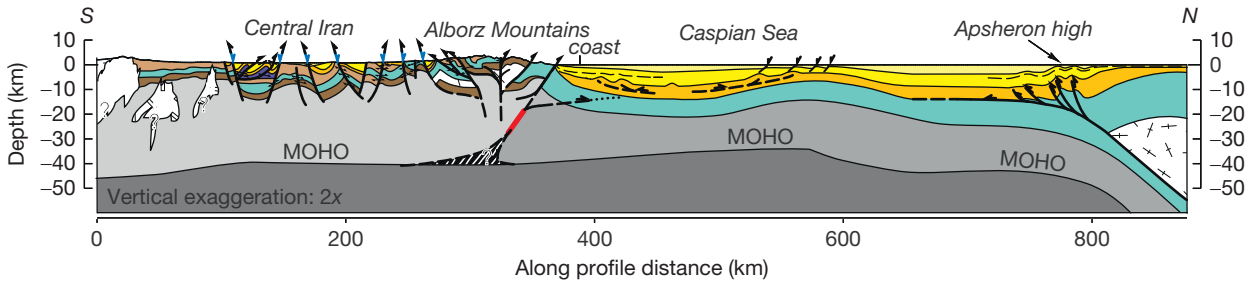

Figure 48 Schematic north–south trending cross section illustrating the basic tectonic setting for northern Iran and the South Caspian Basin (Guest et al., 2007), illustrating basin inversion of the central Iranian basin, pronounced differential topography at the transition of the Alborz Mountains, with a topographic high of several kilometers and the South Caspian Basin with about 20 km of sedimentary infill.

1998) all initiated around 5 ± 2 Ma (e.g., Axen et al., 2001; Smit et al., 2008a,b, 2010), was interpreted by these authors in terms of a widespread tectonic event. Slab detachment could explain part of the recent uplift of Iran, but does not directly explain the simultaneous dramatic subsidence in the adjacent Caspian Basin. However, slab detachment could have an indirect effect if reducing slab pull forces acting on the downgoing lithosphere promote the development of compressional stresses in both the downgoing and the overriding plates (Cloetingh et al., 2004; Matenco et al., 2007).

Guest et al. (2007) argued in favor of compressional deformation of the South Caspian Basin/Alborz Mountains. This interpretation was largely based on available industrial seismic reflection data and gravity data for the basin and followed a similar proposition made for the late-stage deformation of the adjacent Black Sea (Cloetingh et al., 2008; Nikishin et al., 2003). Guest et al. (2007) presented kinematic models, without addressing the reason for the difference in the order of magnitude of the basin depression and the adjacent high. Analog experiments (Sokoutis et al., 2005) show that when compression acts on two blocks with contrasting thickness (and rigidity), a major syncline will develop on top of the suture zone separating these blocks, flanked by an anticline of much lower amplitude. These results are consistent with predictions from folding theory that as a result of the acting gravity field, downwarping is mechanically more effective than upwarping against the action of gravity forces.

6.12.4.2.2.5 Basins on folded lithosphere in Eurasia

Comparison of lithospheric deformation in central Asia, Iberia, the NW European Alpine foreland, and the South Caspian Basin demonstrates common features compatible with an interpretation in terms of basins developed on folded lithosphere. Among these are their symmetrical shape, dimensions, and the temporal association of their basin formation history with the buildup of intraplate stresses. Important differences can be observed between the central Asian and Iberian basins and the South Caspian Basin on one side and the European Alpine foreland on the other side.

The central Asian basins and the basins of the Iberian Plate were initiated by Tertiary folding, whereas the European Alpine foreland underwent a polyphase history, following Carboniferous and Triassic stretching (Le Solleuz et al., 2004; Scheck and Bayer, 1999), prior to Late Cretaceous–early Cenozoic folding. The origin of the South Caspian Basin is not well resolved, but km-scale vertical motions are compatible with a megafold as a prime control on present-day basin geometry. These differences in evolution have a pronounced impact on basin dimensions and on the nature of basin fill. The central Asian basins, the folded basins of Iberia, and the South Caspian Basin have a wavelength compatible with theoretical predictions. In contrast, the fold wavelengths of the European Alpine foreland appear to be primarily controlled by the preexisting geometry of the sediment–basement interface and preexisting Moho topography inherited from the prefolding stage.

Differences occur also in the development of the ranges flanking the basins. In central Asia and Iberia, these highs have amplitudes and widths comparable to the prediction for periodic folding, whereas in the Paris Basin and the North German Basin, these highs are less well developed. The ratio of the depth of the South Caspian Basin to the height of the flanking Alborz Mountains is compatible with a megafold under this area of dramatic differential topography. The large amplitudes of folding at the flanks of the Pannonian Basin system are compatible with its extremely weak rheology. Differences in the amplitude of the highs might also partly result from the differences in neotectonic shortening. The highs bounding the basins of Iberia, South Caspian Basin, and central Asia, located relatively close to the site of ongoing convergence, are still experiencing active uplift. This is much less the case for the low-strain-deforming areas of the NW European Platform and the North German Basin where the peak compression occurred during Late Cretaceous–early Cenozoic. Another difference occurs in the depositional regime prevailing in these basins. The closed basin systems of central Asia and Iberia are dominated by continental and lacustrine deposits, whereas capture is usually a late-stage feature of these basins. The Paris Basin of the NW European Platform has a basin fill largely dominated by marine sediments deposited during the prefolding stage of their evolution, followed by marine Tertiary successions in the basin center with truncated basin margins. The creation of basin highs in this case was in general not capable of interrupting open connections to marine environments.

A general observation for all these basin systems is the flatness of sedimentary sequences in the depocenters. Faulting plays a minor role in the basin development. Faulting appears to be concentrated at the basin margins, with a highly variable depth extent, varying from upper crustal-scale faults bounding pop-up structures in the Iberian Central System to minor faulting in the basement of the North German Basin. The thermal regimes of the basins are similar with thermal histories strongly affected by subsidence and sediment deposition on downflexed lithosphere, preconditioned by its thermomechanical age.

6.12.4.2.3 Basin geometry and accommodation space

6.12.4.2.3.1 Basin shape

Folding of the lithosphere leads to a symmetrical pattern of downwarped areas (synclines) flanked by highs (anticlines) of similar amplitude and wavelength, like the Fergana basin in central Asia (Burov and Molnar, 1998). This symmetry is in marked contrast to the asymmetrical shape of foreland basins, formed by flexure in front of an orogenic wedge, which are flanked by a flexural bulge of which the amplitude is only up to 10% of the maximum depth of the foreland depression (Royden, 1988a,b; Zoetemeijer et al., 1999). Both types of compressional basins show linear nature alignment of parallel depocenters and flanking highs. An important difference is the presence of parallel trending depocenters for lithospheric folding, whereas foreland flexural basins have a single depositional system. In addition, basins developed on folded lithosphere have a static location of the axis of their depocenters, in contrast to foreland basins, where the axis of depocenters can migrate with time (e.g., Zoetemeijer et al., 1993).

In both cases, the integrated strength of the lithosphere (Tesauro et al., 2007; Watts and Burov, 2003) defines the characteristic width of the basins. For folding, the basin width roughly corresponds to one-half of the fold wavelength (λ), which equals 5–10 times the thickness of the strong core of the lithospheric plate, h ($h = 10$–100 km, i.e., $\lambda = 50$–1000 km). In the case of crust–mantle decoupling, which occurs in relatively young plates, two dominant folding wavelengths develop (typically 250–400 km and 50–100 km). Thus, two basin populations may be observed, one imbricated within the other. In the case of flexural foreland deformation, the width of the basin is controlled by the flexural parameter and is thus of the same order as the largest fold wavelength.

6.12.4.2.3.2 Subsidence patterns

Lithospheric folding results from an instability in the lithosphere due to stress/strain incompatibilities that develop in rheologically stratified layers under compressive strain. This process typically operates with timescales of the order of 1–10 My (Cloetingh et al., 1999). The preservation of lithospheric folds appears to depend strongly on the thermomechanical age of the underlying lithosphere (Cloetingh et al., 1999). Folds in young lithosphere will not be preserved upon relaxation of the stress field, whereas ones in cratonic lithosphere will be well preserved (Cloetingh et al., 1999).

Figure 49(a) displays characteristic basin subsidence patterns predicted by folding of 150 and 300 Ma old lithosphere due to a 3 cm year^{-1} shortening rate. As illustrated (**Figure 49(b)**), the differential motions occur in three distinct phases:

- *Stage 1* is the basin formation phase, coinciding with the initiation and development of folding, which is marked by an acceleration of subsidence in the basin and uplift in the flanking highs. As a result of the time lag between sediment supply and the creation of accommodation space, during the few My needed to form the basin, deposition cannot keep up with subsidence causing sediment-starved basins. A similar pattern occurs in pull-apart basins (Pitman and Golovchenko, 1983), which are also associated with ultra-rapid subsidence in their formation stage also lasting only a few My.

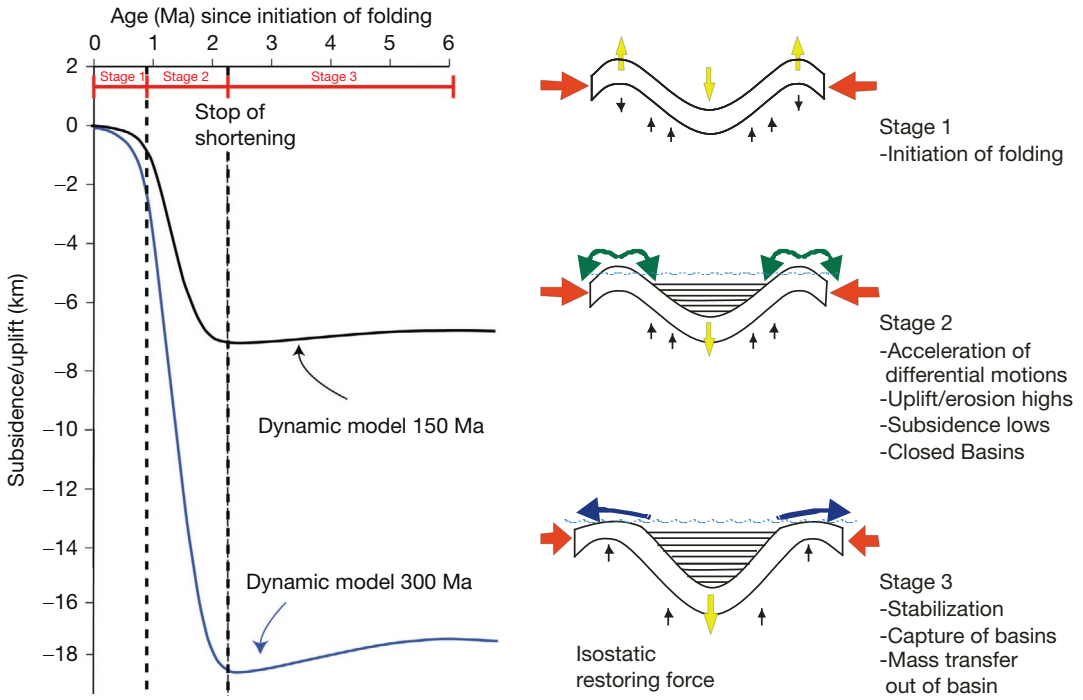

Figure 49 (a) Characteristic subsidence patterns in center of synclinal depression for thermomechanical age of 150 and 300 Ma, respectively. Shortening rate is 3 cm year^{-1}. (b) Characteristic stages in the evolution of a basin formed by lithospheric folding. Stage 1: Basin formation stage, acceleration of subsidence and uplift during folding. Stage 2: Steady state: equilibrium between tectonic subsidence and sediment supply from eroding highs. Stage 3: Capture of folded basin: overall uplift and erosion. Wiggled waved blue line marks position of base level. Reproduced from Cloetingh S and Burov E (2011) Lithospheric folding and sedimentary basin evolution: A review and analysis of formation mechanisms. *Basin Research* 23: 257–290.

- *Stage 2* is the basin preservation stage, where equilibrium develops between sediment supply and sediment deposition. As a result, the basin will be rapidly filled to overfilled.
- *Stage 3* is the basin destruction phase, characterized by basin capture and removal of sediments to areas outside the folding system. During this phase, the size of the accommodation space is reduced and erosion occurs on both flanks and depocenter. Thus, the net effect of these three stages is that lithospheric folding will lead to the development of distinct depositional–erosional cycles.

Characteristic patterns for vertical motions for folding of continental lithosphere of 150 and 300 Ma old (**Figure 49**) demonstrate a remarkably short timescale in which substantial amounts of tectonic subsidence are induced by the process of lithospheric folding. As shown by **Figure 49**, within 1 My after the initiation of folding induced by shortening the lithosphere at a rate of 3 cm year^{-1}, subsidence rates are in the order of 5–15 km My^{-1}, depending on the thermomechanical age of the lithosphere. Thus, folding appears to be more effective in middle-aged lithosphere of 300 Ma than in lithosphere of younger ages (Cloetingh et al., 1999; Burov and Cloetingh, 2009). After 2 My, a slow uplift phase starts of relatively minor magnitude of the order of a few hundreds of meters to a km. The predicted subsidence in **Figure 49** is for the center of the syncline. As pointed out earlier, erosion of the uplifted flanks is taken into account, adopting a diffusive equation approach to erosion (see Burov and Cloetingh, 1997; Cloetingh et al., 1999, for further details).

The alignment of parallel highs and basins of similar dimensions has an important consequence for the areal extent of the source areas for sediments available for deposition in the folded depressions. In comparison with foreland basins, the distribution of sources is more symmetrical, superseding the volume of sediments that can be eroded from, for example, the flexural foreland bulge. As noted earlier, erosion reduces the contribution of gravity-dependent terms and accelerates local deformation. Erosion, therefore, has an important feedback with the geometry of the accommodation space in changing the spectrum of wavelengths (Cloetingh et al., 1999). Erosion acts as a filter, suppressing the shorter wavelengths in folded basin topography. Strong erosion, insufficiently compensated by tectonic deformation, can even wipe out most of the topography. However, if the erosion is tuned to the average elevation rates (**Figure 50**), it may dramatically accelerate folding (Cloetingh et al., 1999).

There has been a rapid development in the application of stratigraphic modeling packages to sequence stratigraphy over the last two decades (e.g., Alzaga-Ruiz et al., 2009; Cross, 1990). Among the different types of modeling programs, the forward stratigraphic modeling approach has been applied extensively by basin modelers from academia and petroleum industry (e.g., Lawrence et al., 1990; Roure et al., 2010b). Forward stratigraphic modeling commonly starts with an estimate of the initial conditions related to an adopted basin formation mechanism and controlling parameters, followed by a forward prediction in time. Most of these software packages are based on sequence stratigraphic concepts (Wilgus et al., 1988). Assumptions for initial subsidence are either ad hoc or related to stretching (e.g., Lawrence et al., 1990) or foreland flexure (Garcia-Castellanos et al., 1997), but to date do not include lithospheric folding as a basin formation mechanism.

6.12.4.2.4 Thermal regime

Lithospheric folding is controlled by the interplay of lithospheric stresses and inherited strength of the lithosphere. The thermal regime controls the rheological profile and differs between folded basins developed in young lithosphere and basins in cratonic lithosphere. The latter are associated with much lower thermal gradients than basins developed on young continental lithosphere. As for foreland basins, the initiation

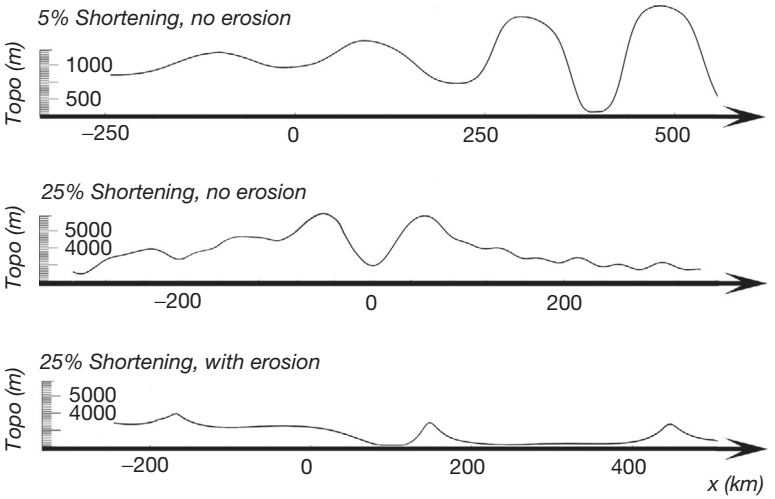

Figure 50 Illustration of the effect of erosion, which acts as a filter suppressing the short wavelengths. In this case, the wavelength and amplitude vary along the cross section at different stages of deformation due to a partial crust–mantle coupling and strain localization for a 400 Ma old lithosphere with weak quartz-dominated rheology. After 5% shortening (top), after 25% shortening (middle), after 25% shortening (bottom), strong zero order diffusional erosion (Avouac and Burov, 1996) tuned to keep mean elevation at the level of 3000 m. Erosion reduces the contribution of gravity-dependent terms (middle wavelength) and accelerates local deformation. Strong erosion, insufficiently compensated by the tectonic deformation wipes out most of the topography. Reproduced from Cloetingh S, Burov E, and Poliakov A (1999) Lithosphere folding: Primary response to compression? (From central Asia to Paris basin). *Tectonics* 18: 1064–1083.

of folding is not associated with a thermal instability, unless folding occurs in conjunction with plume activity (Burov and Cloetingh, 2009). Following the deposition of radiogenic sediments in the folded depression, sediment blanketing will affect the heat flow (Lavier and Steckler, 1997; Stephenson et al., 1990; Van Wees et al., 2009), modifying the surface heat flow in the basin center. As pointed out by Lavier and Steckler (1997) and Ziegler et al. (1998), the effect of sediment fill is to weaken the lithosphere. The low thermal conductivities of the sediments lead to high temperatures in the upper lithosphere and consequently low local yield strength. During basin subsidence, sediments deposited in the central parts of the basin might be exposed to temperature windows corresponding to hydrocarbon generation. At the same time, sediments predating the folding may have undergone extra burial due to synfolding sedimentation. An example is the Paris Basin, where source rocks of Toarcian age were folded in Cenozoic time (Guillocheau et al., 2000; Le Solleuz et al., 2004).

During basin capture, overall cooling takes place. This effect is illustrated by characteristic thermal evolution for different thermotectonic ages of 150 and 300 Ma of the folded continental lithosphere (**Figure 51**), incorporating radioactive heat production in the sediments filling in the synclinal basement depression (**Figure 49(b)**). Subsidence induced by folding is calculated for the center of the basin. Basins developing on folded lithosphere are characterized by their relatively low heat flow at the onset of folding, followed by a steady increase with time, doubling the heat flow over a time interval of the order of 5 My following the cessation of shortening. This increase is primarily due to the contribution of radioactive heat production in the very substantial pile of sediments accumulating in a relatively short time interval. The patterns of heat flow are similar for different thermomechanical ages of the lithosphere, with the oldest lithosphere having the lower heat flow. Older ages enhance the accommodation space and the contribution of the sediments to heat flow but are compensated by a larger decrease in heat flow with aging lithosphere. Another important factor is the mode of folding. Crustal-scale folding, which is characteristic for Lake Issyk-Kul, will be associated with shorter wavelengths, shallower basin depths, and thinner sequences of heat-producing sediments than for mantle–lithospheric folding. This effect might explain the relatively low heat flow observed in Lake Issyk-Kul (Vermeesch et al., 2004).

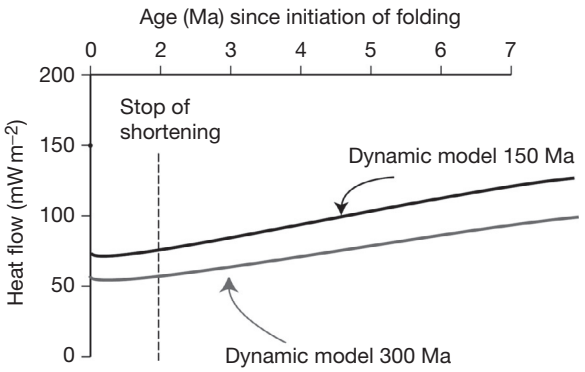

Figure 51 Thermal consequences of lithospheric folding and associated basin evolution depicted in **Figure 49**. The heat flow response is marked by an initial decrease in heat flow as a consequence of rapid sedimentation, followed by a progressive long-term heat flow increase after termination of shortening. Thermal conductivity of sediments is 2.5 $Wm^{-1}\,C^{-1}$. Surface radiogenic heat production H_s is 9.5×10^{-10} W kg^{-1}. Concentration of radiogenic heat sources within sedimentary basin fill is homogeneous. Exponential decay of heat production is assumed for underlying crustal rocks. Note that the figure shows only 7 Ma of thermal evolution. The heat flow does not increase anymore after some tens of Ma and subsequently decreases at later stages. Reproduced from Cloetingh S and Burov E (2011) Lithospheric folding and sedimentary basin evolution: A review and analysis of formation mechanisms. *Basin Research* 23: 257–290.

6.12.4.2.5 Modes of brittle deformation and faulting

The role of preexisting faults on the development of folding has been investigated through numerical experiments on folding of brittle–elastoviscous lithosphere (Beekman et al., 1996; Cloetingh et al., 1999; Gerbault et al., 1999) and through analog experiments on plastic–elastic lithosphere (e.g., Martinod and Davy, 1992; Sokoutis et al., 2005). These studies show that lithospheric folding and faulting can develop simultaneously and that preexisting crustal-scale faults do not prevent but instead promote the development of folding instabilities. The instabilities, in turn, can initiate the formation of new faults at the inflection points of the folds. Although the usual expectation is that faulting prevents folding, this view neglects the role of the gravity and friction on faults in the behavior of the large-scale fault-and-fold systems. As also observed in analog experiments (Martinod and Davy, 1992), this continuous behavior of faulted lithosphere can be explained by fault locking due to gravity and friction. After some sliding (uplift) on a fault, the potential gravitational energy working against friction generated by horizontal shortening forces becomes too high. As a result, the fault locks and the rock mass transmits horizontal stresses as a continuous medium. As the compression continues, one of the folds finally starts to grow faster than others, resulting in a loss of the periodicity and the formation of a megafold (see also the discussion in the context of the Fergana and Tadjik basins of central Asia).

Following the initiation of folding and the further buildup of compressional stresses, folding, therefore, will usually be accompanied by brittle deformation and faulting in the crust and upper lithosphere. The surface expression of folding in uniform lithosphere is frequently in the form of fault-controlled pop-up and pop-down structures and inverted basins (e.g., Cobbold et al., 1993), accompanied by the development of imbrications of bivergent thrust wedges at the areas where shortening is applied (Sokoutis et al., 2005). These findings (see **Figure 52**) are corroborated by observations in the Iberian Central System, where folding of Variscan lithosphere with a thermomechanical age of 280 Ma occurs (Cloetingh et al., 2002). Here, the brittle deformation associated with crustal-scale folding expressed by a folded Moho is mechanically decoupled from folding of the mantle–lithosphere (Fernández-Lozano et al., 2011, 2012; see **Figure 45(b)**).

Crustal and mantle faults may develop as a result of folding (Burov and Molnar, 1998; **Figure 53**). Folding can continue after these faults develop, and folding and faulting can coexist for times of several My (**Figure 45(b)**). For crust–mantle decoupling, a complex distribution of crustal faults and surface undulations can be expected, with crustal faults not necessarily connected to mantle faults. Numerical experiments suggest

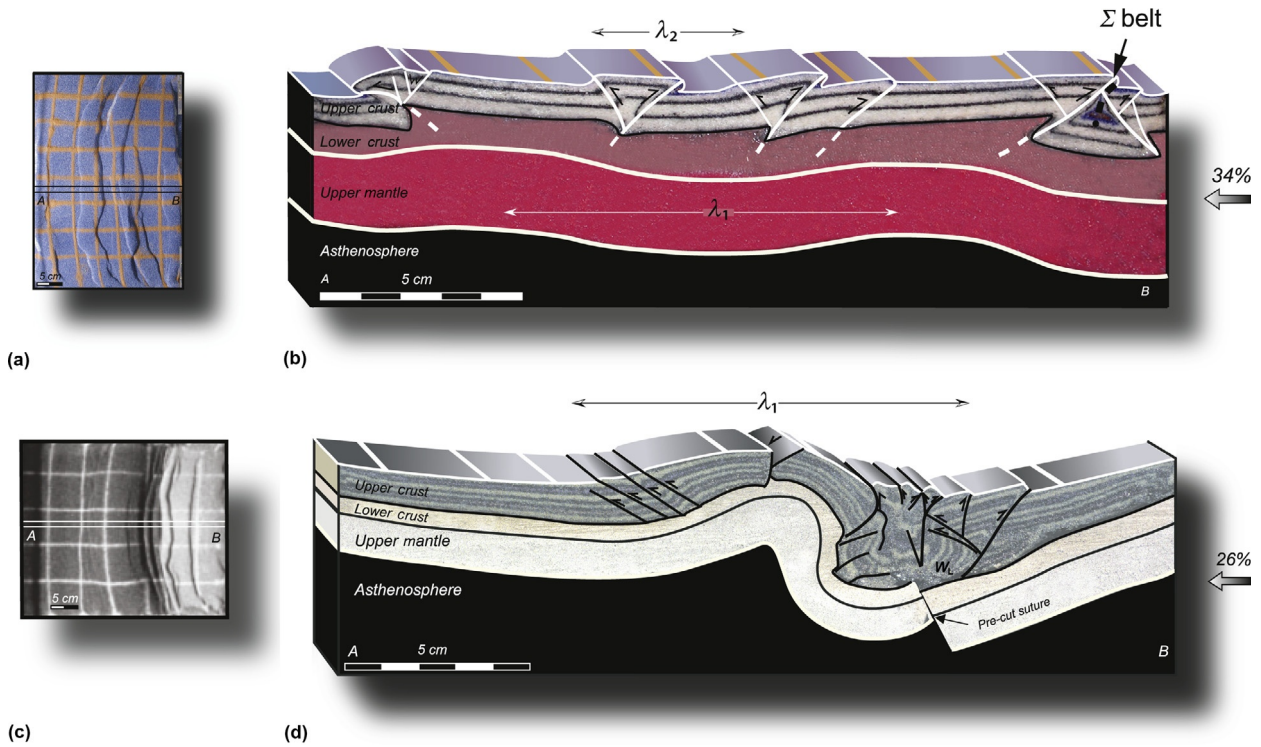

Figure 52 Results of analog tectonic experiments for lithospheric folding. (Top) Folding of uniform lithosphere. Cross section demonstrating pop-up structures in the upper crust above highs induced by lithospheric folding. λ_1 and λ_2 indicate first-order and second-order wavelengths, respectively. Imbrication of bivergent thrust wedges is responsible for the relatively high-topography belt ($\sum$-belt) at the right hand of the model and closure of prismatic basins with a rather undisturbed bottom. The progressive sinking of the prismatic basin allows transferring of the crustal material (i.e., cover sediments) that was initially situated at the surface of the model down to significant depth. (a) Final top view of model after 34% of bulk shortening. (b) Cross section located on the top view. Arrows indicate the direction of the moving wall. Note the similarity to central Iberia (**Figure 45**). (Bottom): Geometries predicted by analog experiment, shortening a lithosphere with two contrasting blocks, bounded by suture. A deep synclinal depocenter develops over the suture zone, flanked by an anticline of smaller amplitude. (c) Final top view of model after 26% of bulk shortening. (d) Cross section located on the top view. λ_1 indicates a first-order wavelength of the folding. Note the striking similarity to the configuration of the South Caspian Basin/Alborz mountain system displayed in **Figure 48**. Reproduced from Sokoutis D, Burg JP, Bonini M, Corti G, and Cloetingh S (2005) Litho spheric-scale structures from the perspective of analog continental collision. *Tectonophysics* 406: 1–15.

that mantle faults are unlikely to be longer than a few km in depth (Burov and Molnar, 1998). Such faults may also not develop at longer wavelengths of folding connected with stronger lithosphere. However, deep-seated faults in mantle–lithosphere can develop when cratonic lithosphere is folded (Cloetingh et al., 1999). The mode of faulting, depth extent, and spacing of faults depend on the thermomechanical age of the lithosphere. Once the development of folding begins in a basin, the intensity and depth penetration of faulting will accelerate. The mode of decoupling between crustal folding and mantle folding is crucial. Discontinuities within the folded lithosphere will localize the development of deep synclines, flanked by more modest anticlines (Sokoutis et al., 2005), and affect the distribution of faulting (**Figure 52**).

During the next phase of basin evolution, when a steady state is reached between the creation of accommodation space and sediment supply, only minor faulting will occur. This is in marked contrast with the later phase of basin capture, which is in general characterized by erosion and narrowing of the basin. Due to erosional unloading, stress relaxation will occur, manifested in upward propagating faults.

6.12.4.2.6 Interaction of folding with other tectonic processes

Folding, in addition to being a basin-forming mechanism, frequently interacts with other tectonic processes. As pointed out by Cloetingh (1988), intraplate compression can modify preexisting basins. As discussed earlier, the Pannonian Basin of central Europe created by Miocene back-arc extension appears to be an example of such a configuration, characterized by atypical aperiodic folding. Other examples are cratonic sag basins where intraplate compression (Cloetingh, 1988) is thought to occur in interaction with phase changes in the lithosphere (Artyushkov, 2007). Examples of these might be the Barents Sea (Ritzmann and Faleide, 2009) and possibly the South Caspian Basin, although in the latter case, preorogenic extension cannot be ruled out (Guest et al., 2007). Basins exposed to changes in tectonic regime will have a polyphase record (Cloetingh and Ziegler, 2007), characterized by a superposition of more than two regimes, such as preorogenic extension, foreland flexure, and late-stage folding. This sequence appears to be characteristic for some very deep foreland basins, such as the Focşani Depression of the Romanian Carpathians,

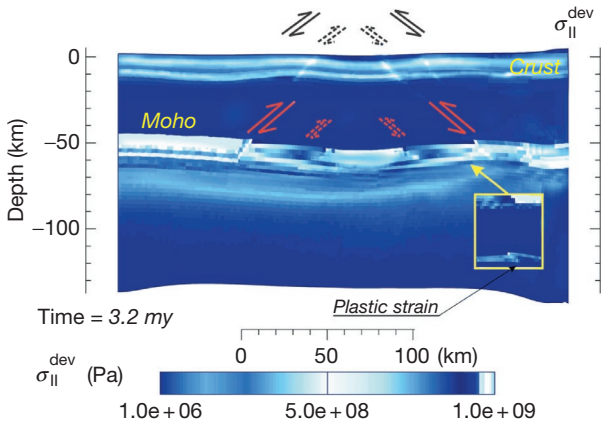

Figure 53 Numerical experiment on faulting developed in folded continental lithosphere of 150 Ma. Note different wavelengths of the crustal and mantle part of the lithosphere and differences in spacing and character of faults that are conditioned by folding. In each layer, two fault spacings occur: A shorter one proportional to layer thickness (also controlled by the strength contrast between the stiff layer and embeddings) and the longer wavelength controlled by the wavelength of folding. The insert shows plastic (brittle) strain localization characterizing initialization of mantle faulting. Reproduced from Burov EB and Molnar P (1998) Gravity anomalies over the Ferghana Valley (central Asia) and intracontinental deformation. *Journal of Geophysical Research-Solid Earth* 103: 18137–18152.

with more than 16 km of sediments, which was affected by extension due to the opening of the Black Sea basin, followed by foreland flexure and overprinted by Late Miocene compression (Tarapoanca et al., 2003). As pointed out earlier (Ziegler and Dèzes, 2007), the northwestern European foreland indicates folding, overprinting, rifting, and foreland flexure. Quantification of the topographies created by rifting and foreland flexure and correcting for them is essential to reconstruct the shape of the additional accommodation shape created by subsequent lithospheric folding (Bourgeois et al., 2007).

The impingement of plumes on the base of continental lithosphere can induce differential topography similar to the surface deflections characteristic for lithospheric folds (Burov et al., 2007; Guillou-Frottier et al., 2007). Plumes and lithospheric folds frequently interact in space and time in the geologic record (Burov and Cloetingh, 2009; Ziegler and Dèzes, 2007). Therefore, the evolution of folded lithosphere basins can be overprinted by the signatures of a plume or vice versa. This will lead to an amplification of the induced vertical motions, particularly significant for young and intermediate age lithosphere. Emplacement of hot upper mantle material will raise temperatures in the lithosphere and increase heat flow. Due to the lag time in the propagation of heat, the effect at the surface might become manifest only after several tens of My. Plume emplacement might also weaken the lithosphere, making it more prone to compressional fault reactivation after cessation of the folding.

Thermomechanical modeling illustrates the relative effectiveness of amplification of lithospheric deformation and topographic effects induced by plumes though folding and vice versa and consequences for basin evolution. Burov and Cloetingh (2009) examined the response times and time lags involved and whether small plumes were more efficient in localizing deformation than large plumes. Plume-affected folding appears to accelerate differential vertical motions (uplift and subsidence) in sedimentary basins. For the discrimination of plumes and folding as mechanisms for sedimentary basin formation, it is critical to access constraints on the presence or absence of radial versus linear symmetry, heat flow anomalies, and gravity and geoid data. Plume activity facilitates folding, by dramatically lowering the stress levels required (Burov and Cloetingh, 2009). Plume impact also reduces the fold wavelength and localizes folding above the plume impact area, with important consequences for the geometry of sedimentary basins.

6.12.5 General Conclusions and Future Perspectives

Sedimentary basin systems are sensitive recorders of dynamic processes controlling the deformation of the lithosphere and its interaction with the deep mantle and surface processes. The thermomechanical structure of the lithosphere exerts a prime control on its response to basin-forming mechanisms, such as rifting and its deflection under vertical loads, as well as its compressional deformation. Table 5 illustrates differences and similarities in basin shape, dimensions, subsidence characteristics, thermal evolution, and faulting histories between various basin types. Polyphase deformation is a common feature of some of Europe's best-documented sedimentary basin systems. The relatively weak lithosphere of intraplate Europe renders many of its sedimentary basins prone to neotectonic reactivation. Tectonic processes operating during basin formation and during the subsequent deformation of basins can generate significant differential topography in basin systems. As there is a close link between erosion of topographic highs and sedimentation in subsiding areas, constraints are needed on uplift and coeval subsidence to validate quantitative process-oriented models for the evolution of sedimentary basins. Integration of analog and numerical modeling provides a novel approach to assess the feedback mechanisms between deep mantle, lithospheric, and surface processes. The analysis of European basin systems demonstrates the importance of preorogenic extension of the lithosphere in the evolution of flexural foreland basins. Furthermore, compressional reactivation of extensional basins during their postrift phase appears to be a common feature of Europe's intraplate rifts and passive margins, reflecting temporal and spatial changes in the orientation and magnitude of the intraplate stress regime. Moreover, in the intraplate domain of continental Europe, which was thermally perturbed by Cenozoic upper mantle plume activity, lithospheric folding plays an important role and strongly affects the pattern of vertical motions, in terms of both the basin subsidence and the uplift of broad arches.

The development of sedimentary basins is, therefore, the intrinsic result of the interplay between lithospheric stresses and rheology and thermal perturbations of the lower lithosphere–upper mantle. The elucidation of paleostresses, paleotemperatures, and paleorheologies of the lithosphere is vital for the reconstruction of dynamically supported paleotopography. Rift shoulder topography and flexural topography

Table 5 Key characteristic features of different classes of sedimentary basins

Basin type	*Basin shape*	*Dimensions*	*Subsidence characteristics*	*Thermal evolution*	*Faulting history*
FLB	Symmetrical	Width: 50–600 km Depth: up to 20 km	Accelerated subsidence, timescales 1–10 My, simultaneously uplift at highs	No initial heating; heat flow increases in first 10s My with sediment deposition and burial and subsequently decreases	Intensive deformation, accelerating trough basin formation phase
FB	Asymmetrical	Width: 50–250 km Depth: up to 10 km	Linear subsidence, interrupted by short-lived faster subsidence during thrusting phases; timescales 10–100 My; simultaneously uplift from thrust front and foreland bulge	No initial heating; heat flow increases with time with sediment deposition and burial	Faulting and thrusting limited to orogenic wedge; minor deformation through faulting in foreland
EB	Symmetrical (pure shear); asymmetrical (simple shear)	Width: 30–500 km Depth up to 10 km	Rapid initial subsidence, followed by postrift decay in subsidence; in case of multiple rifting repeated accelerated subsidence; timescales for postrift subsidence of the order of 70 My. At rifting stage, development takes place of asymmetrical rift-shoulder topography, flanking the rift	Initial heating event, followed by decaying heat flow	Extensional faulting limited to basin formation phase; during postrift absence of faulting
PAB	Symmetrical	Width: 20 km Depth: up to 10 km	Very rapid initial subsidence, followed by postrift decay in subsidence, timescales: 1–10 My. In early stage, sedimentation cannot keep up with subsidence	Initial heating event, followed by very rapid decay in heat flow	Extensional faulting limited to basin formation phase; during postrift absence of faulting
ICB	Symmetrical	Width: 500–1000 km Depth: up to 10 km	Slow subsidence, punctuated by periods of faster subsidence, possibly related to large-scale tectonic events; characteristic timescales: 500–800 My	In the absence of understanding of basin formation mechanism, no prediction for initial heat flow; heat flow at later stage dominated by burial history	Very low level of faulting throughout tectonic history

Reproduced from Cloetingh S and Burov E (2011) Lithospheric folding and sedimentary basin evolution: A review and analysis of formation mechanisms. *Basin Research* 23: 257–290.

in compressional systems are directly linked to the thermomechanical properties and rheological stratification of the underlying lithosphere. The temporal evolution of the strength of continents and the spatial variations in stress and strength at continental margins, rifts, and orogenic belts govern the mechanics of basin development and destruction in time and space. Structural discontinuities and preexisting weakness zones are prone to reactivation in response to the buildup of extensional stresses and thus play an important role in the localization of rifts and related transfer zones. Similarly, their reactivation in response to the buildup of compressional stresses propagating from plate boundaries into continental platform areas controls the inversion of extensional basins and the upthrusting of basement blocks and contributes to the localization of lithospheric folding. The timing and nature of underlying changes in the controlling stress field and the resulting deformation processes can be unraveled by quantitative analyses of the stratigraphic record and the architecture of such complex polyphase sedimentary basins. This permits to assess systematic differences in the timing of the transition from rifting to intraplate compression and the development of foreland fold–thrust belts and lithospheric folds and vice versa.

Sedimentary basin systems are, by their nature, prone to tectonic reactivation and, therefore, frequently characterized by a polyphase evolution. Extensional basins are, for example, often formed in areas previously thickened by tectonic compression and subsequently often subject to late-stage compression. Examples include the Pannonian Basin of Hungary and the North Atlantic rifted margins. Similarly, foreland basins are frequently characterized by preorogenic extension. Examples include the Carpathian foredeep and the Aquitaine Basin of southern France, which was the retroarc foreland basin of the Pyrenees. The actual subsidence patterns of these polyphase systems are often more complex than predicted by the end-member models that only consider the basin formation mechanism.

6.12.5.1 Future Perspectives

The study of sedimentary basins demands added focus on surrounding highs that act as sediment sources as it is recognized that also uplifted/uplifting areas contain valuable information concerning, for instance, underlying deep-seated processes (Cloetingh et al., 2007, 2009, 2011, 2012, 2013;

Matenco et al., 2013). State-of-the art geothermochronology and the study of erosion and river pattern evolution provide major constraints on uplift histories. To elucidate the contribution of internal lithospheric processes and external forcing toward rates of erosion and sedimentation, therefore, presents a major challenge for sedimentary basin studies. This is particularly so as the sedimentary cover of the lithosphere provides a high-resolution record of the changing environment and of deformation and mass transfer at the surface and at different depth levels in the crust, lithosphere, and mantle system. With recent advances in seismic tomography and the development of full-waveform inversion methodologies, our understanding of crust–mantle interactions and their impact on sedimentary basins can be expected to further increase. Particularly striking in this effect is the rapid increase in spatial resolution capable, for example, to image in great detail the presence of mantle plumes in the northern Atlantic (Rickers et al., 2013), which will provide new constraints on the evolution of extensional basin systems in this area.

Tectonic reactivation has strongly affected the structure and fill of many sedimentary basins. The long-lasting rheology memory of the lithosphere appears to play a far more important role in basin reactivation than hitherto assumed. For present-day rheological strength distributions in the lithosphere, regional- and global-scale models have been developed recently (e.g., Tesauro et al., 2009a,b, 2012a,b, 2013). A better understanding of the 3-D linkage between basin formation and basin deformation would also benefit from establishing robust models for paleostrength distributions. Moreover, structural analysis of the basin architecture, including paleostress assessment, will provide important constraints on the transient nature of intraplate stress fields and their effects on the evolution of sedimentary basins (e.g., Roure et al., 2012).

Monitoring lithospheric deformation and its sedimentary record provides constraints on past and present-day structures and on deformation rates. Whereas in the past, tectonics, eustasy, and sediment supply have been commonly treated as separate factors in sedimentary basin analyses, nowadays, an integrated source–sink approach, constrained by fully 3-D quantitative subsidence and exhumation history analyses in carefully selected natural laboratories, is possible and ought to be further pursued (Cloetingh and Willett, 2013; Matenco et al., 2013).

In doing so, future researchers will build on the legacy of Peter Ziegler, coauthor of this chapter, who passed away on 19 July 2013 after the submission of this chapter. Peter Ziegler has been a pioneer in integrating geologic and geophysical information for elucidating lithosphere evolution in space and time. He successfully connected research on sedimentary basins carried out by the energy industry and academia. Peter's fundamental contribution to the paleogeography of Europe and the northern Atlantic and his seminal studies on sedimentary basins will be a solid base for the years to come. Peter's immense overview of the geologic record provided the background for his *Geological Atlas of Western and Central Europe*, which for long has served as a fundamental resource for scientists. Peter Ziegler early understood the importance of integrating different sources of information and that the whole crust and lithosphere are involved in tectonic evolution of basins.

Acknowledgments

The research on sedimentary basin systems reviewed in this chapter was largely carried out in the framework of the International Lithosphere Program (ILP) and the ESF EUROCORES TOPO-EUROPE program. We acknowledge the contributions and efforts made by coworkers from various research institutes in Europe to these projects. Martijn Vlieg is thanked for technical assistance.

References

Abadi AM, Van Wees JD, Van Dijk PM, and Cloetingh SAPL (2008) Tectonics and subsidence evolution of the Sirt Basin, Libya. *AAPG Bulletin* 92: 993–1027.

Ali MY and Watts AB (2009) Subsidence history, gravity anomalies and flexure of the United Arab Emirates (UAE) foreland basin. *GeoArabia* 14: 17–44.

Alinaghi A, Koulakov I, and Thybo H (2007) Seismic tomographic imaging of P- and S-waves velocity perturbations in the upper mantle beneath Iran. *Geophysical Journal International* 169: 1089–1102.

Allen MB and Davies CE (2007) Unstable Asia: Active deformation of Siberia revealed by drainage shifts. *Basin Research* 19: 379–392.

Allen PA, Homewood P, and Williams GD (1986) Foreland basins: An introduction. In: *Foreland Basins*, pp. 3–12. Oxford: Blackwell Publishing Ltd.

Alzaga-Ruiz H, Granjeon D, Lopez M, Seranne M, and Roure F (2009) Gravitational collapse and Neogene sediment transfer across the western margin of the Gulf of Mexico: Insights from numerical models. *Tectonophysics* 470: 21–41.

Anderson DL, Zhang Y-S, and Tanimoto T (1992) Plume heads, continental lithosphere, flood basalts and tomography. *Geological Society, London, Special Publications* 68: 99–124.

Andeweg B (2002) *Cenozoic tectonic evolution of the Iberian Peninsula: Effects and causes of changing stress fields*. Published PhD thesis, Vrije Universiteit Amsterdam, the Netherlands, pp. 178.

Andeweg B and Cloetingh S (1998) Flexure and 'unflexure' of the North Alpine German-Austrian Molasse Basin: Constraints from forward tectonic modelling. *Geological Society, London, Special Publications* 134: 403–422.

Artemieva IM (2006) Global 1 degrees x 1 degrees thermal model TC1 for the continental lithosphere: Implications for lithosphere secular evolution. *Tectonophysics* 416: 245–277.

Artemieva I (2011) *The Lithosphere: An Interdisciplinary Approach*. New York: Cambridge University Press.

Artemieva IM and Mooney WD (2001) Thermal thickness and evolution of Precambrian lithosphere: A global study. *Journal of Geophysical Research-Solid Earth* 106: 16387–16414.

Artemieva IM and Mooney WD (2002) On the relations between cratonic lithosphere thickness, plate motions, and basal drag. *Tectonophysics* 358: 211–231.

Artemieva IM, Thybo H, and Kaban MK (2006) Deep Europe today: Geophysical synthesis of the upper mantle structure and lithospheric processes over 3.5 Ga. *Geological Society, London, Memoirs* 32: 11–41.

Artemjev ME, Kaban MK, Kucherinenko VA, Demyanov GV, and Taranov VA (1994) Subcrustal density inhomogeneities of Northern Eurasia as derived from the gravity data and isostatic models of the lithosphere. *Tectonophysics* 240: 249–280.

Artyushkov EV (2007) Formation of the superdeep South Caspian basin: Subsidence driven by phase change in continental crust. *Russian Geology and Geophysics* 48: 1002–1014.

Artyushkov EV and Baer MA (1990) Formation of hydrocarbon basins: Subsidence without stretching in West Siberia. In: *The Potential of Deep Seismic Profiling for Hydrocarbon Exploration*, pp. 45–61. Paris: Technip.

Athmer W, Groenenberg RM, Luthi SM, et al. (2010) Relay ramps as pathways for turbidity currents: A study combining analogue sandbox experiments and numerical flow simulations. *Sedimentology* 57: 806–823.

Audet P and Burgmann R (2011) Dominant role of tectonic inheritance in supercontinent cycles. *Nature Geoscience* 4: 184–187.

Avouac JP and Burov EB (1996) Erosion as a driving mechanism of intracontinental mountain growth. *Journal of Geophysical Research-Solid Earth* 101: 17747–17769.

Axen GJ, Lam PS, Grove M, Stockli DF, and Hassanzadeh J (2001) Exhumation of the west-central Alborz Mountains, Iran, Caspian subsidence, and collision-related tectonics. *Geology* 29: 559–562.

Babuska V and Plomerova J (1992) The lithosphere in central-Europe – Seismological and petrological aspects. *Tectonophysics* 207: 141–163.

Babuska V and Plomerova J (1993) Lithospheric thickness and velocity anisotropy – Seismological and geothermal aspects. *Tectonophysics* 225: 79–89.

Babuska V and Plomerova J (2001) Subcrustal lithosphere around the Saxothuringian-Moldanubian Suture Zone – A model derived from anisotropy of seismic wave velocities. *Tectonophysics* 332: 185–199.

Bache F, Olivet JL, Gorini C, et al. (2010) Evolution of rifted continental margins: The case of the Gulf of Lions (Western Mediterranean Basin). *Earth and Planetary Science Letters* 292: 345–356.

Bada G, Cloetingh S, Gerner P, and Horváth F (1998) Sources of recent tectonic stress in the Pannonian region: Inferences from finite element modelling. *Geophysical Journal International* 134: 87–101.

Bada G and Horváth F (2001) On the structure and tectonic evolution of the Pannonian basin and surrounding orogens. *Acta Geologica Hungarica* 44: 301–327.

Bada G, Horváth F, Cloetingh S, Coblentz DD, and Toth T (2001) Role of topography-induced gravitational stresses in basin inversion: The case study of the Pannonian basin. *Tectonics* 20: 343–363.

Bada G, Horváth F, Dovenyi P, et al. (2007) Present-day stress field and tectonic inversion in the Pannonian basin. *Global and Planetary Change* 58: 165–180.

Bada G, Horváth F, Gerner P, and Fejes I (1999) Review of the present-day geodynamics of the Pannonian basin: Progress and problems. *Journal of Geodynamics* 27: 501–527.

Bahlburg H and Furlong KP (1996) Lithospheric modeling of the Ordovician foreland basin in the Puna of northwestern Argentina: On the influence of arc loading on foreland basin formation. *Tectonophysics* 259: 245–258.

Balla Z (1986) Paleotectonic reconstruction of the Central Alpine Mediterranean belt for the neogene. *Tectonophysics* 127: 213–243.

Bally AW and Snelson S (1980) Realms of subsidence. *Memoirs Canadian Society of Petroleum Geology* 6: 9–94.

Banks CJ (1998) Basins and thrust belts of the Balkan coast of the Black Sea. *Memoirs-American Association of Petroleum Geologists* 68: 115–128.

Barbeau DL (2003) A flexural model for the Paradox Basin: Implications for the tectonics of the Ancestral Rocky Mountains. *Basin Research* 15: 97–115.

Barbieri C, Bertotti G, Di Giulio A, Fantoni R, and Zoetemeijer R (2004) Flexural response of the Venetian foreland to the Southalpine tectonics along the TRANSALP profile. *Terra nova* 16: 273–280.

Bartol J and Govers R (2009) Flexure due to the Messinian-Pontian sea level drop in the Black Sea. *Geochemistry, Geophysics, Geosystems* 10: Q10013.

Bartol J, Matenco L, Garcia-Castellanos D, and Leever K (2012) Modelling depositional shifts between sedimentary basins: Sediment pathways in Paratethys basins during the Messinian Salinity Crisis. *Tectonophysics* 536: 110–121.

Barton P and Wood R (1984) Tectonic evolution of the north-sea basin – Crustal stretching and subsidence. *Geophysical Journal of the Royal Astronomical Society* 79: 987–1022.

Bassi G (1995) Relative importance of strain-rate and rheology for the mode of continental extension. *Geophysical Journal International* 122: 195–210.

Bassin C (2000) The current limits of resolution for surface wave tomography in North America. *Eos, Transactions of the American Geophysical Union* 81: F897.

Bayasgalan A, Jackson J, and McKenzie D (2005) Lithosphere rheology and active tectonics in Mongolia: Relations between earthquake source parameters, gravity and GPS measurements. *Geophysical Journal International* 163: 1151–1179.

Bayer U, Scheck M, Rabbel W, et al. (1999) An integrated study of the NE German Basin. *Tectonophysics* 314: 285–307.

Beaumont C (1981) Foreland basins. *Geophysical Journal of the Royal Astronomical Society* 65: 291–329.

Beaumont C, Fullsack P, and Hamilton J (1992) Erosional control of active compressional orogens. In: McClay KR (ed.) *Thrust Tectonics*, pp. 1–18. London: Chapman & Hall.

Beaumont C, Keen CE, and Boutilier R (1982) On the evolution of rifted continental margins – Comparison of models and observations for the Nova-Scotian margin. *Geophysical Journal of the Royal Astronomical Society* 70: 667–715.

Beekman F, Bull JM, Cloetingh S, and Scrutton R (1996) Crustal fault reactivation facilitating lithospheric folding/buckling in the central Indian Ocean. *Geological Society, London, Special Publications* 99: 251–263.

Beekman F, Stephenson RA, and Korsch RJ (1997) Mechanical stability of the Redbank Thrust Zone, central Australia: Dynamic and rheological implications. *Australian Journal of Earth Sciences* 44: 215–226.

Beglinger SE, Corver MP, Doust H, Cloetingh S, and Thurmond AK (2012a) A new approach of relating petroleum system and play development to basin evolution: An application to the conjugate margin Gabon coastal and Almada-Camamu basins. *AAPG Bulletin* 96: 953–982.

Beglinger SE, Doust H, and Cloetingh S (2012b) Relating petroleum system and play development to basin evolution: Brazilian South Atlantic margin. *Petroleum Geoscience* 18: 315–336.

Beglinger SE, Doust H, and Cloetingh S (2012c) Relating petroleum system and play development to basin evolution: West African South Atlantic basins. *Marine and Petroleum Geology* 30: 1–25.

Beglinger SE, Van Wees JD, Cloetingh S, and Doust H (2012d) Tectonic subsidence history and source-rock maturation in the Campos Basin, Brazil. *Petroleum Geoscience* 18: 153–172.

Bergerat F (1987) Stress-fields in the european platform at the time of Africa-Eurasia collision. *Tectonics* 6: 99–132.

Bertotti G and Mosca P (2009) Late-orogenic vertical movements within the arc of the SW Alps and Ligurian Alps. *Tectonophysics* 475: 117–127.

Bertotti G, Mosca P, Juez J, et al. (2006) Oligocene to present kilometres scale subsidence and exhumation of the Ligurian Alps and the Tertiary Piedmont Basin (NW Italy) revealed by apatite (U–Th)/He thermochronology: Correlation with regional tectonics. *Terra Nova* 18: 18–25.

Bertotti G, Podladchikov Y, and Daehler A (2000) Dynamic link between the level of ductile crustal flow and style of normal faulting of brittle crust. *Tectonophysics* 320: 195–218.

Bertotti G and Ter Voorde M (1994) Thermal effects of normal faulting during rifted basin formation, 2. The Lugano-Val grande normal-fault and the role of preexisting thermal anomalies. *Tectonophysics* 240: 145–157.

Bertotti G, Ter Voorde M, Cloetingh S, and Picotti V (1997) Thermomechanical evolution of the South Alpine rifted margin (North Italy): Constraints on the strength of passive continental margins. *Earth and Planetary Science Letters* 146: 181–193.

Blundell DJ, Freeman R, Mueller S, and Button S (1992) *A Continent Revealed: The European Geotraverse, Structure and Dynamic Evolution*. Cambridge: Cambridge University Press, 275 pp.

Bocin A (2010) *Crustal Structure of the SE Carpathians and Its Foreland from Densely Spaced Geophysical Data*, 124 pp. PhD Thesis, VU University Amsterdam, Amsterdam.

Bond GC and Kominz MA (1984) Construction of tectonic subsidence curves for the early paleozoic Miogeocline, southern Canadian rocky mountains – Implications for subsidence mechanisms, age of breakup, and crustal thinning. *Geological Society of America Bulletin* 95: 155–173.

Bonjer KP (1997) Seismicity pattern and style of seismic faulting at the eastern borderfault of the southern Rhine Graben. *Tectonophysics* 275: 41–69.

Bonnet S (2009) Shrinking and splitting of drainage basins in orogenic landscapes from the migration of the main drainage divide. *Nature Geoscience* 2: 766–771.

Bonnet S, Guillocheau F, Brun JP, and Van den Driessche J (2000) Large-scale relief development related to Quaternary tectonic uplift of a Proterozoic-Paleozoic basement: The Armorican Massif, NW France. *Journal of Geophysical Research: Solid Earth* 105: 19273–19288.

Boschi L, Faccenna C, and Becker TW (2010) Mantle structure and dynamic topography in the Mediterranean Basin. *Geophysical Research Letters* 37: L20303.

Bott MHP (1992) Modeling the loading stresses associated with active continental rift systems. *Tectonophysics* 215: 99–115.

Bott MHP (1993) Modeling the plate-driving mechanism. *Journal of the Geological Society* 150: 941–951.

Bott MHP and Kusznir NJ (1979) Stress distributions associated with compensated plateau uplift structures with application to the continental splitting mechanism. *Geophysical Journal of the Royal Astronomical Society* 56: 451–459.

Bott MHP and Stern TA (1992) Finite element analysis of Transantarctic Mountain uplift and coeval subsidence in the Ross Embayment. *Tectonophysics* 201: 341–356.

Bourgeois O, Ford M, Diraison M, et al. (2007) Separation of rifting and lithospheric folding signatures in the NW-Alpine foreland. *International Journal of Earth Sciences* 96: 1003–1031.

Braun J (2006) Recent advances and current problems in modelling surface processes and their interaction with crustal deformation. *Geological Society, London, Special Publications* 253: 307–325.

Braun J and Beaumont C (1989) A physical explanation of the relation between flank uplifts and the breakup unconformity at rifted continental margins. *Geology* 17: 760–764.

Brunet MF (1986) The influence of the evolution of the Pyrenees on adjacent basins. *Tectonophysics* 129: 343–354.

Bry M, White N, Singh S, England R, and Trowell C (2004) Anatomy and formation of oblique continental collision: South Falkland basin. *Tectonics* 23.

Brunet M-F and Cloetingh S (2003) Integrated peri-Tethyan basins studies (peri-Tethys programme). *Sedimentary Geology* 156: 1–10.

Buck WR (1991) Modes of continental lithospheric extension. *Journal of Geophysical Research: Solid Earth* 96: 20161–20178.

Buck WR (2007) The dynamics of continental break-up and extension. In: Watts AB (ed.) *Treatise on Geophysics*. *Crust and Lithosphere Dynamics*, vol. 6, pp. 335–376. New York: Elsevier.

Bull JM and Scrutton RA (1992) Seismic-reflection images of intraplate deformation, central Indian-ocean, and their tectonic significance. *Journal of the Geological Society* 149: 955–966.

Burg J-P and Podladchikov Y (1999) Lithospheric scale folding: Numerical modelling and application to the Himalayan syntaxes. *International Journal of Earth Sciences* 88: 190–200.

Burg JP, Van den Driessche J, and Brun JP (1994) Syn-thickening to post-thickening extension – Mode and consequences. *Comptes Rendus de l'Académie des Sciences – Series II* 319: 1019–1032.

Burov EB (2007) Plate rheology and mechanics. In: Watts AB (ed.) *Treatise on Geophysics*. *Crust and Lithosphere Dynamics*, vol. 6, pp. 99–151. Amsterdam: Elsevier.

Burov E and Cloetingh S (1997) Erosion and rift dynamics: New thermomechanical aspects of post-rift evolution of extensional basins. *Earth and Planetary Science Letters* 150: 7–26.

Burov E and Cloetingh S (2009) Controls of mantle plumes and lithospheric folding on modes of intraplate continental tectonics: Differences and similarities. *Geophysical Journal International* 178: 1691–1722.

Burov E and Cloetingh S (2010) Plume-like upper mantle instabilities drive subduction initiation. *Geophysical Research Letters* 37: L03309.

Burov EB and Diament M (1992) Flexure of the continental lithosphere with multilayered rheology. *Geophysical Journal International* 109: 449–468.

Burov EB and Diament M (1995) The effective elastic thickness (T-E) of continental lithosphere – What does it really mean. *Journal of Geophysical Research: Solid Earth* 100: 3905–3927.

Burov E, Guillou-Frottier L, d'Acremont E, Le Pourhiet L, and Cloetingh S (2007) Plume head-lithosphere interactions near intra-continental plate boundaries. *Tectonophysics* 434: 15–38.

Burov EB, Kogan MG, Lyon-Caen H, and Molnar P (1990) Gravity anomalies, the deep structure, and dynamic processes beneath the Tien Shan. *Earth and Planetary Science Letters* 96: 367–383.

Burov EB and Kogan MG (1990) Mechanical-gravitational model of the interaction of continental plates in the Tien-Shan region. *Doklady Akademii NAUK SSS* 313: 1439–1444.

Burov EB, Lobkovsky LI, Cloetingh S, and Nikishin AM (1993) Continental lithosphere folding in central-Asia. 2. Constraints from gravity and topography. *Tectonophysics* 226: 73–87.

Burov EB and Molnar P (1998) Gravity anomalies over the Ferghana Valley (central Asia) and intracontinental deformation. *Journal of Geophysical Research: Solid Earth* 103: 18137–18152.

Burov E and Toussaint G (2007) Surface processes and tectonics: Forcing of continental subduction and deep processes. *Global and Planetary Change* 58: 141–164.

Burton R, Kendall CGSC, and Lerche I (1987) Out of our depth – On the impossibility of fathoming eustasy from the stratigraphic record. *Earth-Science Reviews* 24: 237–277.

Calcagnile G and Panza GF (1987) Properties of the lithosphere-asthenosphere system in Europe with a view toward earth conductivity. *Pure and Applied Geophysics* 125: 241–254.

Caporali A (1995) Gravity anomalies and the flexure of the lithosphere in the Karakoram, Pakistan. *Journal of Geophysical Research: Solid Earth (1978–2012)* 100: 15075–15085.

Cardozo N (1997) Thermomechanical Modeling of the Llanos Basin Colombia, South America. *American Geophysical Union Spring meeting*. Baltimore: Ohio University.

Carrapa B and Garcia-Castellanos D (2005) Western Alpine back-thrusting as subsidence mechanism in the Tertiary Piedmont Basin (Western Po Plain, NW Italy). *Tectonophysics* 406: 197–212.

Carswell DA (1990) *Eclogite Facies Rocks*. New York: Blackie.

Carter NL and Tsenn MC (1987) Flow properties of continental lithosphere. *Tectonophysics* 136: 27–63.

Casas-Sainz AM and de Vicente G (2009) On the tectonic origin of Iberian topography. *Tectonophysics* 474: 214–235.

Casero P (2004) Structural setting of petroleum exploration plays in Italy. *Special Volume of the Italian Geological Society for the IGC* 32: 189–199.

Catuneanu O, Beaumont C, and Waschbusch P (1997) Interplay of static loads and subduction dynamics in foreland basins: Reciprocal stratigraphies and the "missing" peripheral bulge. *Geology* 25: 1087–1090.

Chang HK, Kowsmann RO, Figueiredo AMF, and Bender AA (1992) Tectonics and stratigraphy of the East Brazil Rift System – An overview. *Tectonophysics* 213: 97–138.

Chu DZ and Gordon RG (1998) Current plate motions across the Red Sea. *Geophysical Journal International* 135: 313–328.

Ciulavu D, Dinu C, and Cloetingh S (2002) Late Cenozoic tectonic evolution of the Transylvanian basin and northeastern part of the Pannonian basin (Romania): Constraints from seismic profiling and numerical modelling. *EGU Stephan Mueller Special Publication Series* 3: 105–120.

Cloetingh S (1988) Intraplate stresses: A new element in basin analysis. In: Kleinspehn K and Paola C (eds.) *Frontiers in Sedimentary Geology – New Perspectives in Basin Analysis*, pp. 205–230. New York: Springer.

Cloetingh S and Burov EB (1996) Thermomechanical structure of European continental lithosphere: Constraints from rheological profiles and EET estimates. *Geophysical Journal International* 124: 695–723.

Cloetingh S and Burov E (2011) Lithospheric folding and sedimentary basin evolution: A review and analysis of formation mechanisms. *Basin Research* 23: 257–290.

Cloetingh S, Beekman F, Ziegler PA, et al. (2008) Post-rift compressional reactivation potential of passive margins and extensional basins. *Geological Society, London, Special Publications* 306: 27–70.

Cloetingh S, Burov E, Beekman F, et al. (2002) Lithospheric folding in Iberia. *Tectonics* 21: 1041.

Cloetingh SAPL, Burov E, Matenco L, et al. (2004) Thermo-mechanical controls on the mode of continental collision in the SE Carpathians (Romania). *Earth and Planetary Science Letters* 218: 57–76.

Cloetingh S, Burov E, Matenco L, et al. (2013) The Moho in extensional tectonic settings: Insights from thermo-mechanical models. *Tectonophysics* 609: 558–604.

Cloetingh S, Burov E, and Poliakov A (1999) Lithosphere folding: Primary response to compression? (from central Asia to Paris basin). *Tectonics* 18: 1064–1083.

Cloetingh S, Cornu T, Ziegler PA, and Beekman F (2006) Neotectonics and intraplate continental topography of the northern Alpine Foreland. *Earth-Science Reviews* 74: 127–196.

Cloetingh S, D'Argenio B, Catalano R, Horváth F, and Sassi W (1995a) Interplay of extension and compression in basin formation: Introduction. *Tectonophysics* 252: 1–5.

Cloetingh S, Durand B, and Puigdefabregas C (eds.) (1995c) Special Issue on integrated basin studies (IBS) – A European Commission (DGXII) project. *Marine and Petroleum Geology* 12(8): 787–963.

Cloetingh S, Gallart J, de Vicente G, and Matenco L (2011) TOPO-EUROPE: From Iberia to the Carpathians and analogues. *Tectonophysics* 502: 1–27.

Cloetingh S, Gradstein FM, Kooi H, Grant AC, and Kaminski M (1990) Plate reorganization: A cause of rapid late Neogene subsidence and sedimentation around the North Atlantic? *Journal of the Geological Society* 147: 495–506.

Cloetingh S and Kooi H (1992a) Intraplate stresses and dynamic aspects of rifted basins. *Tectonophysics* 215: 167–185.

Cloetingh S and Kooi H (1992b) Intraplate stresses and dynamical aspects of rifted basins. *Tectonophysics* 215: 167–185.

Cloetingh S, Lambeck K, and McQueen H (1987) Apparent sealevel fluctuations and a paleo-stress field for the North Sea region. In: Brooks J and Glennie K (eds.) *Petroleum Geology of NorthWest Europe*, pp. 49–55. London: Graham and Trotman.

Cloetingh S, Mcqueen H, and Lambeck K (1985) On a tectonic mechanism for regional sealevel variations. *Earth and Planetary Science Letters* 75: 157–166.

Cloetingh S and Negendank JFW (2010) *New Frontiers in Integrated Solid Earth Sciences*, pp. 414. Springer.

Cloetingh S, Sassi W, Stephenson RA, et al. (1994) The origin of sedimentary basins – A status-report from the task-force of the international lithosphere program. *Marine and Petroleum Geology* 11: 659–683.

Cloetingh S, Spadini G, Van Wees JD, and Beekman F (2003) Thermo-mechanical modelling of Black Sea Basin (de)formation. *Sedimentary Geology* 156: 169–184.

Cloetingh S, Thybo H, and Faccenna C (2009) TOPO-EUROPE: Studying continental topography and Deep Earth-Surface processes in 4D. *Tectonophysics* 474: 4–32.

Cloetingh S, Tibaldi A, and Burov E (2012) Coupled deep earth and surface processes and their impact on geohazards. *Global and Planetary Change* 90–91: 1–19.

Cloetingh S, Van Balen RT, Ter Voorde M, Zoetemeijer BP, and Den Bezemer T (1997) Mechanical aspects of sedimentary basin formation: Development of integrated models for lithospheric and surface processes. *Geologische Rundschau* 86: 226–240.

Cloetingh S and Van Wees JD (2005) Strength reversal in Europe's intraplate lithosphere: Transition from basin inversion to lithospheric folding. *Geology* 33: 285–288.

Cloetingh S, Van Wees JD, Van der Beek PA, and Spadini G (1995b) Role of pre-rift rheology in kinematics of extensional basin formation – Constraints from

thermomechanical models of Mediterranean and Intracratonic basins. *Marine and Petroleum Geology* 12: 793–807.
Cloetingh S, Van Wees JD, Ziegler PA, et al. (2010) Lithosphere tectonics and thermo-mechanical properties: An integrated modelling approach for Enhanced Geothermal Systems exploration in Europe. *Earth-Science Reviews* 102: 159–206.
Cloetingh S and Willett SD (2013) TOPO-EUROPE: Understanding of the coupling between the deep Earth and continental topography. *Tectonophysics* 602: 1–14.
Cloetingh S and Wortel R (1986) Stress in the Indo-Australian plate. *Tectonophysics* 132: 49–67.
Cloetingh S, Wortel R, and Vlaar NJ (1989) On the initiation of subduction zones. *Pure and Applied Geophysics* 129: 7–25.
Cloetingh S and Ziegler PA (2007) Tectonic models for the evolution of sedimentary basins. In: Watts AB, Schubert G, Watts AB, and Schubert G (Eds.) *Treatise on Geophysics* 6: 485–611.
Cloetingh S, Ziegler PA, Beekman F, et al. (2005a) Intraplate deformation and 3D rheological structure of the Rhine Rift System and adjacent areas of the northern Alpine foreland. *International Journal of Earth Sciences* 94: 758–778.
Cloetingh S, Ziegler PA, Beekman F, et al. (2005b) Lithospheric memory, state of stress and rheology: Neotectonic controls on Europe's intraplate continental topography. *Quaternary Science Reviews* 24: 241–304.
Cloetingh SAPL, Ziegler PA, Bogaard PJF, et al. (2007) TOPO-EUROPE: The geoscience of coupled deep Earth-surface processes. *Global and Planetary Change* 58: 1–118.
Cobbold PR, Davy P, Gapais D, et al. (1993) Sedimentary basins and crustal thickening. *Sedimentary Geology* 86: 77–89.
Cogan J, Rigo L, Grasso M, and Lerche I (1989) Flexural tectonics of southeastern Sicily. *Journal of geodynamics* 11: 189–241.
Colletta B, Roure F, DeToni B, et al. (1997) Tectonic inheritance, crystal architecture, and contrasting structural styles in the Venezuela Andes. *Tectonics* 16: 777–794.
Corver MP, Doust H, Van Wees JD, Bada G, and Cloetingh S (2009) Classification of rifted sedimentary basins of the Pannonian Basin System according to the structural genesis, evolutionary history and hydrocarbon maturation zones. *Marine and Petroleum Geology* 26: 1452–1464.
Corver MP, Doust H, Van Wees JD, and Cloetingh S (2011) Source-rock maturation characteristics of symmetric and asymmetric grabens inferred from integrated analogue and numerical modeling: The southern Viking Graben (North Sea). *Marine and Petroleum Geology* 28: 921–935.
Coudert L, Frappa M, Viguier C, and Arias R (1995) Tectonic subsidence and crustal flexure in the Neogene Chaco basin of Bolivia. *Tectonophysics* 243: 277–292.
Cross TA (1990) *Quantitative Dynamic Stratigraphy*. New Jersey: Prentice-Hall.
Csontos L (1995) Tertiary tectonic evolution of the Intra-Carpathian area. *Acta Vulcanologica* 7: 1–14.
Csontos L, Nagymarosy A, Horváth F, and Kovac M (1992) Tertiary evolution of the intra-Carpathian area – A model. *Tectonophysics* 208: 221–241.
Csontos L and Voros A (2004) Mesozoic plate tectonic reconstruction of the Carpathian region. *Palaeogeography Palaeoclimatology Palaeoecology* 210: 1–56.
Curray JR and Moore DG (1971) Growth of Bengal Deep-Sea Fan and denudation in Himalayas. *Geological Society of America Bulletin* 82: 563–572.
Dalmayrac B and Molnar P (1981) Parallel thrust and normal faulting in Peru and constraints on the state of stress. *Earth and Planetary Science Letters* 55: 473–481.
Dando BDE, Stuart GW, Houseman GA, et al. (2011) Teleseismic tomography of the mantle in the Carpathian-Pannonian region of central Europe. *Geophysical Journal International* 186: 11–31.
Dávila FM, Astini RA, Jordan TE, Gehrels G, and Ezpeleta M (2007) Miocene forebulge development previous to broken foreland partitioning in the southern Central Andes, west-central Argentina. *Tectonics* 26: T05016.
De Bruijne CH and Andriessen PAM (2000) Interplay of intraplate tectonics and surface processes in the Sierra de Guadarrama (central Spain) assessed by apatite fission track analysis. *Physics and Chemistry of the Earth, Part A: Solid Earth and Geodesy* 25: 555–563.
De Bruijne CH and Andriessen PAM (2002) Far field effects of Alpine plate tectonism in the Iberian microplate recorded by fault-related denudation in the Spanish Central System. *Tectonophysics* 349: 161–184.
De Vicente G, Cloetingh S, Munoz-Martin A, et al. (2008) Inversion of moment tensor focal mechanisms for active stresses around the microcontinent Iberia: Tectonic implications. *Tectonics* 27: TC1009.
De Vicente G, Vegas R, Martin AM, et al. (2007) Cenozoic thick-skinned deformation and topography evolution of the Spanish Central System. *Global and Planetary Change* 58: 335–381.
DeCelles PG and Giles KA (1996) Foreland basin systems. *Basin Research* 8: 105–123.
Decker K, Lillie RJ, and Tomek C (1998) In: *Dynamics of the Pannonian-Carpathian-Dinaride System*, *PANCARDI: The Lithospheric Structure and Evolution of the Pannonian-Carpathian-Dinaride Region: Selected Papers from the PANCARDI Workshop 1996*, Amsterdam: Elsevier.
Delvaux D, Cloetingh S, Beekman F, et al. (2013) Basin evolution in a folding lithosphere: Altai-Sayan and Tien Shan belts in Central Asia. *Tectonophysics* 602: 194–222.
Desegaulx P, Kooi H, and Cloetingh S (1991) Consequences of foreland basin development on thinned continental lithosphere – Application to the Aquitaine Basin (Sw France). *Earth and Planetary Science Letters* 106: 116–132.
Devlin W, Cogswell J, Gaskins G, et al. (1999) South Caspian basin: Young, cool, and full of promise. *GSA Today* 9: 1–9.
Dewey JF (1980) Episodicity, sequence and style at convergent plate boundaries. In: Strangway DW (ed.) *The Continental Crust and Its Mineral Deposits*. Geological Society of Canada.
Dewey JF (1988) Extensional collapse of orogens. *Tectonics* 7: 1123–1139.
Dewey JF and Burke K (1974) Hot spots and continental break-up: Implications for collisional orogeny. *Geology* 2: 57–60.
Dèzes P, Schmid SM, and Ziegler PA (2004) Evolution of the European Cenozoic Rift System: Interaction of the Alpine and Pyrenean orogens with their foreland lithosphere. *Tectonophysics* 389: 1–33.
Dickinson WR (1974) Plate tectonics and sedimentation. *The Society of Economic Paleontologists and Mineralogists (SEPM)* 22: 1–27.
Dinu C, Wong HK, Tambrea D, and Matenco L (2005) Stratigraphic and structural characteristics of the Romanian Black Sea shelf. *Tectonophysics* 410: 417–435.
Doglioni C, Carminati E, Cuffaro M, and Scrocca D (2007) Subduction kinematics and dynamic constraints. *Earth-Science Reviews* 83: 125–175.
Dombradi E, Sokoutis D, Bada G, Cloetingh S, and Horváth F (2010) Modelling recent deformation of the Pannonian lithosphere: Lithospheric folding and tectonic topography. *Tectonophysics* 484: 103–118.
Dombradi E, Timar G, Bada G, Cloetingh S, and Horváth F (2007) Fractal dimension estimations of drainage network in the Carpathian-Pannonian system. *Global and Planetary Change* 58: 197–213.
Dondurur D, Küçük HM, and Çifçi G (2013) Quaternary mass wasting on the western Black Sea margin, offshore of Amasra. *Global and Planetary Change* 103: 248–260.
Doré A, Auguston J, Hermanrud C, Stewart D, and Sylta O (1993) In: *Basin Modelling: Advances and Applications*. Amsterdam: Elsevier, Applications. Norwegian Petroleum Society Special Publication 3.
Doust H and Omatsola E (1989) Niger delta. *Memoir American Association of Petroleum Geologists* 48: 201–238.
Du ZJ, Michelini A, and Panza GF (1998) EurID: A regionalized 3-D seismological model of Europe. *Physics of the Earth and Planetary Interiors* 106: 31–62.
Dunbar JA and Sawyer DS (1989) How preexisting weaknesses control the style of continental breakup. *Journal of Geophysical Research-Solid Earth and Planets* 94: 7278–7292.
Dupré S, Bertotti G, and Cloetingh S (2007) Tectonic history along the South Gabon Basin: Anomalous early post-rift subsidence. *Marine and Petroleum Geology* 24: 151–172.
Dupré S, Cloetingh S, and Bertotti G (2011) Structure of the Gabon Margin from integrated seismic reflection and gravity data. *Tectonophysics* 506: 31–45.
Durand B, Jolivet L, Horváth E, and Seranne M (eds.) (1999) *The Mediterranean Basins: Tertiary Extension Within the Alpine Orogen*. Geological Society of London, Special Publications 159.
Edwards R, Scott C, Shillington D, et al. (2009) Wide-angle seismic data reveal sedimentary and crustal structure of the Eastern Black Sea. *The Leading Edge* 28: 1056–1065.
Egan SS, Mosar J, Brunet M-F, and Kangarli T (2009) Subsidence and uplift mechanisms within the South Caspian Basin: Insights from the onshore and offshore Azerbaijan region. *Geological Society, London, Special Publications* 312: 219–240.
Elfrink N (2001) Quaternary groundwater avulsions: Evidence for large-scale midcontinent folding. *Association of Engineering Geologists News* 44: 60.
Ershov AV, Brunet M-F, Korotaev MV, Nikishin AM, and Bolotov SN (1999) Late Cenozoic burial history and dynamics of the Northern Caucasus molasse basin: Implications for foreland basin modelling. *Tectonophysics* 313: 219–241.
Faccenna C and Becker TW (2010) Shaping mobile belts by small-scale convection. *Nature* 465: 602–605.
Faccenna C, Piromallo C, Crespo-Blanc A, Jolivet L, and Rossetti F (2004) Lateral slab deformation and the origin of the western Mediterranean arcs. *Tectonics* 23: TC1012.
Fakhari MD, Axen GJ, Horton BK, Hassanzadeh J, and Amini A (2008) Revised age of proximal deposits in the Zagros foreland basin and implications for Cenozoic evolution of the High Zagros. *Tectonophysics* 451: 170–185.

Fan P and Ma BL (1990) General petroleum geology of the Tarim Basin. *Academia Sinica* 1: 1–21.

Fan G, Wallace TC, Beck SL, and Chase CG (1996) Gravity anomaly and flexural model: Constraints on the structure beneath the Peruvian Andes. *Tectonophysics* 255: 99–109.

Favre P and Stampfli GM (1992) From rifting to passive margin – The examples of the Red-Sea, Central Atlantic and Alpine Tethys. *Tectonophysics* 215: 69–97.

Fernández-Lozano J, Sokoutis D, Willingshofer E, Cloetingh S, and De Vicente G (2011) Cenozoic deformation of Iberia: A model for intraplate mountain building and basin development based on analogue modeling. *Tectonics* 30: TC1001.

Fernández-Lozano J, Sokoutis D, Willingshofer E, et al. (2012) Integrated gravity and topography analysis in analog models: Intraplate deformation in Iberia. *Tectonics* 31: TC6005.

Finetti I, Bricchi G, Del Ben A, Pipan M, and Xuan Z (1988) Geophysical study of the Black Sea. *Bollettino di Geofisica Teorica ed Applicata* 30: 197–324.

Flament N, Gurnis M, and Müller RD (2013) A review of observations and models of dynamic topography. *Lithosphere* 5: 189–210.

Fleitout L and Froidevaux C (1982) Tectonics and topography for a lithosphere containing density heterogeneities. *Tectonics* 1: 21–56.

Flemings PB and Jordan TE (1989) A synthetic stratigraphic model of foreland basin development. *Journal of Geophysical Research: Solid Earth (1978–2012)* 94: 3851–3866.

Fodor L, Bada G, Csillag G, et al. (2005) An outline of neotectonic structures and morphotectonics of the western and central Pannonian Basin. *Tectonophysics* 410: 15–41.

Fodor L, Csontos L, Bada G, Györfi I, and Benkovics L (1999) Tertiary tectonic evolution of the Pannonian Basin system and neighbouring orogens: A new synthesis of palaeostress data. *Geological Society, London, Special Publications* 156: 295–334.

Ford M, Lickorish WH, and Kusznir NJ (1999) Tertiary foreland sedimentation in the Southern Subalpine Chains, SE France: A geodynamic appraisal. *Basin Research* 11: 315–336.

Forsyth D and Uyeda S (1975) Relative importance of driving forces of plate motion. *Geophysical Journal of the Royal Astronomical Society* 43: 163–200.

Franke D (2013) Rifting, lithosphere breakup and volcanism: Comparison of magma-poor and volcanic rifted margins. *Marine and Petroleum Geology* 43: 63–87.

Fuis GS, Murphy JM, Lutter WJ, et al. (1997) Deep seismic structure and tectonics of northern Alaska: Crustal-scale duplexing with deformation extending into the upper mantle. *Journal of Geophysical Research: Solid Earth* 102: 20873–20896.

Garcia-Castellanos D (2002) Interplay between lithospheric flexure and river transport in foreland basins. *Basin Research* 14: 89–104.

Garcia-Castellanos D (2007) The role of climate during high plateau formation. Insights from numerical experiments. *Earth and Planetary Science Letters* 257: 372–390.

Garcia-Castellanos D and Cloetingh S (2012) Modeling the interaction between lithospheric and surface processes in foreland basins. In: Busby C and Azor A (eds.) *Tectonics of Sedimentary Basins: Recent Advances*, pp. 152–181.

Garcia-Castellanos D, Cloetingh S, and Van Balen R (2000) Modelling the middle pleistocene uplift in the Ardennes-Rhenish Massif: Thermo-mechanical weakening under the Eifel? *Global and Planetary Change* 27: 39–52.

Garcia-Castellanos D, Fernandez M, and Torne M (1997) Numerical modeling of foreland basin formation: A program relating thrusting, flexure, sediment geometry and lithosphere rheology. *Computers & Geosciences* 23: 993–1003.

Garcia-Castellanos D, Fernandez M, and Torne M (2002) Modeling the evolution of the Guadalquivir foreland basin (southern Spain). *Tectonics* 21: 1018.

Gaspar-Escribano JM, Van Wees JD, Ter Voorde M, et al. (2001) Three-dimensional flexural modelling of the Ebro Basin (NE Iberia). *Geophysical Journal International* 145: 349–367.

Geller CA, Weissel JK, and Anderson RN (1983) Heat-transfer and intraplate deformation in the central Indian-Ocean. *Journal of Geophysical Research* 88: 1018–1032.

Gemmer L and Houseman GA (2007) Convergence and extension driven by lithospheric gravitational instability: Evolution of the Alpine-Carpathian-Pannonian system. *Geophysical Journal International* 168: 1276–1290.

Georgiev G, Dabovski C, and Stanisheva-Vassileva G (2001) East Srednogorie-Balkan rift zone. *Mémoires du Muséum national d'histoire naturelle* 186: 259–293.

Gerbault M (2000) At what stress level is the central Indian Ocean lithosphere buckling? *Earth and Planetary Science Letters* 178: 165–181.

Gerbault M, Burov EB, Poliakov ANB, and Daignières M (1999) Do faults trigger folding in the lithosphere? *Geophysical Research Letters* 26: 271–274.

Ghorbal B, Bertotti G, Foeken J, and Andriessen P (2008) Unexpected Jurassic to Neogene vertical movements in 'stable' parts of NW Africa revealed by low temperature geochronology. *Terra Nova* 20: 355–363.

Gillet H, Lericolais G, and Rehault JP (2007) Messinian event in the black sea: Evidence of a Messinian erosional surface. *Marine Geology* 244: 142–165.

Goes S, Govers R, and Vacher P (2000a) Shallow mantle temperatures under Europe from P and S wave tomography. *Journal of Geophysical Research, Solid Earth* 105: 11153–11169.

Goes S, Loohuis JJP, Wortel MJR, and Govers R (2000b) The effect of plate stresses and shallow mantle temperatures on tectonics of northwestern Europe. *Global and Planetary Change* 27: 23–38.

Goetze C and Evans B (1979) Stress and temperature in the bending lithosphere as constrained by experimental rock mechanics. *Geophysical Journal of the Royal Astronomical Society* 59: 463–478.

Gölke M, Cloetingh S, and Coblentz D (1996) Finite-element modelling of stress patterns along the Mid-Norwegian continental margin, 62 degrees to 68 degrees N. *Tectonophysics* 266: 33–53.

Görür N (1988) Timing of opening of the Black-Sea Basin. *Tectonophysics* 147: 247–262.

Gouiza M, Bertotti G, Hafid M, and Cloetingh S (2010) Kinematic and thermal evolution of the Moroccan rifted continental margin: Doukkala-High Atlas transect. *Tectonics* 29: 1–22.

Govers R and Wortel MJR (1993) Initiation of asymmetric extension in continental lithosphere. *Tectonophysics* 223: 75–96.

Granet M, Wilson M, and Achauer U (1995) Imaging a mantle plume beneath the French Massif Central. *Earth and Planetary Science Letters* 136: 281–296.

Gries R (1983) Oil and gas prospecting beneath Precambrian of foreland thrust plates in rocky mountains. *Bulletin-American Association of Petroleum Geologists* 67: 1–28.

Griffin WL, O'Reilly SY, and Pearson NJ (1990) Eclogite stability near the crust-mantle boundary. In: Carswell DA and Carswell DA (eds.) *Eclogite Facies Rocks*, pp. 291–314.

Grotzinger J and Royden L (1990) Elastic strength of the Slave craton at 1.9 Gyr and implications for the thermal evolution of the continents. *Nature* 347: 64–66.

Grünthal G (1999) Seismic hazard assessment for Central, North and Northwest Europe: GSHAP Region 3. *Annali Di Geofisica* 42: 999–1011.

Guest B, Guest A, and Axen G (2007) Late Tertiary tectonic evolution of northern Iran: A case for simple crustal folding. *Global and Planetary Change* 58: 435–453.

Guillocheau F, Robin C, Allemand P, et al. (2000) Meso-Cenozoic geodynamic evolution of the Paris Basin: 3D stratigraphic constraints. *Geodinamica Acta* 13: 189–245.

Guillou-Frottier L, Burov E, Nehlig P, and Wyns R (2007) Deciphering plume-litho sphere interactions beneath Europe from topographic signatures. *Global and Planetary Change* 58: 119–140.

Gutscher M-A (1995) Crustal structure and dynamics in the Rhine Graben and the Alpine foreland. *Geophysical Journal International* 122: 617–636.

Haddad D and Watts AB (1999) Subsidence history, gravity anomalies, and flexure of the northeast Australian margin in Papua New Guinea. *Tectonics* 18: 827–842.

Hafkenscheid E, Wortel MJR, and Spakman W (2006) Subduction history of the Tethyan region derived from seismic tomography and tectonic reconstructions. *Journal of Geophysical Research: Solid Earth* 111: B08401.

Hall R, Cottam MA, and Wilson MEJ (2011) The SE Asian gateway: History and tectonics of the Australia–Asia collision. *Geological Society, London, Special Publications* 355: 1–6.

Hardebol NJ, Beekman F, and Cloetingh SAPL (2013) Strong lateral strength contrasts in the mantle lithosphere of continents: A case study from the hot SW Canadian Cordillera. *Tectonophysics* 602: 87–105.

Hardebol NJ, Callot JP, Bertotti G, and Faure JL (2009) Burial and temperature evolution in thrust belt systems: Sedimentary and thrust sheet loading in the SE Canadian Cordillera. *Tectonics* 28: TC3003.

Hatzfeld D and Molnar P (2010) Comparisons of the kinematics and deep structures of the Zagros and Himalaya and of the Iranian and Tibetan plateaus and geodynamic implications. *Reviews of Geophysics* 48: RG2005.

Hellinger SJ and Sclater JG (1983) Some comments on 2-layer extensional models for the evolution of sedimentary basins. *Journal of Geophysical Research* 88: 8251–8269.

Hetényi G, Cattin R, Vergne J, and Nábělek JL (2006) The effective elastic thickness of the India Plate from receiver function imaging, gravity anomalies and thermomechanical modelling. *Geophysical Journal International* 167: 1106–1118.

Hinze WJ and Braile LW (1988) Sedimentary cover of the North American Craton. In: *The geology of North America* 2, pp. 5–24. Geological Society of America.

Hippolyte JC, Angelier J, and Roure F (1994) A major geodynamic change revealed by quaternary stress patterns in the Southern Apennines (Italy). *Tectonophysics* 230: 199–210.

Holt WE and Stern TA (1991) Sediment loading on the western platform of the New Zealand continent: Implications for the strength of a continental margin. *Earth and planetary science letters* 107: 523–538.

Horton BK and DeCelles PG (1997) The modern foreland basin system adjacent to the Central Andes. *Geology* 25: 895–898.

Horváth F (1993) Towards a mechanical model for the formation of the Pannonian basin. *Tectonophysics* 226: 333–357.

Horváth F (1995) Phases of compression during the evolution of the Pannonian basin and its bearing on hydrocarbon exploration. *Marine and Petroleum Geology* 12: 837–844.

Horváth F, Bada G, Szafián P, et al. (2006) Formation and deformation of the Pannonian Basin: Constraints from observational data. *Geological Society, London, Memoir* 32: 191–206.

Horváth F and Cloetingh S (1996) Stress-induced late-stage subsidence anomalies in the Pannonian basin. *Tectonophysics* 266: 287–300.

Horváth F, Stegena L, and Géczy B (1975) Ensimatic and ensialic interarc basins: Comments on 'Neogene Carpathian Arc: A continental arc displaying the features of an island arc' by M. D. Bleahu, M. Boccaletti, P. Manetti, and S. Peltz. *Journal of Geophysical Research* 80: 281–283.

Houseman GA and Gemmer L (2007) Intra-orogenic extension driven by gravitational instability: Carpathian-Pannonian orogeny. *Geology* 35: 1135–1138.

Hsü KJ and Giovanoli F (1979) Messinian event in the Black-Sea. *Palaeogeography Palaeoclimatology Palaeoecology* 29: 75–93.

Huismans RS, Podladchikov YY, and Cloetingh S (2001a) Transition from passive to active rifting: Relative importance of asthenospheric doming and passive extension of the lithosphere. *Journal of Geophysical Research: Solid Earth (1978–2012)* 106: 11271–11291.

Huismans RS, Podladchikov YY, and Cloetingh S (2001b) Dynamic modeling of the transition from passive to active rifting, application to the Pannonian basin. *Tectonics* 20: 1021–1039.

Ismail-Zadeh A, Matenco L, Radulian M, Cloetingh S, and Panza G (2012) Geodynamics and intermediate-depth seismicity in Vrancea (the south-eastern Carpathians): Current state-of-the art. *Tectonophysics* 530–531: 50–79.

Jackson J (2002) Strength of the continental lithosphere: Time to abandon the jelly sandwich? *GSA Today* 12: 4–9.

Janssen ME (1996) *Intraplate Deformation in Africa as a Consequence of Plate Boundary Changes*: *Inferences from Subsidence Analysis and Tectonic Modelling of the Early and Middle Cretaceous Period*, 161 pp. PhD Thesis, VU University, Amsterdam.

Janssen ME, Stephenson RA, and Cloetingh S (1995) Temporal and spatial correlations between changes in plate motions and the evolution of rifted basins in Africa. *Geological Society of America Bulletin* 107: 1317–1332.

Japsen P and Chalmers JA (2000) Neogene uplift and tectonics around the North Atlantic: Overview. *Global and Planetary Change* 24: 165–173.

Jarosinski M, Beekman F, Matenco L, and Cloetingh S (2011) Mechanics of basin inversion: Finite element modelling of the Pannonian Basin System. *Tectonophysics* 502: 121–145.

Jarvis GT and Mckenzie DP (1980) Sedimentary basin formation with finite extension rates. *Earth and Planetary Science Letters* 48: 42–52.

Jaupart C and Mareschal JC (2007) Heat flow and thermal structure of the lithosphere. *Treatise on Geophysics*, vol. 6, pp. 217–251. The Netherlands: Elsevier.

Jiménez-Munt I, Garcia-Castellanos D, Negredo AM, and Platt JP (2005) Gravitational and tectonic forces controlling postcollisional deformation and the present-day stress field of the Alps: Constraints from numerical modeling. *Tectonics* 24: 1–15.

Johnson DD and Beaumont C (1995) Preliminary results from a planform kinematic model of orogen evolution, surface processes and the development of clastic foreland basin stratigraphy. In: Doborek SL and Ross GM (eds.) *Stratgraphic evolution of foreland basins, 52, pp. 3–24*. Society of Economic Palaeontologists and Mineralogists Special Publications.

Johnson H, Dore AG, Gatliff RW, et al. (2008) In: *The Nature and Origin of Compression in Passive Margins*. London: Geological Society, Special Publications, 306.

Jolivet L and Brun JP (2010) Cenozoic geodynamic evolution of the Aegean. *International Journal of Earth Sciences* 99: 109–138.

Jolivet L and Faccenna C (2000) Mediterranean extension and the Africa-Eurasia collision. *Tectonics* 19: 1095–1106.

Jolivet L, Huchon P, and Rangin C (1989) Tectonic setting of western Pacific marginal basins. *Tectonophysics* 160: 23–47.

Jones CH, Wernicke BP, Farmer GL, et al. (1992) Variations across and along a major continental rift – An interdisciplinary study of the Basin and Range Province, western USA. *Tectonophysics* 213: 57–96.

Jordan TE (1981) Thrust loads and foreland basin evolution, cretaceous, western United-States. *Bulletin of the American Association of Petroleum Geologists* 65: 2506–2520.

Jordan TE (1982) Tectonic loading and foreland basin subsidence. *International Congress on Sedimentology* 11: 131.

Juhász E, Phillips L, Müller P, et al. (1999) Late Neogene sedimentary facies and sequences in the Pannonian Basin, Hungary. *Geological Society, London, Special Publications* 156: 335–356.

Kaban MK (2002) A gravity model of the north Eurasia crust and upper mantle: 2. The Alpine-Mediterranean fold-belt and adjacent structures of the southern former USSR. *Russian Journal of Earth Sciences* 4: 19–33.

Kaikkonen P, Moisio K, and Heeremans M (2000) Thermomechanical lithospheric structure of the central Fennoscandian Shield. *Physics of the Earth and Planetary Interiors* 119: 209–235.

Karner GD and Watts AB (1983) Gravity anomalies and flexure of the lithosphere at mountain ranges. *Journal of Geophysical Research: Solid Earth (1978–2012)* 88: 10449–10477.

Karner GD, Egan SS, and Weissel JK (1992) Modeling the tectonic development of the Tucano and Sergipe-Alagoas rift basins, Brazil. *Tectonophysics* 215: 133–160.

Kazmin VG (1991) The position of continental flood basalts in rift zones and its bearing on models of rifting. *Tectonophysics* 199: 375–387.

Kazmin VG, Schreider AA, and Bulychev AA (2000) Early stages of evolution of the Black Sea. *Geological Society, London, Special Publications* 173: 235–249.

Keen CE and Boutilier R (1990) Geodynamic modelling of rift basins: The syn-rift evolution of a simple half-graben. In: *The Potential of Deep Seismic Profiling for Hydrocarbon Exploration*, pp. 23–33. Paris: Technip.

Khriachtchevskaia O, Stovba S, and Popadyuk I (2009) Hydrocarbon prospects in the Western Black Sea of Ukraine. *The Leading Edge* 28: 1024–1029.

Kooi H (1991) *Tectonic Modelling of Extensional Basins*: *The Role of Lithospheric Flexure*, *Intraplate Stress and Relative Sea-level Change*, 183 pp. PhD Thesis, VU University, Amsterdam.

Kooi H and Cloetingh S (1989) Intraplate stresses and the stratigraphic evolution of the North Sea Central Graben. In: Tankard AJ and Balkwill HR (eds.) *Extensional Tectonics and Stratigraphy of the North Atlantic Margins*, pp. 49–72 Memoirs American Associations of Petroleum Geologists.

Kooi H, Cloetingh S, and Burrus J (1992) Lithospheric necking and regional isostasy at extensional basins. 1. Subsidence and gravity modeling with an application to the Gulf of Lions Margin (Se France). *Journal of Geophysical Research: Solid Earth* 97: 17553–17571.

Kooi H, Hettema M, and Cloetingh S (1991) Lithospheric dynamics and the rapid pliocene quaternary subsidence phase in the southern north-sea basin. *Tectonophysics* 192: 245–259.

Krezsek C and Bally AW (2006) The Transylvanian Basin (Romania) and its relation to the Carpathian fold and thrust belt: Insights in gravitational salt tectonics. *Marine and Petroleum Geology* 23: 405–442.

Krezsek C, Filipescu S, Silye L, Matenco L, and Doust H (2010) Miocene facies associations and sedimentary evolution of the Southern Transylvanian Basin (Romania): Implications for hydrocarbon exploration. *Marine and Petroleum Geology* 27: 191–214.

Krijgsman W, Hilgen FJ, Raffi I, Sierro FJ, and Wilson DS (1999) Chronology, causes and progression of the Messinian salinity crisis. *Nature* 400: 652–655.

Kroon IC (2002) *Strength of the Adriatic lithosphere: Inferences from tectonic modelling*, 112 pp. Published PhD thesis. Vrije Universiteit Amsterdam, the Netherlands.

Kruse SE and Royden LH (1994) Bending and unbending of an elastic lithosphere: The Cenozoic history of the Apennine and Dinaride foredeep basins. *Tectonics* 13: 278–302.

Kusznir NJ, Marsden G, and Egan SS (1991) A flexural-cantilever simple-shear/pure-shear model of continental lithosphere extension: Applications to the Jeanne d'Arc Basin, Grand Banks and Viking Graben, North Sea. *Geological Society, London, Special Publications* 56: 41–60.

Kusznir NJ and Park RG (1987) The extensional strength of the continental lithosphere: its dependence on geothermal gradient, and crustal composition and thickness. *Geological Society, London, Special Publications* 28: 35–52.

Kusznir NJ, Stovba SM, Stephenson RA, and Poplavskii KN (1996) The formation of the northwestern Dniepr-Donets Basin: 2-D forward and reverse syn-rift and post-rift modelling. *Tectonophysics* 268: 237–255.

Kusznir NJ and Ziegler PA (1992) The mechanics of continental extension and sedimentary basin formation – A simple-shear pure-shear flexural cantilever model. *Tectonophysics* 215: 117–131.

Lagarde JL, Baize S, Amorese D, et al. (2000) Active tectonics, seismicity and geomorphology with special reference to Normandy (France). *Journal of Quaternary Science* 15: 745–758.

Lambeck K (1983) The role of compressive forces in intracratonic basin formation and mid-plate orogenies. *Geophysical Research Letters* 10: 845–848.

Lankreijer AC (1998) *Rheology and Basement Control on Extensional Basin Evolution in Central and Eastern Europe*: *Variscan and Alpine-Carpathian-Pannonian Tectonics*, 158 pp. PhD Thesis. VU University, Amsterdam.

Lankreijer A, Bielik M, Cloetingh S, and Majcin D (1999) Rheology predictions across the western Carpathians, Bohemian massif, and the Pannonian basin: Implications for tectonic scenarios. *Tectonics* 18: 1139–1153.

Lankreijer A, Kovac M, Cloetingh S, et al. (1995) Quantitative subsidence analysis and forward modelling of the Vienna and Danube basins: Thin-skinned versus thick-skinned extension. *Tectonophysics* 252: 433–451.

Larsen RM, Brekke H, Larsen BT, and Talleraas E (1992) *Structural and Tectonic Modelling and its Applications to Petroleum Geology*. 549 pp. Norwegian Petroleum Society Special Publications.

Laske G and Masters G (1997) A global digital map of sediment thickness. *Eos, Transactions of the American Geophysical Union* 78: F483.

Laubscher H (2010) Jura, Alps and the boundary of the Adria subplate. *Tectonophysics* 483: 223–239.

Lavier LL and Steckler MS (1997) The effect of sedimentary cover on the flexural strength of continental lithosphere. *Nature* 389: 476–479.

Lawrence DT, Doyle M, and Aigner T (1990) Stratigraphic simulation of sedimentary basins – Concepts and calibration. *Bulletin of the American Association of Petroleum Geologists* 74: 273–295.

Le Solleuz A, Doin MP, Robin C, and Guillocheau F (2004) From a mountain belt collapse to a sedimentary basin development: 2-D thermal model based on inversion of stratigraphic data in the Paris Basin. *Tectonophysics* 386: 1–27.

Leever KA, Matenco L, Garcia-Castellanos D, and Cloetingh SAPL (2011) The evolution of the Danube gateway between Central and Eastern Paratethys (SE Europe): Insight from numerical modelling of the causes and effects of connectivity between basins and its expression in the sedimentary record. *Tectonophysics* 502: 175–195.

Lefort JP and Agarwal BNP (1996) Gravity evidence for an Alpine buckling of the crust beneath the Paris Basin. *Tectonophysics* 258: 1–14.

Lefort JP and Agarwal BNP (2000) Gravity and geomorphological evidence for a large crustal bulge cutting across Brittany (France): A tectonic response to the closure of the Bay of Biscay. *Tectonophysics* 323: 149–162.

Lefort JP and Agarwal BNP (2002) Topography of the Moho undulations in France from gravity data: Their age and origin. *Tectonophysics* 350: 193–213.

Lenkey L (1999) *Geothermics of the Pannonian Basin and Its Bearing on the Tectonics of Basin Evolution*, 215 pp. PhD Thesis, VU University, Amsterdam.

Lenkey L, Dövényi P, Horváth F, and Cloetingh S (2002) Geothermics of the Pannonian basin and its bearing on the neotectonics. *Neotectonics and Surface Processes: The Pannonian Basin and Alpine/Carpathian System*, vol. 3, 29–40.

Lenotre N, Thierry P, Blanchin R, and Brochard G (1999) Current vertical movement demonstrated by comparative levelling in Brittany (northwestern France). *Tectonophysics* 301: 333–344.

Le Pichon X, Henry P, and Goffé B (1997) Uplift of Tibet: From eclogites to granulites—implications for the Andean Plateau and the Variscan belt. *Tectonophysics* 273: 57–76.

Lericolais G, Bourget J, Popescu I, et al. (2013) Late Quaternary deep-sea sedimentation in the western Black Sea: New insights from recent coring and seismic data in the deep basin. *Global and Planetary Change* 103: 232–247.

Letouzey J (1986) Cenozoic Paleostress pattern in the alpine foreland and structural interpretation in a platform basin. *Tectonophysics* 132: 215–231.

Letouzey J, Biju-Duval B, Dorkel A, et al. (1977) The Black Sea: A marginal basin; geophysical and geological data. In: Biju-Duval B and Montadert L (eds.) *Structural History of the Mediterranean, Basins*, pp. 363–376. Paris: Technip.

Letouzey J, Werner P, and Marty A (1990) Fault reactivation and structural inversion. Backarc and intraplate compressive deformations. Example of the eastern Sunda shelf (Indonesia). *Tectonophysics* 183: 341–362.

Linzer HG (1996) Kinematics of retreating subduction along the Carpathian arc, Romania. *Geology* 24: 167–170.

Lin AT and Watts AB (2002) Origin of the West Taiwan basin by orogenic loading and flexure of a rifted continental margin. *Journal of Geophysical Research: Solid Earth (1978–2012)* 107: ETG-2.

Littke R, Bayer U, Gajewski D, and Nelskamp S (2008) In: *Dynamics of Complex Intracontinental Basins: The Central European Basin System*. Heidelberg: Springer, 520 pp.

Liu MJ, Mooney WD, Li SL, Okaya N, and Detweiler S (2006) Crustal structure of the northeastern margin of the Tibetan plateau from the Songpan-Ganzi terrane to the Ordos basin. *Tectonophysics* 420: 253–266.

Liu YJ, Neubauer F, Genser J, et al. (2007) Geochronology of the initiation and displacement of the Altyn Strike-Slip Fault, western China. *Journal of Asian Earth Sciences* 29: 243–252.

Lobkovsky LI, Cloetingh S, Nikishin AM, et al. (1996) Extensional basins of the former Soviet Union – Structure, basin formation mechanisms and subsidence history. *Tectonophysics* 266: 251–285.

Londoño J and Lorenzo JM (2004) Geodynamics of continental plate collision during late tertiary foreland basin evolution in the Timor Sea: constraints from foreland sequences, elastic flexure and normal faulting. *Tectonophysics* 392: 37–54.

Lorenzo JM, O'Brien GW, Stewart J, and Tandon K (1998) Inelastic yielding and forebulge shape across a modern foreland basin: North West Shelf of Australia, Timor Sea. *Geophysical Research Letters* 25: 1455–1458.

Lyon-Caen H and Molnar P (1984) Gravity anomalies and the structure of western Tibet and the southern Tarim Basin. *Geophysical Research Letters* 11: 1251–1254.

Lyon-Caen H and Molnar P (1985) Gravity anomalies, flexure of the Indian plate, and the structure, support and evolution of the Himalaya and Ganga basin. *Tectonics* 4: 513–538.

Macario A, Malinverno A, and Haxby WF (1995) On the robustness of elastic thickness estimates obtained using the coherence method. *Journal of Geophysical Research: Solid Earth (1978–2012)* 100: 15163–15172.

Mareschal JC and Gliko A (1991) Lithospheric thinning, uplift, and heat-flow preceding rifting. *Tectonophysics* 197: 117–126.

Marotta AM, Bayer U, and Thybo H (2000) The legacy of the NE German Basin – Reactivation by compressional buckling. *Terra Nova* 12: 132–140.

Martin M and Wenzel F (2006) High-resolution teleseismic body wave tomography beneath SE-Romania - II. Imaging of a slab detachment scenario. *Geophysical Journal International* 164: 579–595.

Martinod J and Davy P (1992) Periodic instabilities during compression or extension of the lithosphere 1. Deformation modes from an analytical perturbation method. *Journal of Geophysical Research: Solid Earth* 97: 1999–2014.

Mascle A (ed.) (1998) *Cenozoic Foreland Basins of Western Europe*: Geological Society of London, Special Publications 134.

Matenco L, Andriessen P, and Network S (2013) Quantifying the mass transfer from mountain ranges to deposition in sedimentary basins: Source to sink studies in the Danube Basin-Black Sea system. *Global and Planetary Change* 103: 1–18.

Matenco L and Bertotti G (2000) Tertiary tectonic evolution of the external East Carpathians (Romania). *Tectonophysics* 316: 255–286.

Matenco L, Bertotti G, Cloetingh S, and Dinu C (2003) Subsidence analysis and tectonic evolution of the external Carpathian-Moesian Platform region during Neogene times. *Sedimentary Geology* 156: 71–94.

Matenco L, Bertotti G, Dinu C, and Cloetingh S (1997a) Tertiary tectonic evolution of the external South Carpathians and the adjacent Moesian platform (Romania). *Tectonics* 16: 896–911.

Matenco L, Bertotti G, Leever K, et al. (2007) Large-scale deformation in a locked collisional boundary: Interplay between subsidence and uplift, intraplate stress, and inherited lithospheric structure in the late stage of the SE Carpathians evolution. *Tectonics* 26: TC4011.

Matenco L, Krezsek C, Merten S, et al. (2010) Characteristics of collisional orogens with low topographic build-up: An example from the Carpathians. *Terra Nova* 22: 155–165.

Matenco L and Radivojević D (2012) On the formation and evolution of the Pannonian Basin: Constraints derived from the structure of the junction area between the Carpathians and Dinarides. *Tectonics* 31: TC6007.

Matenco L, Zoetemeijer R, Cloetingh S, and Dinu C (1997b) Lateral variations in mechanical properties of the Romanian external Carpathians: Inferences of flexure and gravity modelling. *Tectonophysics* 282: 147–166.

Mathisen ME and Vondra CF (1983) The fluvial and pyroclastic deposits of the Cagayan Basin, Northern Luzon, Philippines – An example of non-marine volcaniclastic sedimentation in an interarc basin. *Sedimentology* 30: 369–392.

Mazur S, Scheck-Wenderoth M, and Krzywiec P (2005) Different modes of the Late Cretaceous-Early Tertiary inversion in the North German and Polish basins. *International Journal of Earth Sciences* 94: 782–798.

Mcadoo DC and Sandwell DT (1985) Folding of oceanic lithosphere. *Journal of Geophysical Research-Solid Earth and Planets* 90: 8563–8569.

McHargue TR, Heidrick TL, and Livingston J (1992) Episodic structural development of the Central African Rift in Sudan. *Tectonophysics* 213: 187–202.

Mckenzie D (1978) Some remarks on development of sedimentary basins. *Earth and Planetary Science Letters* 40: 25–32.

McNutt MK and Kogan MG (1987) Isostasy in the USSR I: Admittance data. *Composition, Structure and Dynamics of the Lithosphere-Asthenosphere System* 16: 301–307.

McNutt MK, Diament M, and Kogan MG (1988) Variations of elastic plate thickness at continental thrust belts. *Journal of Geophysical Research: Solid Earth (1978–2012)* 93: 8825–8838.

Mercier JL, Sebrier M, Lavenu A, et al. (1992) Changes in the tectonic regime above a subduction zone of andean type – The andes of Peru and Bolivia during the Pliocene-Pleistocene. *Journal of Geophysical Research: Solid Earth* 97: 11945–11982.

Merten S, Matenco L, Foeken JPT, and Andriessen PAM (2011) Toward understanding the post-collisional evolution of an orogen influenced by convergence at adjacent plate margins: Late Cretaceous-Tertiary thermotectonic history of the Apuseni Mountains. *Tectonics* 30: TC6008.

Merten S, Matenco L, Foeken JPT, Stuart FM, and Andriessen PAM (2010) From nappe stacking to out-of-sequence postcollisional deformations: Cretaceous to Quaternary exhumation history of the SE Carpathians assessed by low-temperature thermochronology. *Tectonics* 29: TC3013.

Meschede M and Frisch W (1998) A plate-tectonic model for the Mesozoic and Early Cenozoic history of the Caribbean plate. *Tectonophysics* 296: 269–291.

Meulenkamp JE, Kovac M, and Cicha I (1996) On Late Oligocene to Pliocene depocentre migrations and the evolution of the Carpathian-Pannonian system. *Tectonophysics* 266: 301–317.

Millan H, Den Bezemer T, Vergés J, et al. (1995) Paleo-elevation and effective elastic thickness evolution at mountain ranges: Interference from flexural modelling in the Eastern Pyrenees and Ebro Basin. *Marine and Petroleum Geology* 12: 917–928.

Mohr P (1992) Nature of the crust beneath magmatically active continental rifts. *Tectonophysics* 213: 269–284.

Moisio K, Kaikkonen P, and Beekman F (2000) Rheological structure and dynamical response of the DSS profile BALTIC in the SE Fennoscandian Shield. *Tectonophysics* 320: 175–194.

Moretti I and Royden L (1988) Deflection, gravity anomalies and tectonics of doubly subducted continental lithosphere: Adriatic and Ionian Seas. *Tectonics* 7: 875–893.

Morgan P and Ramberg IB (1987) Physical changes in the lithosphere associated with thermal relaxation after rifting. *Tectonophysics* 143: 1–11.

Morley CK and Westaway R (2006) Subsidence in the super-deep Pattani and Malay basins of Southeast Asia: A coupled model incorporating lower-crustal flow in response to post-rift sediment loading. *Basin Research* 18: 51–84.

Moucha R and Forte AM (2011) Changes in African topography driven by mantle convection. *Nature Geoscience* 4: 707–712.

Muhlhaus HB, Sakaguchi H, and Hobbs BE (1998) Evolution of three-dimensional folds for a non-Newtonian plate in a viscous medium. *Proceedings of the Royal Society A Mathematical Physical and Engineering Sciences* 454: 3121–3143.

Munteanu I (2012) *Evolution of the Western Black Sea*: *Kinematic and Sedimentological Inferences from Geological Observations and Analogue Modelling*. Dissertation, Utrecht University.

Munteanu I, Matenco L, Dinu C, and Cloetingh S (2011) Kinematics of back-arc inversion of the Western Black Sea Basin. *Tectonics* 30: TC5004.

Munteanu I, Matenco L, Dinu C, and Cloetingh S (2012) Effects of large sea-level variations in connected basins: The Dacian-Black Sea system of the Eastern Paratethys. *Basin Research* 24: 583–597.

Munteanu I, Willingshofer E, Sokoutis D, Matenco L, Dinu C, and Cloetingh S (2013) Transfer of deformation in back-arc basins with a laterally variable rheology: Constraints from analogue modelling of the Balkanides–Western Black Sea inversion. *Tectonophysics* 602: 223–236.

Munteanu I, Willingshofer E, Matenco L, Sokoutis D, and Cloetingh S (2014) Far-field contractional polarity changes in models and nature. *Earth and Planetary Science Letters* 395: 101–115.

Nádai A (1963) *Theory of flow and fracture of solids*. New York: McGraw-Hill.

Nadin PA and Kusznir NJ (1995) Paleocene uplift and Eocene subsidence in the northern North-Sea Basin from 2D forward and reverse stratigraphic modeling. *Journal of the Geological Society* 152: 833–848.

Nadirov RS, Bagirov E, Tagiyev M, and Lerche I (1997) Flexural plate subsidence, sedimentation rates, and structural development of the super-deep South Caspian Basin. *Marine and Petroleum Geology* 14: 383–400.

Naylor M and Sinclair HD (2008) Pro- vs. retro-foreland basins. *Basin Research* 20: 285–303.

Necea D (2010) *High-Resolution Morpho-Tectonic Profiling Across an Orogen*: *Tectonic-Controlled Geomorphology and Multiple Dating Approach in the SE Carpathians*, 147 pp. PhD Thesis, VU Vrije Universiteit, Amsterdam.

Necea D, Fielitz W, and Matenco L (2005) Late Pliocene-Quaternary tectonics in the frontal part of the SE Carpathians: Insights from tectonic geomorphology. *Tectonophysics* 410: 137–156.

Nemes F, Neubauer F, Cloetingh S, and Genser J (1997) The Klagenfurt Basin in the Eastern Alps: An intra-orogenic decoupled flexural basin? *Tectonophysics* 282: 189–203.

Neubauer F, Cloetingh S, Dinu C, and Mocanu V (1997) Tectonics of the Alpine-Carpathian-Pannonian region: Introduction. *Tectonophysics* 272: 93–96.

Nikishin AM, Brunet MF, Cloetingh S, and Ershov AV (1997) Northern Peri-Tethyan Cenozoic intraplate deformations: Influence of the Tethyan collision belt on the Eurasian continent from Paris to Tian-Shan. *Comptes rendus de l'Académie des sciences. Série 2, Sciences de la terre et des planètes* 324: 49–57.

Nikishin AM, Cloetingh S, Lobkovsky LI, Burov EB, and Lankreijer AC (1993) Continental lithosphere folding in Central-Asia.1. Constraints from geological observations. *Tectonophysics* 226: 59–72.

Nikishin AM, Korotaev MV, Ershov AV, and Brunet MF (2003) The Black Sea basin: Tectonic history and Neogene-Quaternary rapid subsidence modelling. *Sedimentary Geology* 156: 149–168.

Nikishin AM, Ziegler PA, Abbott D, Brunet MF, and Cloetingh S (2002) Permo-Triassic intraplate magmatism and rifting in Eurasia: Implications for mantle plumes and mantle dynamics. *Tectonophysics* 351: 3–39.

Nikishin A, Ziegler P, Bolotov S, et al. (2012) Late Paleozoic to Cenozoic evolution of the Black Sea-Southern Eastern Europe Region: A view from the Russian Platform. *Turkish Journal of Earth Sciences* 21: 571–634.

Nikishin AM, Ziegler PA, Panov DI, et al. (2001) Mesozoic and Cainozoic evolution of the Scythian platform-Black Sea-Caucasus domain. *Memoires du Museum National d'Histoire Naturelle* 186: 295–346.

Nivière B and Winter T (2000) Pleistocene northwards fold propagation of the Jura within the southern Upper Rhine Graben: Seismotectonic implications. *Global and Planetary Change* 27: 263–288.

Nottvedt A, Gabrielsen RH, and Steel RJ (1995) Tectonostratigraphy and sedimentary architecture of rift basins, with reference to the northern north-sea. *Marine and Petroleum Geology* 12: 881–901.

Nunn JA, Czerniak M, and Pilger RH (1987) Constraints on the structure of Brooks Range and Colville Basin, northern Alaska, from flexure and gravity analysis. *Tectonics* 6: 603–617.

Okay AI, Satir M, Maluski H, et al. (1996) Paleo-and Neo-Tethyan events in northwestern Turkey: Geologic and geochronologic constraints. In: Yin A and Olsen KH (eds.) *The Tectonic Evolution of Asia*, pp. 420–441. Cambridge: Cambridge University Press.

Okay AI, Sengor AMC, and Görür N (1994) Kinematic history of the opening of the Black-Sea and its effect on the surrounding regions. *Geology* 22: 267–270.

Olsen KH and Morgan P (1995) Introduction: progress in understanding continental rifts. In: Olsen KH (Ed.) Developments in Geotectonics: Continental Rifts: Evolution, Structure, *Tectonics* 25: 3–26.

Olsen KH and Morgan P (2006) Chapter 1 Introduction: Progress in understanding continental rifts. In: Olsen KH (ed.) *Developments in Geotectonics*, vol. 25, pp. 3–26. Amsterdam: Elsevier.

Oszczypko N, Krzywiec P, Popadyuk I, and Peryt T (2005) Carpathian Foredeep Basin (Poland and Ukraine) - Its sedimentary, structural and geodynamic evolution. In: Golonka J and Picha FJ (eds.) *The Carpathians and their foreland: Geology and hydrocarbon resources* 84, pp. 293–350. AAPG.

Panza GF (1983) Lateral variations in the European lithosphere and seismic activity. *Physics of the Earth and Planetary Interiors* 33: 194–197.

Parnell J (1994) Geofluids: Origin migration and evolution of fluids in sedimentary basins. *Geological Society, London, Special Publications* 78: 1–372.

Parsons T (1995) The Basin and Range Province. In: Olsen KH (ed.) *Developments in Geotectonics, 25: Continental Rifts: Evolution, Structure*, *Tectonics*, pp. 227–324. Amsterdam: Elsevier.

Parsons T (2006) The basin and range province. In: Olsen KH (ed.) *Developments in Geotectonics*, vol. 25, p. 277. Amsterdam: Elsevier.

Pascal C and Cloetingh SAPL (2009) Gravitational potential stresses and stress field of passive continental margins: Insights from the south-Norway shelf. *Earth and Planetary Science Letters* 277: 464–473.

Patacca E, Scandone P, Di Luzio E, Cavinato GP, and Parotto M (2008) Structural architecture of the central Apennines: Interpretation of the CROP 11 seismic profile from the Adriatic coast to the orographic divide. *Tectonics* 27: TC3006.

Pavoni N (1993) Pattern of mantle convection and Pangaea break-up, as revealed by the evolution of the African plate. *Journal of the Geological Society* 150: 953–964.

Pelletier JD (2007) Erosion-rate determination from foreland basin geometry. *Geology* 35: 5–8.

Peper T, van Balen RT, and Cloetingh S (1995) Implications of Orogenic wedge growth, intraplate stress variations and eustatic sea-level change for Foreland Basin Stratigraphy—Inferences From Numerical Modeling. In: Dorobek S and Ross G (eds.) Stratigraphic developments in foreland basins, pp. 25—35. *Special Publications of Society for Sedimentary Geology 52*.

Peper T, Beekman F, and Cloetingh S (1992) Consequences of thrusting and intraplate stress fluctuations for vertical motions in foreland basins and peripheral areas. *Geophysical Journal International* 111: 104–126.

Pérez-Gussinyé M and Watts AB (2005) The long-term strength of Europe and its implications for plate-forming processes. *Nature* 436: 381–384.

Persson KS, Garcia-Castellanos D, and Sokoutis D (2004) River transport effects on compressional belts: First results from an integrated analogue-numerical model. *Journal of Geophysical Research: Solid Earth* 109: B01409.

Persson KS and Sokoutis D (2002) Analogue models of orogenic wedges controlled by erosion. *Tectonophysics* 356: 323–336.

Petroleum Publishing Co./PenWell (1970) Worldwide offshore activity and sedimentary basins. *Oil and Gas Journal*.

Philip H (1987) Plioquaternary evolution of the stress-field in mediterranean zones of subduction and collision. *Annales Geophysicae, Series B: Terrestrial and Planetary Physics* 5: 301–319.

Philippe Y (1994) Transfer Zone in the Southern Jura Thrust Belt (Eastern France): Geometry, development, and comparison with analogue modeling experiments. In: Mascle A (ed.) *Hydrocarbon and Petroleum Geology of France*, pp. 327–346. Heidelberg: Springer Berlin, Special Publication of the European Association of Petroleum Geoscientists 4.

Pinter N, Grenerczy G, Weber J, and Medak D (2005) *The Adria Microplate: GPS Geodesy, Tectonics and Hazards*, vol. 61, p. 414. Netherlands: Springer.

Pitman WC and Golovchenko X (1983) The effect of sealevel change on the shelfedge and slope of passive margins. *Special Publications of SEPM* 33: 41–58.

Piwowar JM and LeDrew EF (1996) Principal components analysis of Arctic ice conditions between 1978 and 1987 as observed from the SMMR data record. *Canadian journal of remote sensing* 22: 390–403.

Plomerova J, Kouba D, and Babuska V (2002) Mapping the lithosphere-asthenosphere boundary through changes in surface-wave anisotropy. *Tectonophysics* 358: 175–185.

Popescu E and Radulian M (2001) Source characteristics of the seismic sequences in the Eastern Carpathians foredeep region (Romania). *Tectonophysics* 338: 325–337.

Popescu I, Lericolais G, Panin N, Wong HK, and Droz L (2001) Late Quaternary channel avulsions on the Danube deep-sea fan, Black Sea. *Marine Geology* 179: 25–37.

Popov SV, Shcherba IG, Ilyina LB, et al. (2006) Late Miocene to Pliocene palaeogeography of the Paratethys and its relation to the Mediterranean. *Palaeogeography Palaeoclimatology Palaeoecology* 238: 91–106.

Poudjom Djomani YH, Fairhead JD, and Griffin WL (1999) The flexural rigidity of Fennoscandia: Reflection of the tectonothermal age of the lithospheric mantle. *Earth and Planetary Science Letters* 174: 139–154.

Prezzi CB (1999) Diacronismo en la deformación Mio-Pliocena de la Puna Argentina: Un modelo flexural. *Actas Congreso Geologico Argentino* 14: 197–200.

Prezzi CB, Uba CE, and Gotze HJ (2009) Flexural isostasy in the Bolivian Andes: Chaco foreland basin development. *Tectonophysics* 474: 526–543.

Price RA (1973) Large-scale gravitational flow of supracrustal rocks, southern Canadian Rockies. In: Jong K and Scholten RA (eds.) *Gravity and tectonics*, pp. 491–502. New York: John Wiley & Sons.

Pysklywec RN and Mitrovica JX (1997) Mantle avalanches and the dynamic topography of continents. *Earth and Planetary Science Letters* 148: 447–455.

Quinlan GM and Beaumont C (1984) Appalachian thrusting, lithospheric flexure, and the paleozoic stratigraphy of the eastern interior of north-America. *Canadian Journal of Earth Sciences* 21: 973–996.

Raileanu V, Taloş D, Varodin V, and Stiopol D (1993) Crustal seismic reflection profiling in Romania on the Urziceni-Mizil line. *Tectonophysics* 223: 401–409.

Ranalli G (1995) *Rheology of the Earth*. London: Chapman & Hall, 413 pp.

Ranalli G and Murphy DC (1987) Rheological stratification of the lithosphere. *Tectonophysics* 132: 281–295.

Rankin DW, Dillon WP, Black DFB, et al. (1991) *Central Kentucky to the Carolina Trough*. Geological Society of America.

Ravaut P, Alyahyaey A, Bayer R, and Lesquer A (1993) Isostatic response of the Arabian Platform to Ophiolitic Loading in Oman. *Comptes Rendus - Acadamie des Sciences* 317: 463–470.

Ren Y, Stuart GW, Houseman GA, et al. (2012) Upper mantle structures beneath the Carpathian-Pannonian region: Implications for the geodynamics of continental collision. *Earth and Planetary Science Letters* 349: 139–152.

Reston TJ (1990) The lower crust and the extension of the continental lithosphere - Kinematic analysis of birps deep seismic data. *Tectonics* 9: 1235–1248.

Richardson RM (1992) Ridge forces, absolute plate motions, and the intraplate stress-field. *Journal of Geophysical Research: Solid Earth* 97: 11739–11748.

Richter F and Mckenzie D (1978) Simple plate models of mantle convection. *Journal of Geophysics* 44: 441–471.

Rickers F, Fichtner A, and Trampert J (2013) The Iceland-Jan Mayen plume system and its impact on mantle dynamics in the North Atlantic region: Evidence from full-waveform inversion. *Earth and Planetary Science Letters* 367: 39–51.

Ritter JRR, Achauer U, Christensen UR, and the Eifel Plume T (2000) The teleseismic tomography experiment in the eifel region, central Europe: Design and first results. *Seismological Research Letters* 71: 437–443.

Ritter JRR, Jordan M, Christensen UR, and Achauer U (2001) A mantle plume below the Eifel volcanic fields, Germany. *Earth and Planetary Science Letters* 186: 7–14.

Ritzmann O and Faleide JI (2009) The crust and mantle lithosphere in the Barents Sea/Kara Sea region. *Tectonophysics* 470: 89–104.

Roberts AM, Yielding G, Kusznir NJ, Walker I, and Dorn-Lopez D (1993) Mesozoic extension in the North Sea: Constraints from flexural backstripping, forward modelling and fault populations. *Geological Society, London, Conference series* 4: 1123–1136.

Robin C, Allemand P, Burov E, et al. (2003) Vertical movements of the Paris Basin (Triassic-Pleistocene): From 3D stratigraphic database to numerical models. *Geological Society, London, Special Publications* 212: 225–250.

Robinson AG, Rudat JH, Banks CJ, and Wiles RLF (1996) Petroleum geology of the Black Sea. *Marine and Petroleum Geology* 13: 195–223.

Robinson A, Spadini G, Cloetingh S, and Rudat J (1995) Stratigraphic evolution of the Black-Sea – Inferences from basin modeling. *Marine and Petroleum Geology* 12: 821–835.

Roddaz M, Viers J, Brusset S, Baby P, and Herail G (2005) Sediment provenances and drainage evolution of the Neogene Amazonian foreland basin. *Earth and Planetary Science Letters* 239: 57–78.

Rohrman M, Vanderbeek P, Andriessen P, and Cloetingh S (1995) Meso-Cenozoic morphotectonic evolution of southern Norway – Neogene domal uplift inferred from apatite fission-track thermochronology. *Tectonics* 14: 704–718.

Roure F (2008) Foreland and Hinterland basins: What controls their evolution? *Swiss Journal of Geosciences* 101: S5–S29.

Roure F, Alzaga-Ruiz H, Callot JP, et al. (2009) Long lasting interactions between tectonic loading, unroofing, post-rift thermal subsidence and sedimentary transfers along the western margin of the Gulf of Mexico: Some insights from integrated quantitative studies. *Tectonophysics* 475: 169–189.

Roure F, Andriessen P, Callot JP, et al. (2010a) The use of palaeo-thermo-barometers and coupled thermal, fluid flow and pore-fluid pressure modelling for hydrocarbon and reservoir prediction in fold and thrust belts. *Geological Society, London, Special Publications* 348: 87–114.

Roure F, Brun JP, Colletta B, and Vially R (1994) Multiphase Extensional structures, fault reactivation, and petroleum plays in the alpine foreland basin of southeastern France. In: Mascle A (ed.) *Hydrocarbon and Petroleum Geology of France*, pp. 245–268. Springer Berlin Heidelberg, Special Publication of the European Association of Petroleum Geoscientists 4.

Roure F, Casero P, and Addoum B (2012) Alpine inversion of the North African margin and delamination of its continental lithosphere. *Tectonics* 31: TC3006.

Roure F, Choukroune P, Berastegui X, et al. (1989) Ecors deep seismic data and balanced cross-sections – Geometric constraints on the evolution of the pyrenees. *Tectonics* 8: 41–50.

Roure F, Choukroune P, and Polino R (1996) Deep seismic reflection data and new insights on the bulk geometry of mountain ranges. *Comptes rendus de l'Académie des sciences. Série 2, Sciences de la terre et des planètes* 322: 345–359.

Roure F, Cloetingh S, Scheck-Wenderoth M, and Ziegler P (2010b) Achievements and challenges in sedimentary basin dynamics: A review. In: Cloetingh S and Negendank J (eds.) *New Frontiers in Integrated Solid Earth Sciences International Year of Planet Earth*, pp. 145–233. Netherlands: Springer.

Roure F, Colletta B, DeToni B, et al. (1997) Within-plate deformations in the Maracaibo and East Zulia basins, western Venezuela. *Marine and Petroleum Geology* 14: 139–163.

Roure F, Roca E, and Sassi W (1993) The Neogene evolution of the outer Carpathian flysch units (Poland, Ukraine and Romania) – Kinematics of a foreland fold-and-thrust belt system. *Sedimentary Geology* 86: 177–201.

Roure F, Scheck-Wenderoth M, Gahnoog A, and Pharaoh T (2010c) Lithosphere dynamics and sedimentary basins: The Arabian plate and analogues. *Arabian Journal of Geosciences* 3: 327–329.

Rowley DB and Sahagian D (1986) Depth-dependent stretching – A different approach. *Geology* 14: 32–35.

Royden L (1988a) Flexural behavior of the continental lithosphere in Italy – Constraints imposed by gravity and deflection data. *Journal of Geophysical Research-Solid Earth and Planets* 93: 7747–7766.

Royden LH (ed.) (1988b) *The Pannonian Basin*. Tusla, OK: American Association of Petroleum Geologists, AAPG Memoirs 45.

Royden LH (1993) The tectonic expression slab pull at continental convergent boundaries. *Tectonics* 12: 303–325.

Royden L and Burchfiel BC (1989) Are systematic variations in thrust belt style related to plate boundary processes – (the Western Alps Versus the Carpathians). *Tectonics* 8: 51–61.
Royden LH and Dövényi P (1988) Variations in extensional styles at depth across the Pannonian basin system. *American Association of Petroleum Geologists* 45: 235–255.
Royden LH and Horváth F (eds.) (1988) *The Pannonian Basin: A case study in basin evolution,* American Association of Petroleum Geologists, AAPG Memoir 45.
Royden L, Horváth F, Nagymarosy A, and Stegena L (1983) Evolution of the Pannonian basin system. 2. Subsidence and thermal history. *Tectonics* 2: 91–137.
Royden L and Karner GD (1984) Flexure of the continental lithosphere beneath Apennine and Carpathian foredeep basins. *Nature* 309: 142–144.
Royden L and Keen CE (1980) Rifting process and thermal evolution of the continental-margin of eastern Canada determined from subsidence curves. *Earth and Planetary Science Letters* 51: 343–361.
Royden L, Sclater JG, and Von Herzen RP (1980) Continental-margin subsidence and heat-flow – Important parameters in formation of petroleum-hydrocarbons. *American Association of Petroleum Geologists Bulletin* 64: 173–187.
Ruppel C and McNutt M (1987) An elastic plate model for the Caucasus. *Eos Transactions AGU* 68: 420.
Sacchi M, Horváth F, and Magyari O (1999) Role of unconformity-bounded units in the stratigraphy of the continental record: A case study from the Late Miocene of the western Pannonian Basin, Hungary. *Geological Society, London, Special Publications* 156: 357–390.
Sachsenhofer RF, Lankreijer A, Cloetingh S, and Ebner F (1997) Subsidence analysis and quantitative basin modelling in the Styrian basin (Pannonian basin system, Austria). *Tectonophysics* 272: 175–196.
Saintot A, Brunet M, Yakovlev F, et al. (2006) The Mesozoic-Cenozoic tectonic evolution of the Greater Caucasus. *Geological Society, London, Memoirs* 32: 277.
Salveson JO (1976) Variations in the oil and gas geology of rift basins. In: *Egyptian General Petroleum Corporation, 5th Exploration Seminar, Cairo, Egypt*.
Samuelsson J and Middleton MF (1999) The Caledonian foreland basin in Scandinavia: Constrained by the thermal maturation of the alum shale. A reply. *Journal of the Geological Society of Sweden (GFF)* 121: 157–159.
Sanders CAE, Andriessen PAM, and Cloetingh SAPL (1999) Life cycle of the East Carpathian orogen: Erosion history of a doubly vergent critical wedge assessed by fission track thermochronology. *Journal of Geophysical Research: Solid Earth* 104: 29095–29112.
Sassi W, Colletta B, Bale P, and Paquereau T (1993) Modeling of structural complexity in sedimentary basins – The role of preexisting faults in thrust tectonics. *Tectonophysics* 226: 97–112.
Sassi W and Rudkiewicz JL (2000) *Computer Modelling of Petroleum Systems Along Regional Cross-Sections in Foreland and Fold-and-Thrustbelts*. In: Proceedings of the conference on geology and petroleum geology of the Mediterranean and circum Mediterranean Basins. Malta: EAGE.
Scheck M and Bayer U (1999) Evolution of the Northeast German Basin – Inferences from a 3D structural model and subsidence analysis. *Tectonophysics* 313: 145–169.
Schlunegger F, Jordan TE, and Klaper EM (1997) Controls of erosional denudation in the orogen on foreland basin evolution: The Oligocene central Swiss Molasse basin as an example. *Tectonics* 16: 823–840.
Schmalholz SM and Podladchikov YY (2000) Finite amplitude folding: Transition from exponential to layer length controlled growth (vol 179, pg 363, 2000). *Earth and Planetary Science Letters* 181: 617–633.
Schmid SM, Bernoulli D, Fugenschuh B, et al. (2008) The Alpine-Carpathian-Dinaridic orogenic system: Correlation and evolution of tectonic units. *Swiss Journal of Geosciences* 101: 139–183.
Schmid SM, Berza T, Diaconescu V, Froitzheim N, and Fügenschuh B (1998) Orogen-parallel extension in the Southern Carpathians. *Tectonophysics* 297: 209–228.
Sclater JG and Christie PAF (1980) Continental stretching – An explanation of the post-mid-cretaceous subsidence of the central north-sea basin. *Journal of Geophysical Research* 85: 3711–3739.
Sclater J, Royden L, Horváth F, Burchfiel B, Semken S, and Stegena L (1980) The formation of the intra-Carpathian basins as determined from subsidence data. *Earth and Planetary Science Letters* 51: 139–162.
Şengör AMC (1987) Tectonics of the tethysides – Orogenic collage development in a collisional setting. *Annual Review of Earth and Planetary Sciences* 15: 213–244.
Sengör AMC and Burke K (1978) Relative timing of rifting and volcanism on earth and its tectonic implications. *Geophysical Research Letters* 5: 419–421.
Şengör AMC and Yilmaz Y (1981) Tethyan evolution of Turkey – A plate tectonic approach. *Tectonophysics* 75: 181–241.
Serpelloni E, Faccenna C, Spada G, Dong D, and Williams SD (2013) Vertical GPS ground motion rates in the Euro-Mediterranean region: New evidence of vertical velocity gradients at different spatial scales along the Nubia-Eurasia plate boundary. *Journal of Geophysical Research: Solid Earth* 118: 6003–6024.
Sheffels B and McNutt M (1986) Role of subsurface loads and regional compensation in the isostatic balance of the Transverse Ranges, California: Evidence for intracontinental subduction. *Journal of Geophysical Research: Solid Earth (1978–2012)* 91: 6419–6431.
Shillington DJ, White N, Minshull TA, et al. (2008) Cenozoic evolution of the eastern Black Sea: A test of depth-dependent stretching models. *Earth and Planetary Science Letters* 265: 360–378.
Shin YH, Shum CK, Braitenberg C, et al. (2009) Three-dimensional fold structure of the Tibetan Moho from GRACE gravity data. *Geophysical Research Letters* 36: L01302.
Shudofsky GN, Cloetingh S, Stein S, and Wortel R (1987) Unusually deep earthquakes in east-Africa – Constraints on the thermomechanical structure of a continental rift system. *Geophysical Research Letters* 14: 741–744.
Simpson GDH (2006) Modelling interactions between fold-thrust belt deformation, foreland flexure and surface mass transport. *Basin Research* 18: 125–143.
Simpson GDH (2010) Influence of the mechanical behaviour of brittle-ductile fold-thrust belts on the development of foreland basins. *Basin Research* 22: 139–156.
Sinclair HD, Coakley BJ, Allen PA, and Watts AB (1991) Simulation of Foreland Basin stratigraphy using a diffusion-model of mountain belt uplift and erosion – An example from the central Alps, Switzerland. *Tectonics* 10: 599–620.
Sleep NH (1971) Thermal effects of formation of atlantic continental margins by continental break up. *Geophysical Journal of the Royal Astronomical Society* 24: 325–350.
Sleep NH (1973) Crustal thinning on Atlantic continental margins: Evidence from older margins. In: Tarling DH and Runcorn SK (eds.) *Implications of Continental Drift to the Earth Sciences*, vol. 2, 685–692.
Smit J, Brun JP, Cloetingh S, and Ben-Avraham Z (2008a) Pull-apart basin formation and development in narrow transform zones with application to the Dead Sea Basin. *Tectonics* 27: 257–290.
Smit J, Brun JP, Cloetingh S, and Ben-Avraham Z (2010) The rift-like structure and asymmetry of the Dead Sea Fault. *Earth and Planetary Science Letters* 290: 74–82.
Smit J, Brun JP, Fort X, Cloetingh S, and Ben-Avraham Z (2008b) Salt tectonics in pull-apart basins with application to the Dead Sea Basin. *Tectonophysics* 449: 1–16.
Smit JHW, Brun JP, and Sokoutis D (2003) Deformation of brittle-ductile thrust wedges in experiments and nature. *Journal of Geophysical Research: Solid Earth* 108: ETG 9.
Smit JHW, Cloetingh SAPL, Burov E, et al. (2013) Interference of lithospheric folding in western Central Asia by simultaneous Indian and Arabian plate indentation. *Tectonophysics* 602: 176–193.
Smolyaninova EI, Mikhailov VO, and Lyakhovsky VA (1996) Numerical modelling of regional neotectonic movements in the northern Black Sea. *Tectonophysics* 266: 221–231.
Sobel ER, Hilley GE, and Strecker MR (2003) Formation of internally drained contractional basins by aridity-limited bedrock incision. *Journal of Geophysical Research: Solid Earth* 108: ETG 9.
Sokoutis D, Burg JP, Bonini M, Corti G, and Cloetingh S (2005) Lithospheric-scale structures from the perspective of analogue continental collision. *Tectonophysics* 406: 1–15.
Solheim A, Riis F, Elverhøi A, et al. (1996) Impact of glaciations on basin evolution: Data and models from the Norwegian margin and adjacent areas – Introduction and summary. *Global and Planetary Change* 12: 1–9.
Spadini G, Bertotti G, and Cloetingh S (1995a) Tectono-stratigraphic modelling of the Sardinian margin of the Tyrrhenian Sea. *Tectonophysics* 252: 269–284.
Spadini G, Cloetingh S, and Bertotti G (1995b) Thermomechanical modeling of the Tyrrhenian Sea – Lithospheric necking and kinematics of rifting. *Tectonics* 14: 629–644.
Spadini G and Podladchikov Y (1996) Spacing of consecutive normal faulting in the lithosphere: A dynamic model for rift axis jumping (Tyrrhenian Sea). *Earth and Planetary Science Letters* 144: 21–34.
Spadini G, Robinson A, and Cloetingh S (1996) Western versus Eastern Black Sea tectonic evolution: Pre-rift lithospheric controls on basin formation. *Tectonophysics* 266: 139–154.
Spadini G, Robinson AG, and Cloetingh SAPL (1997) Thermomechanical modeling of black sea basin formation, subsidence, and sedimentation. *American Association of Petroleum Geologists Memoir* 68: 19–38.
Spakman W and Hall R (2010) Surface deformation and slab-mantle interaction during Banda arc subduction rollback. *Nature Geoscience* 3: 562–566.
Stampfli GM, Borel GD, Cavazza W, Mosar J, and Ziegler PA (2001) Palaeotectonic and palaeogeographic evolution of the western Tethys and PeriTethyan domain (IGCP Project 369). *Episodes* 24: 222–228.

Starostenko V, Buryanov V, Makarenko I, et al. (2004) Topography of the crust-mantle boundary beneath the Black Sea Basin. *Tectonophysics* 381: 211–233.

Steckler MS and Watts AB (1982) Subsidence history and tectonic evolution of Atlantic-type continental margins. *Dynamics of Passive Margins*, vol. 6, pp. 184–196. American Geophysical Union.

Stein CA, Cloetingh S, and Wortel R (1989) Seasat-derived gravity constraints on stress and deformation in the northeastern Indian-Ocean. *Geophysical Research Letters* 16: 823–826.

Stel H, Cloetingh S, Heeremans M, and Van der Beek P (1993) Anorogenic granites, magmatic underplating and the origin of intracratonic basins in a non-extensional setting. *Tectonophysics* 226: 285–299.

Stephenson RA (1989) Beyond first-order thermal subsidence models for sedimentary basins. In: *Quantitative Dynamic Stratigraphy*, pp. 113–125. Prentice Hall, New Jersey: Englewood Cliffs.

Stephenson RA and Cloetingh SAPL (1991) Some examples and mechanical aspects of continental lithospheric folding. *Tectonophysics* 188: 27–37.

Stephenson R and Lambeck K (1985) Isostatic response of the lithosphere with inplane stress – Application to Central Australia. *Journal of Geophysical Research-Solid Earth and Planets* 90: 8581–8588.

Stephenson RA, Mart Y, Okay A, et al. (2004) TRANSMED Section VIII; East-European Craton-Crimea-Black Sea-Anatolia-Cyprus-Levant Sea-Sinai-Red Sea. In: Cavazza W, Roure F, Spakman W, Stampfli GM, and Ziegler PA (Eds.) *The TRANSMED Atlas: The Mediterranean Region from Crust to Mantle*, pp. 77–98. Berlin: Springer.

Stephenson RA, Ricketts BD, Cloetingh SA, and Beekman F (1990) Lithosphere folds in the Eurekan Orogen, Arctic Canada. *Geology* 18: 603–606.

Stephenson RA, Stovba SM, and Starostenko VI (2001) Pripyat-Dniepr-Donets basin: Implications for dynamics of rifting and the tectonic history of the northern peri-Tethyan platform. *Memoires du Museum National d'Histoire Naturelle* 186: 369–406.

Stern TA (1995) Gravity anomalies and crustal loading at and adjacent to the Alpine Fault, New Zealand. *New Zealand Journal of geology and geophysics* 38: 593–600.

Stern TA, Quinlan GM, and Holt WE (1993) Crustal dynamics associated with the formation of Wanganui Basin, New Zealand. *Sedimentary Basins of the World* 2: 213–223.

Stewart J and Watts AB (1997) Gravity anomalies and spatial variations of flexural rigidity at mountain ranges. *Journal of Geophysical Research: Solid Earth (1978–2012)* 102: 5327–5352.

Stockmal GS, Beaumont C, and Boutilier R (1986) Geodynamic models of convergent margin tectonics – Transition from rifted margin to overthrust belt and consequences for foreland-basin development. *Bulletin of the American Association of Petroleum Geologists* 70: 181–190.

Stovba S, Khriachtchevskaia O, and Popadyuk I (2009) Hydrocarbon-bearing areas in the eastern part of the Ukrainian Black Sea. *Leading Edge (Tulsa, OK)* 28: 1042–1045.

Straume AK and Austrheim H (1999) Importance of fracturing during retro-metamorphism of eclogites. *Journal of Metamorphic Geology* 17: 637–652.

Suhadolc P and Panza GF (1989) Physical properties of the lithosphere-asthenosphere system in Europe from geophysical data. *The lithosphere in Italy* 80: 15–40.

Sunal G and Tüysüz O (2002) Palaeostress analysis of Tertiary post-collisional structures in the Western Pontides, northern Turkey. *Geological Magazine* 139: 343–359.

Suvorov VD, Mishenkina ZM, Petrick GV, et al. (2002) Structure of the crust in the Baikal rift zone and adjacent areas from Deep Seismic Sounding data. *Tectonophysics* 351: 61–74.

Snyder DB and Barazangi M (1986) Deep crustal structure and flexure of the Arabian plate beneath the Zagros collisional mountain belt as inferred from gravity observations. *Tectonics* 5: 361–373.

Sztanó O, Szafián P, Magyar I, et al. (2013) Aggradation and progradation controlled clinothems and deep-water sand delivery model in the Neogene Lake Pannon, Makó Trough, Pannonian Basin, SE Hungary. *Global and Planetary Change* 103: 149–167.

Tandon K, Lorenzo JM, and O'Brien GW (2000) Effective elastic thickness of the northern Australian continental lithosphere subducting beneath the Banda orogen (Indonesia): Inelastic failure at the start of continental subduction. *Tectonophysics* 329: 39–60.

Tang J, Lerche I, and Cogan J (1992) An inverse method for calculating basement geometries in foreland basins. *Journal of geodynamics* 15: 85–106.

Tarapoanca M, Andriessen P, Broto K, et al. (2010) Forward kinematic modelling of a regional transect in the Northern Emirates using geological and apatite fission track age constraints on paleo-burial history. *Arabian Journal of Geosciences* 3: 395–411.

Tarapoanca M, Bertotti G, Matenco L, Dinu C, and Cloetingh SAPL (2003) Architecture of the Focsani Depression: A 13 km deep basin in the Carpathians bend zone (Romania). *Tectonics* 22: 13.

Tarapoanca M, Garcia-Castellanos D, Bertotti G, et al. (2004) Role of the 3-D distributions of load and lithospheric strength in orogenic arcs: Polystage subsidence in the Carpathians foredeep. *Earth and Planetary Science Letters* 221: 163–180.

Tari G, Dövényi P, Dunkl I, et al. (1999) Lithospheric structure of the Pannonian basin derived from seismic, gravity and geothermal data. *Geological Society Special Publication* 156: 215–250.

Tari G, Nemcok M, Tari G, and Nemcok M (2009) Introduction to this special section: The Black Sea Region. *Leading Edge* 28: 1022–1023.

Teixell A, Ayarza P, Zeyen H, Fernandez M, and Arboleya ML (2005) Effects of mantle upwelling in a compressional setting: The Atlas Mountains of Morocco. *Terra Nova* 17: 456–461.

Teng JW (1991) Geophysical fields and hydrocarbon prospects of the Tarim Basin. *Academia Sinica* 2: 24–40.

Ter Voorde M and Bertotti G (1994) Thermal effects of normal faulting during rifted basin formation, 1. A finite difference model. *Tectonophysics* 240: 133–144.

Ter Voorde M and Cloetingh S (1996) Numerical modelling of extension in faulted crust: Effects of localized and regional deformation on basin stratigraphy. In: *Modern Developments in Structural Interpretation, Validation and Modelling*, pp. 283–296. London: Geological Society of London, Special Publication 99.

Ter Voorde M, De Bruijne CH, Cloetingh SAPL, and Andriessen PAM (2004) Thermal consequences of thrust faulting: Simultaneous versus successive fault activation and exhumation. *Earth and Planetary Science Letters* 223: 395–413.

Ter Voorde M, Gaspar-Escribano JM, Juez-Larre J, et al. (2007) Thermal effects of linked lithospheric and upper crustal-scale processes: Insights from numerical modeling of the Cenozoic Central Catalan Coastal Ranges (NE Spain). *Tectonics* 26: TC5018.

Ter Voorde M, Ravnås R, Færseth R, and Cloetingh S (1997) Tectonic modelling of the Middle Jurassic synrift stratigraphy in the Oseberg-Brage area, northern Viking Graben. *Basin Research* 9: 133–150.

Ter Voorde M, Van Balen RT, Bertotti G, and Cloetingh SAPL (1998) The influence of a stratified rheology on the flexural response of the lithosphere to (un)loading by extensional faulting. *Geophysical Journal International* 134: 721–735.

Tesauro M, Audet P, Kaban MK, Burgmann R, and Cloetingh S (2012a) The effective elastic thickness of the continental lithosphere: Comparison between rheological and inverse approaches. *Geochemistry, Geophysics, Geosystems* 13: Q09001.

Tesauro M, Burov EB, Kaban MK, and Cloetingh SAPL (2011) Ductile crustal flow in Europe's lithosphere. *Earth and Planetary Science Letters* 312: 254–265.

Tesauro M, Hollenstein C, Egli R, Geiger A, and Kahle HG (2005) Continuous GPS and broad-scale deformation across the Rhine Graben and the Alps. *International Journal of Earth Sciences* 94: 525–537.

Tesauro M, Kaban MK, and Cloetingh SAPL (2008) EuCRUST-07: A new reference model for the European crust. *Geophysical Research Letters* 35: L05313.

Tesauro M, Kaban MK, and Cloetingh SAPL (2009a) A new thermal and rheological model of the European lithosphere. *Tectonophysics* 476: 478–495.

Tesauro M, Kaban MK, and Cloetingh SAPL (2009b) How rigid is Europe's lithosphere? *Geophysical Research Letters* 36: L16303.

Tesauro M, Kaban M, and Cloetingh SPL (2010a) 3D crustal model of western and central Europe as a basis for modelling mantle structure. In: Cloetingh S and Negendank J (eds.) *New Frontiers in Integrated Solid Earth Sciences*, pp. 39–69. Dordrecht: Springer Heidelberg.

Tesauro M, Kaban M, and Cloetingh SPL (2010b) Thermal and rheological model of the European lithosphere. In: Cloetingh S and Negendank J (eds.) *New Frontiers in Integrated Solid Earth Sciences*, pp. 71–101. Dordrecht: Springer Heidelberg.

Tesauro M, Kaban MK, and Cloetingh SAPL (2012b) Global strength and elastic thickness of the lithosphere. *Global and Planetary Change* 90–91: 51–57.

Tesauro M, Kaban MK, and Cloetingh SAPL (2013) Global model for the lithospheric strength and effective elastic thickness. *Tectonophysics* 602: 78–86.

Tesauro M, Kaban MK, Cloetingh SAPL, Hardebol NJ, and Beekman F (2007) 3D strength and gravity anomalies of the European lithosphere. *Earth and Planetary Science Letters* 263: 56–73.

Teson E, Teixell A, García-Castellanos D, and Amrhar M (2006) *Geometry and Evolution of the Ouarzazate Basin in the Foreland of the High Atlas Mountains (Morocco)*. Vienna: EGU.

Tikoff B and Maxson J (2001) Lithospheric buckling of the Laramide foreland during Late Cretaceous and Paleogene, western United States. *Rocky Mountain Geology* 36: 13–35.

Tilita M, Matenco L, Dinu C, Ionescu L, and Cloetingh S (2013) Understanding the kinematic evolution and genesis of a back-arc continental "sag" basin: The Neogene evolution of the Transylvanian Basin. *Tectonophysics* 602: 237–258.

Tomek C (1993) Deep-crustal structure beneath the central and inner west Carpathians. *Tectonophysics* 226: 417–431.

Toth J, Kusznir NJ, and Flint SS (1996) A flexural isostatic model of lithosphere shortening and foreland basin formation: Application to the Eastern Cordillera and Subandean belt of NW Argentina. *Tectonics* 15: 213–223.

Turcotte DL and Emerman SH (1983) Mechanisms of active and passive rifting. *Tectonophysics* 94: 39–50.

Turcotte DL and Schubert G (2014) *Geodynamics*. Cambridge: Cambridge University Press.

Underhill JR and Partington MA (1993) Jurassic thermal doming and deflation in the North Sea: Implications of the sequence stratigraphic evidence. *Petroleum Geology Conference Proceedings*, vol. 4, pp. 337–345.

Uyeda S and Kanamori H (1979) Back-arc opening and the mode of subduction. *Journal of Geophysical Research* 84: 1049–1061.

Uyeda S and McCabe R (1983) A possible mechanism of episodic spreading of the Philippine Sea. In: Hashimoto M and Uyeda S (eds.) *Accretion Tectonics in the Circum-Pacific Regions*, pp. 291–306. Tokyo: TerraPub.

Van Balen RT and Cloetingh SAPL (1993) Stress-induced fluid flow in rifted basins. In: Horbury AD and Robinson A (eds.) *Diagenesis and Basin Development, Studies in Geology* 38, pp. 9–26. American Association of Petroleum Geologists.

Van Balen R and Cloetingh S (1994) Tectonic control of the sedimentary record and stress-induced fluid flow: Constraints from basin modelling. *Geological Society Special Publication* 78: 9–26.

Van Balen RT, Houtgast RF, Van der Wateren FM, Vandenberghe J, and Bogaart PW (2000) Sediment budget and tectonic evolution of the Meuse catchment in the Ardennes and the Roer Valley Rift System. *Global and Planetary Change* 27: 113–129.

Van Balen RT, Lenkey L, Horváth F, and Cloetingh SAPL (1999) Two-dimensional modelling of stratigraphy and compaction-driven fluid flow in the Pannonian Basin. *Geological Society Special Publication* 156: 391–414.

Van Balen RT, Vanderbeek PA, and Cloetingh SAPL (1995) The effect of rift shoulder erosion on stratal patterns at passive margins – Implications for sequence stratigraphy. *Earth and Planetary Science Letters* 134: 527–544.

Van der Beek P, Andriessen P, and Cloetingh S (1995) Morphotectonic evolution of rifted continental margins – Inferences from a coupled tectonic-surface processes model and fission-track thermochronology. *Tectonics* 14: 406–421.

Van der Beek PA and Cloetingh S (1992) Lithospheric flexure and the tectonic evolution of the Betic Cordilleras (Se Spain). *Tectonophysics* 203: 325–344.

Van der Beek P, Cloetingh S, and Andriessen P (1994) Mechanisms of extensional basin formation and vertical motions at rift flanks – Constraints from tectonic modeling and fission-track thermochronology. *Earth and Planetary Science Letters* 121: 417–433.

Van der Meulen MJ, Kouwenhoven TJ, Van der Zwaan GJ, Meulenkamp JE, and Wortel MJR (1999) Late Miocene uplift in the Romagnan Apennines and the detachment of subducted lithosphere. *Tectonophysics* 315: 319–335.

Van der Pluijm BA, Craddock JP, Graham BR, and Harris JH (1997) Paleostress in cratonic North America: Implications for deformation of continental interiors. *Science* 277: 794–796.

Van Vliet-Lanoë B, Laurent M, Everaerts M, Mansy J-L, and Manby G (2000) Évolution néogène et quaternaire de la Somme, une flexuration tectonique active. *Comptes Rendus de l'Académie des Sciences – Series IIA – Earth and Planetary Science* 331: 151–158.

Van Wees JD (1994) *Tectonic Modelling of Basin Deformation and Inversion Dynamics*: *The Role of Pre-existing Faults and Continental Lithosphere Rheology in Basin Evolution*. PhD Thesis, VU University, Amsterdam.

Van Wees JD, Arche A, Beijdorff CG, Lopez-Gomez J, and Cloetingh SAPL (1998) Temporal and spatial variations in tectonic subsidence in the Iberian Basin (eastern Spain): Inferences from automated forward modelling of high-resolution stratigraphy (Permian-Mesozoic). *Tectonophysics* 300: 285–310.

Van Wees JD and Beekman F (2000) Lithosphere rheology during intraplate basin extension and inversion – Inferences from automated modeling of four basins in western Europe. *Tectonophysics* 320: 219–242.

Van Wees JD and Cloetingh S (1996) 3D Flexure and intraplate compression in the North Sea Basin. *Tectonophysics* 266: 343–359.

Van Wees JD, Stephenson RA, Stovba SM, and Shymanovskyi VA (1996) Tectonic variation in the Dniepr-Donets Basin from automated modelling of backstripped subsidence curves. *Tectonophysics* 268: 257–280.

Van Wees JD, Van Bergen F, David P, et al. (2009) Probabilistic tectonic heat flow modeling for basin maturation: Assessment method and applications. *Marine and Petroleum Geology* 26: 536–551.

Vasiliev I, de Leeuw A, Filipescu S, et al. (2010) The age of the Sarmatian-Pannonian transition in the Transylvanian Basin (Central Paratethys). *Palaeogeography Palaeoclimatology Palaeoecology* 297: 54–69.

Vasiliev I, Reichart GJ, and Krijgsman W (2013) Impact of the Messinian Salinity Crisis on Black Sea hydrology – Insights from hydrogen isotopes analysis on biomarkers. *Earth and Planetary Science Letters* 362: 272–282.

Vauchez A, Tommasi A, and Barruol G (1998) Rheological heterogeneity, mechanical anisotropy and deformation of the continental lithosphere. *Tectonophysics* 296: 61–86.

Vening-Meinesz FA (1941) Gravity over the Hawaiian archipelago and over the Madeira area: Netherlands Acad. *Proceedings of the Netherlands Academie van Wetenschappen* 44: 1–12.

Vermeesch P, Poort J, Duchkov AD, Klerkx J, and de Batist M (2004) Lake Issyk-Kul (Tien Shan): Unusually low heat flow in an active intermontane basin. *Geologiya i Geofizika* 45: 616–625.

Vernant P, Nilforoushan F, Hatzfeld D, et al. (2004) Present-day crustal deformation and plate kinematics in the Middle East constrained by GPS measurements in Iran and northern Oman. *Geophysical Journal International* 157: 381–398.

Verrall P (1989) Speculations on the Mesozoic-Cenozoic tectonic history of the western United States. *The American Association of Petroleum Geologists* 46: 615–631.

Vyssotski AV, Vyssotski VN, and Nezhdanov AA (2006) Evolution of the West Siberian Basin. *Marine and Petroleum Geology* 23: 93–126.

Warners-Ruckstuhl KN, Govers R, and Wortel R (2012) Lithosphere-mantle coupling and the dynamics of the Eurasian Plate. *Geophysical Journal International* 189: 1253–1276.

Waschbusch PJ and Royden LH (1992) Episodicity in foredeep basins. *Geology* 20: 915–918.

Watcharanantakul R and Morley CK (2000) Syn-rift and post-rift modelling of the Pattani Basin, Thailand: Evidence for a ramp-flat detachment. *Marine and Petroleum Geology* 17: 937–958.

Watts AB (2001) *Isostasy and Flexure of the Lithosphere*. Cambridge: Cambridge University Press, 458 pp.

Watts AB (2007) An overview. *Treatise on Geophysics*, vol. 6, pp. 1–48. The Netherlands: Elsevier.

Watts AB and Burov EB (2003) Lithospheric strength and its relationship to the elastic and seismogenic layer thickness. *Earth and Planetary Science Letters* 213: 113–131.

Watts AB and Fairhead JD (1997) Gravity anomalies and magmatism along the western continental margin of the British Isles. *Journal of the Geological Society* 154: 523–529.

Watts AB, Karner GD, and Steckler MS (1982) Lithospheric flexure and the evolution of sedimentary basins. *Philosophical Transactions of the Royal Society A: Physical, Mathematical and Engineering Sciences* 305: 249–281.

Wenzel F, Sperner B, Lorenz F, and Mocanu V (2002) Geodynamics, tomographic images and seismicity of the Vrancea region (SE-Carpathians, Romania). *EGU Stephan Mueller Special Publication Series* 3: 95–104.

Wernicke B (1985) Uniform-sense normal simple shear of the continental lithosphere. *Canadian Journal of Earth Sciences* 22: 108–125.

Wernicke B (1990) The fluid crustal layer and its implications for continental dynamics. In: Salisbury MH and Fountain DM (eds.) *Exposed Cross-Sections of the Continental Crust*, pp. 509–544. The Netherlands: Springer.

Wessel P and Müller RD (2007) Plate tectonics. *Treatise on Geophysics*, vol. 6, pp. 49–98. The Netherlands: Elsevier.

Whipple KX (2009) The influence of climate on the tectonic evolution of mountain belts. *Nature Geoscience* 2: 97–104.

White N and Mckenzie D (1988) Formation of the steers head geometry of sedimentary basins by differential stretching of the crust and mantle. *Geology* 16: 250–253.

White RS and Mckenzie DP (1989) Volcanism at rifts. *Scientific American* 261: 62–71.

Whittaker A, Bott MHP, and Waghorn GD (1992) Stresses and plate boundary forces associated with subduction plate margins. *Journal of Geophysical Research: Solid Earth* 97: 11933–11944.

Wilgus CK, Hastings BS, Kendall CGSC, et al. (1988) Sea-level changes: An integrated approach. *Special Publications – Society of Economical Paleontologists and Mineralogists* 42: 402.

Willett SD (1999) Orogeny and orography: The effects of erosion on the structure of mountain belts. *Journal of Geophysical Research: Solid Earth* 104: 28957–28981.

Willett SD, Schlunegger F, and Picotti V (2006) Messinian climate change and erosional destruction of the central European Alps. *Geology* 34: 613–616.

Wilson M (1993a) Geochemical signatures of oceanic and continental basalts – A key to mantle dynamics. *Journal of the Geological Society* 150: 977–990.

Wilson M (1993b) Magmatism and the geodynamics of basin formation. *Sedimentary Geology* 86: 5–29.

Wilson M (1997) Thermal evolution of the Central Atlantic passive margins: Continental break-up above a Mesozoic superplume. *Journal of the Geological Society* 154: 491–495.

Wilson M and Patterson R (2001) Intraplate magmatism related to short-wavelength convective instabilities in the upper mantle: Evidence from the Tertiary-Quaternary volcanic province of western and central Europe. *Special Paper of the Geological Society of America* 352: 37–58.

Winguth C, Wong HK, Panin N, et al. (2000) Upper Quaternary water level history and sedimentation in the northwestern Black Sea. *Marine Geology* 167: 127–146.

Worrall DM and Snelson S (1989) Evolution of the northern Gulf of Mexico, with emphasis on Cenozoic growth faulting and the role of salt. *The Geology of North America*, vol. 1, pp. 97–138. Boulder, Colorado: Geological Society of America.

Wortel MJR and Spakman W (2000) Geophysics – Subduction and slab detachment in the Mediterranean-Carpathian region. *Science* 290: 1910–1917.

Xie X and Heller PL (2009) Plate tectonics and basin subsidence history. *Geological Society of America Bulletin* 121: 55–64.

Yegorova TP, Stephenson RA, Kozlenko VG, Starostenko VI, and Legostaeva OV (1999) 3-D gravity analysis of the Dniepr-Donets Basin and Donbas Foldbelt, Ukraine. *Tectonophysics* 313: 41–58.

Yilmaz Y, Tuysuz O, Yigitbas E, Genc SC, and Sengor AMC (1997) Geology and tectonic evolution of the Pontides. *Regional and Petroleum Geology of the Black Sea and Surrounding Region*, vol. 68, pp. 183–226, American Association of Petroleum Geologists Memoir.

Yong L, Allen PA, Densmore AL, and Qiang X (2003) Evolution of the Longmen Shan foreland basin (western Sichuan, China) during the Late Triassic Indosinian orogeny. *Basin Research* 15: 117–138.

Zeyen H, Volker F, Wehrle V, et al. (1997) Styles of continental rifting: Crust-mantle detachment and mantle plumes. *Tectonophysics* 278: 329–352.

Zhao JM, Mooney WD, Zhang XK, et al. (2006) Crustal structure across the Altyn Tagh Range at the northern margin of the Tibetan plateau and tectonic implications. *Earth and Planetary Science Letters* 241: 804–814.

Ziegler PA (1983) Crustal thinning and subsidence in the North-Sea. *Nature* 304: 561.

Ziegler PA (1987) Compressional intraplate deformations in the Alpine foreland – An introduction. *Tectonophysics* 137: 1–5.

Ziegler PA (1988) Evolution of the arctic-North Atlantic and the western Tethys – A visual presentation of a series of paleogeographic-paleotectonic maps. *Memoirs – American Association of Petroleum Geologists* 43: 164–196.

Ziegler PA (1989a) Evolution of Laurussia. In: *A Study in Late Paleozoic Plate Tectonics*. Dordrecht: Kluwer Academic.

Ziegler PA (1989b) Evolution of the North Atlantic – An overview. *The American Association of Petroleum Geologists* 46: 111–129.

Ziegler PA (1990a) Collision related intra-plate compression deformations in Western and Central-Europe. *Journal of Geodynamics* 11: 357–388.

Ziegler PA (1990b) *Geological Atlas of Western and Central Europe*. Shell Internationale Petroleum Maatschappij BV/Geological Society of London, Amsterdam: Elsevier, 239.

Ziegler PA (1992) Geodynamics of rifting and implications for hydrocarbon habitat. *Tectonophysics* 215: 221–253.

Ziegler PA (1993a) Smith, William Lecture 1992 – Plate-moving mechanisms – Their relative importance. *Journal of the Geological Society* 150: 927–940.

Ziegler PA (1993b) Plate-moving mechanisms: Their relative importance. *Journal of the Geological Society* 150: 927–940.

Ziegler PA (1994) *Geodynamic Processes Governing Development of Rifted Basins*. Paris: Technip.

Ziegler PA (1996a) Hydrocarbon habitat in rifted basins. In: Roure F, Ellouz N, Shein VS, and Skvortsov I (eds.) *Geodynamic Evolution of Sedimentary Basins*, pp. 85–94. Paris: Technip.

Ziegler PA (1996b) Geodynamic processes governing development of rifted basins. In: Roure F, Shein VS, Ellouz-Zimmermann N, and Skvortsow L (eds.) *Geodynamic Evolution of Sedimentary Basins*, pp. 19–67. Paris: Technip.

Ziegler PA, Bertotti G, and Cloetingh S (2002) In: *Dynamic processes controlling foreland development Â the role of mechanical (de) coupling of orogenic wedges and forelands*. *Stephan Mueller Special Publication Series*, vol. 1, pp. 17–56.

Ziegler PA and Cloetingh S (2004) Dynamic processes controlling evolution of rifted basins. *Earth-Science Reviews* 64: 1–50.

Ziegler PA, Cloetingh S, Guiraud R, and Stampfli GM (2001) Peri-Tethyan platforms: Constraints on dynamics of rifting and basin inversion. *Mémoires du Muséum national d'histoire naturelle*, vol. 186, pp. 9–49.

Ziegler PA, Cloetingh S, and Van Wees JD (1995) Dynamics of intra-plate compressional deformation: The Alpine foreland and other examples. *Tectonophysics* 252: 7–59.

Ziegler PA and Dèzes P (2005) Evolution of the lithosphere in the area of the Rhine Rift System. *International Journal of Earth Sciences* 94: 594–614.

Ziegler PA and Dèzes P (2006) Crustal evolution of Western and Central Europe. *Geological Society, London, Memoirs* 32: 43–56.

Ziegler PA and Dèzes P (2007) Cenozoic uplift of Variscan Massifs in the Alpine foreland: Timing and controlling mechanisms. *Global and Planetary Change* 58: 237–269.

Ziegler PA and Horváth E (1996a) Hydrocarbon habitat in rifted basins. In: Roure F, Ellouz N, Shein VS, and Skvortsow I (eds.) *Geodynamic Evolution of Sedimentary Basins*, pp. 19–67. Paris: Technip.

Ziegler PA and Horváth E (1996b) Peri-Tethys Memoir 2: Structure and prospects of Alpine basins and forelands. *Mémoires du Muséum national d'histoire naturelle*, vol. 170, p. 547.

Ziegler PA and Roure F (1996) Architecture and petroleum systems of the Alpine orogen and associated basins. *Mémoires du Muséum national d'histoire naturelle*, vol. 170.

Ziegler PA, Schumacher ME, Dèzes P, Van Wees JD, and Cloetingh S (2004) Post-Variscan evolution of the lithosphere in the Rhine Graben area: Constraints from subsidence modelling. *Geological Society, London, Special Publications* 223: 289–317.

Ziegler PA, Van Wees JD, and Cloetingh S (1998) Mechanical controls on collision-related compressional intraplate deformation. *Tectonophysics* 300: 103–129.

Zoback ML (1992) 1st-order and 2nd-order patterns of stress in the lithosphere – The World Stress Map Project. *Journal of Geophysical Research: Solid Earth* 97: 11703–11728.

Zoback MD, Stephenson RA, Cloetingh S, et al. (1993) Stresses in the lithosphere and sedimentary basin formation. *Tectonophysics* 226: 1–13.

Zoetemeijer R, Desegaulx P, Cloetingh S, Roure F, and Moretti I (1990) Lithospheric dynamics and tectonic-stratigraphic evolution of the Ebro Basin. *Journal of Geophysical Research: Solid Earth (1978–2012)* 95: 2701–2711.

Zoetemeijer R, Cloetingh S, Sassi W, and Roure F (1993) Modeling of Piggyback-Basin stratigraphy – Record of tectonic evolution. *Tectonophysics* 226: 253–269.

Zoetemeijer R, Tomek C, and Cloetingh S (1999) Flexural expression of European continental lithosphere under the western outer Carpathians. *Tectonics* 18: 843–861.

Zonenshain LP and LePichon X (1986) Deep basins of the Black-Sea and Caspian Sea as remnants of Mesozoic Back-Arc basins. *Tectonophysics* 123: 181–211.